Investigation of host-microbiota communication through diverse signalling pathways

Jemma Justine Taitz

Charles Perkins Centre,

School of Medical Sciences, Faculty of Medicine and Health

The University of Sydney

A thesis submitted to fulfil requirements for the degree of Doctor of Philosophy at The University of Sydney

2025

Table of Contents

Statement of originality

This is to certify that the content of this thesis is my own work. This thesis has not been submitted for any other degree or purpose.

I certify that the intellectual content of this thesis is the product of my own work, and that all assistance received in preparing this thesis and all sources have been acknowledged.

Jemma Taitz

February 2023

Author attribution statement

Chapter 1 (Introduction) contains material from a published review:

Taitz J, Tan JK, Potier-Villette C, Ni D, King NJ, Nanan R, Macia L. Diet, commensal microbiota-derived extracellular vesicles, and host immunity. *Eur J Immunol*. 2023; 53:e2250163

Sections from this review article were only included in this chapter if they were originally written and drafted by me. These sections underwent edits by all listed co-authors and were revised further when incorporating into this thesis.

Chapter 2 (Results I) is presented as the following published article:

Taitz J, Tan J, Ni D, Potier-Villette C, Grau G, Nanan R, Macia L. Antibiotic-mediated dysbiosis leads to activation of inflammatory pathways. *Front Immunol*. 2025; 15:1493991

I designed and carried out the majority of the experiments and collaborated on all of them. I analysed the data, and conducted data interpretation, with data curation from co-authors. I wrote the original manuscript. All co-authors contributed to experiments, analysis and manuscript editing.

Chapter 3 (Results II) is presented as the following published article:

Tan J, Ni D, Taitz J, Pinget GV, Read M, Senior A, Wali JA, Elnour R, Shanahan E, Wu H, Chadban SJ, Nanan R, King NJC, Grau GE, Simpson SJ, Macia L. Dietary Protein Increases T-Cell-Independent sIgA Production through Changes in Gut Microbiota-Derived Extracellular Vesicles. *Nature Communications*. 2022;**13**:4336.

I optimised protocols for EV isolation and analysis which formed the basis of this study. I acquired and analysed IVIS imaging data, and worked jointly on animal experiments (dissections, tissue processing, flow cytometry and flow analysis). I helped develop the study design and collaborated with co-authors in drafting and revising the manuscript. All co-authors contributed to data interpretation and manuscript preparation.

Chapter 4 (Results III) is presented as manuscript submitted for publication. *Since the thesis submission this has been published in Molecular Metabolism* (doi: 10.1016/j.molmet.2025.102180*)*

I optimised protocols for EV isolation and analysis, contributed to EV experiments, and generated and analysed the data presented in Figure 1A-E, G; Figure 2C, D; Figure 3E; and Supplementary Figure 1A, C, D. I performed animal experiment including dissections, tissue processing and sample staining and acquisition. I worked with co-authors on the study

design and drafting and editing of the manuscript. All co-authors contributed to data interpretation and manuscript preparation.

Chapter 5 (Results IV) is formatted as a manuscript due to be submitted for publication in 2025

I took the lead in designing and carrying out the majority of the experiments, with assistance from co-authors. I analysed the data, and wrote the original manuscript. All co-authors contributed to data interpretation and manuscript preparation.

Author attribution statement

In addition to the statements above, in cases where I am not the corresponding author of a published item, permission to include the published material has been granted by the corresponding author.

Jemma Taitz

_____

21st February 2025

As supervisor for the candidature upon which this thesis is based, I can confirm that the authorship attribution statements above are correct.

Laurence Macia

_____

21st February 2025

List of Publications

Contributing directly to this thesis:

Taitz J, Tan JK, Potier-Villette C, Ni D, King NJ, Nanan R, Macia L. Diet, commensal microbiota-derived extracellular vesicles, and host immunity. *Eur J Immunol*. 2023; **53**:e2250163

Text from this review is presented as part of **Chapter 1** (Introduction)

Taitz J, Tan J, Ni D, Potier-Villette C, Grau G, Nanan R, Macia L. Antibiotic-mediated dysbiosis leads to activation of inflammatory pathways. *Front Immunol*. 2025; **15**:1493991

The work from this paper presented as **Chapter 2** (Results I)

Tan J, Ni D, **Taitz J**, Pinget GV, Read M, Senior A, Wali JA, Elnour R, Shanahan E, Wu H, Chadban SJ, Nanan R, King NJC, Grau GE, Simpson SJ, Macia L. Dietary Protein Increases T-Cell-Independent sIgA Production through Changes in Gut Microbiota-Derived Extracellular Vesicles. *Nature Communications*. 2022;**13**:4336.

The work from this paper is presented as **Chapter 3** (Results II)

Tan J, **Taitz J**, Ni D, Potier-Villette C, Pulpitel T, Stanley D, Nanan R, Macia L. "Gut microbiota-derived extracellular vesicles promote hepatic gluconeogenesis via the activation of hepatic circadian", *Science Advances* (currently under review)

The work presented in **Chapter 4** (Results III) is formatted as a manuscript currently under review

Related to the research but not presented in this thesis:

Ni D, Tan J, Reyes J, Senior AM, Andrews C, **Taitz J**, Potier-Villette C, Wishart C, Spiteri A, Piccio L, King NJC, Barres R, Raubenheimer D, Simpson SJ, Nanan, R, Macia L. High fat low carbohydrate diet is linked to CAN autoimmunity protection. *Advanced Science*. 2025. In press

Tan J, Potier-Villette C, Ni D, Hoeckh M, **Taitz J**, Simpson SJ, Nanan R, Macia L. Succinate induces a Th2 environment in the small intestine but does not exacerbate food allergy. *Allergy*. 2024

Tan J, **Taitz J**, Nanan R, Grau G, Macia L. Dysbiotic Gut Microbiota-Derived Metabolites and Their Role in Non-Communicable Diseases. *International Journal of Molecular Sciences*. 2023; **24**:15256

Ni D, Tan J, Robert R, **Taitz J**, Ge A, Potier-Villette C, Reyes JGA, Spiteri A, Wishart C, Mackay C, Piccio L, King NJC, Macia L. GPR109A expressed on medullary thymic epithelial cells affects thymic Treg development. *European Journal of Immunology*. 2023; **53**:2350521

Pinget GV, Tan JK, Ni D, **Taitz J**, Daien CI, Mielle J, Moore RJ, Stanley D, Simpson SJ, King NJC, Macia L. Dysbiosis in imiquimod-induced psoriasis alters gut immunity and exacerbates colitis development. *Cell Rep*. 2022; **40**:111191

Tan J, **Taitz J**, Sun SM, Langford L, Ni D, Macia L. Your Regulatory T Cells Are What You Eat: How Diet and Gut Microbiota Affect Regulatory T Cell Development. *Frontiers in Nutrition*. 2022; **9**

Tan J, Ni D, Wali JA, Cox DA, Pinget GV, **Taitz J**, Daïen CI, Senior A, Read M, Simpson SJ, King NJC, Macia L. Dietary carbohydrate, particularly glucose, drives B cell lymphopoiesis and function. *iScience*. 2021; **24**

Abstract

The gut microbiota plays a fundamental role in shaping host physiology, influencing immune homeostasis, metabolism, and overall health. Disruptions in gut homeostasis, driven by altered dietary patterns and antibiotic exposure, are strongly linked to the rising incidence of non-communicable diseases (NCDs) through microbiota-mediated mechanisms. However, identifying precise signalling pathways and their contributions to disease remains challenging, partly due to the vast diversity of microbiota-derived molecules that can influence host processes. While microbial metabolites and microbe-associated molecular patterns (MAMPs) are well-established mediators of the gut-host axis, emerging evidence suggests that gut microbiota extracellular vesicles (MEVs) represent an additional pathway that integrates metabolite and MAMP signalling. Although specific MEV strains and total MEV profiles are increasingly studied as potential therapeutics and biomarkers, their physiological role in gut-host interactions remains poorly understood. This thesis explores how gut microbiota and MEVs influence key aspects of host physiology, focusing on their roles in immunity, metabolism, and maternal-fetal interactions.

Using a long-term antibiotic model, we examined how antibiotics induced distinct dysbiotic microbiota compositions and altered microbial metabolites. While the host showed no overt inflammation, splenic T cells exhibited increased TNF secretion, linking antibiotic-induced dysbiosis to immune dysregulation and potential autoinflammatory disease. Next, we explored the effects of dietary macronutrients on microbiota composition and host immunity. We identified that dietary protein drove an increase in MEV levels, triggering the production of host immunoglobulin A (sIgA) and revealing a novel role for MEVs as intermediaries in the diet-microbiota-immune axis. We then identified that MEVs are regulators of host metabolism, acting as cues for hepatic gluconeogenesis via the circadian pathway. Gut MEV production aligns with host feeding patterns and glucose demand, but chronic MEV exposure promoted metabolic dysfunction, implicating MEVs in microbiota-associated metabolic disorders. Finally, we established MEVs as a distinct fraction of the gut microbiota that actively shapes its composition during homeostasis. When exposed to MEVs in gestation, offspring showed postnatal changes to microbiota composition, colonic gene expression, and peripheral

immune profiles suggesting MEVs are a pathway through which maternal microbiota influences fetal physiology and thus long-term health.

Collectively, this thesis explores the relationship between microbiota and host physiology, examining how antibiotics and diet influence this interplay and identifying MEVs as key mediators in this cross-talk. While further studies are needed to elucidate the precise molecular mechanisms by which MEVs regulate host biology, these findings highlight their potential as both a therapeutic target and a novel intervention to modulate microbiota-driven pathways in NCD development.

Acknowledgements

I want to express my deepest gratitude to my supervisor, Laurence Macia, whose infectious passion for science and persuasiveness led me to pursue PhD. Your excitement, creativity, and love for discovery have been a source of inspiration, helping me push through even the most challenging experiments. I am especially grateful to your guidance and support this past year, even from afar. Thank you for your dedication and belief in me.

A huge thank you to Ralph Nanan for being a pillar of support and guidance throughout my PhD, and even more so in this final year. Your generosity, especially in the last stretch of this journey, has helped me bring everything together. I am very appreciative and grateful for your help in making it to the finish line.

I am immensely grateful to Jian, without whom many of these experiments would not have been possible. From day one, your patience in teaching and answering a million questions has been a lifesaver. I am especially grateful for your feedback and guidance on putting this thesis together, which has been truly invaluable.

Thank you also to Duan, an encyclopaedia of knowledge and technique, always ready to drop whatever he's doing to help in the lab. Your troubleshooting skills and advice has saved me more times than I can count. A big thank you as well to Gaby for your kindness, encouragement and being a friendly face and ear.

I would also like to thank Professors Georges Grau and Nick King for all their thoughtful insights and discussions during our EV meetings over the years. Their continued interest and wisdom have been instrumental in shaping this project.

Thank you to my best friends, Lana, Camille and Claire, for your unwavering support throughout this journey. I feel incredibly lucky to have your friendships, which have brought me so much comfort and raised my spirts countless times. To Claire especially, my twin in this PhD and in so many other ways, you know how grateful I am. Clemma forever.

To my family, Ma, Mira, D-J and my niblings Joel, Sol, Daniel, Sadie, Levi, and Baby Taitz. Thank you for all your unconditional love and support.

Abbreviations

AHR	aryl hydrocarbon receptor
AIC	Akaike information criterion
AMP	antimicrobial peptide
APC	antigen-presenting cell
APRIL	a proliferation-inducing ligand
ASV	amplicon sequence variant
BAFF	B cell activating factor
BALF	bronchoalveolar lavage
BCA	bicinchoninic acid
BCR	B cell receptor
BEV	bacterial extracellular vesicle
BFA	brefeldin A
BHI	brain heart infusion
CCL28	C-C motif chemokine ligand 28
cDC	conventional dendritic cell
CLP	common lymphoid progenitor
CMP	common myeloid progenitor
CRY	cryptochrome
CSR	class switch recombinase
DC	dendritic cell
DMEM	Dulbecco's Modified Eagle Medium
DN	double negative
DP	double positive
DSS	dextran sodium sulfate
EDTA	ethylenediaminetetraacetic acid
ELISA	enzyme-linked immunosorbent assay
Eos	eosinophils
ER	endoplasmic reticulum
EV	extracellular vesicle
FACS	fluorescence-activated cell sorting
FBS	fetal bovine serum
FMO	fluorescence minus one
FMT	faecal microbiota transplantation
G-	Gram-negative
G+	Gram-positive
G6P	glucose-6-phosphatase
GAM	generalised additive model
GDP	gross domestic product

GF	germ-free
GI	gastrointestinal
GMP	granulocyte-macrophage progenitor
GPCR	G-protein coupled receptor
HBSS	Hanks' Balanced Salt Solution
HC	high carbohydrate
HDAC	histone deacetylase
HDM	house dust mite
HEPES	4-(2-hydroxyethyl)-1-piperazineethanesulfonic acid
HF	high fat
HIF-1α	hypoxia inducible factor 1-alpha
HP	high protein
IBD	inflammatory bowel disease
IEL	intraepithelial lymphocyte
IFNγ	interferon gamma
IgE	immunoglobulin E
IgG	immunoglobulin G
IL-4	interleukin 4
IL-5	interleukin 5
IL-6	interleukin 6
IL-10	interleukin 10
IL-13	interleukin 13
IL-17	interleukin 17
IL-22	interleukin 22
ILC	innate lymphoid cell
IVIS	in vivo imaging system
LB	Luria-Bertani
LPS	lipopolysaccharide
LT-HSC	long-term hematopoietic stem cells
ST-HSC	short-term hematopoietic stem cells
M cell	Microfold cell
MAMP	microbe associated molecular pattern
MEP	megakaryocyte-erythroid progenitor
MEV	microbiota extracellular vesicle
MLN	mesenteric lymph node
MPP	multipotent progenitor
NCD	non-communicable disease
NEC	necrotising enterocolitis
Neuts	neutrophils
NF-κB	nuclear factor kappa B
NK	natural killer

NKT	natural killer T
NLRP3	NOD-, LRR- and pyrin domain-containing protein
NMR	nuclear magnetic resonance
NTA	nanoparticle tracking analysis
PAMP	pathogen-associated molecular pattern
PBS	phosphate buffered saline
PCA	principal component analysis
PCoA	principal coordinates analysis
pDC	plasmacytoid dendritic cell
PEPCK	phosphoenolpyruvate carboxykinase
PER	period
pIgR	polymeric immunoglobulin A receptor
PMA	phorbol 12-myristate 13-acetate
PmB	polymyxin B
PRR	pattern recognition receptor
qPCR	quantitative polymerase chain reaction
RA	rheumatoid arthritis
RBC	red blood cell
ROS	reactive oxygen species
rRNA	ribosomal RNA
SCFA	short-chain fatty acid
SI	small intestine
sIgA	secretory immunoglobulin A
SP	single positive
SPF	specific-pathogen free
TCR	T cell receptor
TEM	transmission electron microscopy
TGF-β	transforming growth factor beta
Th1	T helper 1
Th17	T helper 17
Th2	T helper 2
TJ	tight junction
TLR	toll-like receptor
TNF	tumour necrosis factor
Treg	regulatory T cell
TSLP	thymic stromal lymphopoietin
TUDCA	tauroursodeoxycholic acid
Van	vancomycin
WATe	epididymal white adipose tissue
WATi	inguinal white adipose tissue
WT	wild type

List of Figures

List of Tables

List of Supplementary Figures and Tables

Chapter 1 Introduction

1.1 The role of the gut microbiota in host health

The incidence of non-communicable diseases (NCDs) has risen dramatically in recent decades, particularly in high-income countries (Habib and Saha, 2010). These "Western lifestyle diseases" encompass autoimmune conditions (multiple sclerosis, inflammatory bowel disease (IBD), psoriasis, type 1 diabetes), atopic disease (asthma, food allergy, eczema), metabolic disorders (obesity, type 2 diabetes) and neurodegenerative disorders (Alzheimer's and Parkinson's disease) (Carrera-Bastos et al., 2011; Kopp, 2019). While their aetiologies involve a complex interplay of genetic and environmental factors, disrupted gut homeostasis has emerged as a common feature among these diverse conditions (Carding et al., 2015; Fan and Pedersen, 2021). Modern lifestyle factors, including urbanisation, altered dietary patterns, antibiotic use, and modern hygiene practices, influence gut microbiota composition and are increasingly implicated in NCD pathogenesis (Rinninella et al., 2019). As such, deciphering the molecular mechanisms by which gut bacteria influence host tissues is crucial for understanding how they contribute to NCD development and for identifying novel therapeutic interventions.

The body is host to an extensive community of microorganisms which mostly colonise mucosal surfaces, including the skin, lungs, genital tract, mouth and gastrointestinal (GI) tract. The GI tract harbours the most abundant and diverse community, collectively known as the gut microbiota. This ecosystem comprises predominantly 99% anaerobic bacteria and, along with fungi, viruses, and archaea, represents millions of years of co-

evolution with the host (Sommer and Bäckhed, 2013). This evolutionary process has produced an intricate and mutualistic relationship: the host provides a nutrient-rich, stable habitat, while the microbiota carries out essential functions such as nutrient metabolism, defence against pathogens, and the production of bioactive molecules that influence tissue development, immune education, and overall host physiology (Hooper et al., 2012; Kamada et al., 2013; Rowland et al., 2018).

The pivotal role of the gut microbiota in host physiology was first demonstrated in the 1960s with the derivation of germ-free (GF) mice, which are completely devoid of microbial colonisation. GF mouse studies have revealed widespread alterations spanning almost every bodily system, including cognition, behaviour, tissue architecture, metabolism, reproduction, endocrine function, and immunity, extensively reviewed elsewhere (Kennedy et al., 2018; Luczynski et al., 2016; Smith et al., 2007). These systemic abnormalities reveal how signals transmitted to distal organ systems through the gut-peripheral axis are not merely beneficial, but indispensable for normal host development and physiology.

Among these systemic effects, the impact on immunity is particularly profound, as GF mice exhibit deficiencies in both innate and adaptive immune cell populations and impaired cell functionality (Kennedy et al., 2018). Consequently, GF mice are more susceptible to pathogenic infections (Fagundes et al., 2012; Harp et al., 1992; Inagaki et al., 1996; Oh et al., 2014). They also exhibit compromised mucosal tolerance, characterised by impaired immune regulation at mucosal surfaces. For example, GF mice have elevated immunoglobulin E (IgE) production, along with increased numbers of lung basophils and invariant natural killer T cells in the lung and colon, increasing their

susceptibility to an exacerbated allergic response (Cahenzli et al., 2013; Herbst et al., 2011; Olszak et al., 2012). Importantly, reintroduction of gut microbiota, either with partial or with full microbial transplantation, rescues many GF deficiencies. This approach has enabled identification of the specific microbial molecules and mechanisms critical to proper host processes.

While GF mice demonstrate the necessity of the gut microbiota for normal host physiology, microbiota transplantation studies have shown that disease phenotypes can be transferred through gut microbiota, directly linking microbiota composition to disease development. A seminal example comes from obesity research, where transplantation of microbiota from genetically obese mice into GF recipients increases adiposity, while microbiota from lean donor mice does not (Turnbaugh et al., 2006). This was attributed to an enhanced nutrient-harvesting capacity in the obese microbiota which directly promoted weight gain. Similar microbiota-driven links have been observed for other metabolic disorders, such as non-alcoholic fatty liver disease, allergy, autoimmune disease, neurodevelopmental conditions, and psychiatric conditions (Cekanaviciute et al., 2017; Feehley et al., 2019; Le Roy et al., 2013; Sharon et al., 2019; Zheng et al., 2016). Emerging evidence also links microbiota composition to gastric cancer (Kwon et al., 2022), highlighting the microbiota's dual role to either support health or contribute to disease.

Maintaining gut homeostasis requires layers of regulation in the intestinal barrier, as discussed further below. The host has evolved strategies to simultaneously compartmentalise the microbiota, permit beneficial microbial signals, and maintain a balanced microbiota ecosystem. A state of gut homeostasis, or a "healthy" gut, is the result

of these processes working optimally in concert. However, disruptions in gut homeostasis typically manifest in two interconnected ways: dysbiosis (the loss of beneficial bacteria and expansion of pathogenic or non-beneficial taxa) and a compromised gut barrier (Stolfi et al., 2022). A disturbance in one can initiate a cycle that disrupts the other, consequently extending dysregulation beyond the gut and leading to systemic effects (Takiishi et al., 2017). For example, barrier dysfunction allows translocation of lipopolysaccharide (LPS), a component of Gram-negative bacterial membranes, into systemic circulation via the hepatic portal vein, causing metabolic endotoxemia and contributing to systemic inflammation observed in conditions such as non-alcoholic fatty liver disease (Cani et al., 2007).

While significant progress has been made in understanding the layers that constitute gut homeostasis, crucial questions remain about the precise mechanisms that link microbiota-host interactions to health and disease. Complexity also arises from the interconnected nature of these relationships: while disrupted gut homeostasis can contribute to the onset and progression of disease, disease states can perpetuate gut dysregulation, further driving progression. This interplay is evident in antibiotic use. For example, while antibiotics are associated with increased NCD risk, they can alleviate active IBD by reducing bacterial populations that drive inflammation (Nitzan et al., 2016). Similarly, while GF mice are more susceptible to infections and allergy, the absence of gut microbiota is protective in autoimmune models (such as arthritis and multiple sclerosis), as disease-driving microbiota-dependent T-helper 17 (Th17) cells are absent (Berer et al., 2011; Lee et al., 2011; Wu et al., 2010).

This thesis investigates key pathways of gut bacteria-host communication, focusing particularly on bacterial extracellular vesicles (BEVs) as mediators of these interactions. Chapters 1 - 3 use the term BEVs, consistent with the terminology commonly used in the field at the time of publication. As the field and the work of this thesis progressed, the more specific term, microbiota extracellular vesicles (MEVs), has emerged to describe vesicles isolated from gut microbiota samples. Thus, MEV has been used as the preferred term from Chapter 4 onwards, as it more accurately describes the experimental samples used in this thesis and in the field of gut EV research. By examining these fundamental mechanisms, we aim to improve our understanding of the dual nature of the microbiota, essential for normal development yet potentially pathogenic when dysregulated. Through detailed analysis of how bacterial communication pathways influence gut homeostasis, the research presented in this thesis will advance understanding of the host-microbiota relationship and identify novel therapeutic strategies to address the rising burden of NCDs in modern societies.

1.2 Compartmentalisation of the gut microbiota and host

The coexistence of trillions of microorganisms within the host represents a biological paradox. The host must prevent both commensals and pathogens from triggering sustained activation of host pattern recognition receptors (PRRs) via microbial-associated molecular patterns (MAMPs), as this would result in chronic, detrimental inflammation. However, it must simultaneously permit a controlled level of exposure to microbiota-derived signals to facilitate immune education and physiological development (Belkaid and Harrison, 2017). To achieve this balance, the GI barrier has

evolved numerous mechanisms to minimise direct contact between bacteria and host cells under homeostatic conditions, while simultaneously monitoring the gut microbiota. This compartmentalisation is selectively permeable, allowing for the regulated passage of microbiota-derived components to support physiological processes via direct contact with host cells.

The mucosal interface plays a central role in distinguishing pathogenic threats from innocuous antigens, such as dietary components and commensals, to foster immune tolerance without compromising the ability to mount an effective defensive response. Homeostasis is maintained by a coordinated set of structural, molecular, and cellular mechanisms, which also remain poised to respond rapidly to pathogenic or environmental challenges.

The GI tract is spatially organised into functionally specialised regions, reflected in their tissue architecture and cellular composition. While the stomach contains a small number of bacteria, the majority of gut bacteria occupy the lower intestinal tract. Microbial density increases significantly from the small intestine (SI) to the colon, where the comprehensively studied and complex microbial community resides, with approximately 10^{11} bacterial cells for every gram of intestinal content (Neish, 2009).

The SI, comprising the duodenum, jejunum and ileum, plays a key role in nutrient absorption, with the duodenum and jejunum primarily absorbing most nutrients and water, and the ileum specialised in uptake of vitamin B12, bile salts and remaining nutrients (Thompson et al., 2018). Its epithelium is organised in a “hill and valley” structure of crypts and villi, maximising surface area to facilitate absorption (Barker,

2014). These villi, enriched in absorptive epithelial cells, project into lumen creating a large surface area which optimises the uptake of water, proteins, lipids and simple sugars from digested contents. This interface also represents a significant exposure of the host tissues to the external environment. Unabsorbed dietary components, particularly indigestible fibre, pass into the colon, where the anaerobic bacterial community is specialised in the breakdown of complex polysaccharides into short-chain fatty acid (SCFA) metabolites which include butyrate, acetate, and propionate. The colon also reabsorbs water and compacts remaining content, including microbial and epithelial cell debris, into faeces for excretion. In contrast to the SI, the colon epithelium lacks protruding villi, and is characterised by crypts and flat surface (Barker, 2014).

As shown in Figure 1.1, The SI and colon share a similar basic architecture, comprising (1) a luminal space containing a mix of dietary components and microbes, (2) a mucus layer (3) an epithelial layer and (4) an immunologically rich lamina propria. The GI tract also has associated areas of lymphoid tissue, including Peyer's patches and the gut-draining mesenteric lymph nodes (MLNs), which are essential to the development of adaptive immune responses.

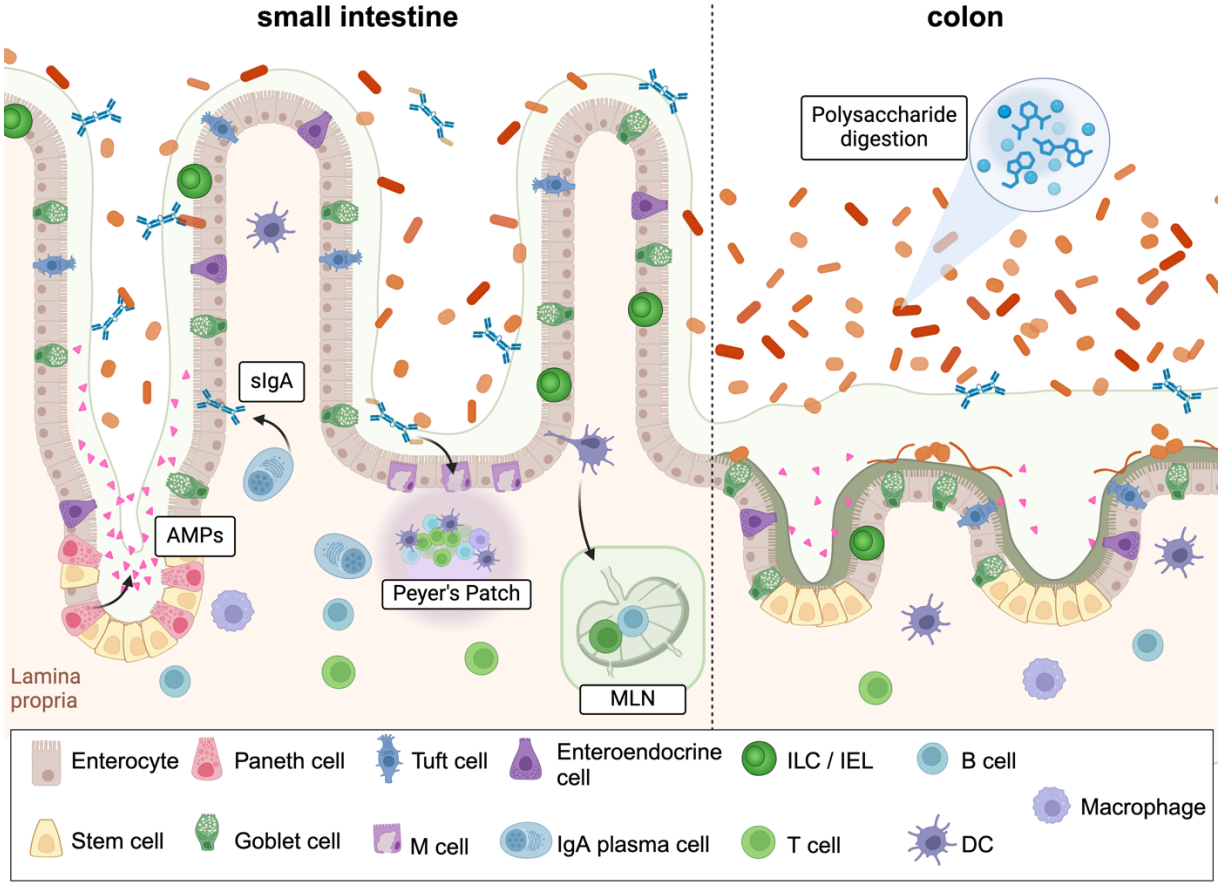

Figure 1.1: Organisation and properties of the intestinal barrier in the small intestine and colon

The intestinal epithelium is continuously renewed by stem cells located at the crypt base, which differentiate into specialised subsets including enterocytes, Paneth cells, goblet cells, tuft cells, enteroendocrine cells and microfold (M) cells. The epithelium is protected by a mucus barrier, which in the small intestine comprises a single, loose layer, and in the colon comprises a dense, adherent inner layer and loose outer layer. Paneth cells and enterocytes secrete antimicrobial peptides (AMPs) that diffuse into the mucus to create an antibacterial zone. Plasma cells in the lamina propria produce secretory IgA (sIgA), which is transported into the lumen to neutralise as well as regulate the microbial community. Immune cells such as intraepithelial lymphocytes (IELs) and innate lymphoid cells (ILCs) patrol the epithelium, while a diverse range of innate and adaptive cells are present in the lamina propria. Compared to the small intestine, the colon has a denser and more complex bacterial community specialised in polysaccharide breakdown, and specific bacteria, such as segmented filamentous bacteria and *Akkermansia muciniphila* colonise the outer mucus layer. Antigen-specific responses are initiated in gut-associated lymphoid tissues such as Peyer's patches and the mesenteric lymph nodes (MLNs), where antigens delivered by M cells or migratory dendritic cells (DCs) trigger the activation of antigen-specific T and B cells. Figure created in BioRender.com

1.2.1 The mucus layer

The mucus layer serves as the outermost barrier between the host and luminal content, with both physical and chemical properties contributing to its protective function. Properties of the mucus layer vary throughout the GI tract: the SI comprises a single layer, while the colon and stomach have both an inner and outer mucus (Ermund et al., 2013). The major structural component of intestinal mucus is the mucin protein MUC2, secreted by goblet cells within the epithelium. Glycosylated mucin monomers polymerize and hydrate with water to form sheets and a gel-like matrix (Birchenough et al., 2015). This net-like structure acts as a molecular sieve, limiting contact between luminal content and the epithelial surface (Pelaseyed et al., 2014).

In the mouse colon, the inner mucus layer is dense (~50μm thick) and adheres to the enterocyte surface (Birchenough et al., 2015; Johansson et al., 2008). This layer is impenetrable to particles equivalent to the size of bacterial cells (~0.5μm) and is effectively sterile under homeostatic conditions (Ermund et al., 2013; Johansson et al., 2008). However, it is permeable to microbial-derived products such as metabolites and toxins, which can diffuse through. The outer mucus (~100μm thick) is formed by endogenous proteolytic cleavage of the inner layer and is looser and non-adherent (Johansson et al., 2008). As such, it has greater penetrability to luminal components, and also serves as a niche for commensal bacteria which utilise its glycans and amino acids as a nutrient source (Arike and Hansson, 2016). These bacteria, positioned near the epithelium, exert significant influence on gut barrier function and host health (Tailford et al., 2015). Reduced abundance of mucus-degrading *Akkermansia muciniphila*, for example, is associated with colitis, obesity, and Type 2 diabetes, while direct

supplementation of this strain improves gut barrier dysfunction in these diseases (Zhao et al., 2023).

In contrast, the SI mucus layer is thinner, non-adherent and more permeable, reflecting its primary role in nutrient absorption and the lower microbial density in this region (Ermund et al., 2013). Despite the increased mucus pore size, however, luminal bacteria are kept at least 50μm from the villi surface, preserving host-microbe segregation (Vaishnava et al., 2011).

The importance of the mucus layer as a foremost protective barrier is shown in *Muc2*-deficient mice, where uncontrolled contact between luminal bacteria and the epithelium results in spontaneous colitis by 5-7 weeks and subsequent colon cancer by six months (Johansson et al., 2008; Van der Sluis et al., 2006). Finally, in addition to acting as a physical "sieve", the mucus layer is enriched with host-derived antimicrobial factors that create an "anti-bacterial gradient" (Pelaseyed et al., 2014), which enhances microbial exclusion, as explored in greater detail in Section 1.2.4 below.

1.2.2 The epithelial barrier

The intestinal epithelial layer is the primary anatomical barrier preventing microbial dissemination while also facilitating host-microbiota interactions through its semi-permeability. It consists of a cell monolayer of various specialised cell types, that maintain homeostasis, conduct immunological surveillance, and mount defensive responses.

Adjacent cells are connected laterally via protein complexes, which collectively form a web-like synapse in the intercellular space (Capaldo et al., 2017). Tight junction (TJ)

complexes play a key role in regulating barrier permeability, and consist of multiple protein families, including the claudins, occludins, and zonulin proteins. Pores allow for the selective passage of solutes and ions critical to cellular homeostasis, while limiting passage of larger molecules (Raya-Sandino et al., 2023; Shen et al., 2011). TJ complexes are also highly dynamic, remodelling in response to environmental cues, including host-derived growth factors, and cytokines such as tumor necrosis factor (TNF) and interferon-γ (IFNγ) (Capaldo and Nusrat, 2015; Ulluwishewa et al., 2011). Similarly, bacterial components can directly modulate their expression, such as the outer membrane protein Amuc from *A. muciniphila* which increases TJ protein expression (Plovier et al., 2017). The dynamic turnover of TJ complexes facilitates the "paracellular leak" pathway, which permits the non-selective passage of larger macromolecules through the epithelial layer (Raya-Sandino et al., 2023).

The intestinal epithelium undergoes continuous renewal by a population of highly proliferative progenitor stem cells located at the base of crypts. These stem cells migrate upwards towards the epithelial surface, and, under the control of the Notch signalling pathway, differentiate into various secretory and non-secretory epithelial lineages, each with distinct functions, as discussed below (Umar, 2010).

1.2.2.1 Epithelial cell types

1.2.2.1.1 Intestinal epithelial cells

Intestinal epithelial cells, or enterocytes, are the predominant cell type in the epithelial layer and perform a wide range of functions. In the SI, their apical microvilli increase surface area to optimise nutrient uptake, while secretion of digestive enzymes aids

nutrient breakdown (Barker, 2014). Enterocytes also serve as first-line microbial sensors, particularly in the colon, through the expression of diverse PRRs.

The differential expression of Toll-like receptors (TLRs) on enterocytes appears to play a pivotal role in maintaining immune homeostasis. For example, apical TLR4 is hypo-responsive to LPS, preventing excessive signalling. This desensitisation is due to the continuous exposure to this MAMP in the lumen, commonly referred to as endotoxin tolerance. In contrast, basolateral expression of TLR5 enables detection of flagellin, typically derived from invasive pathogens such as *Salmonella* enterica (Abreu et al., 2005). Thus, this spatial compartmentalisation of TLRs enables the host to discriminate luminal commensals from invasive pathogens that breach the epithelial barrier.

PRR activation triggers signalling cascades, leading to the activation of transcription factors nuclear factor kappa B (NF-κB) or interferon regulatory factor 3 (IRF3), resulting in the production of various inflammatory mediators that regulate intestinal homeostasis (Price et al., 2018). Enterocytes also participate in antigen surveillance by facilitating the transcytosis of luminal antigens to antigen-presenting cells (APCs), including dendritic cells (DCs) in the underlying lamina propria for processing (Miron and Cristea, 2012). Finally, they also secrete antimicrobial peptides (AMPs), highly conserved innate effector molecules which are critical to controlling the gut microbiota, as described in Section 1.2.4 below.

1.2.2.1.2 Goblet cells

Goblet cells are essential for mucus production, secreting the protein MUC2 to form the mucus layer. MUC2 is tightly packaged and stored in secretory granules within goblet

cells that are released apically into the lumen. Although mucus is constitutively released, granule exocytosis is also regulated by various factors, including Ca^{2+} ion release, microbial SCFAs, cytokines, and activation of the NLRP6 inflammasome (Okumura and Takeda, 2017). After exocytosis into the lumen, the MUC2 protein expands over 1000-fold into a net-like structure, forming stratified sheets that make up the mucus layer (Ambort et al., 2012). Recent studies have identified distinct goblet cell sub-populations, characterised by differences in mucus secretion and expression of effector molecules such as digestive enzymes and AMPs. However the differentiation pathways and regulatory mechanisms behind these specialisations are still being uncovered (Gustafsson and Johansson, 2022). Similar to enterocytes, goblet cells have a high turnover, renewed roughly every 7 days in mice. In the colon, transmembrane mucins at the luminal surface promote tight adherence of the inner mucus layer (Birchenough et al., 2015; Sheng et al., 2013). These mucins also function as PRRs, transducing signals via NF-κB to modulate the inflammatory response and regulate TJ proteins (Segui-Perez et al., 2024; Sheng et al., 2013).

In the SI, goblet cells contribute to antigen surveillance through formation of "goblet cell associated passages", which facilitate antigen transfer to APCs in the lamina propria (McDole et al., 2012), promoting tolerance to by inducing regulatory and stimulating tolerogenic DCs and macrophages phenotypes (Gustafsson and Johansson, 2022). Conversely, "sentinel" goblet cells at the top of colonic crypts act as first-line microbial sensors detect bacteria that have penetrated the mucus barrier (Birchenough et al., 2016). These cells non-specifically sample the microbiota and TLR activation triggers mucin exocytosis from both these sentinel cells and adjacent goblet cells. This facilitates the rapid expulsion of bacteria that have infiltrated close to the crypt base, reinforcing

the spatial segregation between host and microbiota. Collectively, goblet cells play a pivotal role in maintaining mucosal homeostasis by supporting immune exclusion, tolerance and antigen surveillance (Knoop et al., 2015).

1.2.2.1.3 Other cell types

Several less abundant epithelial and lymphoid cell types also contribute to homeostasis and function of the epithelial barrier.

Paneth cells, located exclusively at the base of SI crypts, are specialised in the secretion of various AMPs, as discussed below. Microfold (M) cells are located over Peyer's patches and are highly specialised in antigen uptake and facilitate steady-state transcytosis of luminal antigens to mononuclear phagocytes in the subepithelial dome. This process is crucial for development of tolerance to commensals and dietary antigens, and the mucosal immune response to pathogens (Gullberg and Söderholm, 2006). Tuft cells are rare chemosensory cells that secrete various bioactive molecules in response to a range of extracellular signals such as succinate excreted by protists, and are critical in orchestrating intestinal type 2 immune responses to helminths (Schneider et al., 2019), while enteroendocrine cells sense nutrient and microbial stimuli to regulate digestion, peristalsis, and metabolism via the secretion of hormones including serotonin, ghrelin, and ghrelin like peptide (GLP-1) (Gribble and Reimann, 2019).

Finally, a number of lymphoid-lineage cells are interspersed within the epithelium including intraepithelial lymphocytes (IELs) and innate lymphoid cells (ILCs). IELs, comprising both conventional αβ T cells and non-classical γδ T cells, actively patrol the epithelium and respond rapidly to epithelial stress signals (McDonald et al., 2018). ILCs,

which lack canonical T cell or B cell receptors, are categorised into ILC1, ILC2 and ILC3 subtypes based on their cytokine production, which mirrors those of T helper 1 (Th1), T helper 2 (Th2), and Th17 cells, respectively. These cells contribute to antimicrobial defence and tissue repair in response to cytokine signals in the gut (Fan and Rudensky, 2016). Overall, IELs and ILCs share overlapping effector functions, and this redundancy contributes to the layered immune protection within the gut (McDonald et al., 2018). Although these cells largely exhibit similar roles, specialised roles for individual subsets may still emerge. For example, a distinct tuft cell-ILC2 circuit in response to parasitic infection was identified in 2016. Upon sensing parasitic signals such as parasite-derived succinate, tuft cells secrete IL-25 to activate ILC2s, which then release cytokines that trigger expansion of both goblet and tuft cells, creating a positive feedback mechanism that promotes parasite clearance (Schneider et al., 2019).

1.2.3 The lamina propria and gut-associated lymphoid tissue

The lamina propria underlying the epithelium comprises loose connective tissue densely populated with innate and adaptive immune cells that maintain gut homeostasis, conduct immune surveillance, and execute effector responses. The lamina propria is also highly vascularised, including both blood and lymphatic vessels, which facilitates immune cell trafficking, nutrient absorption, and transport of microbiota-derived components. This network links the intestines to gut-draining lymph nodes via lymphatics, and to the liver via the portal vein, connecting the gut to systemic circulation.

Specialised gut-associated lymphoid tissues serve as key immunological hubs, critical to the development of antigen-specific immune responses, including Peyer's patches in the SI and isolated lymphoid follicles in the colon. Within their follicular domes, APCs

carrying processed luminal antigens prime naive T and B cells, driving antigen-specific responses and enabling the host to develop immunological memory against both innocuous and harmful antigens.

The gut-draining mesenteric lymph nodes (MLNs) also coordinate adaptive immune responses by receiving antigens from the SI and colon. These may be carried directly via efferent lymphatics from the lamina propria, and or via active delivery by migratory DCs. This facilitates the initiation and coordination of antigen-specific T and B cells, which can then migrate back to the lamina propria to regulate gut homeostasis.

1.2.4 Host-secreted defences

1.2.4.1 Antimicrobial peptides

As part of an arsenal of secretory defences, Paneth cells and enterocytes produce a range of AMPs, which are secreted into the mucus layer to contribute to the "antibacterial gradient" that supports microbial exclusion at the gut interface (Meyer-Hoffert et al., 2008; Pelaseyed et al., 2014).

AMPs include α- and β-defensins, cathelicidins, C-type lectins, ribonucleases, and various other molecules, reflecting the diverse complexity of microbial threats the host must contend with (Muniz et al., 2012). AMPs predominantly target cell walls or membranes, disrupting cellular integrity. While some AMPs exhibit broad-spectrum activity, many are highly specific to particular microbes: defensins, for example, are active against bacteria, fungi, viruses, and protozoa, whereas Reg3γ (a C-type lectin) and lysozyme specifically target Gram-positive bacteria (Gallo and Hooper, 2012). Deficiencies in AMPs result in

increased microbiota translocation and susceptibility to enteric pathogens (Wilson et al., 1999). AMPs also play a homeostatic role in shaping microbiota composition, with α-defensin deficiency resulting in loss of specific taxa (Salzman et al., 2010).

1.2.4.2 Secretory IgA

Secretory immunoglobulin A (sIgA) is the most abundant immunoglobulin at mucosal surfaces, where it is crucial to intestinal homeostasis and defence (Corthésy, 2013). sIgA deficiencies correlate with impaired intestinal homeostasis, compromised gut barrier function, and increased bacterial translocation (Sait et al., 2007; Wei et al., 2011). Lamina propria plasma cells produce dimeric IgA, which is transcytosed across the epithelium into the mucus layer via the polymeric immunoglobulin receptor (pIgR). During transcytosis, a portion of the pIgR itself is incorporated into dimeric IgA, forming the secretory component that completes the final sIgA molecule (Sait et al., 2007). Production of sIgA is highly microbiota-dependent, as GF mice show underdeveloped Peyer's patches, few plasma cells, and reduced sIgA levels, all of which can be rescued with microbiota colonisation (Hapfelmeier et al., 2010).

sIgA is generated through either T cell-dependent or -independent pathways, with the latter accounting for most sIgA production. The T-independent pathway is primarily triggered by commensal microbiota and generates low-affinity, polyreactive sIgA that binds to conserved bacterial MAMPs such as LPS, flagellin, and peptidoglycan (Bunker et al., 2015). Microbial TLR signalling triggers epithelial cells to secrete cytokines, including B cell activating factor (BAFF) and a proliferation-inducing ligand (APRIL), which promote B cell class-switching and differentiation to facilitate differentiation of IgA^+ plasma cells (Castigli et al., 2004; He et al., 2007). While this predominantly occurs in the

lamina propria, it can also take place in Peyer's patches and MLNs (Pabst, 2012). In contrast, the T cell-dependent pathway occurs only in lymphoid follicle germinal centres and is typically induced by pathogenic bacteria, where antigen-presenting DCs prime naïve T follicular helper cells, triggering B cell activation, class-switching and somatic hypermutation, resulting in high-affinity and antigen-specific IgA.

sIgA performs numerous functions, but primarily enhances intestinal barrier function by binding to bacteria, antigens, and toxins, neutralising their activity and trapping them within the mucus layer (Boullier et al., 2009; Mantis et al., 2006). These complexes may then be expelled via peristalsis, maintaining microbiota compartmentalisation. Beyond neutralisation, sIgA also facilitates luminal antigen sampling, through retro-transcytosis of antigen-bound sIgA complexes into M cells, delivering antigen to DCs in Peyer's patches (Baumann et al., 2010; Rochereau et al., 2013). This process promotes tolerance to commensals while enabling effective adaptive responses to bacterial and viral pathogens (Fransen et al., 2015; Mathias et al., 2014; Mikulic et al., 2017; Rey et al., 2004; Weltzin et al., 1989). Interestingly, DCs show enhanced tolerogenic and anti-inflammatory phenotypes when recognising IgA-antigen complexes compared to whole bacterial cells, suggesting this mechanism of antigen-sampling fine-tunes tolerogenic responses (Boullier et al., 2009; Mikulic et al., 2017).

A subset of gut bacteria is also constitutively coated with sIgA, and while the repertoire of coated bacteria varies among individuals, it appears to preferentially include taxa that colonise near the epithelium (Pabst et al., 2016). For commensals, this low-affinity IgA coating may be a mechanism to restrict further translocation, limiting their pro-inflammatory potential and preserving homeostasis (Macpherson et al., 2015). sIgA

coating has also been identified as a marker for distinguishing colitogenic commensals, such as *Provetellaceae*, which can drive inflammation during IBD (Palm et al., 2014).

Both T cell-independent and T cell-dependent pathways contribute to the regulation of microbiota composition by sIgA (Fagarasan et al., 2002; Wei et al., 2011). sIgA binding also modulates bacterial gene expression to promote mutualism: in commensal *Bacteroides thetaiotaomicron,* sIgA binding downregulates cognate epitope expression, driving the bacteria's epitope diversification to promote a non-inflammatory interaction with the host (Peterson et al., 2007). Similarly, sIgA binding to proteins of this bacteria's fructan-utilising locus limits its nutrient degradation, controlling for commensal overgrowth (Joglekar et al., 2019).

Altogether, these diverse functions highlight the central role of sIgA in intestinal immunity, by simultaneously regulating homeostasis and composition, preventing pathogenic invasion and commensal outgrowth, and coordinating adaptive responses to both. Chapter 3 of this thesis investigates how diet induces changes in microbiota composition and function to influence the generation of T-cell independent sIgA, with implications for overall host-microbiota communication and homeostasis.

1.3 Gut microbiota methods of communication

The gut microbiota influences host physiology predominantly through two major pathways: (1) metabolite-mediated signalling and (2) MAMP-based signalling.

1.3.1 Metabolites

Bacteria produce diverse metabolites that diffuse across the intestinal barrier to influence host cells both locally and systemically. These molecules, which include SCFAs, amino acid derivatives such as indoles, secondary bile acids, as well as micronutrients like folate and vitamins B and K, profoundly influence host physiology and demonstrate the depth of host-microbe mutualism (Levy et al., 2016). Deficiency of microbial-derived metabolites has been associated with a myriad of inflammatory disorders. They impact host biology through three key mechanisms: direct metabolic effects, receptor-mediated signalling, and epigenetic regulation of host genes.

1.3.1.1 Integration into host metabolism

At the most fundamental level, microbiota-derived metabolites can be utilised as direct substrates in host biosynthetic pathways, reflecting a conserved metabolic interdependence between gut bacteria and host cells. This is exemplified by the SCFA butyrate, which serves as the primary energy source for colonocytes (providing over 60% of energy requirements) (Tan et al., 2014). The preferential metabolism for butyrate by colonocytes also has a secondary effect of deoxygenating the epithelial interface, maintaining anaerobic conditions that support beneficial commensals and inhibit pathogens, reinforcing host-microbiota mutualism (Byndloss et al., 2017). Similarly, vitamins synthesised by gut bacteria, such as vitamin K, B12 and folate can also function as essential substrates or cofactors in many host biosynthetic pathways, highlighting this metabolic dependence (Levy et al., 2016).

While many metabolites can integrate into host metabolism to support homeostasis, in a state of microbiota dysbiosis, the absence or elevation of certain metabolites can disrupt this cooperation and may drive disease pathogenesis, through mechanisms that are still being elucidated (Tan et al., 2023). For example, it was recently identified that pro-inflammatory macrophages increase their uptake of succinate (a metabolite associated with intestinal inflammation) to enhance nitric oxide production, which potentially exacerbates inflammation during IBD (Fremder et al., 2021; Pinget et al., 2022). Thus, these findings highlight that although microbial metabolites have co-evolved to support host homeostasis, their direct utilisation may also trigger inflammatory responses and pathogenesis when microbial homeostasis is disturbed.

1.3.1.2 Receptor-mediated signalling

Metabolites may also bind to specific host receptors to elicit their effects, particularly G-protein coupled receptors (GPCRs) and nuclear receptors. For example, SCFAs bind to GPCRs, such as GPR41, GPR43, and GPR109a with varying affinities which influences their biological effects. Overall, SCFA-GPCR signalling typically promotes anti-inflammatory responses (Tedelind et al., 2007) as demonstrated in models of colitis, arthritis, asthma and infection where GPCR deficiency exacerbates inflammation (Kim et al., 2013; Macia et al., 2015; Maslowski et al., 2009). In addition to their immunomodulatory role, SCFA-GPCR signalling also regulates host energy metabolism (Tan et al., 2014). For example, SCFA-mediated activation of GPR41 and 43 stimulates secretion of PYY, GLP-1 and leptin, hormones that regulate host appetite, insulin sensitivity and glucose homeostasis (Psichas et al., 2015).

The effects of metabolite-receptor interactions may be highly cell- and context specific. For example, succinate binding to GPR91 promotes either pro- or anti-inflammatory signalling in macrophages depending on context. Extracellular succinate acts as a metabolic cue via GPR91, reinforcing a pro-inflammatory feedback loop that promotes cytokine production in arthritis or colitis (Littlewood-Evans et al., 2016; Macias-Ceja et al., 2019). Conversely, basal GPR91-succinate signalling supports anti-inflammatory macrophage polarisation and thus metabolic homeostasis in adipose tissue (Keiran et al., 2019), with dysregulation of this signalling contributing to obesity pathogenesis.

Nuclear receptors and transcription factors, such as the aryl hydrocarbon receptor (AHR) or farnesoid X receptor, can be activated by microbial metabolites, triggering their translocation to the nucleus where they bind to receptor-responsive DNA elements to regulate specific gene programs. The AHR receptor is activated by tryptophan-derived metabolites, such as indoles, and plays an essential role in intestinal homeostasis by modulating TJ expression, goblet cell function, stem cell turnover, and the production of IL-22, a key cytokine for epithelial integrity (Kou and Dai, 2021; Postal et al., 2020). AHR deficiency compromises intestinal immunity by reducing numbers and functionality of IELs and ILCs, impairing control of the microbiota and increasing susceptibility to infection (Li et al., 2011; Qiu et al., 2012). Deficiencies in AHR signalling are linked to IBD and obesity (Monteleone et al., 2011), while indole supplementation improves barrier dysfunction, reducing microbial translocation to alleviate metabolic syndrome in mice (Natividad et al., 2018). AHR signalling also regulates host energy metabolism through modulating GLP-1 production (Natividad et al., 2018).

1.3.1.3 Epigenetic regulation of host genes

Finally, metabolites influence host physiology within in the gut, as well as systemically, through modification of the epigenetic landscape, by altering chromatin accessibility and DNA methylation (Krautkramer et al., 2016). SCFAs are well-characterised histone deacetylase (HDAC) inhibitors, promoting increased chromatin accessibility to enhance gene expression, typically also with anti-inflammatory effects (Tan et al., 2014). For example, butyrate promotes regulatory T cell (Treg) differentiation by enhancing accessibility of the *Foxp3* locus, the master transcriptional regulator for Tregs (Furusawa et al., 2013). In intestinal macrophages, butyrate-mediated HDAC inhibition dampens their pro-inflammatory response to LPS, facilitating tolerance to commensals (Chang et al., 2014). While its tolerogenic effects are the most well-characterised, butyrate also appears to have varied effects on immune cell function. For example, butyrate stimulates an antimicrobial transcriptional program in macrophages via HDAC3 inhibition, enhancing the clearance of intracellular bacteria and limiting pathogen dissemination during infection (Schulthess et al., 2019). Conversely, butyrate-mediated HDAC inhibition dampens neutrophil migration and release of pro-inflammatory mediators, which may be detrimental to the host during acute inflammation but be protective in chronic inflammatory conditions such as IBD (Li et al., 2021).

The microbiota also influences DNA methylation patterns, likely through regulating enzymes such as TET3, as GF mice demonstrate hypermethylation across intestinal epithelial transcriptomes (Ansari et al., 2020). Host DNA methylation enzymes also rely on co-factors such as the methyl donor S-adenosylmethionine, which is generated during microbial folate metabolism, further illustrating the integration of microbial and host signalling pathways (Woo and Alenghat, 2022).

Microbiota-derived metabolites do not act in isolation but function within complex networks of synergistic and antagonistic effects. For example, while SCFAs act as HDAC inhibitors, microbially-produced inositol phosphate promotes HDAC activity (Wu et al., 2020). These interactions highlight the challenges of delineating the specific effects of individual metabolites. Instead, the collective gut metabolite milieu likely integrates signals across multiple pathways to regulate host physiology. The resulting outcomes are highly diverse and context-dependent, shaped by the balance and interplay of these molecules.

1.3.2 MAMPs

Host cells express PRRs that detect conserved MAMPs which include bacterial wall components (LPS, lipoteichoic acid, and peptidoglycan), bacterial proteins (such as flagellin), and nucleic acids. While the intestinal barrier primarily segregates microbiota from host tissues to prevent excessive PRR activation, exposure to gut MAMPs is essential for proper immune development and function (Rakoff-Nahoum et al., 2004).

The fundamental importance of MAMP-PRR signalling to host physiology is demonstrated in GF mice, where treatment with isolated MAMPs such as LPS significantly reduces their infection susceptibility (Beaman et al., 1980; Fagundes et al., 2012) and normalises some physiological aberrations. For example, transferring heat-treated serum from conventional specific-pathogen free (SPF) mice rescues impaired GF myelopoiesis (Balmer et al., 2014). This restoration fails in MyD88-deficient GF mice, revealing that basally circulating gut-derived MAMPs are essential for systemic immune development.

Specific MAMP-PRR interactions can drive highly distinct immunological outcomes. For example, polysaccharide A, from commensal *Bacteroides fragilis* binds to TLR2 on DCs, triggering a tolerogenic phenotype that promotes Treg differentiation via IL-10 (Mazmanian et al., 2005; Shen et al., 2012). This is sufficient to restore intestinal tolerance in GF mice but also reduces inflammation in experimental colitis by promoting Tregs (Mazmanian et al., 2008). Similarly, segmented filamentous bacteria specifically induce intestinal Th17 cells (Ivanov et al., 2009). This taxon colonises in close proximity to epithelial cells, triggering their production of the protein serum amyloid A, which directs Th17 differentiation (Sano et al., 2015).

Overall, MAMP signalling has a crucial role in shaping host health. At homeostasis, basal MAMP signalling supports systemic immune development and enables targeted responses to various microbes. However, during barrier dysfunction associated with NCDs, increased MAMP translocation drives systemic inflammation.

1.4 Bacterial extracellular vesicles

Recently, BEVs have emerged as key mediators of microbe-host communication, capable of signalling via both metabolite- and MAMP-based pathways. Extracellular vesicles (EVs) are universally conserved mechanisms of intercellular communication, produced by eukaryotes, archaea, fungi, and prokaryotes (Schwechheimer and Kuehn, 2015; Yáñez-Mó et al., 2015). BEVs, specifically, are lipid bilayer-enclosed structures, typically ranging 20-400 nm in size, released by both Gram-negative and Gram-positive bacteria (Toyofuku et al., 2019). While the mechanisms of BEV biogenesis differs between bacterial classes,

BEVs generally reflect the molecular composition of their parental cell (Toyofuku et al., 2023), Their lipid bilayer shields internal cargo from degradation, enabling BEVs to deliver bacterial signals to distant targets.

BEVs mediate various biological processes crucial for the survival and competitiveness of the parental cell. They act as "decoys" against environmental threats and mediate self-defence by delivering lysis factors to competitor species (Caruana and Walper, 2020). BEVs also facilitate nutrient acquisition, horizontal gene transfer, cellular waste removal, and the formation of biofilms (Díaz-Garrido et al., 2021; Macia et al., 2019; Toyofuku et al., 2023).

While BEVs are essential for bacteria-bacteria interactions, they also play a significant role in interactions with eukaryotic cells. Enriched with MAMPs, BEVs can engage PRRs, triggering diverse immune signalling cascades. In pathogens, BEVs are well-characterised mediators of virulence, delivering toxins and other effector molecules to host cells while also acting as decoys to evade immune responses (McMillan and Kuehn, 2021).

More recently, BEVs from non-pathogenic or commensal bacteria have been recognised as important mediators of gut-host mutualism, with potent immunomodulatory effects. In the gut, BEVs facilitate bacterial communication and promote survival. For example, *B. fragilis* BEVs deliver AMPs to inhibit competing *Bacteroidales* species (Chatzidaki-Livanis et al., 2014). Additionally, BEVs from a number of *Bacteroides* species have been found to carry various enzymes and metabolites involved in both bacterial as well as host metabolic and biosynthetic pathways (Elhenawy et al., 2014; Rakoff-Nahoum et al., 2014; Stentz et al., 2022; Zakharzhevskaya et al., 2017). Gut BEVs can also mediate antibiotic

resistance by carrying antibiotic-inactivating enzymes such as β-lactamase on their surface, or by transferring antibiotic resistance genes through plasmids (Stentz et al., 2015; Zhao et al., 2024).

1.4.1 BEV composition

The composition of BEVs reflects their origin and is influenced by structural differences between Gram-negative and Gram-positive bacteria. Gram-positive BEVs typically consist of cytosolic components encapsulated by the cytoplasmic membrane and peptidoglycan layer. In contrast, Gram-negative BEVs may contain elements from the inner membrane, outer membrane, periplasm, and cytosol, or a combination of these components (Toyofuku et al., 2019). This results in significant diversity and heterogeneity in the composition and thus functional properties of BEVs within the gut microbiota (Figure 1.2).

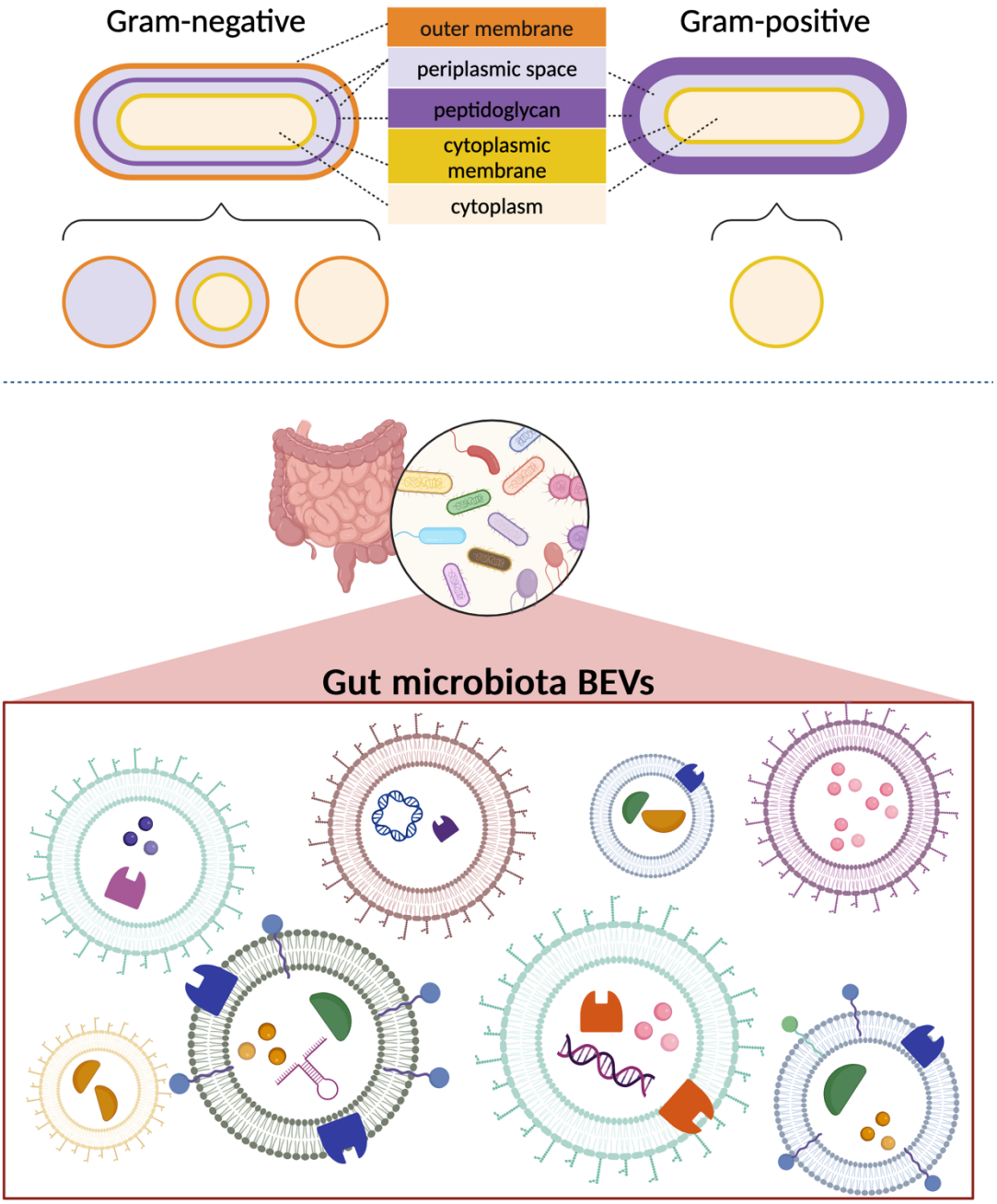

Figure 1.2: Gram-negative and Gram-positive bacteria of the gut microbiota produce BEVs that differ in composition

Gram negative BEVs may incorporate outer membrane, periplasmic, or cytoplasmic contents, while Gram-positive BEVs generally derive from the cytoplasmic membrane and contain cytoplasmic contents. Gut BEVs show significant heterogeneity in size and composition and may be enriched with a range of bioactive cargo including proteins (enzymes, periplasmic/cytoplasmic proteins, outer membrane lipoproteins), DNA, RNA, plasmids, and metabolites. Gram-negative BEVs may also carry LPS on their outer membrane while Gram-positive BEVs may carry lipoteichoic acid. These diverse molecular profiles contribute to the broad functional capacity of BEVs to modulate the gut-host axis, the extent of which is only starting to be uncovered. Figure created in BioRender.com

In addition to being enriched with surface MAMPs, BEVs can carry a diverse cargo of bioactive molecules which can include proteins, lipids, nucleic acids, and metabolites (Díaz-Garrido et al., 2021; Macia et al., 2019). Interestingly, BEVs may elicit broader immune responses than exposure to their parental bacteria, due to their enriched MAMP content (Gilmore et al., 2022). Thus, by integrating both metabolite- and MAMP-based signalling pathways, BEVs function as complex molecular packages that mediate host-gut microbiota communication to influence host physiology.

1.4.2 BEV biogenesis

While BEV production is constitutive, it is significantly influenced by environmental stressors, such as temperature, pH, nutrient availability, antibiotics, and altered oxygen levels (Klimentová and Stulík, 2015; McMillan and Kuehn, 2021). Vesiculation generally increases under stress conditions and appears to be a conserved response across bacterial species (Toyofuku et al., 2023). Environmental stressors not only affect the quantity of BEVs produced but also their molecular composition. For example, iron-limiting conditions promote production of BEVs enriched with iron-binding proteins and siderophores, enhancing bacterial iron-acquisition and survival (Prados-Rosales et al., 2014). Genetic factors also appear to regulate vesiculation, with mutations in membrane-associated genes leading to hyper- or hypo-vesiculating strains (Avila-Calderón et al., 2021).

The selective enrichment of specific cargo in BEVs relative to the parental cell suggests the presence of active sorting or enrichment mechanisms. However, further studies are needed to determine the specific molecular mechanisms involved, which also likely vary across different species (Briaud and Carroll, 2020). This stands in contrast to eukaryotic

EVs, whose biogenesis pathways have been extensively described (Yáñez-Mó et al., 2015). Eukaryotic EV formation is regulated by well-characterised universal molecular mechanisms, such as the ESCRT pathway, tetraspanin enriched microdomains, or lipid raft domains (Catalano and O'Driscoll, 2020; Dixson et al., 2023; Fang et al., 2022). In the gut, BEV production is likely regulated by various factors, but particularly nutrient availability and bacterial stress signals. Consequently, BEVs likely serve as important molecular markers of how gut bacteria may respond and adapt to various environmental challenges. Although this thesis focuses on gut microbiota BEVs, other bacterial communities in the body, including the skin and lung, have also been shown to produce EVs which may similarly reflect microbial activity and serve as markers of microbiota-status (Kim et al., 2017; Zhou et al., 2025). However, as the gut microbiota is significantly more diverse and abundant than the microbiota at these sites, the majority of current literature has focused on gut-derived BEVs, particularly in relation to their pathogenic, therapeutic and diagnostic potential, as explored further below and throughout this thesis.

1.4.3 Gut BEVs cross the intestinal barrier

Despite the host's efforts to compartmentalise the gut microbiota, due to their nanoscale size BEVs can cross the intestinal barrier and interact directly with host cells via multiple pathways (O'Donoghue and Krachler, 2016). At the epithelial surface, BEVs can engage PRRs to trigger signalling pathways and or/direct internalisation. Enterocytes take up BEVs through all known endocytic pathways, processing them intracellularly or transcyotosing them to the basolateral side (Jones et al., 2020; Rubio et al., 2020). Although not demonstrated experimentally, M cells may also contribute to BEV

transcytosis (Stentz et al., 2018). BEVs also traverse the epithelium paracellularly through the TJ paracellular leak pathway (Jones et al., 2020)

Notably, BEVs themselves can alter intestinal barrier permeability to modulate their transit. For example, colitogenic *B. thetaiotaomicron* BEVs carry mucin-degrading enzymes to facilitate epithelial access (Hickey et al., 2015). Conversely, BEVs from probiotic strains, such as *A. muciniphila* and *Escherichia coli* Nissle 1917, enhance barrier function via upregulation of TJ proteins (Alvarez et al., 2016; Chelakkot et al., 2018).

Once in the lamina propria BEVs may interact with resident immune cells, particularly phagocytes such as DCs (Shen et al., 2012). BEVs can also access lymphatics and blood circulation, allowing them to influence distal organs. BEVs from pathogenic bacteria can directly fuse with host membranes, mediating delivery of their cargo, although this has not yet been demonstrated for commensals (Gan et al., 2023).

1.4.4 Gut BEVs in health and disease

Under homeostatic conditions, BEVs routinely cross the intestinal barrier to systemic circulation and are detectable in the blood of healthy individuals (Tulkens et al., 2020). This transit has been proposed as an explanation for the phenomenon of the "blood microbiota", where bacterial DNA signatures have been frequently detected in serum and brain samples (Gosiewski et al., 2017; Santacroce et al., 2024; Stentz et al., 2018). BEV transit, however, increases significantly in conditions associated with compromised barrier function, with elevated levels first detected in plasma of patients with IBD, HIV and cancer-associated mucositis (Tulkens et al., 2020). Interestingly, BEVs may also display tissue tropism in their biodistribution: for example *Pseudomonas panacis*-derived

BEVs distribute to insulin-sensitive tissues, while *A. muciniphila* BEVs remain in the GI tract (Chelakkot et al., 2018; Choi et al., 2015).

The detection of BEVS in various bodily fluids has generated growing interest in their potential as diagnostic and prognostic biomarkers. Studies have examined microbial BEV profiles in a wide range of conditions, including metabolic disorders, inflammatory diseases, and cancer. As summarised in Table 1.1, many disease states show alterations in BEV diversity and composition, compared to healthy controls. However, understanding whether these changes are causative or consequential in disease requires further investigation.

Table 1.1: Summary of studies examining microbial BEV profiles across diseases and biofluids

Biofluid	Disease focus	Key finding	Reference
Serum	Gestational diabetes mellitus vs HC pregnancy	↑ Diversity, richness ↑ *Actinobacteria, Firmicutes* ↓ *Bacteroidetes, Proteobacteria*	(Chang et al., 2024)
	Acute vs chronic cholecystitis	↓ Diversity, richness in acute ↑ *Proteobacteria* in acute ↑*Actinobacteria, Firmicutes*, *Bacteroides* in chronic	(Zhu et al., 2024)
	Atopic dermatitis vs HC	No change in richness, diversity but distinct clustering Various changes in composition for disease sample vs HC	(Yang et al., 2020)
	Breast cancer vs HC	↓ Diversity, richness ↑ *Bacteroidetes* ↓ *Actinobacteria, Cyanobacteria* Used to develop diagnostic model	(An et al., 2023)
	Ovarian cancer vs benign ovarian tumours	No differences in diversity or clustering Identified genus-level biomarkers, used to develop diagnostic model	(Kim et al., 2020)
	Renal cell carcinoma vs HC	No changes in diversity, richness ↑ *BacteroidiaTM7-1, Sphingomonadales* High sensitivity diagnostic model constructed, correlated with disease progression	(Uemura et al., 2023)
	Bipolar disorder, major depressive disorder vs HC	No differences in diversity, richness ↑ *Firmicutes*, *Bacteroidetes* in bipolar and major depressive disorder ↑ *Prevotella* and *Rumonococcaceae* in major depressive disorder Differences in microbial functional prediction analysis	(Rhee et al., 2020)
	Obsessive compulsive disorder vs HC	↓ Diversity, richness Relative differences in genus composition Compositional differences in early onset vs late onset subtypes	(Kang et al., 2023)
Plasma	Mechanically ventilated patients with and without pneumonia	No change in diversity or richness, but distinct clustering Differences in functional profiling of pneumonia vs non pneumonia patients Longitudinal BEV composition changes correlate with survival	(Park et al., 2022)
	Colitis vs HC	No differences in diversity, richness or composition	(Jones et al., 2021)
	Polycystic ovary syndrome and insulin resistance before/after metformin treatment	↑ Diversity, richness after metformin Significant compositional differences from treatment, particularly ↑*Streptococcus salivarius*	(Hu et al., 2024)
	Psoriasis vs HC	↓ Diversity, richness ↓ *Firmicutes, Fusobacteria* Predicted microbial metabolism pathways altered in psoriasis	(Chang et al., 2021)

Urine	Children with allergic airway and atopy vs HC	↑ Phylogenetic diversity ↓ functional diversity Compositional and metabolic pathway changes correlate with IgE, eosinophils	(Samra et al., 2019)
	Colorectal cancer vs HC	↓ Diversity, richness ↑ *Firmicutes, Actinobacteria, Proteobacteria* ↓ *Bacteroidetes, Verrucomicrobia*	(Yoon et al., 2023)
	Prospective study of 10-year obesity risk	No association for risk of obesity Risk of abdominal obesity associated with ↑ *Firmicutes* ↓ *Proteobacteria*	(Shin and Baik, 2023)
	Children with asthma vs HC	↓ Richness ↑ *Cyanobacteria* ↓ *Verrucomicrobia* Differences in functional profiling	(Lee et al., 2020)
	Autism spectrum disorder vs HC	No changes in diversity ↑ *Verrucomicrobia*, *Firmicutes* ↓ *Cyanobacteria*, *Proteobacteria*	(Lee et al., 2017)
Stool	Colorectal cancer vs HC	↓ Diversity, richness ↑ *Firmicutes* ↓ *Verrucomicrobia* Compositional differences between early vs late and distal vs proximal cancers	(J. Park et al., 2021)
	Intestinal pathologies/diseases (obesity, diarrhea, Crohn's disease) vs HC	No differences in diversity, richness Various compositional differences identified between HC and disease groups, and between disease groups	(Rodríguez-Díaz et al., 2023)
	Crohn's Disease vs HC	↓ Richness ↓ *Bifidobacteriaceae, Lactobacillaceae*	(Kameli et al., 2021) k
	IBD vs HC	↓ Diversity, richness ↑ *Firmicutes* ↓ *Verrucomicrobia, Proteobacteria* Differences in composition more prominent in BEVs than stool microbiota	(Heo et al., 2023)
	Type 2 diabetes vs HC	↑ *Proteobacteria*, particularly *Akkermansia muciniphila*	(Chelakkot et al., 2018)
Urine, serum	Atopic dermatitis vs HC	↓ Diversity ↑ *Proteobacteria* ↓ *Firmicutes*. Lactic acid bacteria particularly decreased in disease	(Kim et al., 2018)
Stool, serum, urine	Gastric cancer vs HC	↓ Diversity, richness for urine and serum in cancer group Various compositional differences across stool, serum and urine BEV profiles between cancer and HC Urine-based biomarker model was best for diagnostic prediction model	(J.-Y. Park et al., 2021)

HC: Healthy control

1.4.5 Current understandings of gut BEV-host interactions

Research on BEVs from gut bacterial species has largely focused on examining immunomodulatory effects of single bacterial strains (either pathogenic or probiotic) or utilising total gut microbiota-derived BEVs as biomarkers, as discussed above. The effects of BEVs on host physiology are complex and context-dependent, and vary with bacterial origin, cargo, route of cellular uptake, target cell type, and broader disease context.

The diverse roles of gut BEVs have been reviewed extensively across different contexts. Several reviews have examined their fundamental contribution to intestinal homeostasis (Díaz-Garrido et al., 2021; Melo-Marques et al., 2024; Zeng et al., 2024), while others have focused on the therapeutic potential of probiotic-derived BEVs (Chen et al., 2024; Domínguez Rubio et al., 2022; Molina-Tijeras et al., 2019). The dual pathogenic and probiotic roles of BEVs have been explored in specific conditions including metabolic disorders (Verbunt et al., 2024), colorectal cancer (Meng et al., 2023; Song et al., 2024), IBD (Kim et al., 2024; Olovo et al., 2024; Shen et al., 2021; Zubair et al., 2024), reproductive disorders (Wagner et al., 2024; Yang et al., 2024), atherosclerosis (Lin et al., 2025), and neurological and psychiatric conditions (Guo et al., 2024; Sun et al., 2023).

Most mechanistic studies have investigated single-strain BEV interactions with intestinal epithelial cells or immune cells, focusing on their influence on intestinal barrier integrity or immune regulation. Overall, commensal and probiotic-derived BEVs typically promote homeostasis and exert anti-inflammatory effects. *In vivo*, probiotic BEVs are often as effective as their parental strains in ameliorating inflammation in models of colitis and obesity (Chelakkot et al., 2018; Chu et al., 2016; Fábrega et al., 2017; Seo et al., 2018).

These therapeutic effects may occur through multiple mechanisms, but particularly through enhancement of the intestinal barrier, promoting homeostatic pathways such as sIgA production, and the induction of tolerogenic DCs and Treg differentiation (Chelakkot et al., 2018; Fábrega et al., 2017; López et al., 2012; Shen et al., 2012; Yamasaki-Yashiki et al., 2019).

Studies examining total fecal BEVs reveal that the vesicle secretome can be significantly altered in disease conditions, with specific bacterial populations showing differential enrichment within the BEV profile across various disease states (Chelakkot et al., 2018; Choi et al., 2015).

These findings implicate BEV composition plays a role in disease pathogenesis, while also highlighting the potential therapeutic applications of strain-specific BEVs.

1.4.6 Gaps in current knowledge

It has become increasingly clear that BEVs are not minor bacterial by-products, but are a significant component of the bacterial secretome, alongside metabolites and MAMPs, that can regulate host processes. While BEV production in the gut likely fluctuates significantly (as explored in Chapters 3 and 4 of this thesis), it is reasonable to assume their numbers surpass those of bacterial cells at any given time, indicating a substantial presence in the gut environment. For example, if each bacterial cell in the gut were to produce a single vesicle, this would result in an equal vesicle-to-cell ratio. However, this ratio is likely much higher: a study of marine bacteria found that among various strains, a single cell can release between 4 and 58 vesicles per cell division cycle under optimal culturing conditions (Biller et al., 2023). One estimate suggests BEVs outnumber bacterial

cells by a factor of 10, reaching approximately 4 x 10^{14} BEVs in the human gut microbiota (Schaack et al., 2022).

Precise gut BEV-to-bacteria ratios have not been well-characterised, which is likely due to the dynamic nature of BEV production. As discussed below and explored in Chapters 3 and 4 of thesis, BEV production in the gut is influenced by environmental factors that affect bacterial stress responses and membrane integrity, such as antibiotic exposure, nutrient composition, and nutrient availability. Given this, we hypothesise that under certain conditions, BEVs outnumber bacterial cells by *more* than 10-fold. Due to their capacity to be enriched with bioactive molecules, including metabolites and MAMPs, BEVs likely serve as particularly potent mediators of host-gut communication. Despite substantial advancements in gut BEV research in the last decade, major gaps remain in our understanding of gut BEV-host interactions. While studies focusing on single bacterial strains provide mechanistic insights, they do not capture the complexity and heterogeneity of the total BEV population to which the host is exposed. As a result, these studies do not fully represent the physiological interactions between the host and BEVs within the gut.

Similarly, although the past five years have seen a rise in investigations into total gut microbiota BEV profiles, research has primarily focused on their role in pathological conditions, such as diabetes and obesity. Thus, the broader, homeostatic role of gut BEVs remains largely unexplored. There is also limited understanding of how environmental factors such as diet, which strongly influences gut microbiota composition, affect BEV production, composition, and function.

Greater understanding of how the total microbiota BEV population influences host physiology through their diverse signalling pathways will provide greater insights into the fundamental nature of the gut-host relationship and advance our understanding of how gut bacteria drive health and disease.

1.5 Establishment of the gut microbiota

1.5.1 Is there a microbiota *in utero?*

The gut microbiota has traditionally thought to be established at birth when newborns encounter maternal microbes at delivery. However, the possibility of this initial colonisation beginning *in utero* has been the subject of ongoing scientific debate (Banchi et al., 2024; Perez-Muñoz et al., 2017). While some studies suggest the existence of a low-biomass *in utero* microbiota in mammals (Aagaard et al., 2014; Dera et al., 2024; Jiménez et al., 2005; Moore et al., 2017), numerous studies report these positive results reflect contamination during sample collection or processing rather than a viable, colonising microbiota (Banchi et al., 2023; Malmuthuge and Griebel, 2018; Panzer et al., 2023; Sterpu et al., 2021; Theis et al., 2020, 2019; Winters et al., 2022).

While there is currently no consensus on the existence of bonafide microbiota *in utero*, it is widely accepted that the fetus encounters gut microbial components via maternal circulation (Li et al., 2020). Metabolites such as SCFAs, as well as antigenic components, can directly cross the placenta to influence fetal development (Gomez de Agüero et al., 2016; Husso et al., 2023; Kimura et al., 2020; Pessa-Morikawa et al., 2022; Thorburn et al., 2015). Moreover, evidence suggests that maternal serum components such as

immunoglobulin G (IgG) may actively facilitate the transfer of antigens across the placental barrier (Gomez de Agüero et al., 2016).

1.5.2 The significance of the early-life period

Early life, particularly gestation, represents a critical period for immune system development and physiological programming. During this time, microbial-derived signals play an essential role in optimal development, with exposure to gut microbiota components being key for tissue maturation and establishing immunological tolerance. Mucosal organs such as the lungs, GI tract, and skin commence development and are seeded with self-renewing cell populations *in utero*, and evidence suggests these organs are especially sensitive to microbial-derived signalling *in utero* (Ignacio et al., 2024; Jain, 2020).

The hygiene hypothesis proposes that modern lifestyles and hygienic practices have reduced microbial exposures, leading to immune dysregulation and contributing to increasing rates of NCDs (Okada et al., 2010). In support of this, maternal exposure to farm living and unpasteurised milk during pregnancy correlates with decreased offspring allergy incidence (Schaub et al., 2009; von Mutius, 2012). Various factors affecting the maternal gut microbiota during pregnancy, including environment, diet, and antibiotic use, may therefore impact fetal physiology by modulating the exposure to microbial components and metabolites (Gao et al., 2021). For instance, maternal consumption of a high-fibre diet, or the presence of specific species, such as *Prevotella copri*, is associated with offspring protection from allergic disease (Thorburn et al., 2015; Vuillermin et al., 2020). Protection is mediated through multiple mechanisms, including maternally-

derived SCFAs promoting Treg induction, as well as the early provision of antigenic stimuli that educate the fetal immune system via TLR-signalling.

Conversely, maternal diets high in fat or representative of the Western diet are associated with offspring metabolic impairments and increased disease susceptibility (Myles et al., 2013; Seet et al., 2015; Xie et al., 2018). These findings highlight gestation as a key developmental and programming window, where the maternal gut microbiota can have life-long consequences on offspring health.

Chapter 5 of this thesis examines how gestational exposure to BEVs derived from maternal gut microbiota influences offspring physiology, including the gut barrier and systemic immune development, and potential susceptibility to disease in adulthood.

1.6 Regulation of gut microbiota composition and gut BEVs

Gut microbiota composition is shaped by numerous environmental factors, with diet and antibiotics being major modulators. While these factors directly influence the abundance of microbial communities, emerging evidence suggests they also significantly impact BEV production and composition. Moreover, BEVs themselves, as mediators of bacterial communication, may actively regulate composition, adding an additional layer of complexity.

1.6.1 The impact of antibiotics on gut microbiota composition

Antimicrobial agents represent a significant modulator of gut microbiota composition. Global antibiotic consumption has increased dramatically in recent decades, contributing to declining infection rates in Western countries alongside improved hygiene practices. However, this has coincided with rising incidence of NCDs (Donald and Finlay, 2024; Guarner et al., 2024). Given dysbiosis and gut pathologies often accompany NCDs, mounting evidence implicates antibiotic exposure in disease development via detrimental impacts on gut microbiota (Donald and Finlay, 2024; Guarner et al., 2024). While the mechanistic links are still being uncovered, antibiotics can be major disruptors of commensal flora, eliminating beneficial taxa and facilitating conditions that favour opportunistic pathogens such as *Clostridium difficile* (Ramirez et al., 2020).

The effects of antibiotics on microbiota composition vary considerably among individuals, influenced by factors such as antibiotic class, course length, pre-existing microbiota composition, and timing of exposure (e.g. adulthood vs childhood). While the microbiota shows some resilience, evidence suggests the adult microbiota never fully recovers to its initial state, retaining a "scarred" composition with marked loss of diversity and increased presence of antibiotic resistance genes (Anthony et al., 2022; Dethlefsen and Relman, 2011). Indeed, compositional fluctuations can stabilise 8-31 months post-exposure, however, long-term alterations in function can persist, such as reduced capacity to generate butyrate (Haak et al., 2019). Some beneficial taxa such as *Bacteroides* may never recover, even two years post-exposure (Jernberg et al., 2007), and compositional changes have been observed up to four years after antibiotic treatment (Jakobsson et al., 2010). Each antibiotic exposure may represent “another roll of the dice” (Dethlefsen and Relman, 2011), potentially displacing beneficial strains with

opportunistic members of the microbiota, with significant ramifications on host health that are still being uncovered.

Another critical consideration in increasing antibiotic exposure is the acquisition and spread of antibiotic resistance genes. Interestingly, the resilience of the microbiota to antibiotics is in part dependent on pre-existing antibiotic resistance genes that "deactivate" antibiotics, suggesting spread of antibiotic resistance may paradoxically be advantageous for retaining beneficial commensals (Bhattarai et al., 2024; d'Humières et al., 2024). However, antibiotics-induced expansion of resistance genes can persist at high levels years after exposure, raising concerns about long-term implications for individual and public health (Jakobsson et al., 2010),

Thus, the long-term consequences of antibiotics exposure in adults remain complex and are still being elucidated. Chapter 2 of this thesis explores how antibiotics differentially targeting Gram-negative and Gram-positive species impacts mouse gut microbiota composition, and the accompanying downstream effects on local and systemic immunity, providing insight into potential mechanisms linking antibiotic exposure and NCDs.

1.6.2 The impact of diet on microbiota composition and BEVs

Diet is a major regulator of gut microbiota composition, with specific nutrients directly supporting the growth and expansion of particular taxa (David et al., 2014; Singh et al., 2017). Indeed, consumption of a Western diet, characterised by high intake of animal products, refined carbohydrates, and fats, is associated with distinct microbiota composition from that of individuals following a Mediterranean or traditional plant-based diet (García-Montero et al., 2021; Soldán et al., 2024). While dietary changes induce

compositional changes within 24 hours, some evidence suggests the microbiota is resilient and has a tendency to retain an individual-specific "core" composition (Voreades et al., 2014). A lack of long-term studies limits our understanding of whether sustained dietary changes produce stable and lasting alterations in composition. Long-term dietary patterns, however, do appear to associate with specific microbial taxa. For example, the phylum *Bacteroides* strongly associates with Western diet components such as animal proteins and saturated fat, whereas *Prevotella* correlates with plant-based diets, rich in carbohydrates and simple sugars (Wu et al., 2011).

Beyond compositional changes, dietary components can significantly influence the bacterial secretome, modulating outputs such as metabolites and BEVs, without necessarily altering microbial abundance as typically detected by bacterial 16S rRNA gene sequencing. The intake of nutrients, including carbohydrates, fats and proteins, may regulate BEV production differentially across gut species, shaping host-gut interactions through changes in BEVs-mediated signalling pathways.

1.6.2.1 Carbohydrates

Fibre supplementation supports the expansion of polysaccharide-digesting bacteria in vivo, particularly those expressing carbohydrate-active enzymes that catalyse fibre breakdown (Wastyk et al., 2021). These enzymes can be directly carried by BEVs and may be important for supporting a healthy gut microbiota, as glycosidase-enriched BEVs released by Bacteroides mediate fibre digestion, facilitating "cross-feeding" for non-polysaccharide-utilizing species, (Elhenawy et al., 2014). Similarly, cellulose-degrading enzymes have been identified in ruminant microbiota BEVs (Arntzen et al., 2017). In vitro, carbohydrates can modulate BEV production, for example, with beta-mannan

supplementation stimulating BEV release from isolated porcine gut microbiota (Lagos et al., 2020). While beta-mannan exposure altered BEV protein composition, however, it did not enrich the presence of polysaccharide-digesting enzymes. Thus, while fibre supplementation in vivo may increase BEV production by supporting expansion of carbohydrate-digesting bacteria, it may not impact the functional properties of BEVs.

1.6.2.2 Fats

High-fat diets alter microbiota composition and also faecal BEV profiles, increasing BEV size as well as protein and LPS content in mice (Choi et al., 2015). Fatty acid composition, particularly the ratio of saturated to unsaturated fatty acids, influences the rigidity of the bacterial membrane (Zhang and Rock, 2008) and bacteria modulate their incorporation of fatty acids during stress (Zhu et al., 2014), which may influence BEV biogenesis.

In vitro supplementation with saturated or unsaturated fatty acid modulated BEV production in *Bacteroides* taxa, with strain-specific effects (Mirjafari Tafti et al., 2019). These BEVs in turn upregulated expression of cholesterol transporters in a colonic cell line (Badi et al., 2020). This suggests that dietary fatty acid intake may influence vesiculation in a complex manner *in vivo*, and further work is needed to delineate the effects of specific saturated and unsaturated fatty acids. Total dietary lipid intake may also indirectly affect gut BEV production via stimulating host bile acid secretion. Bile acids have antimicrobial properties (Islam et al., 2011), and stimulate commensal BEV generation *in vitro* (Kawasaki et al., 2018; Pumbwe et al., 2007). Supporting this, BEVs from *B. thetaiotaomicron* were found to carry bile-degrading enzymes, suggesting a role for BEVs in modulating host biosynthetic pathways (Stentz et al., 2022).

1.6.2.3 Proteins

The availability of different amino acids also influences BEV generation. Glycine weakens peptidoglycan structure, inhibiting bacterial growth at high concentrations (Hammes et al., 1973) and promotes vesiculation for *E. coli* Nissle 1917 *in vitro* (Hirayama and Nakao, 2020). These BEVs also exhibited altered size, protein profiles, and lowered LPS activity.

Interestingly, D-form amino acids isomers can also regulate peptidoglycan structure (Cava et al., 2011) and synergise with antimicrobials to disrupt bacterial cell integrity (Sanchez et al., 2014). In mammals, most D-form amino acids derive from either gut microbiota metabolism or through intake of fermented foods (Bastings et al., 2019). Whether fermented foods directly modulate gut BEV production is unknown, but this could be a factor underlying their health benefits. Additionally N-acetyl cysteine, a cysteine precursor found in protein-rich foods, and also marketed as an antioxidant supplement, has been shown to alter BEV production in respiratory pathogens, and blunt their immunogenicity *in vitro* (Volgers et al., 2017).

Altogether, the ratio and availability of these various macronutrients not only influence both microbiota composition and metabolism,but may also directly impact BEV production and functional activity. This is explored in Chapter 3 of this thesis, where a high-protein diet was found to shift gut microbiota metabolism towards succinate production, leading to increased overall BEV release via induction of the bacterial stress response. Increased BEV levels activated epithelial TLR4, subsequently promoting the generation of T-cell independent sIgA, and demonstrating a direct link between diet, BEVs and host physiology.

1.6.2.4 Fasting

In the gut, the microbiota experience natural cycles of nutrient availability based on host feeding patterns. Thus, fasting represents a period of nutrient deprivation for gut bacteria where BEV production is likely to be significantly increased. However, this concept has not been investigated before *in vivo* to our knowledge, nor has the potential impact of fasting-induced BEVs on host metabolism and homeostasis.

Chapter 4 of this thesis addresses this gap, by examining BEV dynamics *in vivo* and identifies BEVs as key regulators of host hepatic gluconeogenesis via the circadian CLOCK pathway. This finding suggests that BEVs act as an environmental cue to support the host's glucose demands during periods of glucose scarcity, such as in fasting. This discovery highlights a previously unrecognised synchronisation between host and gut microbiota metabolism, mediated through gut BEVs.

1.7 Aims and rationale

The research undertaken in this thesis aimed to investigate the role of the gut microbiota in regulating host physiology, and whether BEVs are key mediators of these effects.

Substantial evidence indicates antibiotics are major disruptors of microbiota composition and are linked to increased risk of autoimmune and allergic diseases in humans. However, the variability of antibiotic regimens, the complexity of the human gut microbiota, and the poorly understood aetiologies of these diseases makes this relationship difficult to elucidate. Therefore, a study investigating the effects of antibiotics that differentially target the two major bacterial classes, along with the

subsequent changes in microbiota composition, metabolite production, and host immunity, is crucial for understanding the link between antibiotics, gut microbiota, and immune dysregulation.

BEVs are emerging as important mediators of microbiota-host communication in regulating host physiology. However, the role of total microbiota-derived BEVs in this dynamic remains underexplored. Critical gaps remain in our understanding of how antibiotics and nutrient intake (including dietary components and fasting) influences BEV production and its downstream effects on gut homeostasis. Additionally, it is unclear whether BEVs contribute to homeostatic regulation of gut bacterial composition and whether maternal BEVs influence gestational programming of the fetus.

To address these gaps in BEV knowledge, this thesis comprises studies investigating: (1) the effects of diet on total BEVs and downstream impacts on mucosal immunity, (2) the influence of fasting on BEV production and its effects on host metabolism, and (3), the role of total BEVs in shaping gut microbiota composition, and their impact on fetal physiology following gestational exposure.

These studies provide valuable insights into how BEVs mediate gut-host crosstalk, uncovering novel pathways that advance our understanding of gut-host mutualism. This knowledge could drive the development of targeted therapeutics, aimed at optimising GI health, regulating host metabolism, and supporting fetal development during gestation.

1.7.1 Aims

1. To determine the impact of antibiotic-mediated dysbiosis on gut bacterial composition, metabolites, and host immune profiles
2. To explore the effects of dietary composition on gut BEVs, and their influence on gut homeostasis, particularly sIgA production
3. To investigate the effects of fasting on gut BEVs and their role in regulating host metabolic homeostasis.
4. To investigate the role of BEVs in shaping gut bacterial composition, and how maternal gut BEVs contribute to fetal programming of the gut, immune organs, and the lung.

References

Aagaard, K., Ma, J., Antony, K.M., Ganu, R., Petrosino, J., Versalovic, J., 2014. The placenta harbors a unique microbiome. Sci Transl Med 6, 237ra65. https://doi.org/10.1126/scitranslmed.3008599

Abreu, M.T., Fukata, M., Arditi, M., 2005. TLR signaling in the gut in health and disease. J Immunol 174, 4453–4460. https://doi.org/10.4049/jimmunol.174.8.4453

Alvarez, C.-S., Badia, J., Bosch, M., Giménez, R., Baldomà, L., 2016. Outer Membrane Vesicles and Soluble Factors Released by Probiotic Escherichia coli Nissle 1917 and Commensal ECOR63 Enhance Barrier Function by Regulating Expression of Tight Junction Proteins in Intestinal Epithelial Cells. Front Microbiol 7, 1981. https://doi.org/10.3389/fmicb.2016.01981

Ambort, D., Johansson, M.E.V., Gustafsson, J.K., Nilsson, H.E., Ermund, A., Johansson, B.R., Koeck, P.J.B., Hebert, H., Hansson, G.C., 2012. Calcium and pH-dependent packing and release of the gel-forming MUC2 mucin. Proceedings of the National Academy of Sciences 109, 5645–5650. https://doi.org/10.1073/pnas.1120269109

An, J., Yang, J., Kwon, H., Lim, W., Kim, Y.-K., Moon, B.-I., 2023. Prediction of breast cancer using blood microbiome and identification of foods for breast cancer prevention. Sci Rep 13, 5110. https://doi.org/10.1038/s41598-023-32227-x

Ansari, I., Raddatz, G., Gutekunst, J., Ridnik, M., Cohen, D., Abu-Remaileh, M., Tuganbaev, T., Shapiro, H., Pikarsky, E., Elinav, E., Lyko, F., Bergman, Y., 2020. The microbiota programs DNA methylation to control intestinal homeostasis and inflammation. Nat Microbiol 5, 610–619. https://doi.org/10.1038/s41564-019-0659-3

Anthony, W.E., Wang, B., Sukhum, K.V., D'Souza, A.W., Hink, T., Cass, C., Seiler, S., Reske, K.A., Coon, C., Dubberke, E.R., Burnham, C.-A.D., Dantas, G., Kwon, J.H., 2022. Acute and persistent effects of commonly used antibiotics on the gut microbiome and resistome in healthy adults. Cell Rep 39, 110649. https://doi.org/10.1016/j.celrep.2022.110649

Arike, L., Hansson, G.C., 2016. The Densely O-glycosylated MUC2 Mucin Protects the Intestine and Provides Food for the Commensal Bacteria. J Mol Biol 428, 3221–3229. https://doi.org/10.1016/j.jmb.2016.02.010

Arntzen, M.Ø., Várnai, A., Mackie, R.I., Eijsink, V.G.H., Pope, P.B., 2017. Outer membrane vesicles from Fibrobacter succinogenes S85 contain an array of carbohydrate-active enzymes with versatile polysaccharide-degrading capacity. Environ Microbiol 19, 2701–2714. https://doi.org/10.1111/1462-2920.13770

Avila-Calderón, E.D., Ruiz-Palma, M. del S., Aguilera-Arreola, Ma.G., Velázquez-Guadarrama, N., Ruiz, E.A., Gomez-Lunar, Z., Witonsky, S., Contreras-Rodríguez, A., 2021. Outer Membrane Vesicles of Gram-Negative Bacteria: An Outlook on Biogenesis. Front Microbiol 12, 557902. https://doi.org/10.3389/fmicb.2021.557902

Badi, S.A., Motahhary, A., Bahramali, G., Masoumi, M., Khalili, S.F.S., Ebrahimzadeh, N., Nouri, P., Rahimi, A., Masotti, A., Moshiri, A., Siadat, S.D., 2020. The regulation of Niemann-Pick C1-Like 1 (NPC1L1) gene expression in opposite direction by Bacteroides spp. and related outer membrane vesicles in Caco-2 cell line. J Diabetes Metab Disord 19, 415–422. https://doi.org/10.1007/s40200-020-00522-3

Balmer, M.L., Schürch, C.M., Saito, Y., Geuking, M.B., Li, H., Cuenca, M., Kovtonyuk, L.V., McCoy, K.D., Hapfelmeier, S., Ochsenbein, A.F., Manz, M.G., Slack, E., Macpherson, A.J., 2014. Microbiota-derived compounds drive steady-state granulopoiesis via MyD88/TICAM signaling. J Immunol 193, 5273–5283. https://doi.org/10.4049/jimmunol.1400762

Banchi, P., Colitti, B., Del Carro, Andrea, Corrò, M., Bertero, A., Ala, U., Del Carro, Angela, Van Soom, A., Bertolotti, L., Rota, A., 2023. Challenging the Hypothesis of in Utero Microbiota Acquisition in Healthy Canine and Feline Pregnancies at Term: Preliminary Data. Vet Sci 10, 331. https://doi.org/10.3390/vetsci10050331

Banchi, P., Colitti, B., Opsomer, G., Rota, A., Van Soom, A., 2024. The dogma of the sterile uterus revisited: does microbial seeding occur during fetal life in humans and animals? Reproduction 167, e230078. https://doi.org/10.1530/REP-23-0078

Barker, N., 2014. Adult intestinal stem cells: critical drivers of epithelial homeostasis and regeneration. Nat Rev Mol Cell Biol 15, 19–33. https://doi.org/10.1038/nrm3721

Bastings, J.J.A.J., van Eijk, H.M., Olde Damink, S.W., Rensen, S.S., 2019. d-amino Acids in Health and Disease: A Focus on Cancer. Nutrients 11, 2205. https://doi.org/10.3390/nu11092205

Baumann, J., Park, C.G., Mantis, N.J., 2010. Recognition of secretory IgA by DC-SIGN: Implications for immune surveillance in the intestine. Immunol Lett 131, 59–66. https://doi.org/10.1016/j.imlet.2010.03.005

Beaman, B.L., Gershwin, M.E., Scates, S.S., Ohsugi, Y., 1980. Immunobiology of germfree mice infected with Nocardia asteroides. Infect Immun 29, 733–743. https://doi.org/10.1128/iai.29.2.733-743.1980

Belkaid, Y., Harrison, O.J., 2017. Homeostatic Immunity and the Microbiota. Immunity 46, 562–576. https://doi.org/10.1016/j.immuni.2017.04.008

Berer, K., Mues, M., Koutrolos, M., Rasbi, Z.A., Boziki, M., Johner, C., Wekerle, H., Krishnamoorthy, G., 2011. Commensal microbiota and myelin autoantigen cooperate to trigger autoimmune demyelination. Nature 479, 538–541. https://doi.org/10.1038/nature10554

Bhattarai, S.K., Du, M., Zeamer, A.L., M Morzfeld, B., Kellogg, T.D., Firat, K., Benjamin, A., Bean, J.M., Zimmerman, M., Mardi, G., Vilbrun, S.C., Walsh, K.F., Fitzgerald, D.W., Glickman, M.S., Bucci, V., 2024. Commensal antimicrobial resistance mediates microbiome resilience to antibiotic disruption. Sci Transl Med 16, eadi9711. https://doi.org/10.1126/scitranslmed.adi9711

Biller, S.J., Coe, A., Arellano, A.A., Dooley, K., Silvestri, S.M., Gong, J.S., Yeager, E.A., Becker, J.W., Chisholm, S.W., 2023. Environmental and Taxonomic Drivers of Bacterial Extracellular Vesicle Production in Marine Ecosystems. Applied and Environmental Microbiology 89, e00594-23. https://doi.org/10.1128/aem.00594-23

Birchenough, G.M.H., Johansson, M.E.V., Gustafsson, J.K., Bergström, J.H., Hansson, G.C., 2015. New developments in goblet cell mucus secretion and function. Mucosal Immunol 8, 712–719. https://doi.org/10.1038/mi.2015.32

Birchenough, G.M.H., Nyström, E.E.L., Johansson, M.E.V., Hansson, G.C., 2016. A sentinel goblet cell guards the colonic crypt by triggering Nlrp6-dependent Muc2 secretion. Science 352, 1535–1542. https://doi.org/10.1126/science.aaf7419

Boullier, S., Tanguy, M., Kadaoui, K.A., Caubet, C., Sansonetti, P., Corthésy, B., Phalipon, A., 2009. Secretory IgA-Mediated Neutralization of Shigella flexneri Prevents Intestinal Tissue Destruction by Down-Regulating Inflammatory Circuits1. The Journal of Immunology 183, 5879–5885. https://doi.org/10.4049/jimmunol.0901838

Briaud, P., Carroll, R.K., 2020. Extracellular Vesicle Biogenesis and Functions in Gram-Positive Bacteria. Infection and Immunity 88, 10.1128/iai.00433-20. https://doi.org/10.1128/iai.00433-20

Bunker, J.J., Flynn, T.M., Koval, J.C., Shaw, D.G., Meisel, M., McDonald, B.D., Ishizuka, I.E., Dent, A.L., Wilson, P.C., Jabri, B., Antonopoulos, D.A., Bendelac, A., 2015. Innate and Adaptive Humoral Responses Coat Distinct Commensal Bacteria with Immunoglobulin A. Immunity 43, 541–553. https://doi.org/10.1016/j.immuni.2015.08.007

Byndloss, M.X., Olsan, E.E., Rivera-Chávez, F., Tiffany, C.R., Cevallos, S.A., Lokken, K.L., Torres, T.P., Byndloss, A.J., Faber, F., Gao, Y., Litvak, Y., Lopez, C.A., Xu, G., Napoli, E., Giulivi, C., Tsolis, R.M., Revzin, A., Lebrilla, C., Bäumler, A.J., 2017. Microbiota-activated PPAR-γ-signaling inhibits dysbiotic Enterobacteriaceae expansion. Science 357, 570–575. https://doi.org/10.1126/science.aam9949

Cahenzli, J., Köller, Y., Wyss, M., Geuking, M.B., McCoy, K.D., 2013. Intestinal microbial diversity during early-life colonization shapes long-term IgE levels. Cell Host Microbe 14, 559–570. https://doi.org/10.1016/j.chom.2013.10.004

Cani, P.D., Amar, J., Iglesias, M.A., Poggi, M., Knauf, C., Bastelica, D., Neyrinck, A.M., Fava, F., Tuohy, K.M., Chabo, C., Waget, A., Delmée, E., Cousin, B., Sulpice, T., Chamontin, B., Ferrières, J., Tanti, J.-F., Gibson, G.R., Casteilla, L., Delzenne, N.M., Alessi, M.C., Burcelin, R., 2007. Metabolic endotoxemia initiates obesity and insulin resistance. Diabetes 56, 1761–1772. https://doi.org/10.2337/db06-1491

Capaldo, C.T., Nusrat, A., 2015. Claudin switching: Physiological plasticity of the Tight Junction. Semin Cell Dev Biol 42, 22–29. https://doi.org/10.1016/j.semcdb.2015.04.003

Capaldo, C.T., Powell, D.N., Kalman, D., 2017. Layered defense: how mucus and tight junctions seal the intestinal barrier. J Mol Med 95, 927–934. https://doi.org/10.1007/s00109-017-1557-x

Carding, S., Verbeke, K., Vipond, D.T., Corfe, B.M., Owen, L.J., 2015. Dysbiosis of the gut microbiota in disease. Microbial Ecology in Health and Disease 26, 26191. https://doi.org/10.3402/mehd.v26.26191

Carrera-Bastos, P., Fontes-Villalba, M., O'Keefe, J.H., Lindeberg, S., Cordain, L., 2011. The western diet and lifestyle and diseases of civilization. Research Reports in Clinical Cardiology.

Caruana, J.C., Walper, S.A., 2020. Bacterial Membrane Vesicles as Mediators of Microbe - Microbe and Microbe - Host Community Interactions. Front Microbiol 11, 432. https://doi.org/10.3389/fmicb.2020.00432

Castigli, E., Scott, S., Dedeoglu, F., Bryce, P., Jabara, H., Bhan, A.K., Mizoguchi, E., Geha, R.S., 2004. Impaired IgA class switching in APRIL-deficient mice. Proceedings of the National Academy of Sciences 101, 3903–3908. https://doi.org/10.1073/pnas.0307348101

Catalano, M., O'Driscoll, L., 2020. Inhibiting extracellular vesicles formation and release: a review of EV inhibitors. Journal of Extracellular Vesicles 9, 1703244. https://doi.org/10.1080/20013078.2019.1703244

Cava, F., Lam, H., de Pedro, M.A., Waldor, M.K., 2011. Emerging knowledge of regulatory roles of D-amino acids in bacteria. Cell Mol Life Sci 68, 817–831. https://doi.org/10.1007/s00018-010-0571-8

Cekanaviciute, E., Yoo, B.B., Runia, T.F., Debelius, J.W., Singh, S., Nelson, C.A., Kanner, R., Bencosme, Y., Lee, Y.K., Hauser, S.L., Crabtree-Hartman, E., Sand, I.K., Gacias, M., Zhu, Y., Casaccia, P., Cree, B.A.C., Knight, R., Mazmanian, S.K., Baranzini, S.E., 2017. Gut bacteria from multiple sclerosis patients modulate human T cells and exacerbate symptoms in mouse models. Proc Natl Acad Sci U S A 114, 10713–10718. https://doi.org/10.1073/pnas.1711235114

Chang, C.-J., Bai, Y.-C., Jiang, H., Ma, Q.-W., Hsieh, C.-H., Liu, C.-C., Huang, H.-C., Chen, T.-J., 2024. Microbiome analysis of serum extracellular vesicles in gestational diabetes patients. Acta Diabetol. https://doi.org/10.1007/s00592-024-02358-2

Chang, C.-J., Zhang, J., Tsai, Y.-L., Chen, C.-B., Lu, C.-W., Huo, Y.-P., Liou, H.-M., Ji, C., Chung, W.-H., 2021. Compositional Features of Distinct Microbiota Base on Serum Extracellular Vesicle Metagenomics Analysis in Moderate to Severe Psoriasis Patients. Cells 10, 2349. https://doi.org/10.3390/cells10092349

Chang, P.V., Hao, L., Offermanns, S., Medzhitov, R., 2014. The microbial metabolite butyrate regulates intestinal macrophage function via histone deacetylase inhibition. Proc Natl Acad Sci U S A 111, 2247–2252. https://doi.org/10.1073/pnas.1322269111

Chatzidaki-Livanis, M., Coyne, M.J., Comstock, L.E., 2014. An antimicrobial protein of the gut symbiont Bacteroides fragilis with a MACPF domain of host immune proteins. Mol Microbiol 94, 1361–1374. https://doi.org/10.1111/mmi.12839

Chelakkot, C., Choi, Y., Kim, D.-K., Park, H.T., Ghim, J., Kwon, Y., Jeon, J., Kim, M.-S., Jee, Y.-K., Gho, Y.S., Park, H.-S., Kim, Y.-K., Ryu, S.H., 2018. Akkermansia muciniphila-derived extracellular vesicles

influence gut permeability through the regulation of tight junctions. Exp Mol Med 50, e450. https://doi.org/10.1038/emm.2017.282

Chen, X., Li, Q., Xie, J., Nie, S., 2024. Immunomodulatory Effects of Probiotic-Derived Extracellular Vesicles: Opportunities and Challenges. J. Agric. Food Chem. 72, 19259–19273. https://doi.org/10.1021/acs.jafc.4c04223

Choi, Y., Kwon, Y., Kim, D.-K., Jeon, J., Jang, S.C., Wang, T., Ban, M., Kim, M.-H., Jeon, S.G., Kim, M.-S., Choi, C.S., Jee, Y.-K., Gho, Y.S., Ryu, S.H., Kim, Y.-K., 2015. Gut microbe-derived extracellular vesicles induce insulin resistance, thereby impairing glucose metabolism in skeletal muscle. Sci Rep 5, 15878. https://doi.org/10.1038/srep15878

Chu, H., Khosravi, A., Kusumawardhani, I.P., Kwon, A.H.K., Vasconcelos, A.C., Cunha, L.D., Mayer, A.E., Shen, Y., Wu, W.-L., Kambal, A., Targan, S.R., Xavier, R.J., Ernst, P.B., Green, D.R., McGovern, D.P.B., Virgin, H.W., Mazmanian, S.K., 2016. Gene-microbiota interactions contribute to the pathogenesis of inflammatory bowel disease. Science 352, 1116–1120. https://doi.org/10.1126/science.aad9948

Corthésy, B., 2013. Multi-Faceted Functions of Secretory IgA at Mucosal Surfaces. Front Immunol 4, 185. https://doi.org/10.3389/fimmu.2013.00185

d'Humières, C., Delavy, M., Alla, L., Ichou, F., Gauliard, E., Ghozlane, A., Levenez, F., Galleron, N., Quinquis, B., Pons, N., Mullaert, J., Bridier-Nahmias, A., Condamine, B., Touchon, M., Rainteau, D., Lamazière, A., Lesnik, P., Ponnaiah, M., Lhomme, M., Sertour, N., Devente, S., Docquier, J.-D., Bougnoux, M.-E., Tenaillon, O., Magnan, M., Ruppé, E., Grall, N., Duval, X., Ehrlich, D., Mentré, F., Denamur, E., Rocha, E.P.C., Le Chatelier, E., Burdet, C., PrediRes study group, 2024. Perturbation and resilience of the gut microbiome up to 3 months after β-lactams exposure in healthy volunteers suggest an important role of microbial β-lactamases. Microbiome 12, 50. https://doi.org/10.1186/s40168-023-01746-0

David, L.A., Maurice, C.F., Carmody, R.N., Gootenberg, D.B., Button, J.E., Wolfe, B.E., Ling, A.V., Devlin, A.S., Varma, Y., Fischbach, M.A., Biddinger, S.B., Dutton, R.J., Turnbaugh, P.J., 2014. Diet rapidly and reproducibly alters the human gut microbiome. Nature 505, 559–563. https://doi.org/10.1038/nature12820

Dera, N., Żeber-Lubecka, N., Ciebiera, M., Kosińska-Kaczyńska, K., Szymusik, I., Massalska, D., Dera, K., Bubień, K., 2024. Intrauterine Shaping of Fetal Microbiota. J Clin Med 13, 5331. https://doi.org/10.3390/jcm13175331

Dethlefsen, L., Relman, D.A., 2011. Incomplete recovery and individualized responses of the human distal gut microbiota to repeated antibiotic perturbation. Proc Natl Acad Sci U S A 108, 4554–4561. https://doi.org/10.1073/pnas.1000087107

Díaz-Garrido, N., Badia, J., Baldomà, L., 2021. Microbiota-derived extracellular vesicles in interkingdom communication in the gut. J Extracell Vesicles 10, e12161. https://doi.org/10.1002/jev2.12161

Dixson, A.C., Dawson, T.R., Di Vizio, D., Weaver, A.M., 2023. Context-specific regulation of extracellular vesicle biogenesis and cargo selection. Nat Rev Mol Cell Biol 24, 454–476. https://doi.org/10.1038/s41580-023-00576-0

Domínguez Rubio, A.P., D'Antoni, C.L., Piuri, M., Pérez, O.E., 2022. Probiotics, Their Extracellular Vesicles and Infectious Diseases. Front Microbiol 13, 864720. https://doi.org/10.3389/fmicb.2022.864720

Donald, K., Finlay, B.B., 2024. Experimental models of antibiotic exposure and atopic disease. Front Allergy 5, 1455438. https://doi.org/10.3389/falgy.2024.1455438

Elhenawy, W., Debelyy, M.O., Feldman, M.F., 2014. Preferential packing of acidic glycosidases and proteases into Bacteroides outer membrane vesicles. mBio 5, e00909-00914. https://doi.org/10.1128/mBio.00909-14

Ermund, A., Schütte, A., Johansson, M.E.V., Gustafsson, J.K., Hansson, G.C., 2013. Studies of mucus in mouse stomach, small intestine, and colon. I. Gastrointestinal mucus layers have different properties depending on location as well as over the Peyer's patches. Am J Physiol Gastrointest Liver Physiol 305, G341–G347. https://doi.org/10.1152/ajpgi.00046.2013

Fábrega, M.-J., Rodríguez-Nogales, A., Garrido-Mesa, J., Algieri, F., Badía, J., Giménez, R., Gálvez, J., Baldomà, L., 2017. Intestinal Anti-inflammatory Effects of Outer Membrane Vesicles from Escherichia coli Nissle 1917 in DSS-Experimental Colitis in Mice. Front Microbiol 8, 1274. https://doi.org/10.3389/fmicb.2017.01274

Fagarasan, S., Muramatsu, M., Suzuki, K., Nagaoka, H., Hiai, H., Honjo, T., 2002. Critical roles of activation-induced cytidine deaminase in the homeostasis of gut flora. Science 298, 1424–1427. https://doi.org/10.1126/science.1077336

Fagundes, C.T., Amaral, F.A., Vieira, A.T., Soares, A.C., Pinho, V., Nicoli, J.R., Vieira, L.Q., Teixeira, M.M., Souza, D.G., 2012. Transient TLR activation restores inflammatory response and ability to control pulmonary bacterial infection in germfree mice. J Immunol 188, 1411–1420. https://doi.org/10.4049/jimmunol.1101682

Fan, X., Rudensky, A.Y., 2016. Hallmarks of Tissue-Resident Lymphocytes. Cell 164, 1198–1211. https://doi.org/10.1016/j.cell.2016.02.048

Fan, Y., Pedersen, O., 2021. Gut microbiota in human metabolic health and disease. Nat Rev Microbiol 19, 55–71. https://doi.org/10.1038/s41579-020-0433-9

Fang, Y., Wang, Z., Liu, X., Tyler, B.M., 2022. Biogenesis and Biological Functions of Extracellular Vesicles in Cellular and Organismal Communication With Microbes. Front Microbiol 13, 817844. https://doi.org/10.3389/fmicb.2022.817844

Feehley, T., Plunkett, C.H., Bao, R., Choi Hong, S.M., Culleen, E., Belda-Ferre, P., Campbell, E., Aitoro, R., Nocerino, R., Paparo, L., Andrade, J., Antonopoulos, D.A., Berni Canani, R., Nagler, C.R., 2019. Healthy infants harbor intestinal bacteria that protect against food allergy. Nat Med 25, 448–453. https://doi.org/10.1038/s41591-018-0324-z

Fransen, F., Zagato, E., Mazzini, E., Fosso, B., Manzari, C., El Aidy, S., Chiavelli, A., D'Erchia, A.M., Sethi, M.K., Pabst, O., Marzano, M., Moretti, S., Romani, L., Penna, G., Pesole, G., Rescigno, M., 2015. BALB/c and C57BL/6 Mice Differ in Polyreactive IgA Abundance, which Impacts the Generation of Antigen-Specific IgA and Microbiota Diversity. Immunity 43, 527–540. https://doi.org/10.1016/j.immuni.2015.08.011

Fremder, M., Kim, S.W., Khamaysi, A., Shimshilashvili, L., Eini-Rider, H., Park, I.S., Hadad, U., Cheon, J.H., Ohana, E., 2021. A transepithelial pathway delivers succinate to macrophages, thus perpetuating their pro-inflammatory metabolic state. Cell Reports 36. https://doi.org/10.1016/j.celrep.2021.109521

Furusawa, Y., Obata, Y., Fukuda, S., Endo, T.A., Nakato, G., Takahashi, D., Nakanishi, Y., Uetake, C., Kato, K., Kato, T., Takahashi, M., Fukuda, N.N., Murakami, S., Miyauchi, E., Hino, S., Atarashi, K., Onawa, S., Fujimura, Y., Lockett, T., Clarke, J.M., Topping, D.L., Tomita, M., Hori, S., Ohara, O., Morita, T., Koseki, H., Kikuchi, J., Honda, K., Hase, K., Ohno, H., 2013. Commensal microbe-derived butyrate induces the differentiation of colonic regulatory T cells. Nature 504, 446–450. https://doi.org/10.1038/nature12721

Gallo, R.L., Hooper, L.V., 2012. Epithelial antimicrobial defence of the skin and intestine. Nat Rev Immunol 12, 503–516. https://doi.org/10.1038/nri3228

Gan, Y., Zhao, G., Wang, Z., Zhang, X., Wu, M.X., Lu, M., 2023. Bacterial Membrane Vesicles: Physiological Roles, Infection Immunology, and Applications. Advanced Science 10, 2301357. https://doi.org/10.1002/advs.202301357

Gao, Y., Nanan, R., Macia, L., Tan, J., Sominsky, L., Quinn, T.P., O'Hely, M., Ponsonby, A.-L., Tang, M.L.K., Collier, F., Strickland, D.H., Dhar, P., Brix, S., Phipps, S., Sly, P.D., Ranganathan, S., Stokholm, J., Kristiansen, K., Gray, L.E.K., Vuillermin, P., 2021. The maternal gut microbiome during pregnancy

and offspring allergy and asthma. Journal of Allergy and Clinical Immunology 148, 669–678. https://doi.org/10.1016/j.jaci.2021.07.011

García-Montero, C., Fraile-Martínez, O., Gómez-Lahoz, A.M., Pekarek, L., Castellanos, A.J., Noguerales-Fraguas, F., Coca, S., Guijarro, L.G., García-Honduvilla, N., Asúnsolo, A., Sanchez-Trujillo, L., Lahera, G., Bujan, J., Monserrat, J., Álvarez-Mon, M., Álvarez-Mon, M.A., Ortega, M.A., 2021. Nutritional Components in Western Diet Versus Mediterranean Diet at the Gut Microbiota–Immune System Interplay. Implications for Health and Disease. Nutrients 13, 699. https://doi.org/10.3390/nu13020699

Gilmore, W.J., Johnston, E.L., Bitto, N.J., Zavan, L., O'Brien-Simpson, N., Hill, A.F., Kaparakis-Liaskos, M., 2022. Bacteroides fragilis outer membrane vesicles preferentially activate innate immune receptors compared to their parent bacteria. Front Immunol 13, 970725. https://doi.org/10.3389/fimmu.2022.970725

Gomez de Agüero, M., Ganal-Vonarburg, S.C., Fuhrer, T., Rupp, S., Uchimura, Y., Li, H., Steinert, A., Heikenwalder, M., Hapfelmeier, S., Sauer, U., McCoy, K.D., Macpherson, A.J., 2016. The maternal microbiota drives early postnatal innate immune development. Science 351, 1296–1302. https://doi.org/10.1126/science.aad2571

Gosiewski, T., Ludwig-Galezowska, A.H., Huminska, K., Sroka-Oleksiak, A., Radkowski, P., Salamon, D., Wojciechowicz, J., Kus-Slowinska, M., Bulanda, M., Wolkow, P.P., 2017. Comprehensive detection and identification of bacterial DNA in the blood of patients with sepsis and healthy volunteers using next-generation sequencing method - the observation of DNAemia. Eur J Clin Microbiol Infect Dis 36, 329–336. https://doi.org/10.1007/s10096-016-2805-7

Gribble, F.M., Reimann, F., 2019. Function and mechanisms of enteroendocrine cells and gut hormones in metabolism. Nat Rev Endocrinol 15, 226–237. https://doi.org/10.1038/s41574-019-0168-8

Guarner, F., Bustos Fernandez, L., Cruchet, S., Damião, A., Maruy Saito, A., Riveros Lopez, J.P., Rodrigues Silva, L., Valdovinos Diaz, M.A., 2024. Gut dysbiosis mediates the association between antibiotic exposure and chronic disease. Front Med (Lausanne) 11, 1477882. https://doi.org/10.3389/fmed.2024.1477882

Gullberg, E., Söderholm, J.D., 2006. Peyer's Patches and M Cells as Potential Sites of the Inflammatory Onset in Crohn's Disease. Annals of the New York Academy of Sciences 1072, 218–232. https://doi.org/10.1196/annals.1326.028

Guo, C., Bai, Y., Li, P., He, K., 2024. The emerging roles of microbiota-derived extracellular vesicles in psychiatric disorders. Front Microbiol 15, 1383199. https://doi.org/10.3389/fmicb.2024.1383199

Gustafsson, J.K., Johansson, M.E.V., 2022. The role of goblet cells and mucus in intestinal homeostasis. Nat Rev Gastroenterol Hepatol 19, 785–803. https://doi.org/10.1038/s41575-022-00675-x

Haak, B.W., Lankelma, J.M., Hugenholtz, F., Belzer, C., de Vos, W.M., Wiersinga, W.J., 2019. Long-term impact of oral vancomycin, ciprofloxacin and metronidazole on the gut microbiota in healthy humans. J Antimicrob Chemother 74, 782–786. https://doi.org/10.1093/jac/dky471

Habib, S.H., Saha, S., 2010. Burden of non-communicable disease: Global overview. Diabetes & Metabolic Syndrome: Clinical Research & Reviews 4, 41–47. https://doi.org/10.1016/j.dsx.2008.04.005

Hammes, W., Schleifer, K.H., Kandler, O., 1973. Mode of action of glycine on the biosynthesis of peptidoglycan. J Bacteriol 116, 1029–1053. https://doi.org/10.1128/jb.116.2.1029-1053.1973

Hapfelmeier, S., Lawson, M.A.E., Slack, E., Kirundi, J.K., Stoel, M., Heikenwalder, M., Cahenzli, J., Velykoredko, Y., Balmer, M.L., Endt, K., Geuking, M.B., Curtiss, R., McCoy, K.D., Macpherson, A.J., 2010. Reversible microbial colonization of germ-free mice reveals the dynamics of IgA immune responses. Science 328, 1705–1709. https://doi.org/10.1126/science.1188454

Harp, J.A., Chen, W., Harmsen, A.G., 1992. Resistance of severe combined immunodeficient mice to infection with Cryptosporidium parvum: the importance of intestinal microflora. Infection and Immunity 60, 3509–3512. https://doi.org/10.1128/iai.60.9.3509-3512.1992

He, B., Xu, W., Santini, P.A., Polydorides, A.D., Chiu, A., Estrella, J., Shan, M., Chadburn, A., Villanacci, V., Plebani, A., Knowles, D.M., Rescigno, M., Cerutti, A., 2007. Intestinal bacteria trigger T cell-independent immunoglobulin A(2) class switching by inducing epithelial-cell secretion of the cytokine APRIL. Immunity 26, 812–826. https://doi.org/10.1016/j.immuni.2007.04.014

Heo, M., Park, Y.S., Yoon, H., Kim, N.-E., Kim, K., Shin, C.M., Kim, N., Lee, D.H., 2023. Potential of Gut Microbe-Derived Extracellular Vesicles to Differentiate Inflammatory Bowel Disease Patients from Healthy Controls. Gut Liver 17, 108–118. https://doi.org/10.5009/gnl220081

Herbst, T., Sichelstiel, A., Schär, C., Yadava, K., Bürki, K., Cahenzli, J., McCoy, K., Marsland, B.J., Harris, N.L., 2011. Dysregulation of allergic airway inflammation in the absence of microbial colonization. Am J Respir Crit Care Med 184, 198–205. https://doi.org/10.1164/rccm.201010-1574OC

Hickey, C.A., Kuhn, K.A., Donermeyer, D.L., Porter, N.T., Jin, C., Cameron, E.A., Jung, H., Kaiko, G.E., Wegorzewska, M., Malvin, N.P., Glowacki, R.W.P., Hansson, G.C., Allen, P.M., Martens, E.C., Stappenbeck, T.S., 2015. Colitogenic Bacteroides thetaiotaomicron Antigens Access Host Immune Cells in a Sulfatase-Dependent Manner via Outer Membrane Vesicles. Cell Host Microbe 17, 672–680. https://doi.org/10.1016/j.chom.2015.04.002

Hirayama, S., Nakao, R., 2020. Glycine significantly enhances bacterial membrane vesicle production: a powerful approach for isolation of LPS-reduced membrane vesicles of probiotic Escherichia coli. Microb Biotechnol 13, 1162–1178. https://doi.org/10.1111/1751-7915.13572

Hooper, L.V., Littman, D.R., Macpherson, A.J., 2012. Interactions between the microbiota and the immune system. Science 336, 1268–1273. https://doi.org/10.1126/science.1223490

Hu, L., Hong, G., Li, J., Chen, M., Chang, C.-J., Cheng, P.-J., Zhang, Z., Zhang, X., Chen, H., Zhuang, Y., Li, Y., 2024. Metformin modifies plasma microbial-derived extracellular vesicles in polycystic ovary syndrome with insulin resistance. J Ovarian Res 17, 136. https://doi.org/10.1186/s13048-024-01444-x

Husso, A., Pessa-Morikawa, T., Koistinen, V.M., Kärkkäinen, O., Kwon, H.N., Lahti, L., Iivanainen, A., Hanhineva, K., Niku, M., 2023. Impacts of maternal microbiota and microbial metabolites on fetal intestine, brain, and placenta. BMC Biology 21, 207. https://doi.org/10.1186/s12915-023-01709-9

Ignacio, A., Czyz, S., McCoy, K.D., 2024. Early life microbiome influences on development of the mucosal innate immune system. Seminars in Immunology 73, 101885. https://doi.org/10.1016/j.smim.2024.101885

Inagaki, H., Suzuki, T., Nomoto, K., Yoshikai, Y., 1996. Increased susceptibility to primary infection with Listeria monocytogenes in germfree mice may be due to lack of accumulation of L-selectin+ CD44+ T cells in sites of inflammation. Infect Immun 64, 3280–3287. https://doi.org/10.1128/iai.64.8.3280-3287.1996

Islam, K.B.M.S., Fukiya, S., Hagio, M., Fujii, N., Ishizuka, S., Ooka, T., Ogura, Y., Hayashi, T., Yokota, A., 2011. Bile acid is a host factor that regulates the composition of the cecal microbiota in rats. Gastroenterology 141, 1773–1781. https://doi.org/10.1053/j.gastro.2011.07.046

Ivanov, I.I., Atarashi, K., Manel, N., Brodie, E.L., Shima, T., Karaoz, U., Wei, D., Goldfarb, K.C., Santee, C.A., Lynch, S.V., Tanoue, T., Imaoka, A., Itoh, K., Takeda, K., Umesaki, Y., Honda, K., Littman, D.R., 2009. Induction of intestinal Th17 cells by segmented filamentous bacteria. Cell 139, 485–498. https://doi.org/10.1016/j.cell.2009.09.033

Jain, N., 2020. The early life education of the immune system: Moms, microbes and (missed) opportunities. Gut Microbes 12, 1824564. https://doi.org/10.1080/19490976.2020.1824564

Jakobsson, H.E., Jernberg, C., Andersson, A.F., Sjölund-Karlsson, M., Jansson, J.K., Engstrand, L., 2010. Short-Term Antibiotic Treatment Has Differing Long-Term Impacts on the Human Throat and Gut Microbiome. PLoS One 5, e9836. https://doi.org/10.1371/journal.pone.0009836

Jernberg, C., Löfmark, S., Edlund, C., Jansson, J.K., 2007. Long-term ecological impacts of antibiotic administration on the human intestinal microbiota. ISME J 1, 56–66. https://doi.org/10.1038/ismej.2007.3

Jiménez, E., Fernández, L., Marín, M.L., Martín, R., Odriozola, J.M., Nueno-Palop, C., Narbad, A., Olivares, M., Xaus, J., Rodríguez, J.M., 2005. Isolation of commensal bacteria from umbilical cord blood of healthy neonates born by cesarean section. Curr Microbiol 51, 270–274. https://doi.org/10.1007/s00284-005-0020-3

Joglekar, P., Ding, H., Canales-Herrerias, P., Pasricha, P.J., Sonnenburg, J.L., Peterson, D.A., 2019. Intestinal IgA Regulates Expression of a Fructan Polysaccharide Utilization Locus in Colonizing Gut Commensal Bacteroides thetaiotaomicron. mBio 10, e02324-19. https://doi.org/10.1128/mBio.02324-19

Johansson, M.E.V., Phillipson, M., Petersson, J., Velcich, A., Holm, L., Hansson, G.C., 2008. The inner of the two Muc2 mucin-dependent mucus layers in colon is devoid of bacteria. Proceedings of the National Academy of Sciences 105, 15064–15069. https://doi.org/10.1073/pnas.0803124105

Jones, E., Stentz, R., Telatin, A., Savva, G.M., Booth, C., Baker, D., Rudder, S., Knight, S.C., Noble, A., Carding, S.R., 2021. The Origin of Plasma-Derived Bacterial Extracellular Vesicles in Healthy Individuals and Patients with Inflammatory Bowel Disease: A Pilot Study. Genes (Basel) 12, 1636. https://doi.org/10.3390/genes12101636

Jones, E.J., Booth, C., Fonseca, S., Parker, A., Cross, K., Miquel-Clopés, A., Hautefort, I., Mayer, U., Wileman, T., Stentz, R., Carding, S.R., 2020. The Uptake, Trafficking, and Biodistribution of Bacteroides thetaiotaomicron Generated Outer Membrane Vesicles. Front Microbiol 11, 57. https://doi.org/10.3389/fmicb.2020.00057

Kamada, N., Seo, S.-U., Chen, G.Y., Núñez, G., 2013. Role of the gut microbiota in immunity and inflammatory disease. Nat Rev Immunol 13, 321–335. https://doi.org/10.1038/nri3430

Kameli, N., Becker, H.E.F., Welbers, T., Jonkers, D.M.A.E., Penders, J., Savelkoul, P., Stassen, F.R., 2021. Metagenomic Profiling of Fecal-Derived Bacterial Membrane Vesicles in Crohn's Disease Patients. Cells 10, 2795. https://doi.org/10.3390/cells10102795

Kang, J.I., Seo, J.H., Park, C.I., Kim, S.T., Kim, Y.-K., Jang, J.-K., Kwon, C.-O., Jeon, S., Kim, H.W., Kim, S.J., 2023. Microbiome analysis of circulating bacterial extracellular vesicles in obsessive-compulsive disorder. Psychiatry Clin Neurosci 77, 646–652. https://doi.org/10.1111/pcn.13593

Kawasaki, S., Watanabe, M., Fukiya, S., Yokota, A., 2018. Chapter 7 - Stress Responses of Bifidobacteria: Oxygen and Bile Acid as the Stressors, in: Mattarelli, P., Biavati, B., Holzapfel, W.H., Wood, B.J.B. (Eds.), The Bifidobacteria and Related Organisms. Academic Press, pp. 131–143. https://doi.org/10.1016/B978-0-12-805060-6.00007-7

Keiran, N., Ceperuelo-Mallafré, V., Calvo, E., Hernández-Alvarez, M.I., Ejarque, M., Núñez-Roa, C., Horrillo, D., Maymó-Masip, E., Rodríguez, M.M., Fradera, R., de la Rosa, J.V., Jorba, R., Megia, A., Zorzano, A., Medina-Gómez, G., Serena, C., Castrillo, A., Vendrell, J., Fernández-Veledo, S., 2019. SUCNR1 controls an anti-inflammatory program in macrophages to regulate the metabolic response to obesity. Nat Immunol 20, 581–592. https://doi.org/10.1038/s41590-019-0372-7

Kennedy, E.A., King, K.Y., Baldridge, M.T., 2018. Mouse Microbiota Models: Comparing Germ-Free Mice and Antibiotics Treatment as Tools for Modifying Gut Bacteria. Front. Physiol. 9. https://doi.org/10.3389/fphys.2018.01534

Kim, H.J., Kim, Y.-S., Kim, K.-H., Choi, J.-P., Kim, Y.-K., Yun, S., Sharma, L., Dela Cruz, C.S., Lee, J.S., Oh, Y.-M., Lee, S.-D., Lee, S.W., 2017. The microbiome of the lung and its extracellular vesicles in nonsmokers, healthy smokers and COPD patients. Exp Mol Med 49, e316–e316. https://doi.org/10.1038/emm.2017.7

Kim, M.H., Choi, S.J., Choi, H.I., Choi, J.P., Park, H.K., Kim, E.K., Kim, M.J., Moon, B.S., Min, T.K., Rho, M., Cho, Y.J., Yang, S., Kim, Y.K., Kim, Y.Y., Pyun, B.Y., 2018. Lactobacillus plantarum-derived Extracellular Vesicles Protect Atopic Dermatitis Induced by Staphylococcus aureus-derived Extracellular Vesicles. Allergy Asthma Immunol Res 10, 516–532. https://doi.org/10.4168/aair.2018.10.5.516

Kim, M.H., Kang, S.G., Park, J.H., Yanagisawa, M., Kim, C.H., 2013. Short-chain fatty acids activate GPR41 and GPR43 on intestinal epithelial cells to promote inflammatory responses in mice. Gastroenterology 145, 396-406.e1–10. https://doi.org/10.1053/j.gastro.2013.04.056

Kim, S.H., Keum, B., Kwak, S., Byun, J., Shin, J.M., Kim, T.H., 2024. Therapeutic Applications of Extracellular Vesicles in Inflammatory Bowel Disease. Int J Mol Sci 25, 745. https://doi.org/10.3390/ijms25020745

Kim, S.I., Kang, N., Leem, S., Yang, J., Jo, H., Lee, M., Kim, H.S., Dhanasekaran, D.N., Kim, Y.-K., Park, T., Song, Y.S., 2020. Metagenomic Analysis of Serum Microbe-Derived Extracellular Vesicles and Diagnostic Models to Differentiate Ovarian Cancer and Benign Ovarian Tumor. Cancers (Basel) 12, 1309. https://doi.org/10.3390/cancers12051309

Kimura, I., Miyamoto, J., Ohue-Kitano, R., Watanabe, K., Yamada, T., Onuki, M., Aoki, R., Isobe, Y., Kashihara, D., Inoue, D., Inaba, A., Takamura, Y., Taira, S., Kumaki, S., Watanabe, M., Ito, M., Nakagawa, F., Irie, J., Kakuta, H., Shinohara, M., Iwatsuki, K., Tsujimoto, G., Ohno, H., Arita, M., Itoh, H., Hase, K., 2020. Maternal gut microbiota in pregnancy influences offspring metabolic phenotype in mice. Science 367, eaaw8429. https://doi.org/10.1126/science.aaw8429

Klimentová, J., Stulík, J., 2015. Methods of isolation and purification of outer membrane vesicles from gram-negative bacteria. Microbiological Research 170, 1–9. https://doi.org/10.1016/j.micres.2014.09.006

Knoop, K.A., McDonald, K.G., McCrate, S., McDole, J.R., Newberry, R.D., 2015. Microbial Sensing by Goblet Cells Controls Immune Surveillance of Luminal Antigens in the Colon. Mucosal Immunol 8, 198–210. https://doi.org/10.1038/mi.2014.58

Kopp, W., 2019. How Western Diet And Lifestyle Drive The Pandemic Of Obesity And Civilization Diseases. Diabetes, Metabolic Syndrome and Obesity 12, 2221–2236. https://doi.org/10.2147/DMSO.S216791

Kou, Z., Dai, W., 2021. Aryl hydrocarbon receptor: Its roles in physiology. Biochemical Pharmacology 185, 114428. https://doi.org/10.1016/j.bcp.2021.114428

Krautkramer, K.A., Kreznar, J.H., Romano, K.A., Vivas, E.I., Barrett-Wilt, G.A., Rabaglia, M.E., Keller, M.P., Attie, A.D., Rey, F.E., Denu, J.M., 2016. Diet-microbiota interactions mediate global epigenetic programming in multiple host tissues. Mol Cell 64, 982–992. https://doi.org/10.1016/j.molcel.2016.10.025

Kwon, S.-K., Park, J.C., Kim, K.H., Yoon, J., Cho, Y., Lee, B., Lee, J.-J., Jeong, H., Oh, Y., Kim, S.-H., Lee, S.D., Hwang, B.R., Chung, Y., Kim, J.F., Nam, K.T., Lee, Y.C., 2022. Human gastric microbiota transplantation recapitulates premalignant lesions in germ-free mice. Gut 71, 1266–1276. https://doi.org/10.1136/gutjnl-2021-324489

Lagos, L., Leanti La Rosa, S., Ø Arntzen, M., Ånestad, R., Terrapon, N., Gaby, J.C., Westereng, B., 2020. Isolation and Characterization of Extracellular Vesicles Secreted In Vitro by Porcine Microbiota. Microorganisms 8, 983. https://doi.org/10.3390/microorganisms8070983

Le Roy, T., Llopis, M., Lepage, P., Bruneau, A., Rabot, S., Bevilacqua, C., Martin, P., Philippe, C., Walker, F., Bado, A., Perlemuter, G., Cassard-Doulcier, A.-M., Gérard, P., 2013. Intestinal microbiota determines development of non-alcoholic fatty liver disease in mice. Gut 62, 1787–1794. https://doi.org/10.1136/gutjnl-2012-303816

Lee, Y., Park, J.-Y., Lee, E.-H., Yang, J., Jeong, B.-R., Kim, Y.-K., Seoh, J.-Y., Lee, S., Han, P.-L., Kim, E.-J., 2017. Rapid Assessment of Microbiota Changes in Individuals with Autism Spectrum Disorder Using Bacteria-derived Membrane Vesicles in Urine. Exp Neurobiol 26, 307–317. https://doi.org/10.5607/en.2017.26.5.307

Lee, Y.K., Menezes, J.S., Umesaki, Y., Mazmanian, S.K., 2011. Proinflammatory T-cell responses to gut microbiota promote experimental autoimmune encephalomyelitis. Proc Natl Acad Sci U S A 108 Suppl 1, 4615–4622. https://doi.org/10.1073/pnas.1000082107

Lee, Y.S., Kim, J.H., Lim, D.H., 2020. Urine Microbe-Derived Extracellular Vesicles in Children With Asthma. Allergy Asthma Immunol Res 13, 75–87. https://doi.org/10.4168/aair.2021.13.1.75

Levy, M., Thaiss, C.A., Elinav, E., 2016. Metabolites: messengers between the microbiota and the immune system. Genes Dev 30, 1589–1597. https://doi.org/10.1101/gad.284091.116

Li, G., Lin ,Jian, Zhang ,Cui, Gao ,Han, Lu ,Huiying, Gao ,Xiang, Zhu ,Ruixin, Li ,Zhitao, Li ,Mingsong, and Liu, Z., 2021. Microbiota metabolite butyrate constrains neutrophil functions and ameliorates mucosal inflammation in inflammatory bowel disease. Gut Microbes 13, 1968257. https://doi.org/10.1080/19490976.2021.1968257

Li, Y., Innocentin, S., Withers, D.R., Roberts, N.A., Gallagher, A.R., Grigorieva, E.F., Wilhelm, C., Veldhoen, M., 2011. Exogenous stimuli maintain intraepithelial lymphocytes via aryl hydrocarbon receptor activation. Cell 147, 629–640. https://doi.org/10.1016/j.cell.2011.09.025

Li, Y., Toothaker, J.M., Ben-Simon, S., Ozeri, L., Schweitzer, R., McCourt, B.T., McCourt, C.C., Werner, L., Snapper, S.B., Shouval, D.S., Khatib, S., Koren, O., Agnihorti, S., Tseng, G., Konnikova, L., 2020. In utero human intestine harbors unique metabolome, including bacterial metabolites. JCI Insight 5, e138751. https://doi.org/10.1172/jci.insight.138751

Lin, Y., Wang, Jingyu, Bu, F., Zhang, R., Wang, Junhui, Wang, Y., Huang, M., Huang, Y., Zheng, L., Wang, Q., Hu, X., 2025. Bacterial extracellular vesicles in the initiation, progression and treatment of atherosclerosis. Gut Microbes 17, 2452229. https://doi.org/10.1080/19490976.2025.2452229

Littlewood-Evans, A., Sarret, S., Apfel, V., Loesle, P., Dawson, J., Zhang, J., Muller, A., Tigani, B., Kneuer, R., Patel, S., Valeaux, S., Gommermann, N., Rubic-Schneider, T., Junt, T., Carballido, J.M., 2016. GPR91 senses extracellular succinate released from inflammatory macrophages and exacerbates rheumatoid arthritis. J Exp Med 213, 1655–1662. https://doi.org/10.1084/jem.20160061

López, P., González-Rodríguez, I., Sánchez, B., Gueimonde, M., Margolles, A., Suárez, A., 2012. Treg-inducing membrane vesicles from Bifidobacterium bifidum LMG13195 as potential adjuvants in immunotherapy. Vaccine 30, 825–829. https://doi.org/10.1016/j.vaccine.2011.11.115

Luczynski, P., McVey Neufeld, K.-A., Oriach, C.S., Clarke, G., Dinan, T.G., Cryan, J.F., 2016. Growing up in a Bubble: Using Germ-Free Animals to Assess the Influence of the Gut Microbiota on Brain and Behavior. Int J Neuropsychopharmacol 19, pyw020. https://doi.org/10.1093/ijnp/pyw020

Macia, L., Nanan, R., Hosseini-Beheshti, E., Grau, G.E., 2019. Host- and Microbiota-Derived Extracellular Vesicles, Immune Function, and Disease Development. Int J Mol Sci 21, 107. https://doi.org/10.3390/ijms21010107

Macia, L., Tan, J., Vieira, A.T., Leach, K., Stanley, D., Luong, S., Maruya, M., Ian McKenzie, C., Hijikata, A., Wong, C., Binge, L., Thorburn, A.N., Chevalier, N., Ang, C., Marino, E., Robert, R., Offermanns, S., Teixeira, M.M., Moore, R.J., Flavell, R.A., Fagarasan, S., Mackay, C.R., 2015. Metabolite-sensing receptors GPR43 and GPR109A facilitate dietary fibre-induced gut homeostasis through regulation of the inflammasome. Nat Commun 6, 6734. https://doi.org/10.1038/ncomms7734

Macias-Ceja, D.C., Ortiz-Masiá, D., Salvador, P., Gisbert-Ferrándiz, L., Hernández, C., Hausmann, M., Rogler, G., Esplugues, J.V., Hinojosa, J., Alós, R., Navarro, F., Cosin-Roger, J., Calatayud, S., Barrachina, M.D., 2019. Succinate receptor mediates intestinal inflammation and fibrosis. Mucosal Immunol 12, 178–187. https://doi.org/10.1038/s41385-018-0087-3

Macpherson, A.J., Köller, Y., McCoy, K.D., 2015. The bilateral responsiveness between intestinal microbes and IgA. Trends in Immunology 36, 460–470. https://doi.org/10.1016/j.it.2015.06.006

Malmuthuge, N., Griebel, P.J., 2018. Fetal environment and fetal intestine are sterile during the third trimester of pregnancy. Vet Immunol Immunopathol 204, 59–64. https://doi.org/10.1016/j.vetimm.2018.09.005

Mantis, N.J., McGuinness, C.R., Sonuyi, O., Edwards, G., Farrant, S.A., 2006. Immunoglobulin A Antibodies against Ricin A and B Subunits Protect Epithelial Cells from Ricin Intoxication. Infect Immun 74, 3455–3462. https://doi.org/10.1128/IAI.02088-05

Maslowski, K.M., Vieira, A.T., Ng, A., Kranich, J., Sierro, F., Yu, D., Schilter, H.C., Rolph, M.S., Mackay, F., Artis, D., Xavier, R.J., Teixeira, M.M., Mackay, C.R., 2009. Regulation of inflammatory responses by gut microbiota and chemoattractant receptor GPR43. Nature 461, 1282–1286. https://doi.org/10.1038/nature08530

Mathias, A., Pais, B., Favre, L., Benyacoub, J., Corthésy, B., 2014. Role of secretory IgA in the mucosal sensing of commensal bacteria. Gut Microbes 5, 688–695. https://doi.org/10.4161/19490976.2014.983763

Mazmanian, S.K., Liu, C.H., Tzianabos, A.O., Kasper, D.L., 2005. An immunomodulatory molecule of symbiotic bacteria directs maturation of the host immune system. Cell 122, 107–118. https://doi.org/10.1016/j.cell.2005.05.007

Mazmanian, S.K., Round, J.L., Kasper, D.L., 2008. A microbial symbiosis factor prevents intestinal inflammatory disease. Nature 453, 620–625. https://doi.org/10.1038/nature07008

McDole, J.R., Wheeler, L.W., McDonald, K.G., Wang, B., Konjufca, V., Knoop, K.A., Newberry, R.D., Miller, M.J., 2012. Goblet cells deliver luminal antigen to CD103+ DCs in the small intestine. Nature 483, 345–349. https://doi.org/10.1038/nature10863

McDonald, B.D., Jabri, B., Bendelac, A., 2018. Diverse developmental pathways of intestinal intraepithelial lymphocytes. Nat Rev Immunol 18, 514–525. https://doi.org/10.1038/s41577-018-0013-7

McMillan, H.M., Kuehn, M.J., 2021. The extracellular vesicle generation paradox: a bacterial point of view. EMBO J 40, e108174. https://doi.org/10.15252/embj.2021108174

Melo-Marques, I., Cardoso, S.M., Empadinhas, N., 2024. Bacterial extracellular vesicles at the interface of gut microbiota and immunity. Gut Microbes 16, 2396494. https://doi.org/10.1080/19490976.2024.2396494

Meng, R., Zeng, M., Ji, Y., Huang, X., Xu, M., 2023. The potential role of gut microbiota outer membrane vesicles in colorectal cancer. Front Microbiol 14, 1270158. https://doi.org/10.3389/fmicb.2023.1270158

Meyer-Hoffert, U., Hornef, M.W., Henriques-Normark, B., Axelsson, L.-G., Midtvedt, T., Pütsep, K., Andersson, M., 2008. Secreted enteric antimicrobial activity localises to the mucus surface layer. Gut 57, 764–771. https://doi.org/10.1136/gut.2007.141481

Mikulic, J., Longet, S., Favre, L., Benyacoub, J., Corthesy, B., 2017. Secretory IgA in complex with Lactobacillus rhamnosus potentiates mucosal dendritic cell-mediated Treg cell differentiation via TLR regulatory proteins, RALDH2 and secretion of IL-10 and TGF-β. Cell Mol Immunol 14, 546–556. https://doi.org/10.1038/cmi.2015.110

Mirjafari Tafti, Z.S., Moshiri, A., Ettehad Marvasti, F., Tarashi, S., Sadati Khalili, S.F., Motahhary, A., Fateh, A., Vaziri, F., Ahmadi Badi, S., Siadat, S.D., 2019. The effect of saturated and unsaturated fatty acids on the production of outer membrane vesicles from Bacteroides fragilis and Bacteroides thetaiotaomicron. Gastroenterol Hepatol Bed Bench 12, 155–162.

Miron, N., Cristea, V., 2012. Enterocytes: active cells in tolerance to food and microbial antigens in the gut. Clin Exp Immunol 167, 405–412. https://doi.org/10.1111/j.1365-2249.2011.04523.x

Molina-Tijeras, J.A., Gálvez, J., Rodríguez-Cabezas, M.E., 2019. The Immunomodulatory Properties of Extracellular Vesicles Derived from Probiotics: A Novel Approach for the Management of Gastrointestinal Diseases. Nutrients 11, 1038. https://doi.org/10.3390/nu11051038

Monteleone, I., Rizzo, A., Sarra, M., Sica, G., Sileri, P., Biancone, L., MacDonald, T.T., Pallone, F., Monteleone, G., 2011. Aryl Hydrocarbon Receptor-Induced Signals Up-regulate IL-22 Production and Inhibit Inflammation in the Gastrointestinal Tract. Gastroenterology 141, 237-248.e1. https://doi.org/10.1053/j.gastro.2011.04.007

Moore, S.G., Ericsson, A.C., Poock, S.E., Melendez, P., Lucy, M.C., 2017. Hot topic: 16S rRNA gene sequencing reveals the microbiome of the virgin and pregnant bovine uterus. J Dairy Sci 100, 4953–4960. https://doi.org/10.3168/jds.2017-12592

Muniz, L.R., Knosp, C., Yeretssian, G., 2012. Intestinal antimicrobial peptides during homeostasis, infection, and disease. Front Immunol 3, 310. https://doi.org/10.3389/fimmu.2012.00310

Myles, I.A., Fontecilla, N.M., Janelsins, B.M., Vithayathil, P.J., Segre, J.A., Datta, S.K., 2013. Parental dietary fat intake alters offspring microbiome and immunity. J Immunol 191, 10.4049/jimmunol.1301057. https://doi.org/10.4049/jimmunol.1301057

Natividad, J.M., Agus, A., Planchais, J., Lamas, B., Jarry, A.C., Martin, R., Michel, M.-L., Chong-Nguyen, C., Roussel, R., Straube, M., Jegou, S., McQuitty, C., Gall, M.L., Costa, G. da, Lecornet, E., Michaudel, C., Modoux, M., Glodt, J., Bridonneau, C., Sovran, B., Dupraz, L., Bado, A., Richard, M.L., Langella, P., Hansel, B., Launay, J.-M., Xavier, R.J., Duboc, H., Sokol, H., 2018. Impaired Aryl Hydrocarbon Receptor Ligand Production by the Gut Microbiota Is a Key Factor in Metabolic Syndrome. Cell Metabolism 28, 737-749.e4. https://doi.org/10.1016/j.cmet.2018.07.001

Neish, A.S., 2009. Microbes in Gastrointestinal Health and Disease. Gastroenterology 136, 65–80. https://doi.org/10.1053/j.gastro.2008.10.080

Nitzan, O., Elias, M., Peretz, A., Saliba, W., 2016. Role of antibiotics for treatment of inflammatory bowel disease. World J Gastroenterol 22, 1078–1087. https://doi.org/10.3748/wjg.v22.i3.1078

O'Donoghue, E.J., Krachler, A.M., 2016. Mechanisms of outer membrane vesicle entry into host cells. Cell Microbiol 18, 1508–1517. https://doi.org/10.1111/cmi.12655

Oh, J.Z., Ravindran, R., Chassaing, B., Carvalho, F.A., Maddur, M.S., Bower, M., Hakimpour, P., Gill, K.P., Nakaya, H.I., Yarovinsky, F., Sartor, R.B., Gewirtz, A.T., Pulendran, B., 2014. TLR5-mediated sensing of gut microbiota is necessary for antibody responses to seasonal influenza vaccination. Immunity 41, 478–492. https://doi.org/10.1016/j.immuni.2014.08.009

Okada, H., Kuhn, C., Feillet, H., Bach, J.-F., 2010. The 'hygiene hypothesis' for autoimmune and allergic diseases: an update. Clin Exp Immunol 160, 1–9. https://doi.org/10.1111/j.1365-2249.2010.04139.x

Okumura, R., Takeda, K., 2017. Roles of intestinal epithelial cells in the maintenance of gut homeostasis. Exp Mol Med 49, e338–e338. https://doi.org/10.1038/emm.2017.20

Olovo, C.V., Wiredu Ocansey, D.K., Ji, Y., Huang, X., Xu, M., 2024. Bacterial membrane vesicles in the pathogenesis and treatment of inflammatory bowel disease. Gut Microbes 16, 2341670. https://doi.org/10.1080/19490976.2024.2341670

Olszak, T., An, D., Zeissig, S., Vera, M.P., Richter, J., Franke, A., Glickman, J.N., Siebert, R., Baron, R.M., Kasper, D.L., Blumberg, R.S., 2012. Microbial Exposure During Early Life Has Persistent Effects on Natural Killer T Cell Function. Science 336, 489–493. https://doi.org/10.1126/science.1219328

Pabst, O., 2012. New concepts in the generation and functions of IgA. Nat Rev Immunol 12, 821–832. https://doi.org/10.1038/nri3322

Pabst, O., Cerovic, V., Hornef, M., 2016. Secretory IgA in the Coordination of Establishment and Maintenance of the Microbiota. Trends in Immunology 37, 287–296. https://doi.org/10.1016/j.it.2016.03.002

Palm, N.W., de Zoete, M.R., Cullen, T.W., Barry, N.A., Stefanowski, J., Hao, L., Degnan, P.H., Hu, J., Peter, I., Zhang, W., Ruggiero, E., Cho, J.H., Goodman, A.L., Flavell, R.A., 2014. Immunoglobulin A coating identifies colitogenic bacteria in inflammatory bowel disease. Cell 158, 1000–1010. https://doi.org/10.1016/j.cell.2014.08.006

Panzer, J.J., Romero, R., Greenberg, J.M., Winters, A.D., Galaz, J., Gomez-Lopez, N., Theis, K.R., 2023. Is there a placental microbiota? A critical review and re-analysis of published placental microbiota datasets. BMC Microbiol 23, 76. https://doi.org/10.1186/s12866-023-02764-6

Park, J., Kim, N.-E., Yoon, H., Shin, C.M., Kim, N., Lee, D.H., Park, J.Y., Choi, C.H., Kim, J.G., Kim, Y.-K., Shin, T.-S., Yang, J., Park, Y.S., 2021. Fecal Microbiota and Gut Microbe-Derived Extracellular Vesicles in Colorectal Cancer. Front Oncol 11, 650026. https://doi.org/10.3389/fonc.2021.650026

Park, J., Lee, J.J., Hong, Y., Seo, H., Shin, T.-S., Hong, J.Y., 2022. Metagenomic Analysis of Plasma Microbial Extracellular Vesicles in Patients Receiving Mechanical Ventilation: A Pilot Study. J Pers Med 12, 564. https://doi.org/10.3390/jpm12040564

Park, J.-Y., Kang, C.-S., Seo, H.-C., Shin, J.-C., Kym, S.-M., Park, Y.-S., Shin, T.-S., Kim, J.-G., Kim, Y.-K., 2021. Bacteria-Derived Extracellular Vesicles in Urine as a Novel Biomarker for Gastric Cancer: Integration of Liquid Biopsy and Metagenome Analysis. Cancers 13, 4687. https://doi.org/10.3390/cancers13184687

Pelaseyed, T., Bergström, J.H., Gustafsson, J.K., Ermund, A., Birchenough, G.M.H., Schütte, A., van der Post, S., Svensson, F., Rodríguez-Piñeiro, A.M., Nyström, E.E.L., Wising, C., Johansson, M.E.V., Hansson, G.C., 2014. The mucus and mucins of the goblet cells and enterocytes provide the first defense line of the gastrointestinal tract and interact with the immune system. Immunol Rev 260, 8–20. https://doi.org/10.1111/imr.12182

Perez-Muñoz, M.E., Arrieta, M.-C., Ramer-Tait, A.E., Walter, J., 2017. A critical assessment of the "sterile womb" and "in utero colonization" hypotheses: implications for research on the pioneer infant microbiome. Microbiome 5, 48. https://doi.org/10.1186/s40168-017-0268-4

Pessa-Morikawa, T., Husso, A., Kärkkäinen, O., Koistinen, V., Hanhineva, K., Iivanainen, A., Niku, M., 2022. Maternal microbiota-derived metabolic profile in fetal murine intestine, brain and placenta. BMC Microbiology 22, 46. https://doi.org/10.1186/s12866-022-02457-6

Peterson, D.A., McNulty, N.P., Guruge, J.L., Gordon, J.I., 2007. IgA response to symbiotic bacteria as a mediator of gut homeostasis. Cell Host Microbe 2, 328–339. https://doi.org/10.1016/j.chom.2007.09.013

Pinget, G.V., Tan, J.K., Ni, D., Taitz, J., Daien, C.I., Mielle, J., Moore, R.J., Stanley, D., Simpson, S., King, N.J.C., Macia, L., 2022. Dysbiosis in imiquimod-induced psoriasis alters gut immunity and exacerbates colitis development. Cell Rep 40, 111191. https://doi.org/10.1016/j.celrep.2022.111191

Plovier, H., Everard, A., Druart, C., Depommier, C., Van Hul, M., Geurts, L., Chilloux, J., Ottman, N., Duparc, T., Lichtenstein, L., Myridakis, A., Delzenne, N.M., Klievink, J., Bhattacharjee, A., van der Ark, K.C.H., Aalvink, S., Martinez, L.O., Dumas, M.-E., Maiter, D., Loumaye, A., Hermans, M.P., Thissen, J.-P., Belzer, C., de Vos, W.M., Cani, P.D., 2017. A purified membrane protein from Akkermansia muciniphila or the pasteurized bacterium improves metabolism in obese and diabetic mice. Nat Med 23, 107–113. https://doi.org/10.1038/nm.4236

Postal, B.G., Ghezzal, S., Aguanno, D., André, S., Garbin, K., Genser, L., Brot-Laroche, E., Poitou, C., Soula, H., Leturque, A., Clément, K., Carrière, V., 2020. AhR activation defends gut barrier integrity against damage occurring in obesity. Molecular Metabolism 39, 101007. https://doi.org/10.1016/j.molmet.2020.101007

Prados-Rosales, R., Weinrick, B.C., Piqué, D.G., Jacobs, W.R., Casadevall, A., Rodriguez, G.M., 2014. Role for Mycobacterium tuberculosis membrane vesicles in iron acquisition. J Bacteriol 196, 1250–1256. https://doi.org/10.1128/JB.01090-13

Price, A.E., Shamardani, K., Lugo, K.A., Deguine, J., Roberts, A.W., Lee, B.L., Barton, G.M., 2018. A map of Toll-like receptor expression in the intestinal epithelium reveals distinct spatial, cell type-specific, and temporal patterns. Immunity 49, 560-575.e6. https://doi.org/10.1016/j.immuni.2018.07.016

Psichas, A., Sleeth, M.L., Murphy, K.G., Brooks, L., Bewick, G.A., Hanyaloglu, A.C., Ghatei, M.A., Bloom, S.R., Frost, G., 2015. The short chain fatty acid propionate stimulates GLP-1 and PYY secretion via free fatty acid receptor 2 in rodents. Int J Obes (Lond) 39, 424–429. https://doi.org/10.1038/ijo.2014.153

Pumbwe, L., Skilbeck, C.A., Nakano, V., Avila-Campos, M.J., Piazza, R.M.F., Wexler, H.M., 2007. Bile salts enhance bacterial co-aggregation, bacterial-intestinal epithelial cell adhesion, biofilm formation

and antimicrobial resistance of Bacteroides fragilis. Microb Pathog 43, 78–87. https://doi.org/10.1016/j.micpath.2007.04.002

Qiu, J., Heller, J.J., Guo, X., Chen, Z.E., Fish, K., Fu, Y.-X., Zhou, L., 2012. The aryl hydrocarbon receptor regulates gut immunity through modulation of innate lymphoid cells. Immunity 36, 92–104. https://doi.org/10.1016/j.immuni.2011.11.011

Rakoff-Nahoum, S., Coyne, M.J., Comstock, L.E., 2014. An ecological network of polysaccharide utilization among human intestinal symbionts. Curr Biol 24, 40–49. https://doi.org/10.1016/j.cub.2013.10.077

Rakoff-Nahoum, S., Paglino, J., Eslami-Varzaneh, F., Edberg, S., Medzhitov, R., 2004. Recognition of commensal microflora by toll-like receptors is required for intestinal homeostasis. Cell 118, 229–241. https://doi.org/10.1016/j.cell.2004.07.002

Ramirez, J., Guarner, F., Bustos Fernandez, L., Maruy, A., Sdepanian, V.L., Cohen, H., 2020. Antibiotics as Major Disruptors of Gut Microbiota. Front Cell Infect Microbiol 10, 572912. https://doi.org/10.3389/fcimb.2020.572912

Raya-Sandino, A., Lozada-Soto, K.M., Rajagopal, N., Garcia-Hernandez, V., Luissint, A.-C., Brazil, J.C., Cui, G., Koval, M., Parkos, C.A., Nangia, S., Nusrat, A., 2023. Claudin-23 reshapes epithelial tight junction architecture to regulate barrier function. Nat Commun 14, 6214. https://doi.org/10.1038/s41467-023-41999-9

Rey, J., Garin, N., Spertini, F., Corthésy, B., 2004. Targeting of secretory IgA to Peyer's patch dendritic and T cells after transport by intestinal M cells. J Immunol 172, 3026–3033. https://doi.org/10.4049/jimmunol.172.5.3026

Rhee, S.J., Kim, H., Lee, Y., Lee, H.J., Park, C.H.K., Yang, J., Kim, Y.-K., Kym, S., Ahn, Y.M., 2020. Comparison of serum microbiome composition in bipolar and major depressive disorders. J Psychiatr Res 123, 31–38. https://doi.org/10.1016/j.jpsychires.2020.01.004

Rinninella, E., Raoul, P., Cintoni, M., Franceschi, F., Miggiano, G.A.D., Gasbarrini, A., Mele, M.C., 2019. What is the Healthy Gut Microbiota Composition? A Changing Ecosystem across Age, Environment, Diet, and Diseases. Microorganisms 7, 14. https://doi.org/10.3390/microorganisms7010014

Rochereau, N., Drocourt, D., Perouzel, E., Pavot, V., Redelinghuys, P., Brown, G.D., Tiraby, G., Roblin, X., Verrier, B., Genin, C., Corthésy, B., Paul, S., 2013. Dectin-1 Is Essential for Reverse Transcytosis of Glycosylated SIgA-Antigen Complexes by Intestinal M Cells. PLoS Biol 11, e1001658. https://doi.org/10.1371/journal.pbio.1001658

Rodríguez-Díaz, C., Martín-Reyes, F., Taminiau, B., Ho-Plágaro, A., Camargo, R., Fernandez-Garcia, F., Pinazo-Bandera, J., Toro-Ortiz, J.P., Gonzalo, M., López-Gómez, C., Rodríguez-Pacheco, F., Rodríguez de Los Ríos, D., Daube, G., Alcain-Martinez, G., García-Fuentes, E., 2023. The Metagenomic Composition and Effects of Fecal-Microbe-Derived Extracellular Vesicles on Intestinal Permeability Depend on the Patient's Disease. Int J Mol Sci 24, 4971. https://doi.org/10.3390/ijms24054971

Rowland, I., Gibson, G., Heinken, A., Scott, K., Swann, J., Thiele, I., Tuohy, K., 2018. Gut microbiota functions: metabolism of nutrients and other food components. Eur J Nutr 57, 1–24. https://doi.org/10.1007/s00394-017-1445-8

Rubio, A.P.D., Martínez, J., Palavecino, M., Fuentes, F., López, C.M.S., Marcilla, A., Pérez, O.E., Piuri, M., 2020. Transcytosis of Bacillus subtilis extracellular vesicles through an in vitro intestinal epithelial cell model. Sci Rep 10, 3120. https://doi.org/10.1038/s41598-020-60077-4

Sait, L.C., Galic, M., Price, J.D., Simpfendorfer, K.R., Diavatopoulos, D.A., Uren, T.K., Janssen, P.H., Wijburg, O.L.C., Strugnell, R.A., 2007. Secretory antibodies reduce systemic antibody responses against the gastrointestinal commensal flora. Int Immunol 19, 257–265. https://doi.org/10.1093/intimm/dxl142

Salzman, N.H., Hung, K., Haribhai, D., Chu, H., Karlsson-Sjöberg, J., Amir, E., Teggatz, P., Barman, M., Hayward, M., Eastwood, D., Stoel, M., Zhou, Y., Sodergren, E., Weinstock, G.M., Bevins, C.L., Williams, C.B., Bos, N.A., 2010. Enteric defensins are essential regulators of intestinal microbial ecology. Nat Immunol 11, 76–83. https://doi.org/10.1038/ni.1825

Samra, M., Nam, S.K., Lim, D.H., Kim, D.H., Yang, J., Kim, Y.-K., Kim, J.H., 2019. Urine Bacteria-Derived Extracellular Vesicles and Allergic Airway Diseases in Children. Int Arch Allergy Immunol 178, 150–158. https://doi.org/10.1159/000492677

Sanchez, C.J., Akers, K.S., Romano, D.R., Woodbury, R.L., Hardy, S.K., Murray, C.K., Wenke, J.C., 2014. D-amino acids enhance the activity of antimicrobials against biofilms of clinical wound isolates of Staphylococcus aureus and Pseudomonas aeruginosa. Antimicrob Agents Chemother 58, 4353–4361. https://doi.org/10.1128/AAC.02468-14

Sano, T., Huang, W., Hall, J.A., Yang, Y., Chen, A., Gavzy, S.J., Lee, J.-Y., Ziel, J.W., Miraldi, E.R., Domingos, A.I., Bonneau, R., Littman, D.R., 2015. An IL-23R/IL-22 Circuit Regulates Epithelial Serum Amyloid A to Promote Local Effector Th17 Responses. Cell 163, 381–393. https://doi.org/10.1016/j.cell.2015.08.061

Santacroce, L., Charitos, I.A., Colella, M., Palmirotta, R., Jirillo, E., 2024. Blood Microbiota and Its Products: Mechanisms of Interference with Host Cells and Clinical Outcomes. Hematol Rep 16, 440–453. https://doi.org/10.3390/hematolrep16030043

Schaack, B., Hindré, T., Quansah, N., Hannani, D., Mercier, C., Laurin, D., 2022. Microbiota-Derived Extracellular Vesicles Detected in Human Blood from Healthy Donors. Int J Mol Sci 23, 13787. https://doi.org/10.3390/ijms232213787

Schaub, B., Liu, J., Höppler, S., Schleich, I., Huehn, J., Olek, S., Wieczorek, G., Illi, S., von Mutius, E., 2009. Maternal farm exposure modulates neonatal immune mechanisms through regulatory T cells. J Allergy Clin Immunol 123, 774-782.e5. https://doi.org/10.1016/j.jaci.2009.01.056

Schneider, C., O'Leary, C.E., Locksley, R.M., 2019. Regulation of immune responses by tuft cells. Nat Rev Immunol 19, 584–593. https://doi.org/10.1038/s41577-019-0176-x

Schulthess, J., Pandey, S., Capitani, M., Rue-Albrecht, K.C., Arnold, I., Franchini, F., Chomka, A., Ilott, N.E., Johnston, D.G.W., Pires, E., McCullagh, J., Sansom, S.N., Arancibia-Cárcamo, C.V., Uhlig, H.H., Powrie, F., 2019. The Short Chain Fatty Acid Butyrate Imprints an Antimicrobial Program in Macrophages. Immunity 50, 432-445.e7. https://doi.org/10.1016/j.immuni.2018.12.018

Schwechheimer, C., Kuehn, M.J., 2015. Outer-membrane vesicles from Gram-negative bacteria: biogenesis and functions. Nat Rev Microbiol 13, 605–619. https://doi.org/10.1038/nrmicro3525

Seet, E.L., Yee, J.K., Jellyman, J.K., Han, G., Ross, M.G., Desai, M., 2015. Maternal High-Fat-Diet Programs Rat Offspring Liver Fatty Acid Metabolism. Lipids 50, 565–573. https://doi.org/10.1007/s11745-015-4018-8

Segui-Perez, C., Stapels, D.A.C., Ma, Z., Su, J., Passchier, E., Westendorp, B., Wubbolts, R.W., Wu, W., van Putten, J.P.M., Strijbis, K., 2024. MUC13 negatively regulates tight junction proteins and intestinal epithelial barrier integrity via protein kinase C. J Cell Sci 137, jcs261468. https://doi.org/10.1242/jcs.261468

Seo, M.K., Park, E.J., Ko, S.Y., Choi, E.W., Kim, S., 2018. Therapeutic effects of kefir grain Lactobacillus-derived extracellular vesicles in mice with 2,4,6-trinitrobenzene sulfonic acid-induced inflammatory bowel disease. J Dairy Sci 101, 8662–8671. https://doi.org/10.3168/jds.2018-15014

Sharon, G., Cruz, N.J., Kang, D.-W., Gandal, M.J., Wang, B., Kim, Y.-M., Zink, E.M., Casey, C.P., Taylor, B.C., Lane, C.J., Bramer, L.M., Isern, N.G., Hoyt, D.W., Noecker, C., Sweredoski, M.J., Moradian, A., Borenstein, E., Jansson, J.K., Knight, R., Metz, T.O., Lois, C., Geschwind, D.H., Krajmalnik-Brown, R., Mazmanian, S.K., 2019. Human Gut Microbiota from Autism Spectrum Disorder Promote Behavioral Symptoms in Mice. Cell 177, 1600-1618.e17. https://doi.org/10.1016/j.cell.2019.05.004

Shen, L., Weber, C.R., Raleigh, D.R., Yu, D., Turner, J.R., 2011. Tight Junction Pore and Leak Pathways: A Dynamic Duo. Annu Rev Physiol 73, 283–309. https://doi.org/10.1146/annurev-physiol-012110-142150

Shen, Q., Huang, Z., Yao, J., Jin, Y., 2021. Extracellular vesicles-mediated interaction within intestinal microenvironment in inflammatory bowel disease. J Adv Res 37, 221–233. https://doi.org/10.1016/j.jare.2021.07.002

Shen, Y., Giardino Torchia, M.L., Lawson, G.W., Karp, C.L., Ashwell, J.D., Mazmanian, S.K., 2012. Outer membrane vesicles of a human commensal mediate immune regulation and disease protection. Cell Host Microbe 12, 509–520. https://doi.org/10.1016/j.chom.2012.08.004

Sheng, Y.H., Triyana, S., Wang, R., Das, I., Gerloff, K., Florin, T.H., Sutton, P., McGuckin, M.A., 2013. MUC1 and MUC13 differentially regulate epithelial inflammation in response to inflammatory and infectious stimuli. Mucosal Immunol 6, 557–568. https://doi.org/10.1038/mi.2012.98

Shin, C., Baik, I., 2023. Bacterial Extracellular Vesicle Composition in Human Urine and the 10-Year Risk of Abdominal Obesity. Metabolic Syndrome and Related Disorders 21, 233–242. https://doi.org/10.1089/met.2022.0109

Singh, R.K., Chang, H.-W., Yan, D., Lee, K.M., Ucmak, D., Wong, K., Abrouk, M., Farahnik, B., Nakamura, M., Zhu, T.H., Bhutani, T., Liao, W., 2017. Influence of diet on the gut microbiome and implications for human health. J Transl Med 15, 73. https://doi.org/10.1186/s12967-017-1175-y

Smith, K., McCoy, K.D., Macpherson, A.J., 2007. Use of axenic animals in studying the adaptation of mammals to their commensal intestinal microbiota. Semin Immunol 19, 59–69. https://doi.org/10.1016/j.smim.2006.10.002

Soldán, M., Argalášová, Ľ., Hadvinová, L., Galileo, B., Babjaková, J., 2024. The Effect of Dietary Types on Gut Microbiota Composition and Development of Non-Communicable Diseases: A Narrative Review. Nutrients 16, 3134. https://doi.org/10.3390/nu16183134

Sommer, F., Bäckhed, F., 2013. The gut microbiota--masters of host development and physiology. Nat Rev Microbiol 11, 227–238. https://doi.org/10.1038/nrmicro2974

Song, Y., Shi, M., Wang, Y., 2024. Deciphering the role of host-gut microbiota crosstalk via diverse sources of extracellular vesicles in colorectal cancer. Mol Med 30, 200. https://doi.org/10.1186/s10020-024-00976-8

Stentz, R., Carvalho, A.L., Jones, E.J., Carding, S.R., 2018. Fantastic voyage: the journey of intestinal microbiota-derived microvesicles through the body. Biochem Soc Trans 46, 1021–1027. https://doi.org/10.1042/BST20180114

Stentz, R., Horn, N., Cross, K., Salt, L., Brearley, C., Livermore, D.M., Carding, S.R., 2015. Cephalosporinases associated with outer membrane vesicles released by Bacteroides spp. protect gut pathogens and commensals against β-lactam antibiotics. J Antimicrob Chemother 70, 701–709. https://doi.org/10.1093/jac/dku466

Stentz, R., Jones, E., Juodeikis, R., Wegmann, U., Guirro, M., Goldson, A.J., Brion, A., Booth, C., Sudhakar, P., Brown, I.R., Korcsmáros, T., Carding, S.R., 2022. The Proteome of Extracellular Vesicles Produced by the Human Gut Bacteria Bacteroides thetaiotaomicron In Vivo Is Influenced by Environmental and Host-Derived Factors. Appl Environ Microbiol 88, e0053322. https://doi.org/10.1128/aem.00533-22

Sterpu, I., Fransson, E., Hugerth, L.W., Du, J., Pereira, M., Cheng, L., Radu, S.A., Calderón-Pérez, L., Zha, Y., Angelidou, P., Pennhag, A., Boulund, F., Scheynius, A., Engstrand, L., Wiberg-Itzel, E., Schuppe-Koistinen, I., 2021. No evidence for a placental microbiome in human pregnancies at term. Am J Obstet Gynecol 224, 296.e1-296.e23. https://doi.org/10.1016/j.ajog.2020.08.103

Stolfi, C., Maresca, C., Monteleone, G., Laudisi, F., 2022. Implication of Intestinal Barrier Dysfunction in Gut Dysbiosis and Diseases. Biomedicines 10, 289. https://doi.org/10.3390/biomedicines10020289

Sun, B., Sawant, H., Borthakur, A., Bihl, J.C., 2023. Emerging therapeutic role of gut microbial extracellular vesicles in neurological disorders. Front Neurosci 17, 1241418. https://doi.org/10.3389/fnins.2023.1241418

Tailford, L.E., Crost, E.H., Kavanaugh, D., Juge, N., 2015. Mucin glycan foraging in the human gut microbiome. Front Genet 6, 81. https://doi.org/10.3389/fgene.2015.00081

Takiishi, T., Fenero, C.I.M., Câmara, N.O.S., 2017. Intestinal barrier and gut microbiota: Shaping our immune responses throughout life. Tissue Barriers 5, e1373208. https://doi.org/10.1080/21688370.2017.1373208

Tan, J., McKenzie, C., Potamitis, M., Thorburn, A.N., Mackay, C.R., Macia, L., 2014. The role of short-chain fatty acids in health and disease. Adv Immunol 121, 91–119. https://doi.org/10.1016/B978-0-12-800100-4.00003-9

Tan, J., Taitz, J., Nanan, R., Grau, G., Macia, L., 2023. Dysbiotic Gut Microbiota-Derived Metabolites and Their Role in Non-Communicable Diseases. Int J Mol Sci 24, 15256. https://doi.org/10.3390/ijms242015256

Tedelind, S., Westberg, F., Kjerrulf, M., Vidal, A., 2007. Anti-inflammatory properties of the short-chain fatty acids acetate and propionate: A study with relevance to inflammatory bowel disease. World J Gastroenterol 13, 2826–2832. https://doi.org/10.3748/wjg.v13.i20.2826

Theis, K.R., Romero, R., Greenberg, J.M., Winters, A.D., Garcia-Flores, V., Motomura, K., Ahmad, M.M., Galaz, J., Arenas-Hernandez, M., Gomez-Lopez, N., 2020. No Consistent Evidence for Microbiota in Murine Placental and Fetal Tissues. mSphere 5, e00933-19. https://doi.org/10.1128/mSphere.00933-19

Theis, K.R., Romero, R., Winters, A.D., Greenberg, J.M., Gomez-Lopez, N., Alhousseini, A., Bieda, J., Maymon, E., Pacora, P., Fettweis, J.M., Buck, G.A., Jefferson, K.K., Strauss, J.F., Erez, O., Hassan, S.S., 2019. Does the human placenta delivered at term have a microbiota? Results of cultivation, quantitative real-time PCR, 16S rRNA gene sequencing, and metagenomics. Am J Obstet Gynecol 220, 267.e1-267.e39. https://doi.org/10.1016/j.ajog.2018.10.018

Thompson, C.A., DeLaForest, A., Battle, M.A., 2018. Patterning the gastrointestinal epithelium to confer regional-specific functions. Developmental Biology 435, 97–108. https://doi.org/10.1016/j.ydbio.2018.01.006

Thorburn, A.N., McKenzie, C.I., Shen, S., Stanley, D., Macia, L., Mason, L.J., Roberts, L.K., Wong, C.H.Y., Shim, R., Robert, R., Chevalier, N., Tan, J.K., Mariño, E., Moore, R.J., Wong, L., McConville, M.J., Tull, D.L., Wood, L.G., Murphy, V.E., Mattes, J., Gibson, P.G., Mackay, C.R., 2015. Evidence that asthma is a developmental origin disease influenced by maternal diet and bacterial metabolites. Nat Commun 6, 7320. https://doi.org/10.1038/ncomms8320

Toyofuku, M., Nomura, N., Eberl, L., 2019. Types and origins of bacterial membrane vesicles. Nat Rev Microbiol 17, 13–24. https://doi.org/10.1038/s41579-018-0112-2

Toyofuku, M., Schild, S., Kaparakis-Liaskos, M., Eberl, L., 2023. Composition and functions of bacterial membrane vesicles. Nat Rev Microbiol 21, 415–430. https://doi.org/10.1038/s41579-023-00875-5

Tulkens, J., Vergauwen, G., Van Deun, J., Geeurickx, E., Dhondt, B., Lippens, L., De Scheerder, M.-A., Miinalainen, I., Rappu, P., De Geest, B.G., Vandecasteele, K., Laukens, D., Vandekerckhove, L., Denys, H., Vandesompele, J., De Wever, O., Hendrix, A., 2020. Increased levels of systemic LPS-positive bacterial extracellular vesicles in patients with intestinal barrier dysfunction. Gut 69, 191–193. https://doi.org/10.1136/gutjnl-2018-317726

Turnbaugh, P.J., Ley, R.E., Mahowald, M.A., Magrini, V., Mardis, E.R., Gordon, J.I., 2006. An obesity-associated gut microbiome with increased capacity for energy harvest. Nature 444, 1027–1031. https://doi.org/10.1038/nature05414

Uemura, T., Kawashima, A., Jingushi, K., Motooka, D., Saito, T., Nesrine, S., Oka, T., Okuda, Y., Yamamoto, A., Yamamichi, G., Tomiyama, E., Ishizuya, Y., Yamamoto, Y., Kato, T., Hatano, K., Tsujikawa, K.,

Wada, H., Nonomura, N., 2023. Bacteria-derived DNA in serum extracellular vesicles are biomarkers for renal cell carcinoma. Heliyon 9, e19800. https://doi.org/10.1016/j.heliyon.2023.e19800

Ulluwishewa, D., Anderson, R.C., McNabb, W.C., Moughan, P.J., Wells, J.M., Roy, N.C., 2011. Regulation of Tight Junction Permeability by Intestinal Bacteria and Dietary Components1,2. The Journal of Nutrition 141, 769–776. https://doi.org/10.3945/jn.110.135657

Umar, S., 2010. Intestinal Stem Cells. Curr Gastroenterol Rep 12, 340–348. https://doi.org/10.1007/s11894-010-0130-3

Vaishnava, S., Yamamoto, M., Severson, K.M., Ruhn, K.A., Yu, X., Koren, O., Ley, R., Wakeland, E.K., Hooper, L.V., 2011. The antibacterial lectin RegIIIγ promotes the spatial segregation of microbiota and host in the intestine. Science 334, 255–258. https://doi.org/10.1126/science.1209791

Van der Sluis, M., De Koning, B.A.E., De Bruijn, A.C.J.M., Velcich, A., Meijerink, J.P.P., Van Goudoever, J.B., Büller, H.A., Dekker, J., Van Seuningen, I., Renes, I.B., Einerhand, A.W.C., 2006. Muc2-deficient mice spontaneously develop colitis, indicating that MUC2 is critical for colonic protection. Gastroenterology 131, 117–129. https://doi.org/10.1053/j.gastro.2006.04.020

Verbunt, J., Jocken, J., Blaak, E., Savelkoul, P., Stassen, F., 2024. Gut-bacteria derived membrane vesicles and host metabolic health: a narrative review. Gut Microbes 16, 2359515. https://doi.org/10.1080/19490976.2024.2359515

Volgers, C., Benedikter, B.J., Grauls, G.E., Hellebrand, P.H.M., Savelkoul, P.H.M., Stassen, F.R.M., 2017. Effects of N-acetyl-L-cysteine on the membrane vesicle release and growth of respiratory pathogens. FEMS Microbiol Lett 364. https://doi.org/10.1093/femsle/fnx087

von Mutius, E., 2012. Maternal farm exposure/ingestion of unpasteurized cow's milk and allergic disease. Current Opinion in Gastroenterology 28, 570. https://doi.org/10.1097/MOG.0b013e32835955d3

Voreades, N., Kozil, A., Weir, T.L., 2014. Diet and the development of the human intestinal microbiome. Front Microbiol 5, 494. https://doi.org/10.3389/fmicb.2014.00494

Vuillermin, P.J., O'Hely, M., Collier, F., Allen, K.J., Tang, M.L.K., Harrison, L.C., Carlin, J.B., Saffery, R., Ranganathan, S., Sly, P.D., Gray, L., Molloy, J., Pezic, A., Conlon, M., Topping, D., Nelson, K., Mackay, C.R., Macia, L., Koplin, J., Dawson, S.L., Moreno-Betancur, M., Ponsonby, A.-L., 2020. Maternal carriage of Prevotella during pregnancy associates with protection against food allergy in the offspring. Nat Commun 11, 1452. https://doi.org/10.1038/s41467-020-14552-1

Wagner, M., Hicks, C., El-Omar, E., Combes, V., El-Assaad, F., 2024. The Critical Role of Host and Bacterial Extracellular Vesicles in Endometriosis. Biomedicines 12, 2585. https://doi.org/10.3390/biomedicines12112585

Wastyk, H.C., Fragiadakis, G.K., Perelman, D., Dahan, D., Merrill, B.D., Yu, F.B., Topf, M., Gonzalez, C.G., Van Treuren, W., Han, S., Robinson, J.L., Elias, J.E., Sonnenburg, E.D., Gardner, C.D., Sonnenburg, J.L., 2021. Gut-microbiota-targeted diets modulate human immune status. Cell 184, 4137-4153.e14. https://doi.org/10.1016/j.cell.2021.06.019

Wei, M., Shinkura, R., Doi, Y., Maruya, M., Fagarasan, S., Honjo, T., 2011. Mice carrying a knock-in mutation of Aicda resulting in a defect in somatic hypermutation have impaired gut homeostasis and compromised mucosal defense. Nat Immunol 12, 264–270. https://doi.org/10.1038/ni.1991

Weltzin, R., Lucia-Jandris, P., Michetti, P., Fields, B.N., Kraehenbuhk, J.P., Neutra, M.R., 1989. Binding and transepithelial transport of immunoglobulins by intestinal M cells: demonstration using monoclonal IgA antibodies against enteric viral proteins. J Cell Biol 108, 1673–1685.

Wilson, C.L., Ouellette, A.J., Satchell, D.P., Ayabe, T., López-Boado, Y.S., Stratman, J.L., Hultgren, S.J., Matrisian, L.M., Parks, W.C., 1999. Regulation of Intestinal α-Defensin Activation by the Metalloproteinase Matrilysin in Innate Host Defense. Science 286, 113–117. https://doi.org/10.1126/science.286.5437.113

Winters, A.D., Romero, R., Greenberg, J.M., Galaz, J., Shaffer, Z.D., Garcia-Flores, V., Kracht, D.J., Gomez-Lopez, N., Theis, K.R., 2022. Does the Amniotic Fluid of Mice Contain a Viable Microbiota? Front Immunol 13, 820366. https://doi.org/10.3389/fimmu.2022.820366

Woo, V., Alenghat, T., 2022. Epigenetic regulation by gut microbiota. Gut Microbes 14, 2022407. https://doi.org/10.1080/19490976.2021.2022407

Wu, G.D., Chen, J., Hoffmann, C., Bittinger, K., Chen, Y.-Y., Keilbaugh, S.A., Bewtra, M., Knights, D., Walters, W.A., Knight, R., Sinha, R., Gilroy, E., Gupta, K., Baldassano, R., Nessel, L., Li, H., Bushman, F.D., Lewis, J.D., 2011. Linking long-term dietary patterns with gut microbial enterotypes. Science 334, 105–108. https://doi.org/10.1126/science.1208344

Wu, H.-J., Ivanov, I.I., Darce, J., Hattori, K., Shima, T., Umesaki, Y., Littman, D.R., Benoist, C., Mathis, D., 2010. Gut-residing segmented filamentous bacteria drive autoimmune arthritis via T helper 17 cells. Immunity 32, 815–827. https://doi.org/10.1016/j.immuni.2010.06.001

Wu, S., Hashimoto-Hill, S., Woo, V., Eshleman, E.M., Whitt, J., Engleman, L., Karns, R., Denson, L.A., Haslam, D.B., Alenghat, T., 2020. Microbiota-derived metabolite promotes HDAC3 activity in the gut. Nature 586, 108–112. https://doi.org/10.1038/s41586-020-2604-2

Xie, R., Sun, Y., Wu, J., Huang, S., Jin, G., Guo, Z., Zhang, Y., Liu, T., Liu, X., Cao, X., Wang, B., Cao, H., 2018. Maternal High Fat Diet Alters Gut Microbiota of Offspring and Exacerbates DSS-Induced Colitis in Adulthood. Front Immunol 9, 2608. https://doi.org/10.3389/fimmu.2018.02608

Yamasaki-Yashiki, S., Miyoshi, Y., Nakayama, T., Kunisawa, J., Katakura, Y., 2019. IgA-enhancing effects of membrane vesicles derived from Lactobacillus sakei subsp. sakei NBRC15893. Biosci Microbiota Food Health 38, 23–29. https://doi.org/10.12938/bmfh.18-015

Yáñez-Mó, M., Siljander, P.R.-M., Andreu, Z., Zavec, A.B., Borràs, F.E., Buzas, E.I., Buzas, K., Casal, E., Cappello, F., Carvalho, J., Colás, E., Cordeiro-da Silva, A., Fais, S., Falcon-Perez, J.M., Ghobrial, I.M., Giebel, B., Gimona, M., Graner, M., Gursel, I., Gursel, M., Heegaard, N.H.H., Hendrix, A., Kierulf, P., Kokubun, K., Kosanovic, M., Kralj-Iglic, V., Krämer-Albers, E.-M., Laitinen, S., Lässer, C., Lener, T., Ligeti, E., Linē, A., Lipps, G., Llorente, A., Lötvall, J., Manček-Keber, M., Marcilla, A., Mittelbrunn, M., Nazarenko, I., Nolte-'t Hoen, E.N.M., Nyman, T.A., O'Driscoll, L., Olivan, M., Oliveira, C., Pállinger, É., Del Portillo, H.A., Reventós, J., Rigau, M., Rohde, E., Sammar, M., Sánchez-Madrid, F., Santarém, N., Schallmoser, K., Ostenfeld, M.S., Stoorvogel, W., Stukelj, R., Van der Grein, S.G., Vasconcelos, M.H., Wauben, M.H.M., De Wever, O., 2015. Biological properties of extracellular vesicles and their physiological functions. J Extracell Vesicles 4, 27066. https://doi.org/10.3402/jev.v4.27066

Yang, J., McDowell, A., Seo, H., Kim, S., Min, T.K., Jee, Y.K., Choi, Y., Park, H.S., Pyun, B.Y., Kim, Y.K., 2020. Diagnostic Models for Atopic Dermatitis Based on Serum Microbial Extracellular Vesicle Metagenomic Analysis: A Pilot Study. Allergy Asthma Immunol Res 12, 792–805. https://doi.org/10.4168/aair.2020.12.5.792

Yang, L., Liu, T., Liao, Y., Ren, Y., Zheng, Z., Zhang, M., Yu, Y., Liu, C., Wang, C., Chen, T., Zhang, L., Zheng, D., Zhao, H., Ni, Z., Liu, X., 2024. Potential therapeutic application and mechanism of gut microbiota-derived extracellular vesicles in polycystic ovary syndrome. Biomedicine & Pharmacotherapy 180, 117504. https://doi.org/10.1016/j.biopha.2024.117504

Yoon, H., Kim, N.-E., Park, J., Shin, C.M., Kim, N., Lee, D.H., Park, J.Y., Choi, C.H., Kim, J.G., Park, Y.S., 2023. Analysis of the gut microbiome using extracellular vesicles in the urine of patients with colorectal cancer. Korean J Intern Med 38, 27–38. https://doi.org/10.3904/kjim.2022.112

Zakharzhevskaya, N.B., Vanyushkina, A.A., Altukhov, I.A., Shavarda, A.L., Butenko, I.O., Rakitina, D.V., Nikitina, A.S., Manolov, A.I., Egorova, A.N., Kulikov, E.E., Vishnyakov, I.E., Fisunov, G.Y., Govorun, V.M., 2017. Outer membrane vesicles secreted by pathogenic and nonpathogenic Bacteroides fragilis represent different metabolic activities. Sci Rep 7, 5008. https://doi.org/10.1038/s41598-017-05264-6

Zeng, Y., Yin, Y., Zhou, X., 2024. Insights into Microbiota–Host Crosstalk in the Intestinal Diseases Mediated by Extracellular Vesicles and Their Encapsulated MicroRNAs. Int J Mol Sci 25, 13001. https://doi.org/10.3390/ijms252313001

Zhang, Y.-M., Rock, C.O., 2008. Membrane lipid homeostasis in bacteria. Nat Rev Microbiol 6, 222–233. https://doi.org/10.1038/nrmicro1839

Zhao, M., He, S., Wen, R., Li, C., Chen, X., Lin, X., Wang, H., Tang, Y., 2024. Membrane vesicles derived from Enterococcus faecalis promote the co-transfer of important antibiotic resistance genes located on both plasmids and chromosomes. Journal of Antimicrobial Chemotherapy 79, 320–326. https://doi.org/10.1093/jac/dkad381

Zhao, Q., Yu, J., Hao, Y., Zhou, H., Hu, Y., Zhang, C., Zheng, H., Wang, X., Zeng, F., Hu, J., Gu, L., Wang, Z., Zhao, F., Yue, C., Zhou, P., Zhang, H., Huang, N., Wu, W., Zhou, Y., Li, J., 2023. Akkermansia muciniphila plays critical roles in host health. Critical Reviews in Microbiology 49, 82–100. https://doi.org/10.1080/1040841X.2022.2037506

Zheng, P., Zeng, B., Zhou, C., Liu, M., Fang, Z., Xu, X., Zeng, L., Chen, J., Fan, S., Du, X., Zhang, X., Yang, D., Yang, Y., Meng, H., Li, W., Melgiri, N.D., Licinio, J., Wei, H., Xie, P., 2016. Gut microbiome remodeling induces depressive-like behaviors through a pathway mediated by the host's metabolism. Mol Psychiatry 21, 786–796. https://doi.org/10.1038/mp.2016.44

Zhou, H., Tan, X., Chen, G., Liu, X., Feng, A., Liu, Z., Liu, W., 2025. Extracellular Vesicles of Commensal Skin Microbiota Alleviate Cutaneous Inflammation in Atopic Dermatitis Mouse Model by Re-Establishing Skin Homeostasis. Journal of Investigative Dermatology 145, 312-322.e9. https://doi.org/10.1016/j.jid.2023.02.023

Zhu, B., Xia, X., Xia, N., Zhang, S., Guo, X., 2014. Modification of Fatty acids in membranes of bacteria: implication for an adaptive mechanism to the toxicity of carbon nanotubes. Environ Sci Technol 48, 4086–4095. https://doi.org/10.1021/es404359v

Zhu, Q., Li, M.-X., Yu, M.-C., Ma, Q.-W., Huang, M.-J., Lu, C.-W., Chen, C.-B., Chung, W.-H., Chang, C.-J., 2024. Altered microbiome of serum exosomes in patients with acute and chronic cholecystitis. BMC Microbiol 24, 133. https://doi.org/10.1186/s12866-024-03269-6

Zubair, M., Abouelnazar, F.A., Dawood, A.S., Pan, J., Zheng, X., Chen, T., Liu, P., Mao, F., Yan, Y., Chu, Y., 2024. Microscopic messengers: microbiota-derived bacterial extracellular vesicles in inflammatory bowel disease. Front Microbiol 15, 1481496. https://doi.org/10.3389/fmicb.2024.1481496

Chapter 2 Antibiotic-mediated dysbiosis leads to activation of inflammatory pathways

This chapter has been published as:
Taitz J, Tan J, Ni D, Potier-Villette C, Grau G, Nanan R, Macia L. "Antibiotic-mediated dysbiosis leads to activation of inflammatory pathways" *Front Immunol*. 2025; **15**:1493991
I designed and carried out the majority of the experiments and collaborated on all of them. I analysed the data, and conducted data interpretation, with data curation from co-authors. I wrote the original manuscript. All co-authors contributed to experiments, analysis and manuscript editing.

This work in the context of this thesis:

The gut microbiota is a key determinant of overall host physiology, shaping immune regulation and balance. Antibiotics are major disruptors of gut bacterial communities, and their increasing use is linked to dysregulated gut homeostasis and the rise of NCDs. While early-life exposure to antibiotics is linked to disease by disrupting immune education, how antibiotic exposure in adulthood contributes to NCD development remains poorly understood. This knowledge gap is partly due to variability in antibiotic class and duration, as well as an absence of robust antibiotic mouse models that comprehensively characterise changes to host immunity. This study aimed to address this gap by using vancomycin and polymyxin B to selectively target Gram-positive or Gram-negative bacteria, and provide a comprehensive characterisation of bacterial composition, microbial metabolites, and host immune profiles.

To investigate the impact of extended antibiotic exposures which may occur throughout adulthood, we employed a long-term, twice-daily gavage model, the most consistent

approach for modulating microbiota composition (25). Five weeks of antibiotic treatment significantly altered gut bacterial composition, reducing diversity, and shifting the microbiota towards dysbiosis without affecting total bacterial load or promoting fungal overgrowth (Chapter 2, Figure 1 and Supplementary Figure 1 D, E). Both antibiotics disrupted key bacterial metabolites, reducing butyrate and acetate, while differentially affecting propionate and succinate levels, highlighting that distinct compositional shifts have metabolite-specific consequences (Chapter 2 Figure 2). Vancomycin enhanced the SI sIgA response (Figure 2D), whereas both antibiotics expanded DC populations in the spleen and MLNs, potentially reflecting altered antigen presentation and immune surveillance (Figures 3-4). Notably, antibiotic-treated mice exhibited heightened splenic T cell cytokine production *ex vivo*, with significantly elevated TNF expression (Figure 5).

While we did not directly investigate BEVs in this chapter, it is highly likely they contributed to the findings. As discussed in Chapter 1.4.4, changes in gut microbiota composition have also been linked to shifts in BEV production. Bacterial vesiculation is a stress response, which may be triggered by various factors including nutrient deprivation and exposure to antimicrobials. For example, fasting induces greater vesicle production *in vivo* (shown in Chapter 4 of this thesis), and *in vitro* antibiotics induce vesiculation by triggering bacterial stress and through their cell wall-targeting activity (Chapter 1.4.2). To our knowledge, the impact of oral antibiotics on gut BEV levels *in vivo* has not been studied. However, preliminary analysis from this study (data not shown in following publication) revealed increased faecal BEV levels in antibiotics-treated mice, suggesting that antibiotics do alter BEV levels *in vivo*. While we did not assess the bacterial composition of BEVs, it is likely that shifts in bacterial composition would have led to

corresponding changes in BEV profiles. Given the emerging role of BEVs as key mediators of gut-host cross-talk, further investigation is warranted to investigate how antibiotics and antimicrobials may influence their composition and abundance.

Since the antibiotics used in this study selectively depleted different bacterial species, differences in both the abundance and origin of BEVs may help explain several key findings. For example, increased BEV levels may have triggered the elevated sIgA we observed in vancomycin-treated mice. This would be consistent with our later findings in Chapter 3, where elevated BEV levels promoted T-cell independent IgA production. BEVs are also known to translocate beyond the gut to reach systemic organs, where they can modulate cell function (Chapter 1.4.3). It is plausible that increased circulating BEV levels in antibiotics-treated mice contributed to the heightened TNF expression by splenic T cells *ex vivo*, potentially acting as antigenic stimuli that primed these cells for a heightened response. Thus, while BEVs were not directly investigated in this chapter, they represent a key mechanism of microbiota-host communication that is sensitive to antibiotics. Thus, further investigation is warranted into how BEVs may influence host immunity during antibiotics-induced dysbiosis.

This study provides insight into how antibiotic-induced dysbiosis influences host immune homeostasis and may predispose to disease. Our findings suggest that in otherwise healthy mice, prolonged antibiotic exposure and dysbiosis do not trigger overt inflammation but may prime the immune system for dysregulation. Overall, this work strengthens the epidemiological link between antibiotics and TNF-associated autoinflammatory diseases, suggesting that even subtle immune priming from antibiotic-mediated dysbiosis in adulthood could contribute to disease development.

frontiers | Frontiers in Immunology

TYPE Original Research
PUBLISHED 09 January 2025
DOI 10.3389/fimmu.2024.1493991

OPEN ACCESS

EDITED BY
Mats Bemark,
Lund University, Sweden

REVIEWED BY
Roberto Rosales-Reyes,
National Autonomous University of Mexico, Mexico
Carolyn Thomson,
University of Calgary, Canada

*CORRESPONDENCE
Laurence Macia
Laurence.macia@sanofi.com

RECEIVED 10 September 2024
ACCEPTED 19 December 2024
PUBLISHED 09 January 2025

CITATION
Taitz JJ, Tan J, Ni D, Potier-Villette C, Grau G, Nanan R and Macia L (2025) Antibiotic-mediated dysbiosis leads to activation of inflammatory pathways.
Front. Immunol. 15:1493991.
doi: 10.3389/fimmu.2024.1493991

Antibiotic-mediated dysbiosis leads to activation of inflammatory pathways

Jemma J. Taitz[1,2], Jian Tan[1,2], Duan Ni[1,2], Camille Potier-Villette[1,2], Georges Grau[2,3], Ralph Nanan[1,2,4] and Laurence Macia[1,2,4]*

[1]Charles Perkins Centre, The University of Sydney, Sydney, NSW, Australia, [2]School of Medical Sciences, Faculty of Medicine and Health, The University of Sydney, Sydney, NSW, Australia, [3]Vascular Immunology Unit, Discipline of Pathology, School of Medical Sciences, University of Sydney, Sydney, NSW, Australia, [4]Sydney Medical School Nepean, The University of Sydney, Sydney, NSW, Australia

Introduction: The gut microbiota plays a pivotal role in influencing host health, through the production of metabolites and other key signalling molecules. While the impact of specific metabolites or taxa on host cells is well-documented, the broader impact of a disrupted microbiota on immune homeostasis is less understood, which is particularly important in the context of the increasing overuse of antibiotics.

Methods: Female C57BL/6 mice were gavaged twice daily for four weeks with Vancomycin, Polymyxin B, or PBS (control). Caecal microbiota composition was assessed via 16S rRNA sequencing and caecal metabolites were quantified with NMR spectroscopy. Immune profiles of spleen and mesenteric lymph nodes (MLNs) were assessed by flow cytometry, and splenocytes assessed for *ex vivo* cytokine production. A generalised additive model approach was used to examine the relationship between global antibiotic consumption and IBD incidence.

Results: Antibiotics significantly altered gut microbiota composition, reducing alpha-diversity. Acetate and butyrate were significantly reduced in antibiotic groups, while propionate and succinate increased in Vancomycin and PmB-treated mice, respectively. The MLNs and spleen showed changes only to DC numbers. Splenocytes from antibiotic-treated mice stimulated ex vivo exhibited increased production of TNF. Epidemiological analysis revealed a positive correlation between global antibiotic consumption and IBD incidence.

Discussion: Our findings demonstrate that antibiotic-mediated dysbiosis results in significantly altered short-chain fatty acid levels but immune homeostasis in spleen and MLNs at steady state is mostly preserved. Non-specific activation of splenocytes ex vivo, however, revealed mice with perturbed microbiota had

10.3389/fimmu.2024.1493991

significantly elevated production of TNF. Thus, this highlights antibiotic-mediated disruption of the gut microbiota may program the host towards dysregulated immune responses, predisposing to the development of TNF-associated autoimmune or chronic inflammatory disease.

KEYWORDS

gut microbiota, dysbiosis, antibiotics, vancomycin, Polymyxin B, TNF, IBD, autoimmunity

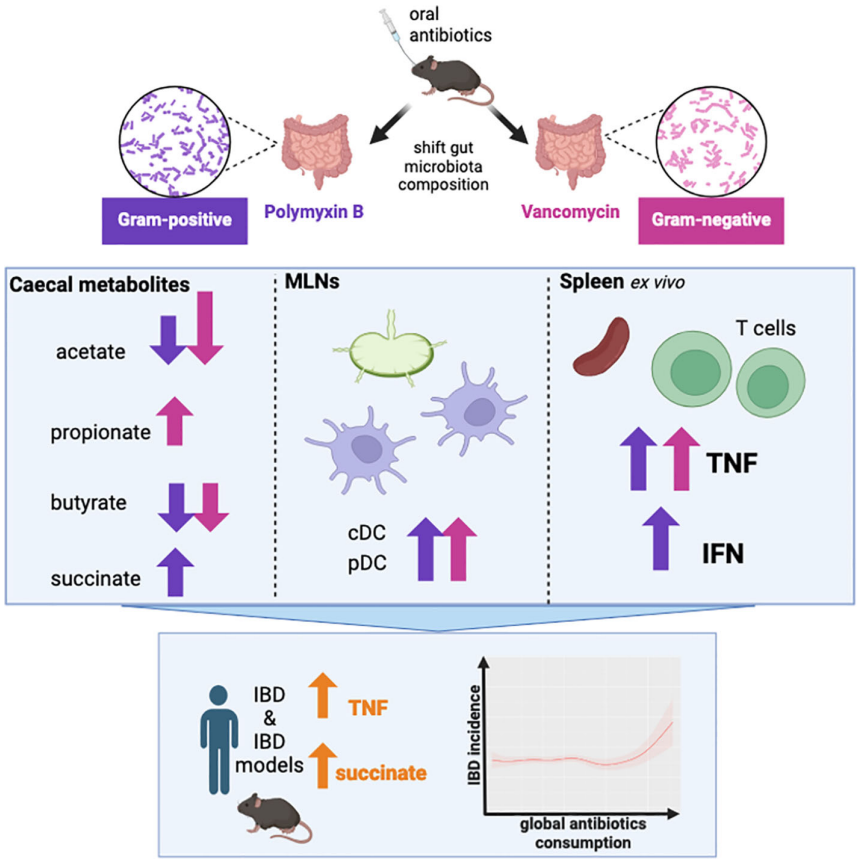

GRAPHICAL ABSTRACT

1 Introduction

The gut microbiota comprises trillions of microorganisms, predominantly bacteria, which have a profound impact on host physiology, including on metabolism and immunity. Studies of germ-free mice reveal that the absence of gut microbiota results in impaired development across multiple bodily systems, particularly the immune system (1). Gut bacteria are essential for immune cell development, including regulatory T cells (Tregs) (2) and T helper 17 cells (3), and they play a key role in regulating the function of both innate (4, 5) and adaptive immune cells (6).

Although there is no consensus as to what constitutes a healthy or ideal microbiota composition, dysbiosis - defined as detrimental changes to the gut microbiota - has been implicated in a range of diseases including allergies and autoimmune diseases (7). Most notably, dysbiosis is strongly associated with the rise of chronic

diseases, such as metabolic syndrome, cardiovascular disease and obesity (8). A growing body of research suggests that dysbiosis not only contributes to the onset and progression of disease (9) but may also influence effectiveness of treatments (10).

The gut microbiota can affect host immunity through the release of metabolites, which interact with specific receptors expressed on host cells. For example, the fermentation of dietary fibre by gut bacteria generates short-chain fatty acids (SCFAs), which bind to G-protein coupled receptors to modulate immune cells (11). Expression of these receptors, along with other metabolite receptors such as the aryl hydrocarbon receptor and the farnesoid X receptor, are not confined to the gut, but are broadly expressed in distal organs such as the liver, lung and brain (12, 13). This widespread distribution accounts in part for the systemic impact of the gut microbiota on the host.

Bacteria can be classified as gram-negative (G-) and gram-positive (G+), based on their membrane structure, and the host immune system has evolved to effectively discriminate between these distinct bacterial components. For example, lipopolysaccharide (LPS) from G- bacteria can activate Toll-like receptor 4, while peptidoglycans and polysaccharides, predominantly from G+ bacteria, activate receptors such as NOD-like receptors and Toll-like receptor 2 (14, 15). Although the immune response to G- or G+ bacteria has been extensively studied in the context of infections (16, 17), the effects of a skewed commensal composition are less well understood. Emerging research indicates that dysbiotic shifts towards predominantly G+ or G- bacteria are associated with distinct diseases (18–21), highlighting the need for further investigation into how gut bacterial composition influences health and disease.

Antibiotics can be a useful tool in the study of gut-microbiota host interactions, allowing researchers to examine the effects of specific bacterial communities on the host. Alongside this, global antibiotic use is rising and raises significant concerns about their impact on gut microbiota. Antibiotics can significantly alter microbiota composition, indiscriminately targeting pathogenic or non-pathogenic species, leading to a reduction in diversity and the loss of key species that are beneficial to host health (22). This disruption often results in dysbiosis, and antibiotic exposure has been correlated with chronic disease development (9, 23).

Here we used aimed to use antibiotics as a tool to shift gut microbiota composition to a predominantly G+ or G- composition to interrogate the impacts of a perturbed microbiota on immune homeostasis in the host.

2 Methods

2.1 Mice and housing

6-week old female C57BL/6 mice (Australian BioResources, NSW, Australia) were housed under specific-pathogen-free conditions in the animal facility of Charles Perkins Centre, The University of Sydney. Mice were given *ad libitum* access to standardised rodent diet AIN-93G (Specialty Feeds, Glen Forrest, Australia) and drinking water. Mice were weighed twice weekly and monitored for humane endpoints. Humane endpoints for this study included greater than 15% loss of bodyweight, as well as observed changes in behaviour such as hunching, ruffled fur, and inactivity persisting over 24 hours. Loose stool consistency over a 24-hour period was also used as a parameter to assess animal wellbeing. All experiments were performed with approval from the University of Sydney Animal Ethics Committee (2023/2308).

2.2 Antibiotics administration

To deplete gram-positive or gram-negative gut bacteria, mice were gavaged with either Vancomycin (5mg/mL; targeting gram-positives) or Polymyxin B (7.5mg/mL; targeting gram-negatives) dissolved in PBS, based on previous studies (24, 25) (n=10 mice per group). Mice were also gavaged with the anti-fungal Amphotericin B (1mg/mL in PBS) (Sigma-Aldrich) for 1 week prior to, and throughout the antibiotic regimen. Mice were gavaged twice daily for all antibiotic treatments, in a maximum volume of 200uL per gavage. Control mice (PBS group) were administered PBS for all gavages.

2.3 Metabolites quantification

Caecal content was weighed and homogenised in deuterium oxide (Sigma-Aldrich) at a concentration of 100mg/mL. The sample was centrifuged 5 mins at 14 000 xg at 4°C, caecal pellet was retained for DNA extraction. The supernatant was filtered through 3kDa centrifugal filtration unit (Merck Millipore) and added to chloroform-D/methanol-D (Sigma Aldrich). The upper aqueous phase was diluted into sodium triphosphate buffer with 4,4-dimethyl-4-silapentane-1-sulfomnic acid spiked in as an internal standard. Samples were run on a Bruker 600 MHz spectrometer and data was analysed with Chenomx Profiler software (V10.0).

2.4 DNA extraction and 16S rRNA sequencing

DNA from pelleted caecal content was extracted using the FastDNA SPIN Kit for Feces (MP Biomedicals) according to manufacturer's instructions, and quantified with the Nanodrop for normalisation to caecal weight. The V3–V4 region of the 16S rRNA gene was amplified with Q5® High-Fidelity 2X Master Mix (New England Biolabs) using the Pro341F (5′- CCTACGGGNBGCASCAG -3′) and Pro805R (5′- GACTACNVGGGTATCTAATCC -3′) primers as previously described (26). Following amplification, library cleanup was performed using AMPure XP reagent (Beckman Coulter). Amplicon sequencing was done on the Illumina MiSeq system (2x250 bp PE). Data was analysed using the dada2 package (1.30.0) using R software (4.3.1) to generate Amplicon sequence variants (ASV). ASV were classified according to taxonomy using the Ribosomal Database Project classifier (27). Analysis was performed with the phyloseq (1.46.0), vegan (2.6-4) and microbiome (1.24.0) R packages and differentially abundant taxa were analysed using ALDEx2 (1.34.0). Bacterial load was assessed by absolute 16S copy number per gram of caecal content, as described previously (28). Copy number was determined by qPCR with

the 16S rDNA universal primers, UniF: GTGSTGCAYG GYYGTCGTCA and UniR: ACGTCRTCCMCNCCTTCCTC, and compared with a standard curve (10^2 to 10^8 copies per uL). Fungal load was determined using primers for the Fungal ITS1 rRNA region (ITS1-30F: GTCCCTGCCCTTTGTACACA, ITS1-217R: TTTCGC TGCGTTCTTCATCG) (29) and the 18S region (F: GGRAAACTCA CCAGGTCCAG, R: GSWCTATCCCCAKCACGA) (30), following the relevant cycling conditions.

2.5 Immunoglobulin A quantification

Small intestinal content was homogenised at 100mg/mL in PBS with complete Protease Inhibitor cocktail (Roche). Samples were centrifuged 14 000x g for 10 min at 4°C and supernatant collected. Immunoglobulin A (IgA) was assessed with the Mouse IgA Quantitation Set (Bethyl Laboratories) following the manufacturer's instructions.

2.6 Flow cytometry tissue processing

Mice were euthanised via CO_2 and mesenteric lymph nodes (MLNs) and spleens were collected and processed into single cell suspension. Tissues were disrupted in FACS buffer (2% FCS, 0.5M EDTA in PBS). Red blood cells were lysed for spleen samples using RBC Lysis Buffer 10X (Biolegend). Cell suspensions were passed through a 100µm mesh filter and resuspended in FACS buffer for counting with trypan blue (0.4%) on a haemocytometer to exclude dead cells.

TABLE 1 Flow cytometry antibodies.

Antibody	Manufacturer	Catalog #	Clone
anti-mouse B220 BUV661	BD	612972	RA3-6B2
anti-mouse CD3 PE-CF594	BD	562286	145-2C11
anti-mouse CD4 BV750	BioLegend	100467	GK1.5
anti-mouse CD8 BUV805	BD	612896	53-6.7
anti-mouse CD11b BUV395	BD	563553	M1/70
anti-mouse CD11c BV786	BD	563735	HL3
anti-mouse CD25 PE-Cy7	BioLegend	102016	PC61
anti-mouse CD45 Alexa Fluor 700	BioLegend	103128	30-F11
anti-mouse NK1.1 PE/Cy5	BioLegend	108716	PK136
anti-mouse F4/80 BV711	BioLegend	123147	BM8
anti-mouse FoxP3 APC	Miltenyi	130-111-601	REA788
anti-mouse Ly6C FITC	BD	553104	AL-21
anti-mouse Ly6G BV650	BioLegend	127641	1A8
anti-mouse MHCII BV510	BioLegend	107636	M5/114.15.2
anti-mouse TCRγδ APC-Fire 750	Biolegend	118136	GL3
anti-mouse FoxP3 Vio515	Miltenyi	130-111-603	REA788
anti-mouse IFN-γ BV650	BioLegend	505832	XMG1.2
anti-mouse IL-10 APC	BioLegend	505010	JES5-16E3
anti-mouse IL-17 PE	BioLegend	506904	TC11-18H10.1
anti-mouse TNF-a BV510	BD	563386	MP6-XT22
anti-mouse MHCII Pacific Blue	BioLegend	107620	M5/114.15.2
anti-mouse Ly6C BV605	BioLegend	128036	HK1.4
anti-mouse CD103 Vio515	Miltenyi	130-111-609	REA789
anti-mouse CD11b PerCP	BioLegend	101230	M1/70
anti-mouse IL-6 PE	BioLegend	504504	MP5-20F3
anti-mouse F480 PE/Cy7	BioLegend	123113	BM8
anti-mouse iNOS APC	eBioscience	17-5920-82	CXNFT

2.7 Flow cytometry staining

Cells were stained for viability using LIVE/DEAD™ Fixable Blue Dead Cell Stain (ThermoFisher Scientific), and non-specific binding was prevented using anti-mouse CD16/32 (BioLegend). Surface antigen and intracellular staining was performed using antibodies listed in Table 1. For intracellular staining of cytokines and FoxP3, cells were fixed and permeabilised using the Foxp3/Transcription Factor Staining Buffer Set (eBioscience) according to the manufacturer's instructions. Cells were washed and then acquired on the Aurora (Cytek) with SpectroFlo software (Cytek) and data was analysed in FlowJo (Treestar Inc. Ashland, OR, USA), based on the gating strategies in Supplementary Figures 4–9.

2.8 *In vitro* stimulations

Splenocytes (10^6 cells) were stimulated with either lipopolysaccharide (LPS) (100ng/mL) (Invivogen) for 48 hours, or with phorbol 12-myristate 13-acetate (PMA) (50ng/mL) (Sigma Aldrich), ionomycin (500ng/mL) (Sigma Aldrich), and brefeldin A (BFA) (5µg/mL) (Sigma Aldrich) for 4 hours. Cells were incubated at 37°C 5% CO2, then washed and stained for intracellular cytokines as described above.

2.9 Data collection and processing

Global antibiotic consumption data was sourced from the Global Research on Antimicrobial Resistance (GRAM) database (31). Antibiotic usage was documented as defined daily doses per 1000 population per day (DDD/1000 inhabitants/day). Age-standardised incidence rates of inflammatory bowel disease (IBD) was collated from Global Burden of Disease (GBD) Study 2021 (https://vizhub.healthdata.org/gbd-results/). Global gross domestic product (GDP) data was obtained from the Maddison project (32). Countries or timepoints without available data were excluded from analysis, and the final dataset included data from close to 200 countries, spanning the years 2000 to 2018.

2.10 Generalised additive models

Details of analysis were adapted from our previous works (33, 34). Generalised additive model (GAM) is a statistical tool facilitating the simultaneous analyses of multiple parameters, including their plausible interactions and non-linear effects (35–37). They are modelled using non-parametric smoothed functions, which are generally in forms of splines and represent flexible manners to examine non-linear associations. In this study, GAMs were used to model age-standardised IBD incidence rates, using antibiotic consumption, GDP and time as predictors with the "*gam*" function from the *mgcv* package (37, 38). When modelling, countries that the data were based on were corrected as random effects. An array of GAMs were run using aforementioned predictors as well as their different combinations, capturing their individual, additive and interactive effects. Effects from each parameters were modelled as smooth terms with the "s()" function, and their interactions were modelled with the "ti()" or "te()" functions, considering their different scales, such as antibiotic consumption and GDP. Modelling results were evaluated following the Akaike information criterion (AIC) (39), and the one with the lowest AIC was chosen.

2.11 Statistics

Comparisons between groups were performed with GraphPad Prism (v10) with ordinary one ANOVA, repeated measures two-way ANOVA, or a mixed-effects model with Geisser-Greenhouse correction, followed by Tukey's multiple comparisons test. Differences were considered statistically significant when $p<0.05$, with *p<0.05, **p<0.01, ***p<0.001, **** p<.0001

3 Results

3.1 Both polymyxin B and vancomycin treatments significantly alter gut microbiota composition and diversity

In order to understand the broad impact of G- or G+ bacteria on immune homeostasis we used antibiotics to selectively eliminate G+ or G- taxa within the gut microbiota towards a dominantly G+ or G- composition. We utilised Polymyxin B (PmB), a cationic peptide that binds to LPS to weaken the bacterial outer membrane to target G- species and skew the microbiota towards a G+ composition (40). To shift the microbiota towards a G- composition we used vancomycin, which is active against most enteric G+ species. Before beginning the antibiotic regimen, mice were administered the antifungal amphotericin B (1mg/mL) for 1 week, to avoid expansion of enteric fungi that often occurs with antibiotic treatment. Mice were then maintained on amphotericin B and gavaged either vancomycin (5mg/mL), PmB (7.5mg/mL) or PBS twice daily for 4 weeks (Figure 1A), to generate microbiota that was G- or G+ dominant, respectively. All three drugs are reported to have poor bioavailability after oral administration, with little systemic absorption (41–47). Therefore, we expect minimal absorption into peripheral circulation, and the drugs' primary activity to be confined to the gastrointestinal tract. We selected to administer antibiotic treatments via oral gavage to allow for a standardised dose to be delivered and avoid dehydration and severe weight loss often observed if antibiotics are given in drinking water (25, 48). We observed, however, that vancomycin-treated mice had significant increase in percentage weight gain compared to PmB treated mice, and PmB mice tended to have reduced weight compared to PBS mice towards the end of the experiment (Figure 1B). Vancomycin has been linked to weight gain in humans (49) and was found to promote food intake and weight gain in mice (50), which may explain this discrepancy. Caecal weight was also significantly increased by vancomycin treatment (Supplementary Figure 1A), as previously

10.3389/fimmu.2024.1493991

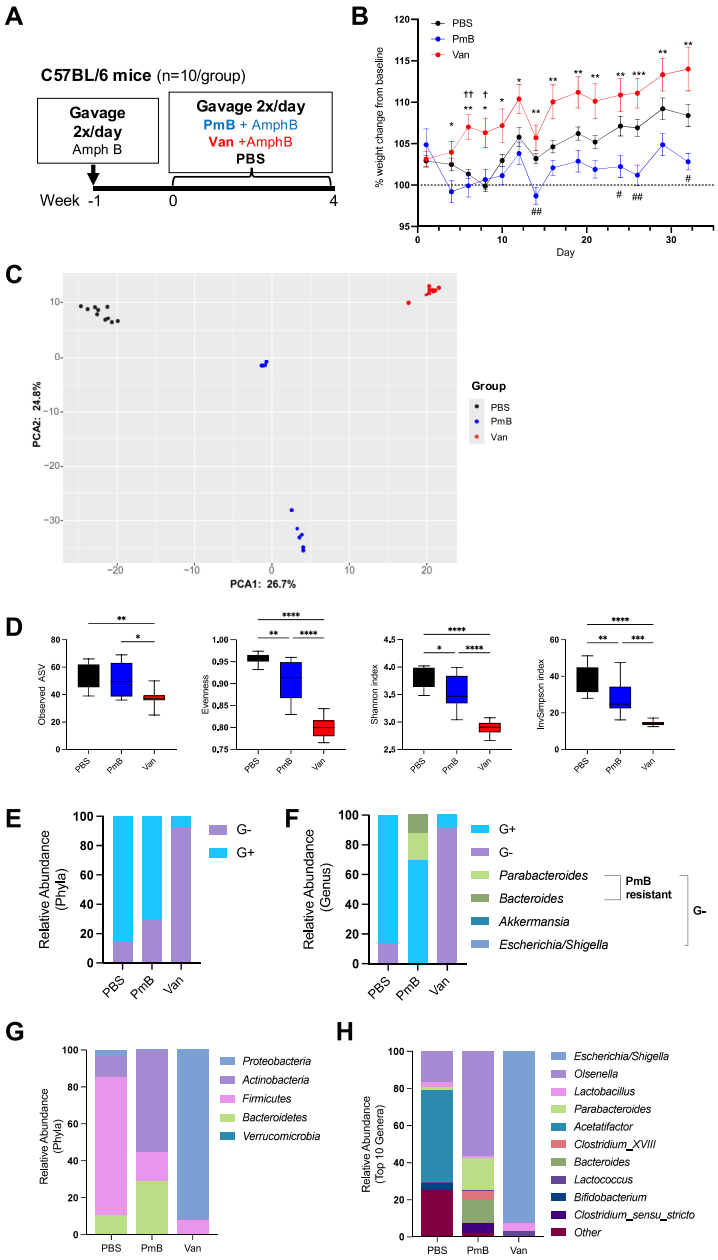

FIGURE 1
aqr rid="aq1" qside="l" boffset="10"/>Administration of Polymyxin B or vancomycin significantly alters microbiota composition, eliminating to a G+ or G- taxa. **(A)** Diagram of experimental set up. C57BL/6 mice were gavaged amphotericin B (Amph B) (1mg/mL) 1 week prior to commencing 2x daily gavages of vancomycin (Van) (5mg/mL), Polymyxin B (PmB) (7.5mg/mL), or PBS, for 4 weeks (n=10 mice per group). **(B)** Bodyweight as percent of baseline weight, using mixed-effects model with Geisser-Greenhouse correction, followed by Tukey's multiple comparisons test. * indicates differences between Van and PmB, † between Van and PBS, # between PmB and PBS **(C)** Differences in microbiota composition shown as principal component analysis (PCA) of Aitchison distance. **(D)** Alpha diversity measures of microbiota composition, showing richness (observed ASV), Evenness, Shannon Diversity index and Inverse Simpson index. **(E)** Phyla and genera were classified as gram-positive (G+) or gram-negative (G-) and relative abundance was graphed for phyla **(E)** and genera **(F)**, also indicating PmB-resistant and susceptible strains. **(G)** Relative abundance of bacteria at phyla level **(H)** and genus level (top 10 genera). Data are represented as mean ± SEM. *p<0.05, **<0.01, ***0.001, ****<0.0001, , †<0.05, ††<0.01, #<0.05, ##<0.01, by ordinary one-way ANOVA followed by Tukey's multiple comparisons test.

described (50, 51), likely due to elimination of fibre-digesting bacteria. While histopathological analysis was beyond the scope of this study, previous studies suggest vancomycin does not induce gross changes to the colonic epithelium (52). However, short-term oral vancomycin was found to disrupt the colonic mucus barrier by inducing ER stress in goblet cells that impaired mucus secretion in goblet cells (53), and both vancomycin and PmB may impair colonic permeability (54).

To confirm our treatments were successful in manipulating gut microbiota composition, we extracted caecal DNA and performed 16S rRNA sequencing. Principal component analysis based on Aitchison distance revealed that all three groups had a distinct microbiota composition (Figure 1C). Measures of alpha diversity, which evaluate the species richness and evenness within the gut microbiota, were also examined (Figure 1D). Mice treated with vancomycin had a significantly reduced richness compared to PBS and PmB-treated mice, as shown by the decreased number of unique amplicon sequence variants (ASV). Observed ASV was unchanged in PmB-treated mice compared to PBS, indicating this treatment did not significantly reduce the number of unique taxa. Other measures of alpha diversity, including Evenness and Shannon and Inverse Simpson indices, were also significantly reduced in antibiotics-treated groups compared to PBS (Figure 1D), however, vancomycin-treated mice exhibited a more pronounced reduction across these measures and were significantly lower compared to PmB-treated mice (Figure 1D).

Next, to confirm the efficacy of antibiotic treatment, we examined the relative abundance of phyla in the gut microbiota and classified these as G- or G+ (Figure 1E). Basally, the composition of PBS microbiota was mostly G+. As expected, vancomycin treatment led to predominantly G- phyla and PmB resulted in predominantly G+ phyla. Surprisingly, PmB-treated mice had a slightly reduced abundance of G+ phyla compared to PBS. Examination of the G- phyla at the genus level for PmB mice revealed that G- species comprised *Parabacteroides* and *Bacteroides* spp (Figure 1F). PmB resistance in commensal *Bacteroides* and *Parabacteroides* has been reported previously, and has been attributed to enzyme modifications to the lipid A component of LPS, which disrupts PmB binding (55–57). Remaining G- genera, *Akkermansia* and *Escherichia/Shigella*, were present at relative abundance of <1% (Supplementary Figures 1B, C), indicating that susceptible G- species were successfully eliminated by PmB treatment. Altogether, this demonstrates that our treatments were successful in eliminating the majority of susceptible G+ or G- species within the gut microbiota.

To gain further insight into the gut microbiota composition, we examined the relative abundance of Phyla (Figure 1G) and Genus (top 10 genera) (Figure 1H). The mostly G+ composition of PBS microbiota was attributed to the presence of *Firmicutes*, primarily represented by the genus *Acetatifactor* (Figures 1G, H), which is strongly associated with the rodent gut (58, 59). As described earlier, PmB led to expansion of G- phyla *Bacteroidetes* (comprising genera *Bacteroides* and *Parabacteroides*) and G+ *Actinobacteria* (comprising the genus *Olsenella*). Vancomycin resulted in a microbiota primarily composed of G- *Proteobacteria* phyla, which was due to expansion of the genus *Escherichia/Shigella*, which likely represents the proliferation of a commensal or facultatively pathogenic species (pathobiont) within the existing gut microbiota. Altogether these data further confirm that our treatments effectively targeted susceptible bacteria to significantly perturb gut microbiota composition and induce a shift to a G+ or G- dominant composition.

We also measured 16S copy number, as a readout of bacterial load in the gut, which is an influential factor on host immunity (Supplementary Figure 1D). We found antibiotics decreased bacterial load compared to PBS mice, and PmB treated mice had significantly reduced load compared to vancomycin treated mice. Thus, the selective antibiotic treatments effectively targeted their respective species and reduced overall bacterial burden in the gut. We also assessed fungal load within the microbiota, which, despite comprising only 1% of gut microbiota, play a critical role in systemic immune development and responses (60, 61). We observed that vancomycin-treated mice had increased fungal load compared to PBS, as quantified by the relative expression of 18S rRNA, however, there were no significant differences between groups for ITS rRNA expression (Supplementary Figure 1E). Altogether, these findings reveal the differential impact of select antibiotic treatments on the bacterial and fungal compartments of the gut microbiota.

3.2 Differential production of G+ or G- dominant microbiota metabolites and impact on host sIgA

Gut microbiota-derived metabolites, particularly SCFAs, profoundly influence host physiology and immunity. To assess how antibiotic-mediated changes in microbiota composition impact the production of these metabolites, we quantified the levels of caecal SCFAs by nuclear magnetic resonance spectroscopy. We examined levels of the major SCFAs, acetate, propionate, and butyrate, as these play a key role in promoting tolerance (11, 62). Moreover, the majority of SCFA-generating bacteria belong to the predominantly G+ phyla *Firmicutes* (63), which was decreased in abundance in antibiotic-treated groups. Accordingly, these mice had decreased total SCFA levels, with vancomycin-treated mice having the most altered ratios of SCFAs (Figures 2A, B). Compared to PBS, acetate was significantly decreased in PmB-treated mice, and close to undetectable in vancomycin-treated mice (Figure 2B). Surprisingly, a proportion of vancomycin mice had significantly elevated propionate levels, whereas propionate was undetectable in the PBS and PmB mice (Figure 2B). Butyrate was reduced in both antibiotic-treated groups to a similar extent (Figure 2B). Finally, succinate, another metabolite that has significant associations with dysbiosis as well as intestinal inflammation and stress (64, 65), was significantly elevated in PmB mice (Figure 2C) compared to other groups.

Next, we measured intestinal secretory Immunoglobulin A (sIgA), a key component of the host's luminal response to the gut microbiota, which has also been linked to high levels of acetate (66). One function of sIgA is binding to luminal bacteria to maintain exclusion of the microbiota from the host epithelium. sIgA was substantially elevated in vancomycin mice, approximately two-fold compared to other groups (Figure 2D) suggesting a potential expansion of colitogenic bacteria (67).

Finally, we performed a correlation analysis between bacterial-derived metabolites, host sIgA, and the composition of the gut microbiota (Figure 2E). We identified a positive correlation with acetate and butyrate with some G- genera (*Desulfovibrio, Alistipes, Oscillibacter*) and many G+ genera (including *Bifidobacterium*,

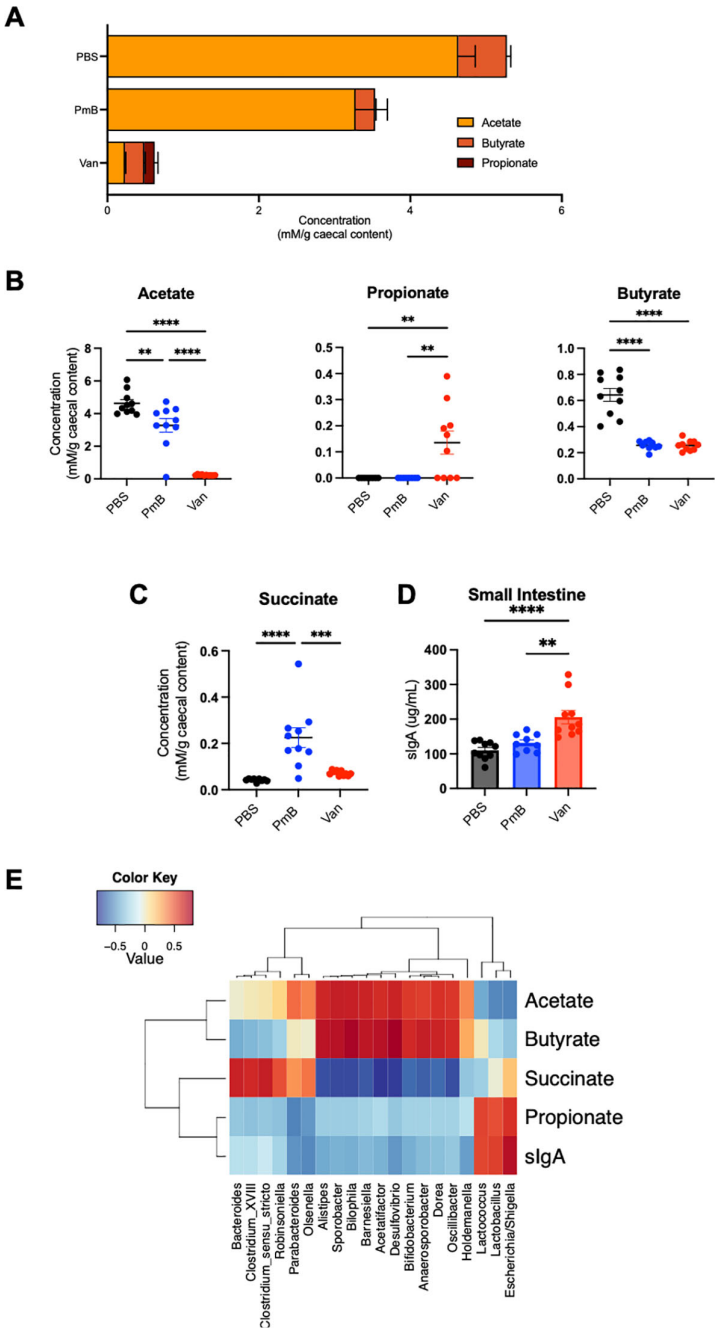

FIGURE 2
Antibiotic-shifted microbiota have significantly altered metabolite profiles **(A)** Ratios and total amounts of SCFAs (acetate, butyrate and propionate) in caecal content, as quantified by nuclear magnetic resonance (NMR) spectroscopy. **(B, C)** Concentrations of acetate, propionate, butyrate, and succinate in caecal content. **(D)** Levels of sIgA in small intestinal content, as quantified by ELISA. **(E)** Correlation between metabolites, sIgA level, and 16S genera results. Data are represented as mean ± SEM with **p<0.01, ***0.001, ****<0.0001 by ordinary one-way ANOVA followed by Tukey's multiple comparisons test.

Sporobacter, *Acetatifactor*, *Anaerosporobacter*, and *Dorea*). Similarly, succinate levels correlated with both G- taxa (*Bacteroides* and *Parabacteroides*) and G+ phyla *Firmicutes* (including *Clostridia* spp). Although propionate production is commonly correlated with G- *Bacteroides* in human microbiota (68), we observed propionate correlated highly with G- *Escherichia/Shigella* as well as G+ *Lactococcus* and *Lactobacillus* spp, all of which have the capacity to generate propionate (69, 70). Similarly, sIgA correlated strongly with *Escherichia/Shigella*, *Lactococcus* and *Lactobacillus* spp, in line with a previous study in humans treated

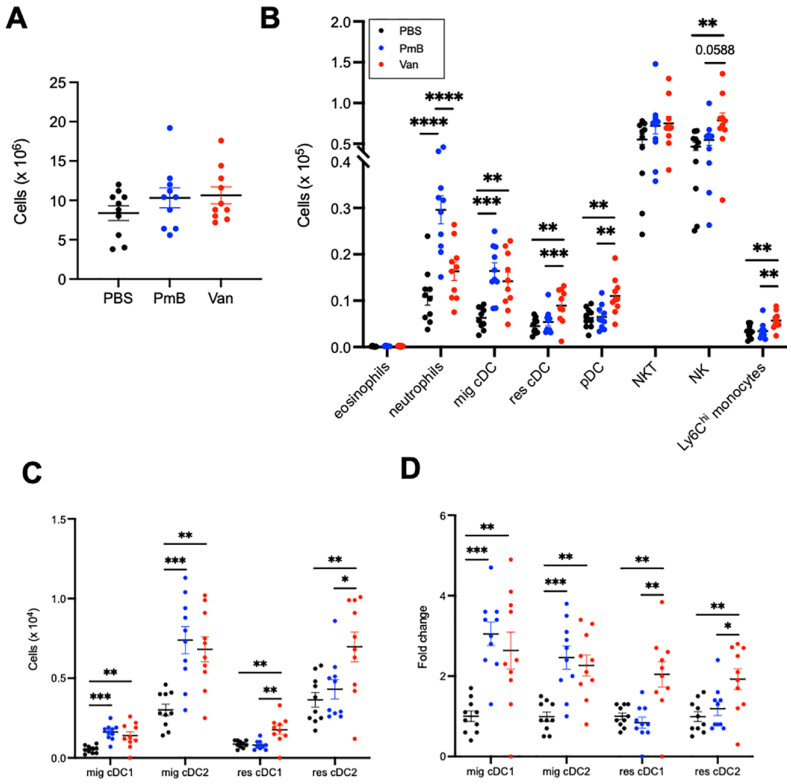

FIGURE 3
Dendritic cells in mesenteric lymph nodes are mainly impacted by antibiotics-induced dysbiosis **(A)** Total cellularity of the mesenteric lymph nodes (MLNs). **(B)** Absolute cell numbers of eosinophils, neutrophils, migratory conventional dendritic cells (mig cDC), resident cDC (res cDC), plasmacytoid dendritic cells (pDC), Natural Killer T cells (NKT) and Natural Killer cells (NK), and Ly6C^{hi} monocytes were quantified by flow cytometry. **(C)** Numbers of migratory and resident cDC1 (CD11b$^-$ CD8$^+$) and cDC2 (CD11b$^+$CD8$^-$) subsets **(D)** and fold change across groups. Data are represented as mean ± SEM with *p<0.05, **<0.01, ***0.001, ****<0.0001 by ordinary one-way ANOVA followed by Tukey's multiple comparisons test.

with vancomycin (71). Together these findings suggest that perturbing microbiota composition can dramatically alter gut microbiota-derived metabolites, some of which may be attributed to the large reduction in *Firmicutes* phyla we observed.

3.3 Antibiotic-mediated dysbiosis predominantly affects dendritic cells in the mesenteric lymph nodes

As the mesenteric lymph nodes (MLNs) drain the gut and are the critical sites of antigen-specific response against gut bacteria, we first assessed impact of antibiotic-mediated changes in gut bacteria on this site. To identify how these changes may influence the local immune system in the gut, we quantified proportions and absolute numbers of innate and adaptive immune cells in the MLNs (gating strategy shown in Supplementary Figure 4).

Total MLN cellularity was similar among groups (Figure 3A), suggesting changes to gut microbiota composition did not induce a localised immune response in this site. We observed that compared to PBS control, a antibiotics-perturbed microbiota impacted the proportions of a range of innate and adaptive immune cell subsets (Supplementary Figures 2A, B). Both antibiotics treated groups had increased proportions of migratory conventional DCs (MHCII^{hi} cDCs), and PmB mice had increased neutrophils compared to vancomycin and PBS mice. Vancomycin treatment increased proportions of plasmacytoid DCs (pDCs), resident cDCs, Natural Killer (NK) cells, Ly6C$^+$ inflammatory monocytes compared to the other groups, and led to decreases in TCRγδ$^+$ T cells compared to PBS and decreased CD4$^+$ T cells compared to PmB mice (Supplementary Figures 2A, B). For absolute cell number, we found mainly innate cells were influenced by antibiotic treatment (Figure 3B, Supplementary Figure 2C). PmB treated mice had increased neutrophils compared to PBS and vancomycin mice, while vancomycin mice had increased NK cells and Ly6C$^+$ monocytes compared to the other groups (Figure 3B). We found both antibiotic-treated groups had significantly increased numbers of migratory DCs compared to PBS, while vancomycin mice had increased numbers of resident cDCs and pDCs compared to PmB and PBS mice (Figure 3B). DCs are key antigen-presenting cells that are crucial for the development of antigen-specific responses in the gut and in the induction of tolerance, and cDCs and pDCs differ in their ontogeny as well as their functional role, with cDCs being highly efficient in antigen-presentation and activation of naïve T-cells whereas pDCs play a key role in production of type I interferons and the anti-viral response (72). Altogether our

findings suggest that skewing the microbiota towards a dysbiotic composition mainly impacts innate cell numbers, primarily DCs.

Migratory and resident cDCs can be further classified into cDC1 ($CD8a^+CD11b^-$) and cDC2 ($CD8a^-CD11b^+$) subsets, which are also functionally specialised: cDC1 are key in the cytotoxic immune response and presentation to $CD8^+$ T cells, and cDC2s are key in helper T cell responses and presentation to $CD4^+$ T cells. Both migratory cDC subsets were increased in proportion and number for antibiotics-treated mice (Figure 3C, Supplementary Figure 2D). For vancomycin mice, both resident cDC1 and cDC2 subsets were also increased in number compared to other groups (Figure 3C). The fold-change for increased migratory cDC numbers was approximately 3 times greater for both antibiotics-treated groups compared to the PBS group, while the increase in resident cDC in vancomycin mice was twice that of PBS and PmB groups (Figure 3D). Altogether, these data indicate that a dramatically altered microbiota composition impacts innate cells in the gut-draining lymph nodes, and a PmB- or vancomycin-skewed microbiota appear to differentially impact neutrophils and pDCs, but both increasing migratory cDC numbers.

As we observed DC numbers were highly impacted by a skewed microbiota, we next examined the impact on T cells. Neither the proportion nor the number of total T cells, $CD4^+$ T cell or $CD8^+$ T cell subsets were altered in mice with perturbed microbiota compared to PBS (Supplementary Figures 2B, C), suggesting there was no initiation of an antigen-specific immune response, consistent with the unchanged MLN cellularity. This further confirms that antibiotic treatments perturbing the microbiota mainly impact innate, and not adaptive cell subsets, in the MLNs.

Altogether these results suggest that an antibiotics-perturbed microbiota increase recruitment of DC to the MLNs, but without initiation of an antigen-induced T cell response.

3.4 Perturbed gut microbiota minimally impacts cell numbers in the spleen but increases their pro-inflammatory profile

To determine if a dramatically skewed microbiota had a systemic impact on immunity, we next investigated proportions and numbers of innate and adaptive cells among splenocytes, as well as their cytokine secretion profile.

Similar to the MLN we found no changes in overall splenic cellularity (Supplementary Figure 3A). However, mice with perturbed microbiota had altered proportions of immune subsets including eosinophils, cDCs, putative red pulp macrophages ($F480^+Ly6C^-$ cells) and $Ly6C^{med}$ monocytes, as well as T cell subsets (Supplementary Figures 3B, C; gating strategy shown in Supplementary Figure 5), suggesting the systemic impact of the microbiota shift. As in the MLNs, DC subset numbers were primarily impacted, with a significant reduction of total cDCs as well as cDC1 and cDC2 subsets in PmB-treated mice compared to other groups (Figures 4A, B). Contrary to the MLNs, we found no change to pDC numbers.

To further investigate the impact of antibiotic-mediated dysbiosis on immune function, we quantified the cytokine secretion before and after challenge *in vitro*. To do this, we stimulated splenocytes with LPS from *E. coli* for 48 hours and examined the intracellular production of pro-inflammatory cytokines IL-6 and TNF by flow cytometry (Figures 4C–E; gating strategy shown in Supplementary Figure 6). As expected, LPS treatment in pDC from PBS-treated mice led to increased production of IL-6 but this was to the same extent as pDC from vancomycin mice (Figure 4C). Interestingly, there was no effect of LPS on pDCs from PmB mice (Figure 4C). This differential effect of the gut microbiota on IL-6 was not observed for TNF, as pDCs across groups produced comparable levels of TNF upon LPS treatment (Figure 4C). LPS stimulation of cDCs induced robust IL-6 expression for all groups, however, cDCs from vancomycin mice showed reduced expression compared to PBS and PmB mice (Figure 4D). Although we did not measure circulating or faecal LPS levels in our mice, which may reflect differences in LPS tolerance, the fact that LPS is the primary antigen of the G- membrane suggests that reduced LPS levels in PmB mice may affect the DC response to this stimulus. This may be supported by the fact that *Bacteroides* is the only G- phyla present in PmB-treated microbiota, and *Bacteroides*-derived LPS is well-known to be less immunogenic than *E. coli*-derived LPS (73). Although PmB is known for its endotoxin-binding capability, the low likelihood of systemically circulating PmB suggests that the gut microbiota remains a critical source of antigens that shapes immune responses in distal organs. LPS stimulation did not induce TNF expression in cDCs, and there was in fact a slight reduction in TNF levels in PmB mice (Figure 4D). Overall, these results indicate that a PmB treated microbiota primarily impacts cDC activation by LPS, possibly reducing cDC capacity to respond to stimuli from immunogenic G- bacteria.

To further examine the impact of antibiotic-mediated dysbiosis on immune cells, we measured the expression of the cytokines IL-17, IFN-γ IL-10 and TNF, in splenocytes after PMA/ionomycin stimulation (Figure 5; gating strategy and FMOs shown in Supplementary Figures 7-9). Many studies have identified G+ and G- bacteria induce differing cytokine immune profiles *in vitro* (74–77), as well as during sepsis (78), highlighting the capacity of the immune system to discriminate between the two classes of bacteria. We first examined levels of IL-17 and IL-10, as these cytokines are highly influenced by gut microbiota composition (1, p. 20). The development of IL17-producing cells $TCR\gamma\delta^+$ T cells in the intestines, as well as in the liver and lungs, is regulated by the gut microbiota (79, p. 201; 3, 80). We observed antibiotics-treated mice showed no changes in $IL\text{-}17^+$ cells for $CD4^+$ T cells. $TCR\gamma\delta^+$ and $CD8^+$ T cells (Figure 5A). The induction of intestinal Th17 cells is highly dependent on a subset of G+ bacteria known as segmented filamentous bacteria (3), thus while we did not observe changes in IL-17 production in the spleen, measuring production of IL-17 in gut-local T cells may provide more relevant insights into the influence of antibiotics-perturbed microbiota. The anti-inflammatory cytokine IL-10 is primarily derived from Tregs that are induced by tolerogenic DCs. The generation of tolerogenic DCs is also strongly associated with G+ species, highly prevalent in PmB treated mice (81, 82). In line with this, we found PmB mice had significantly elevated IL-10 expression across T-cell subsets, including Tregs, non-Treg $CD4^+$ cells, as well as $CD8^+$ T cells (Figure 5B). Vancomycin mice also had

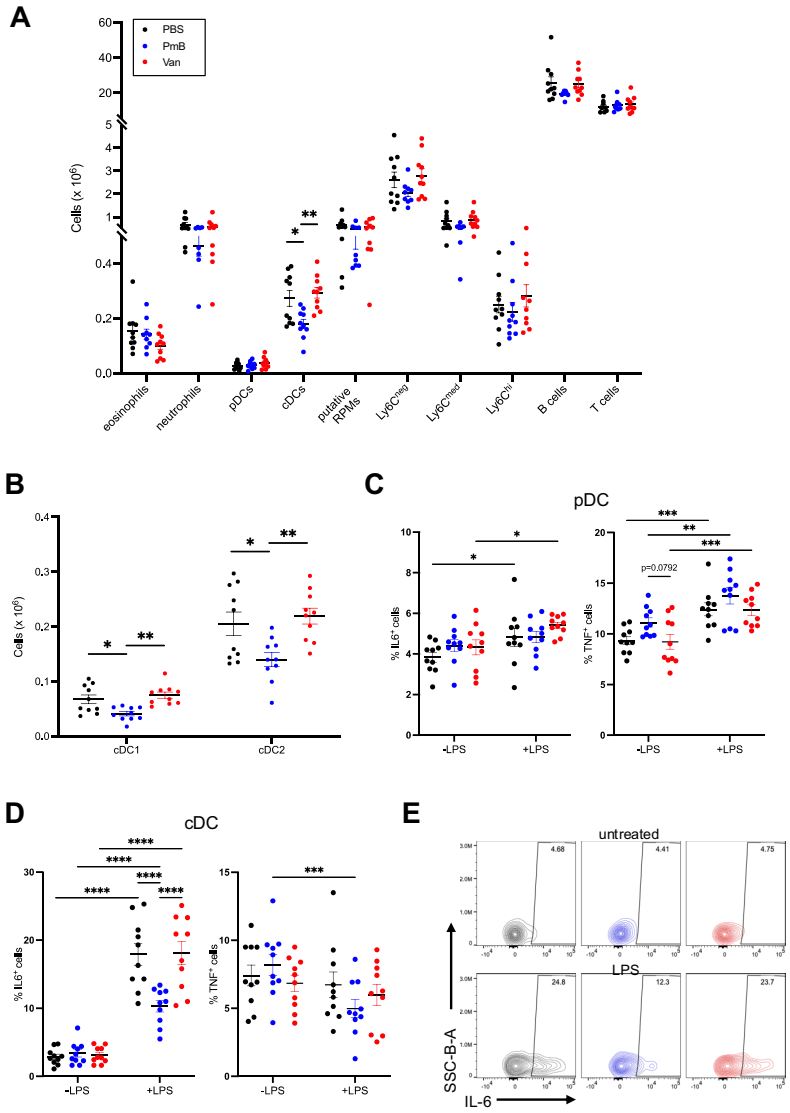

FIGURE 4
Perturbed microbiota has minimal impact on spleen immune composition **(A)** Absolute cell numbers of innate and adaptive cell subsets in the spleen, including eosinophils, neutrophils, plasmacytoid dendritic cells (pDCs), conventional dendritic cells (cDCs), putative red pulp macrophage (RPMs), monocyte subsets (Ly6C^{hi}Ly6C^{mid} Ly6C^{neg}), B cells and T cells as quantified by flow cytometry. **(B)** Numbers of cDC1 (CD11b^{-} CD8^{+}) and cDC2 (CD11b^{+}CD8^{-}) subsets in the spleen. **(C)** Expression of IL-6 and TNF in pDCs stimulated with lipopolysaccharide (LPS) for 48 hours *in vitro*, as quantified by flow cytometry. **(D)** Expression of IL-6 and TNF in cDCs stimulated with LPS for 48 hours *in vitro*, as quantified by flow cytometry and **(E)** representative plots of proportions of IL-6 expressing cells in LPS-stimulated and unstimulated cDCs. Data are represented as mean ± SEM with *p<0.05, **<0.01, ***0.001, ****<0.0001 by ordinary one-way ANOVA followed by Tukey's multiple comparisons test or repeated measures two-way ANOVA followed by Tukey's multiple comparisons test.

elevated proportions of non-Treg IL10^{+} CD4^{+} T cells and tended to have elevated IL10^{+} CD8^{+} T cells (p=0.0603) compared to PBS mice (Figure 5B).

Finally, we examined the expression of IFN-γ and TNF, pleiotropic cytokines that are instrumental in regulating immune response and also associated with autoimmune diseases. IFN-γ, a type II interferon, is thought to contribute to the pathological intestinal inflammation seen in irritable bowel disease (IBD) (83, 84) and TNF is widely recognised for its involvement across autoimmune conditions such as IBD, arthritis, psoriasis, and systemic lupus erythematosus (85). Previous studies have also identified increases in TNF mRNA in colon tissue after PmB and vancomycin treatment (54, 86). While these studies differed from ours in antibiotic administration methods and resulting microbiota compositional changes, they are suggestive of a link between antibiotics exposure and a pro-inflammatory response. We observed that compared to PBS, PmB mice showed IFN-γ production across a range of subsets including NK cells, TCRγδ $^{+}$ T cells, CD4^{+} and CD8^{+} T cells, as well as B cells (Figure 5C). IFN-γ^{+} cells also tended to be increased compared to vancomycin mice for NK, TCRγδ^{+},and CD8^{+} T cell

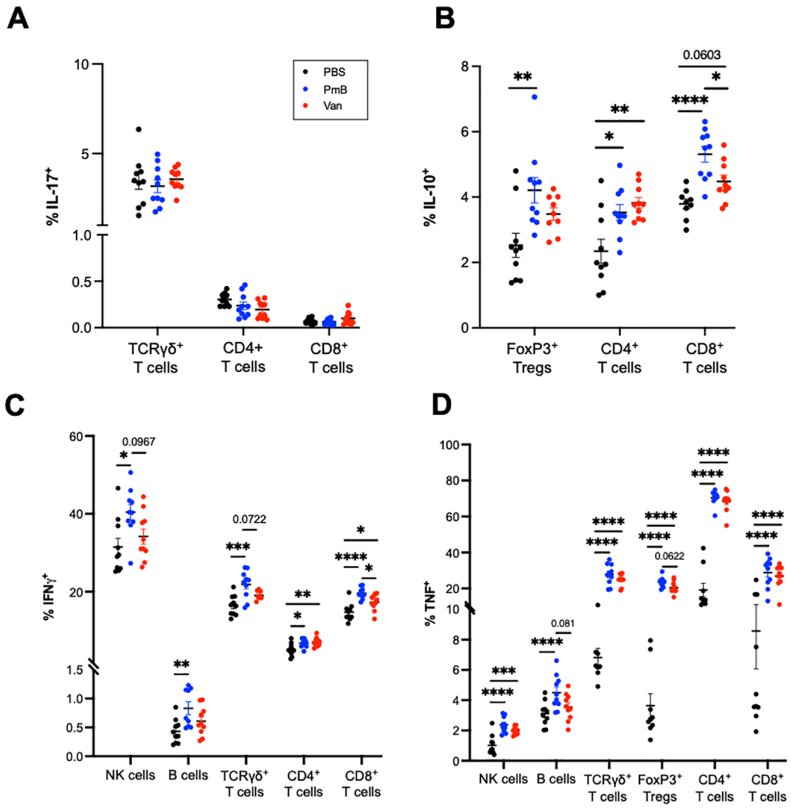

FIGURE 5
Adaptive splenocytes from antibiotics-shifted microbiota shifted mice show greater cytokine expression under stimulation conditions. Splenocytes were stimulated with PMA/ionomycin/BFA for 4 hours and cytokine expression was quantified by flow cytometry. **(A)** IL-17 expression in TCRγδ$^+$, CD4$^+$ and CD8$^+$ T cells **(B)** IL-10 expression in Tregs, CD4$^+$ and CD8$^+$ T cells. **(C)** IFN-γ expression in NK cells, B cells, and TCRγδ$^+$, CD4$^+$ and CD8$^+$ T cells **(D)** TNF expression in NK cells, B cells, TCRγδ$^+$ T cells, FoxP3$^+$ Tregs and CD4$^+$ and CD8$^+$ T cell subsets. Data are represented as mean ± SEM with *p<0.05, **<0.01, ***0.001, ****<0.0001 by ordinary one-way ANOVA followed by Tukey's multiple comparisons test.

subsets. Vancomycin mice exhibited IFN-γ CD8$^+$ T cells only, compared to PBS (Figure 5C). Strikingly, we observed that an antibiotics-skewed microbiota, resulted in a significantly increased TNF expression across a variety of cell types, including NK cells, TCRγδ$^+$ T cells, Tregs, CD4$^+$ T-cells and CD8$^+$ T-cells (Figure 5D). This increase was most prominent for TCRγδ$^+$ and CD4 subsets, where the average % of TNF positive cells was more than double the PBS group (Figure 5D). Altogether these data show that while PmB may promote IL-10 expression, contributing to a protective response, both PmB and vancomycin-treated microbiota significantly upregulate TNF expression, which may potentially exacerbate inflammation.

Given antibiotic-treated mice showed significant upregulation of TNF and IFN-γ, critical mediators of IBD, this prompted us to examine the link between antibiotic consumption and global burden of IBD. Previous studies have identified associations between antibiotic exposure and development of chronic inflammatory diseases, such as metabolic disease, allergies, and autoimmune conditions, including colitis (23). Therefore, we gathered antibiotic usage data from the Global Research on Antimicrobial Resistance database, as well as age-standardised IBD incidence rates from Global Burden of Disease 2021 (GBD2021) and analysed their relationship using a generalised additive model (GAM). GAMs allow for comprehensive analysis of multiple parameters, simultaneously covering their individual, interactive effects, including non-linear effects. Our GAM also adjusted for confounders such as socioeconomics, reflected by gross domestic product (GDP), and corrected for inter-country differences as random effects (see Supplementary Information in Supplementary Data Sheet 1).

Figure 6 presents the modelling results for 2018, the most recent timepoint with complete data coverage, illustrating the predicted response curve of IBD incidence rate as a function of antibiotic consumption (Defined Daily Dose per 1000 inhabitants) at the median-grouped GDP. Globally, increased antibiotic consumption correlated with higher IBD disease burden. However, this relationship was also influenced by GDP, as the association dissipates at a high GDP bracket (Supplementary Figure 10). Here, our global analysis aligns with previous observational studies, which have demonstrated an association with antibiotics exposure and IBD incidence rates (87–89).

Overall, these data suggest a perturbed microbiota primes host cells for heightened pro-inflammatory expression under activation conditions. A PmB-treated microbiota in particular may skew the

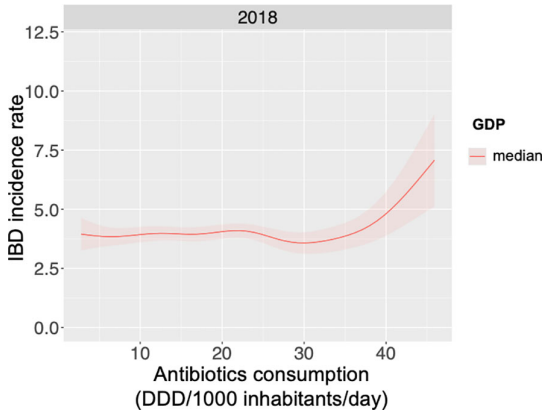

FIGURE 6
Global IBD incidence increases with increasing antibiotics consumption for median GDP. Global antibiotic consumption data, as Defined Daily Doses per 1000 inhabitants per day (DDD/1000 inhabitants/day) for 2018, was collected along with age-standardised incidence rates of irritable bowel disease (IBD) and data of gross domestic product (GDP). A generalised additive model was used to examine the relationship between antibiotic consumption, GDP and IBD incidence, with results for the year 2018 and median GDP presented.

host towards a Th1-biased phenotype, in line with data that found G+ bacteria preferentially induce IFN-γ and TNF in human PBMCs (90).

4 Discussion

The aim of this project was to investigate how antibiotic-mediated shifts in gut microbiota composition, impact the gut microbiota-host immune interaction. We utilised two antibiotic regimens to alter gut flora and found that while gut-derived SCFAs were highly impacted, the profile of immune cells in the spleen and MLNs were largely unchanged, suggesting minimal distal immune perturbations under basal conditions. While the MLNs showed minor changes in specific cell populations, it is important to note we did not assess other components of the mucosal immune system (i.e. intestinal lamina propia or epithelia), which have been shown to exhibit localised changes in response to antibiotics, as discussed below. *Ex vivo* stimulation revealed that adaptive cells from antibiotics-treated mice show greater pro-inflammatory cytokine expression, suggesting that immune function is impacted under challenged conditions. Altogether this highlights the need to better understand how dysbiosis may predispose the host to disease development, and how antibiotics may set the scene for inflammatory disease (Graphical Abstract).

While our study focused primarily of the impact on the spleen and MLNs, there is extensive body of literature highlighting their impact on mucosal immunity. For example, vancomycin specifically depletes intestinal Th17 and Treg populations (81, 91), demonstrating the importance of gram-positive segmented filamentous bacteria and *Clostridia* species in the induction of these T cell populations in the intestines. Antibiotics also reduce intestinal epithelial cell proliferation, and deplete innate cell populations, such as macrophages and monocytes in the ileum and colon (4). Notably, these perturbations can remain despite attempts to restore the microbiota via faecal transplantation, revealing their long-term impacts on immune homeostasis. Recent studies also reveal the short-term impact of antibiotics, with even a brief (3-day) course of broad-spectrum antibiotics significantly altering colonic innate lymphoid cell populations (92). As reviewed in Kennedy et al. (1) antibiotics also alter various components of intestinal immunity (such as antimicrobial peptides production, TLR expression, etc.), and the specific alteration varies depending on the antibiotic regimen, tissue examined, and the experimental model (1). For an overview of broad-spectrum antibiotic regimens and their impact on immunity, refer to Kennedy et al. (1),

Antibiotic treatment also impacts systemic immunity beyond the mucosal compartment. For example, disruption of commensal signalling with broad spectrum antibiotics influences haematopoiesis via STAT1 to reduce bone marrow progenitors (93), and also influences basophil development and IgE levels, via MyD88-dependent pathways (94). Scott et al. (95) further showed that antibiotic treatment followed by recolonisation results in persistent changes to the colonic lamina propria, including elevated Th1 responses driven by infiltrating pro-inflammatory macrophages. These macrophages produced high levels of TNF and IL6, contributing to a sustained inflammatory environment and enhancing the Th1 response. Altogether, these findings reveal the widespread and persistent impact of antibiotics, which can significantly perturb multiple immune compartments.

While previous studies have explored the effects of vancomycin and PmB on gut microbiota and host tissues, these studies focused on changes in faecal metabolites (51, 54) and characteristics of colon tissue (86). Methodological differences in these studies also limit the relevance of their findings to the influence of gut microbiota on host immunity. Zhang et al. (51) and Sun et al. (54) found PmB did not alter microbiota composition to be significantly different than vehicle controls, which may have resulted from inconsistent dosing associated with antibiotics in drinking water. Consequently, these studies do not provide clear links between how gut microbiota composition may influence observed changes in metabolites. These studies also used mice younger than 6-weeks old, which may limit relevance to mature adult immune systems. Ran et al. (86) found PmB and vancomycin increased colonic permeability *ex vivo*, and increased TNF expression in colonic tissue. However, their study used a short 7-day regimen of antibiotics in drinking water, and only reported minor changes to PmB microbiota at the genus level. Thus we have aimed to address a critical gap by characterising the long-term (4+ week) impact of antibiotics and how this may influence immune responses in gut local and systemic organs in otherwise healthy mice.

It is also important to note each antimicrobial in our study has been shown to exert immunomodulatory effects on cytokine production *in vitro*. PmB is a protein kinase C inhibitor, and thus would likely decrease cytokine production when directly exposed to T cells (96). Vancomycin appears to have context-dependent effects,

with differential regulation of TNF mRNA in primary PBMCs versus the Thp-1 monocyte cell line (97, 98). More recently, vancomycin was found also to directly interact with specific HLA alleles (99) and affect macrophage mitochondrial function (100). Similarly, amphotericin B, while primarily targeting ergosterol in fungal cells, has weak affinity for mammalian cholesterol and TLRs (46, 101). The drug also induces pro inflammatory cytokines such as TNF via the MyD88 pathway, although this may vary according to cell type and drug formulation (101).

Although these drugs demonstrate immunomodulatory effects *in vitro*, the oral administration route in our study makes it unlikely the drugs reached significant circulating concentrations to directly influence distal immune cells. Thus, we attribute the increase of TNF production in splenocytes to perturbations in microbiota-derived signalling, rather than a direct impact of the drugs themselves.

Another important methodological consideration of our study was the lack of an Amphotericin-only control group, to account for potential effects of the mycobiome. Interestingly, we observed vancomycin treatment resulted in increased fungal DNA levels compared to PBS groups, as determined by fungal 18S rRNA expression. Previously, vancomycin impaired gut antifungal immunity Th17 cells in the small intestinal lamina propria, likely due to the loss of segmented filamentous bacteria (102). Although we did not assess intestinal T cells, this impact of vancomycin could explain our observed increase in fungal DNA. Amphotericin B has broad-spectrum antifungal activity, and is commonly used in microbiota depletion studies to prevent fungal overgrowth, rather than achieve complete depletion (103, 104). Hence some alteration in fungal load is not unexpected. However, we cannot fully exclude that changes in mycobiome composition may have occurred due to our treatment, which could be potential confounding factor in our immunological findings.

We observed a significant increase in TNF expression in immune cells from antibiotic-treated mice after non-specific activation, particularly in TCR$\gamma\delta$ and $CD4^+$ T cells. Although TNF is a key mediator of the host defence response, it also plays a pathological role in autoimmune diseases, with elevated TNF levels observed in arthritis, psoriasis and IBD (83, 105–107). While the exact mechanisms by which TNF may initiate or sustain immune dysregulation in these conditions is still under investigation, TNF can be regarded as the "apex of a pro-inflammatory cascade" (85). This is demonstrated by the effectiveness of anti-TNF therapies which are widely used to neutralise TNF signalling, alleviating symptoms and improving outcomes in chronic inflammatory diseases. Dysbiosis is also considered a component of chronic inflammatory diseases, with the gut microbiota thought to contribute to inflammation and disease progression (108, 109). Previously we found that Imiquimod-induced psoriasis triggered dysbiosis, leading to a microbiota that produced elevated caecal succinate (65). This rise in succinate promoted the proliferation of a homeostatic population of colonic macrophages, which aggravated the symptoms of DSS-induced colitis. Indeed, psoriasis has a significant association with IBD, with evidence suggesting that IBD may be a causal risk factor for psoriasis, though not vice versa (110, 111). This highlights the possibility that alterations to gut microbiota homeostasis could be a fundamental contributor in the development of extra-intestinal autoinflammatory diseases.

Numerous studies have linked antibiotic exposure in high income countries with later development of autoimmune or chronic diseases, particularly when exposure occurs in early life (23). Our findings suggest that an antibiotics-perturbed microbiota results in an immune system that is basally predisposed for a heightened TNF response, which could help explain this association. This could be further explored using an autoimmune disease model, particularly one that may be T-cell mediated such as experimental autoimmune encephalitis or collagen-induced arthritis models (112, 113). While the precise relationship between TNF, gut dysbiosis and autoimmune disease is under investigation, our study highlights this as a crucial area for future research.

The broader context in which antibiotics are used is also key when considering their secondary impacts. For example, administration of the broad-spectrum antibiotic azithromycin (given biannually over two years) was found to reduce all-cause mortality in children under five across several sub-Saharan African countries (114). Thus, while antibiotics exposure may be a contributing factor to chronic disease in low-infection risk environments (such as high GDP countries), they provide significant health benefits in high-infection risk settings. Moreover, the increased basal immune activation we observed in our study may also be beneficial in such high-risk settings, although further investigation is warranted.

Although our findings indicate the immune system may be primed for heightened response, we found that dramatic changes in microbiota composition did not broadly modify host immunity in distal lymphoid organs during homeostasis, except for alterations in DC numbers in the spleen and MLN. Given the rising and widespread use of antibiotics and concerns about their adverse impact on gut flora, this finding is reassuring as it suggests the systemic immune compartment largely maintains homeostasis, despite substantial shifts in the gut microbiota. While we did not examine the recovery of microbiota after the cessation of antibiotics, most healthy humans recover baseline composition and richness two months after antibiotics exposure, but with a significant increase in the prevalence of antibiotic resistance genes (115, 116). Some individuals, however, do not fully recover, maintaining a "scarred" composition that resembles critically ill ICU patients (115). This emphasises the importance of prudent antibiotic usage as well as the need for greater understanding of the long-term consequences of a "scarred" microbiota: whether specific bacteria or metabolites that are important for host health are most likely to be impacted. While we focused on the impact of the gut microbiota on immunity under homeostatic conditions, many have observed that antibiotic-induced disruption to gut flora is associated with worse outcomes in various conditions such as infection, stroke, cancer and allergy (117–121). Therefore, it would be important to investigate our model under conditions particularly where the gut immune system is challenged, such as enteric infection or food

allergy, to fully understand the impact of antibiotic-mediated dysbiosis on the host.

We observed primarily DC subsets were altered in the spleen and MLNs. One potential mechanism for these changes could be through microbiota-derived signalling on haematopoiesis. The microbiota drives haematopoiesis primarily via TLR signalling (5, 93, 122) and is necessary for proper neutrophil and NK cell function (123, 124). While some studies suggest antibiotics do not impact DC progenitors in bone marrow (125, 126), others have identified an impact via FLT3L, a key DC growth factor (117). Recently, gut microbiota-derived propionate, delivered via breastmilk, was identified as essential for FLT3L signalling and thus pDC development in the neonatal gut (127). While we did not assess FLT3L expression, this may explain the increase in MLN pDCs we observed only in vancomycin mice who had elevated propionate levels. However, a more likely explanation for our observation is increased DC maturation and migration from the intestinal lamina propria, in response to our antibiotic regimen, which likely induced local inflammation.

We found perturbing the microbiota increased the numbers of migratory cDCs in the MLNs, identified as $CD11c^{+}$ $MHCII^{hi}$ cells. This finding aligns with previous observations by Diehl et al. (128), where antibiotic-induced dysbiosis during *Salmonella* infection promoted antigen uptake by $CD11c^{+}$ CX_3CR1^{hi} mononuclear phagocytes, that trafficked to the MLNs to induce a *Salmonella*-specific T cell response (128). Although we did not measure CX_3CR1 or CD103 (a migratory DC marker) expression, these markers would confirm migratory cDC identity. We did not observe changes to adaptive cell numbers in the MLNs and spleen, suggestive of no overt immune response. However, a comprehensive profile of the mucosal T cell compartment, particularly using approaches to track T cell migration (such as FTY720 to block egress), would be needed to fully assess potential antigen-specific responses to long-term antibiotic-mediated dysbiosis. Notably, the gut microbiota appears to influence vaccine efficacy (129). Human trials examining impact of antibiotics on vaccine efficacy show mixed results but are often limited by small sample size ($n<100$) (129). However, there is extensive evidence in mice indicating that antibiotics exposure or impaired TLR recognition has a detrimental effect on antibody response (129–131). While the mechanisms underlying this are still under investigation, the gut microbiota seems to have an adjuvant effect: as a source of pattern-recognition receptor ligands for antigen-presenting cells; through production of immunomodulatory metabolites that regulate host cells; and as a source of cross-reactive epitopes (132). Infancy also seems to be the crucial period in which the gut microbiota influences vaccination outcomes, for mice and humans (129), again highlighting the importance of the early life period on life-long immunity and the need for cautious use of antibiotics during this time.

In the study of microbiota-host interactions, SCFA represent a particularly important class of metabolites, given their extensive role in maintaining immune homeostasis and gut health (11). Here, perturbing the microbiota composition reduced overall levels of SCFAs, particularly acetate and butyrate. Reduced SCFAs are implicated in a range of conditions, including inflammatory bowel disease, arthritis, and allergies (11), with decreased maternal acetate levels in pregnancy linked to atopy, for example (133, 134). SCFAs also have links to DC functionality, impairing DC cytokine secretion and antigen presentation ability *in vitro* (135, 136). Urribe-Herranz et al. found vancomycin-mediated depletion of butyrate augmented the antitumour response in a murine radiotherapy model, through enhanced DC cross-presentation of tumour antigens (136). This suggests that antibiotics could be used to modulate DC antigen-presentation capacity via their impact on the gut microbiota, which could be advantageous in contexts such as cancer treatment or autoimmune disease. Conversely, reductions in SCFA caused by antibiotics could be mitigated through prebiotic or probiotic supplementation, to encourage growth of SCFA-generating species, or by direct supplementation with SCFAs.

In summary, we aimed to examine the impact of an antibiotics-induced dysbiosis on host immune homeostasis. Our findings reveal that while perturbation of the gut microbiota reduces levels of immunomodulatory SCFAs, the immune profiles in the spleen and MLNs remain largely unaffected under basal conditions. However, host cells may be programmed towards a greater immune response when challenged, suggesting a potential predisposition to inflammation. This study adds to the growing body of research highlighting the importance of understanding short- and long-term impacts of dysbiosis, particularly when triggered by antibiotics, and how it may set the stage for development of chronic diseases.

Data availability statement

The datasets presented in this study can be found in online repositories. The names of the repository/repositories and accession number(s) can be found below: https://www.ebi.ac.uk/ena, PRJEB79918.

Ethics statement

The animal study was approved by Australian Ethics Committee, The University of Sydney. The study was conducted in accordance with the local legislation and institutional requirements.

Author contributions

JJT: Data curation, Formal analysis, Investigation, Methodology, Writing – original draft. JT: Data curation, Investigation, Methodology, Writing – review & editing. DN: Data curation, Formal analysis, Writing – review & editing. CP-V: Data curation, Writing – review & editing. GG: Funding acquisition, Writing – review & editing. RN: Conceptualization, Funding acquisition, Investigation, Supervision, Writing – review & editing. LM: Conceptualization, Funding acquisition, Investigation, Supervision, Writing – review & editing.

Funding

The author(s) declare financial support was received for the research, authorship, and/or publication of this article. This work was supported with funding by ARC DP210102943.

Acknowledgments

The authors acknowledge the Sydney Cytometry Core Research Facility, a joint initiative of Centenary Institute and the University of Sydney, for providing access to flow cytometers. The authors acknowledge the facilities and the scientific and technical assistance of Sydney Analytical, a core research facility at The University of Sydney. We acknowledge the University of Sydney Laboratory animal services. We acknowledge Dr. Dana Stanley and Dr Yagav Bajagai for performing 16S Amplicon sequencing at Central Queensland University. Graphical abstract was created with BioRender.com.

Conflict of interest

LM is a current employee of the Translational Science Hub Global Sanofi Vaccines R&D Brisbane, Australia. Her contribution to this manuscript was when she was an employee of the University of Sydney.

The remaining authors declare that the research was conducted in the absence of any commercial or financial relationships that could be construed as a potential conflict of interest.

The author(s) declared that they were an editorial board member of Frontiers, at the time of submission. This had no impact on the peer review process and the final decision.

Publisher's note

Supplementary material

The Supplementary Material for this article can be found online at: https://www.frontiersin.org/articles/10.3389/fimmu.2024.1493991/full#supplementary-material.

References

1. Kennedy EA, King KY, Baldridge MT. Mouse microbiota models: comparing germ-free mice and antibiotics treatment as tools for modifying gut bacteria. *Front Physiol*. (2018) 9:1534. doi: 10.3389/fphys.2018.01534

2. Tan J, Taitz J, Sun SM, Langford L, Ni D, Macia L. Your regulatory T cells are what you eat: how diet and gut microbiota affect regulatory T cell development. *Front Nutr*. (2022) 9. doi: 10.3389/fnut.2022.878382

3. Ivanov II, Atarashi K, Manel N, Brodie EL, Shima T, Karaoz U, et al. Induction of intestinal Th17 cells by segmented filamentous bacteria. *Cell*. (2009) 139:485–98. doi: 10.1016/j.cell.2009.09.033

4. Ekmekciu I, von Klitzing E, Fiebiger U, Escher U, Neumann C, Bacher P, et al. Immune responses to broad-spectrum antibiotic treatment and fecal microbiota transplantation in mice. *Front Immunol*. (2017) 8:397. doi: 10.3389/fimmu.2017.00397

5. Khosravi A, Yáñez A, Price JG, Chow A, Merad M, Goodridge HS, et al. Gut microbiota promote hematopoiesis to control bacterial infection. *Cell Host Microbe*. (2014) 15:374–81. doi: 10.1016/j.chom.2014.02.006

6. Ochoa-Repáraz J, Mielcarz DW, Ditrio LE, Burroughs AR, Foureau DM, Haque-Begum S, et al. Role of gut commensal microflora in the development of experimental autoimmune encephalomyelitis. *J Immunol*. (2009) 183:6041–50. doi: 10.4049/jimmunol.0900747

7. Miyauchi E, Shimokawa C, Steimle A, Desai MS, Ohno H. The impact of the gut microbiome on extra-intestinal autoimmune diseases. *Nat Rev Immunol*. (2023) 23:9–23. doi: 10.1038/s41577-022-00727-y

8. Carding S, Verbeke K, Vipond DT, Corfe BM, Owen LJ. Dysbiosis of the gut microbiota in disease. *Microb Ecol Health Dis*. (2015) 26:26191. doi: 10.3402/mehd.v26.26191

9. Wilkins LJ, Monga M, Miller AW. Defining dysbiosis for a cluster of chronic diseases. *Sci Rep*. (2019) 9:12918. doi: 10.1038/s41598-019-49452-y

10. Memon H, Abdulla F, Reljic T, Alnuaimi S, Serdarevic F, Asimi ZV, et al. Effects of combined treatment of probiotics and metformin in management of type 2 diabetes: A systematic review and meta-analysis. *Diabetes Res Clin Pract*. (2023) 202:110806. doi: 10.1016/j.diabres.2023.110806

11. Tan J, McKenzie C, Potamitis M, Thorburn AN, Mackay CR, Macia L. The role of short-chain fatty acids in health and disease. *Adv Immunol*. (2014) 121:91–119. doi: 10.1016/B978-0-12-800100-4.00003-9

12. Ferrell JM, Chiang JYL. Bile acid receptors and signaling crosstalk in the liver, gut and brain. *Liver Research Bile Acids Metab liver Dis*. (2021) 5:105–18. doi: 10.1016/j.livres.2021.07.002

13. Zhou L. Ahr function in lymphocytes: emerging concepts. *Trends Immunol*. (2016) 37:17–31. doi: 10.1016/j.it.2015.11.007

14. Franchi L, Warner N, Viani K, Nuñez G. Function of nod-like receptors in microbial recognition and host defense. *Immunol Rev*. (2009) 227:106–28. doi: 10.1111/j.1600-065X.2008.00734.x

15. Mogensen TH. Pathogen recognition and inflammatory signaling in innate immune defenses. *Clin Microbiol Rev*. (2009) 22:240–73. doi: 10.1128/CMR.00046-08

16. Hoerr V, Zbytnuik L, Leger C, Tam PPC, Kubes P, Vogel HJ. Gram-negative and gram-positive bacterial infections give rise to a different metabolic response in a mouse model. *J Proteome Res*. (2012) 11:3231–45. doi: 10.1021/pr201274r

17. Wang Q, Li X, Tang W, Guan X, Xiong Z, Zhu Y, et al. Differential gene sets profiling in gram-negative and gram-positive sepsis. *Front Cell Infect Microbiol*. (2022) 12:801232. doi: 10.3389/fcimb.2022.801232

18. Liu P, Wu L, Peng G, Han Y, Tang R, Ge J, et al. Altered microbiomes distinguish Alzheimer's disease from amnestic mild cognitive impairment and health in a Chinese cohort. *Brain Behav Immun*. (2019) 80:633–43. doi: 10.1016/j.bbi.2019.05.008

19. Magne F, Gotteland M, Gauthier L, Zazueta A, Pesoa S, Navarrete P, et al. The firmicutes/bacteroidetes ratio: A relevant marker of gut dysbiosis in obese patients? *Nutrients*. (2020) 12:1474. doi: 10.3390/nu12051474

20. Pushpanathan P, Srikanth P, Seshadri KG, Selvarajan S, Pitani RS, Kumar TD, et al. Gut microbiota in type 2 diabetes individuals and correlation with monocyte chemoattractant protein1 and interferon gamma from patients attending a tertiary care centre in chennai, India. *Indian J Endocrinol Metab*. (2016) 20:523–30. doi: 10.4103/2230-8210.183474

21. Salguero MV, Al-Obaide MAI, Singh R, Siepmann T, Vasylyeva TL. Dysbiosis of Gram-negative gut microbiota and the associated serum lipopolysaccharide exacerbates inflammation in type 2 diabetic patients with chronic kidney disease. *Exp Ther Med*. (2019) 18:3461–9. doi: 10.3892/etm.2019.7943

22. Patangia DV, Anthony Ryan C, Dempsey E, Paul Ross R, Stanton C. Impact of antibiotics on the human microbiome and consequences for host health. *Microbiologyopen*. (2022) 11:e1260. doi: 10.1002/mbo3.1260

23. Queen J, Zhang J, Sears CL. Oral antibiotic use and chronic disease: long-term health impact beyond antimicrobial resistance and Clostridioides difficile. *Gut Microbes*. (2020) 11:1092–103. doi: 10.1080/19490976.2019.1706425

24. Song W, Tiruthani K, Wang Y, Shen L, Hu M, Dorosheva O, et al. Trapping lipopolysaccharide to promote immunotherapy against colorectal cancer and attenuate liver metastasis. *Adv Mater*. (2018) 30:e1805007. doi: 10.1002/adma.201805007

25. Tirelle P, Breton J, Riou G, Déchelotte P, Coëffier M, Ribet D. Comparison of different modes of antibiotic delivery on gut microbiota depletion efficiency and body composition in mouse. *BMC Microbiol*. (2020) 20:340. doi: 10.1186/s12866-020-02018-9

26. Joat N, Bajagai YS, Van TTH, Stanley D, Chousalkar K, Moore RJ. The temporal fluctuations and development of faecal microbiota in commercial layer flocks. *Anim Nutr*. (2023) 15:197–209. doi: 10.1016/j.aninu.2023.07.006

27. Callahan B. *RDP taxonomic training data formatted for DADA2 (RDP trainset 16/release 11.5)*. Zenodo (2017). doi: 10.5281/zenodo.801828.

28. Tan J, Ni D, Taitz J, Pinget GV, Read M, Senior A, et al. Dietary protein increases T-cell-independent sIgA production through changes in gut microbiota-derived extracellular vesicles. *Nat Commun*. (2022) 13:4336. doi: 10.1038/s41467-022-31761-y

29. Usyk M, Zolnik CP, Patel H, Levi MH, Burk RD. Novel ITS1 fungal primers for characterization of the mycobiome. *mSphere*. (2017) 2:e00488–17. doi: 10.1128/mSphere.00488-17

30. Boutin RCT, Sbihi H, McLaughlin RJ, Hahn AS, Konwar KM, Loo RS, et al. Composition and associations of the infant gut fungal microbiota with environmental factors and childhood allergic outcomes. *mBio*. (2021) 12:e0339620. doi: 10.1128/mBio.03396-20

31. Browne AJ, Chipeta MG, Haines-Woodhouse G, Kumaran EPA, Hamadani BHK, Zaraa S, et al. Global antibiotic consumption and usage in humans 2000-18: a spatial modelling study. *Lancet Planet Health*. (2021) 5:e893–904. doi: 10.1016/S2542-5196(21)00280-1

32. Inklaar R, de Jong H, Bolt J, van Zanden JL. Rebasing "Maddison": new income comparisons and the shape of long-run economic development. Groningen Growth and Development Center. *GGDC Res Memorandum*. (2018) GD-174.

33. Ni D, Nanan R. Global and regional associations of enteric infections and asthma. *medRxiv*. (2024). doi: 10.1101/2024.05.21.24307671

34. Ni D, Nanan R. Global associations of maternal hypertensive disorders and offspring allergic disease burden. *Clin Exp Allergy*. (2024) 54:1024–6. doi: 10.1111/cea.14566

35. Diederich A. Generalized additive models. *introduction R J Math Psychol*. (2007) 51:339.

36. Lane P, Wood S, Jones M, Nelder J, Lee Y, Cortina-Borja M, et al. Generalized additive models for location, scale and shape - Discussion. *Appl Stat*. (2005) 54:544–54.

37. Verbeke T. Generalized additive models: an introduction with R by S. N. Wood. *J R Stat Soc Ser A: Stat Soc*. (2007) 170:262. doi: 10.1111/j.1467-985X.2006.00455_15.x

38. Wood SN. *Generalized additive models: an introduction with R. 2nd ed*. New York: Chapman and Hall/CRC (2017).

39. Akaike H. Information theory and an extension of the maximum likelihood principle. In: Parzen E, Tanabe K, Kitagawa G, editors. *Selected papers of hirotugu akaike*. Springer, New York, NY (1998). p. 199–213. doi: 10.1007/978-1-4612-1694-0_15

40. Trimble MJ, Mlynárčik P, Kolář M, Hancock REW. Polymyxin: alternative mechanisms of action and resistance. *Cold Spring Harb Perspect Med*. (2016) 6:a025288. doi: 10.1101/cshperspect.a025288

41. Avedissian SN, Liu J, Rhodes NJ, Lee A, Pais GM, Hauser AR, et al. A review of the clinical pharmacokinetics of polymyxin B. *Antibiotics*. (2019) 8:31. doi: 10.3390/antibiotics8010031

42. Eubank TA, Hu C, Gonzales-Luna AJ, Garey KW. Detectable vancomycin stool concentrations in hospitalized patients with diarrhea given intravenous vancomycin. *Pharmacoepidemiology*. (2023) 2:283–8. doi: 10.3390/pharma2040024

43. Falagas ME, Kasiakou SK, Saravolatz LD. Colistin: the revival of polymyxins for the management of multidrug-resistant gram-negative bacterial infections. *Clin Infect Dis*. (2005) 40:1333–41. doi: 10.1086/429323

44. Gonzales M, Pepin J, Frost EH, Carrier JC, Sirard S, Fortier L-C, et al. Faecal pharmacokinetics of orally administered vancomycin in patients with suspected Clostridium difficile infection. *BMC Infect Dis*. (2010) 10:363. doi: 10.1186/1471-2334-10-363

45. Kaye KS, Pogue JM, Kaye D. 31 - polymyxins (Polymyxin B and colistin). In: Bennett JE, Dolin R, Blaser MJ, editors. *Mandell, douglas, and bennett's principles and practice of infectious diseases, Eighth Edition*. W.B. Saunders, Philadelphia (2015). p. 401–405.e1. doi: 10.1016/B978-1-4557-4801-3.00031-X

46. Liu M, Chen M, Yang Z. Design of amphotericin B oral formulation for antifungal therapy. *Drug Delivery*. (2017) 24:1–9. doi: 10.1080/10717544.2016.1225852

47. Pettit NN, DePestel DD, Fohl AL, Eyler R, Carver PL. Risk factors for systemic vancomycin exposure following administration of oral vancomycin for the treatment of clostridium difficile infection. *Pharmacotherapy: J Hum Pharmacol Drug Ther*. (2015) 35:119–26. doi: 10.1002/phar.1538

48. Reikvam DH, Erofeev A, Sandvik A, Grcic V, Jahnsen FL, Gaustad P, et al. Depletion of murine intestinal microbiota: effects on gut mucosa and epithelial gene expression. *PloS One*. (2011) 6:e17996. doi: 10.1371/journal.pone.0017996

49. Thuny F, Richet H, Casalta J-P, Angelakis E, Habib G, Raoult D. Vancomycin treatment of infective endocarditis is linked with recently acquired obesity. *PloS One*. (2010) 5:e9074. doi: 10.1371/journal.pone.0009074

50. Inoue Y, Fukui H, Xu X, Ran Y, Tomita T, Oshima T, et al. Colonic M1 macrophage is associated with the prolongation of gastrointestinal motility and obesity in mice treated with vancomycin. *Mol Med Rep*. (2019) 19:2591–8. doi: 10.3892/mmr.2019.9920

51. Zhang N, Liu J, Chen Z, Chen N, Gu F, He Q. Integrated analysis of the alterations in gut microbiota and metabolites of mice induced after long-term intervention with different antibiotics. *Front Microbiol*. (2022) 13:832915. doi: 10.3389/fmicb.2022.832915

52. Xu X, Fukui H, Ran Y, Tomita T, Oshima T, Watari J, et al. Alteration of GLP-1/GPR43 expression and gastrointestinal motility in dysbiotic mice treated with vancomycin. *Sci Rep*. (2019) 9:4381. doi: 10.1038/s41598-019-40978-9

53. Sawaed J, Zelik L, Levin Y, Feeney R, Naama M, Gordon A, et al. Antibiotics damage the colonic mucus barrier in a microbiota-independent manner. *Sci Adv*. (2024) 10:eadp4119. doi: 10.1126/sciadv.adp4119

54. Sun L, Zhang X, Zhang Y, Zheng K, Xiang Q, Chen N, et al. Antibiotic-induced disruption of gut microbiota alters local metabolomes and immune responses. *Front Cell Infect Microbiol*. (2019) 9:99. doi: 10.3389/fcimb.2019.00099

55. Buchholz KR, Reichelt M, Johnson MC, Robinson SJ, Smith PA, Rutherford ST, et al. Potent activity of polymyxin B is associated with long-lived super-stoichiometric accumulation mediated by weak-affinity binding to lipid A. *Nat Commun*. (2024) 15:4733. doi: 10.1038/s41467-024-49200-5

56. Cullen TW, Schofield WB, Barry NA, Putnam EE, Rundell EA, Trent MS, et al. Antimicrobial peptide resistance mediates resilience of prominent gut commensals during inflammation. *Science*. (2015) 347:170–5. doi: 10.1126/science.1260580

57. Ingham HR, Selkon JB, Codd AA, Hale JH. A study *in vitro* of the sensitivity to antibiotics of Bacteroides fragilis. *J Clin Pathol*. (1968) 21:432–6. doi: 10.1136/jcp.21.4.432

58. Lagkouvardos I, Joseph D, Kapfhammer M, Giritli S, Horn M, Haller D, et al. IMNGS: A comprehensive open resource of processed 16S rRNA microbial profiles for ecology and diversity studies. *Sci Rep*. (2016) 6:33721. doi: 10.1038/srep33721

59. Pfeiffer N, Desmarchelier C, Blaut M, Daniel H, Haller D, Clavel T. Acetatifactor muris gen. nov., sp. nov., a novel bacterium isolated from the intestine of an obese mouse. *Arch Microbiol*. (2012) 194:901–7. doi: 10.1007/s00203-012-0822-1

60. Huffnagle GB, Noverr MC. The emerging world of the fungal microbiome. *Trends Microbiol*. (2013) 21:334. doi: 10.1016/j.tim.2013.04.002

61. van Tilburg Bernardes E, Pettersen VK, Gutierrez MW, Laforest-Lapointe I, Jendzjowsky NG, Cavin J-B, et al. Intestinal fungi are causally implicated in microbiome assembly and immune development in mice. *Nat Commun*. (2020) 11:2577. doi: 10.1038/s41467-020-16431-1

62. Daïen CI, Tan J, Audo R, Mielle J, Quek LE, Krycer JR, et al. Gut-derived acetate promotes B10 cells with antiinflammatory effects. *JCI Insight*. (2021) 6:e144156. doi: 10.1172/jci.insight.144156

63. Fusco W, Lorenzo MB, Cintoni M, Porcari S, Rinninella E, Kaitsas F, et al. Short-chain fatty-acid-producing bacteria: key components of the human gut microbiota. *Nutrients*. (2023) 15:2211. doi: 10.3390/nu15092211

64. Fernández-Veledo S, Vendrell J. Gut microbiota-derived succinate: Friend or foe in human metabolic diseases? *Rev Endocr Metab Disord*. (2019) 20:439–47. doi: 10.1007/s11154-019-09513-z

65. Pinget GV, Tan JK, Ni D, Taitz J, Daien CI, Mielle J, et al. Dysbiosis in imiquimod-induced psoriasis alters gut immunity and exacerbates colitis development. *Cell Rep*. (2022) 40:111191. doi: 10.1016/j.celrep.2022.111191

66. Takeuchi T, Miyauchi E, Kanaya T, Kato T, Nakanishi Y, Watanabe T, et al. Acetate differentially regulates IgA reactivity to commensal bacteria. *Nature*. (2021) 595:560–4. doi: 10.1038/s41586-021-03727-5

67. Gupta S, Basu S, Bal V, Rath S, George A. Gut IgA abundance in adult life is a major determinant of resistance to dextran sodium sulfate-colitis and can compensate for the effects of inadequate maternal IgA received by neonates. *Immunology*. (2019) 158:19–34. doi: 10.1111/imm.13091

68. Salonen A, Lahti L, Salojärvi J, Holtrop G, Korpela K, Duncan SH, et al. Impact of diet and individual variation on intestinal microbiota composition and fermentation products in obese men. *ISME J*. (2014) 8:2218–30. doi: 10.1038/ismej.2014.63

69. Fang S, Qin T, Yu T, Zhang G. Improvement of the gut microbiota *in vivo* by a short-chain fatty acids-producing strain lactococcus garvieae CF11. *Processes*. (2022) 10:604. doi: 10.3390/pr10030604

70. Louis P, Flint HJ. Formation of propionate and butyrate by the human colonic microbiota. *Environ Microbiol*. (2017) 19:29–41. doi: 10.1111/1462-2920.13589

71. Scheithauer TPM, Bakker GJ, Winkelmeijer M, Davids M, Nieuwdorp M, van Raalte DH, et al. Compensatory intestinal immunoglobulin response after vancomycin treatment in humans. *Gut Microbes*. (2021) 13:1875109. doi: 10.1080/19490976.2021.1875109

72. Sun T, Nguyen A, Gommerman JL. Dendritic cell subsets in intestinal immunity and inflammation. *J Immunol*. (2020) 204:1075–83. doi: 10.4049/jimmunol.1900710

73. Vatanen T, Kostic AD, d'Hennezel E, Siljander H, Franzosa EA, Yassour M, et al. Variation in microbiome LPS immunogenicity contributes to autoimmunity in humans. *Cell*. (2016) 165:842. doi: 10.1016/j.cell.2016.04.007

74. Hessle C, Andersson B, Wold AE. Gram-positive bacteria are potent inducers of monocytic interleukin-12 (IL-12) while gram-negative bacteria preferentially stimulate

IL-10 production. *Infect Immun*. (2000) 68:3581–6. doi: 10.1128/IAI.68.6.3581-3586.2000

75. Hessle CC, Andersson B, Wold AE. Gram-positive and Gram-negative bacteria elicit different patterns of pro-inflammatory cytokines in human monocytes. *Cytokine*. (2005) 30:311–8. doi: 10.1016/j.cyto.2004.05.008

76. Karlsson H, Larsson P, Wold AE, Rudin A. Pattern of Cytokine Responses to Gram-Positive and Gram-Negative Commensal Bacteria is Profoundly Changed when Monocytes Differentiate into Dendritic Cells. *Scandinavian J Immunol*. (2004) 59:628–8. doi: 10.1111/j.0300-9475.2004.01423at.x

77. Tietze K, Dalpke A, Morath S, Mutters R, Heeg K, Nonnenmacher C. Differences in innate immune responses upon stimulation with gram-positive and gram-negative bacteria. *J Periodontal Res*. (2006) 41:447–54. doi: 10.1111/j.1600-0765.2006.00890.x

78. Surbatovic M, Popovic N, Vojvodic D, Milosevic I, Acimovic G, Stojicic M, et al. Cytokine profile in severe Gram-positive and Gram-negative abdominal sepsis. *Sci Rep*. (2015) 5:11355. doi: 10.1038/srep11355

79. Cheng M, Qian L, Shen G, Bian G, Xu T, Xu W, et al. Microbiota modulate tumoral immune surveillance in lung through a γδT17 immune cell-dependent mechanism. *Cancer Res*. (2014) 74:4030–41. doi: 10.1158/0008-5472.CAN-13-2462

80. Li F, Hao X, Chen Y, Bai L, Gao X, Lian Z, et al. The microbiota maintain homeostasis of liver-resident γδT-17 cells in a lipid antigen/CD1d-dependent manner. *Nat Commun*. (2017) 8:13839. doi: 10.1038/ncomms13839

81. Atarashi K, Tanoue T, Shima T, Imaoka A, Kuwahara T, Momose Y, et al. Induction of colonic regulatory T cells by indigenous Clostridium species. *Science*. (2011) 331:337–41. doi: 10.1126/science.1198469

82. Mazmanian SK, Liu CH, Tzianabos AO, Kasper DL. An immunomodulatory molecule of symbiotic bacteria directs maturation of the host immune system. *Cell*. (2005) 122:107–18. doi: 10.1016/j.cell.2005.05.007

83. Kamada N, Hisamatsu T, Okamoto S, Chinen H, Kobayashi T, Sato T, et al. Unique CD14 intestinal macrophages contribute to the pathogenesis of Crohn disease via IL-23/IFN-gamma axis. *J Clin Invest*. (2008) 118:2269–80. doi: 10.1172/JCI34610

84. Langer V, Vivi E, Regensburger D, Winkler TH, Waldner MJ, Rath T, et al. IFN-γ drives inflammatory bowel disease pathogenesis through VE-cadherin–directed vascular barrier disruption. *J Clin Invest*. (2019) 129:4691–707. doi: 10.1172/JCI124884

85. Monaco C, Nanchahal J, Taylor P, Feldmann M. Anti-TNF therapy: past, present and future. *Int Immunol*. (2015) 27:55–62. doi: 10.1093/intimm/dxu102

86. Ran Y, Fukui H, Xu X, Wang X, Ebisutani N, Tanaka Y, et al. Alteration of colonic mucosal permeability during antibiotic-induced dysbiosis. *Int J Mol Sci*. (2020) 21:6108. doi: 10.3390/ijms21176108

87. Faye AS, Allin KH, Iversen AT, Agrawal M, Faith J, Colombel J-F, et al. Antibiotic use as a risk factor for inflammatory bowel disease across the ages: a population-based cohort study. *Gut*. (2023) 72:663–70. doi: 10.1136/gutjnl-2022-327845

88. Nguyen LH, Örtqvist AK, Cao Y, Simon TG, Roelstraete B, Song M, et al. Antibiotic use and the development of inflammatory bowel disease: a national case/control study in Sweden. *Lancet Gastroenterol Hepatol*. (2020) 5:986–95. doi: 10.1016/S2468-1253(20)30267-3

89. Theochari NA, Stefanopoulos A, Mylonas KS, Economopoulos KP. Antibiotics exposure and risk of inflammatory bowel disease: a systematic review. *Scandinavian J Gastroenterol*. (2018) 53:1–7. doi: 10.1080/00365521.2017.1386711

90. Skovbjerg S, Martner A, Hynsjö L, Hessle C, Olsen I, Dewhirst FE, et al. Gram-positive and gram-negative bacteria induce different patterns of cytokine production in human mononuclear cells irrespective of taxonomic relatedness. *J Interferon Cytokine Res*. (2010) 30:23–32. doi: 10.1089/jir.2009.0033

91. Ivanov II, de Llanos Frutos R, Manel N, Yoshinaga K, Rifkin DB, Sartor RB, et al. Specific microbiota direct the differentiation of Th17 cells in the mucosa of the small intestine. *Cell Host Microbe*. (2008) 4:337–49. doi: 10.1016/j.chom.2008.09.009

92. Uddin MJ, Thompson B, Leslie JL, Fishman C, Sol-church K, Kumar P, et al. Investigating the impact of antibiotic-induced dysbiosis on protection from Clostridium difficile colitis by mouse colonic innate lymphoid cells. *mBio*. (2024) 15:e03338–23. doi: 10.1128/mbio.03338-23

93. Josefsdottir KS, Baldridge MT, Kadmon CS, King KY. Antibiotics impair murine hematopoiesis by depleting the intestinal microbiota. *Blood*. (2017) 129:729–39. doi: 10.1182/blood-2016-03-708594

94. Hill DA, Siracusa MC, Abt MC, Kim BS, Kobuley D, Kubo M, et al. Commensal bacterial–derived signals regulate basophil hematopoiesis and allergic inflammation. *Nat Med*. (2012) 18:538–46. doi: 10.1038/nm.2657

95. Scott NA, Andrusaite A, Andersen P, Lawson M, Alcon-Giner C, Leclaire C, et al. Antibiotics induce sustained dysregulation of intestinal T cell immunity by perturbing macrophage homeostasis. *Sci Transl Med*. (2018) 10:eaao4755. doi: 10.1126/scitranslmed.aao4755

96. Baliga BS, Sindel LJ, Jenkins LD, Sachen JB. Effect of polymyxin-B on T-lymphocyte protein synthesis. *Biochem Biophys Res Commun*. (1986) 135:649–54. doi: 10.1016/0006-291X(86)90042-2

97. Bode C, Muenster S, Diedrich B, Jahnert S, Weisheit C, Steinhagen F, et al. Linezolid, vancomycin and daptomycin modulate cytokine production, Toll-like receptors and phagocytosis in a human *in vitro* model of sepsis. *J Antibiot*. (2015) 68:485–90. doi: 10.1038/ja.2015.18

98. Siedlar M, Szczepanik A, Więckiewicz J, Pituch-Noworolska A, Zembala M. Vancomycin down-regulates lipopolysaccharide-induced tumour necrosis factor alpha (TNFα) production and TNFa-mRNA accumulation in human blood monocytes. *Immunopharmacology*. (1997) 35:265–71. doi: 10.1016/S0162-3109(96)00156-7

99. Ogese MO, Lister A, Gardner J, Meng X, Alfirevic A, Pirmohamed M, et al. Deciphering adverse drug reactions: *in vitro* priming and characterization of vancomycin-specific T cells from healthy donors expressing HLA-A*32:01. *Toxicol Sci*. (2021) 183:139–53. doi: 10.1093/toxsci/kfab084

100. Bojang E, Sheriff L, Fu MS, Wellings C, Abdissa K, Stavrou V, et al. Vancomycin impairs macrophage fungal killing by disrupting mitochondrial morphology and function. *bioRxiv*. (2024). doi: 10.1101/2024.06.25.600580

101. Mesa-Arango AC, Scorzoni L, Zaragoza O. It only takes one to do many jobs: Amphotericin B as antifungal and immunomodulatory drug. *Front Microbiol*. (2012) 3:286. doi: 10.3389/fmicb.2012.00286

102. Drummond RA, Desai JV, Ricotta EE, Swamydas M, Deming C, Conlan S, et al. Long-term antibiotic exposure promotes mortality after systemic fungal infection by driving lymphocyte dysfunction and systemic escape of commensal bacteria. *Cell Host Microbe*. (2022) 30:1020–33.e6. doi: 10.1016/j.chom.2022.04.013

103. Lee Y, Robbins N, Cowen LE. Molecular mechanisms governing antifungal drug resistance. *NPJ Antimicrob Resist*. (2023) 1:5. doi: 10.1038/s44259-023-00007-2

104. O'Shaughnessy EM, Lyman CA, Walsh TJ. "Amphotericin B: Polyene Resistance Mechanisms." In *Antimicrobial Drug Resistance: Mechanisms of Drug Resistance*, edited by Douglas L. Mayers. (Totowa: Humana Press). (2009) pp. 295–305. doi: 10.1007/978-1-59745-180-2_25

105. Atreya R, Zimmer M, Bartsch B, Waldner MJ, Atreya I, Neumann H, et al. Antibodies against tumor necrosis factor (TNF) induce T-cell apoptosis in patients with inflammatory bowel diseases via TNF receptor 2 and intestinal $CD14^+$ macrophages. *Gastroenterology*. (2011) 141:2026–38. doi: 10.1053/j.gastro.2011.08.032

106. Singh UP, Singh NP, Murphy EA, Price RL, Fayad R, Nagarkatti M, et al. Chemokine and cytokine levels in inflammatory bowel disease patients. *Cytokine*. (2016) 77:44–9. doi: 10.1016/j.cyto.2015.10.008

107. Tetta C, Camussi G, Modena V, Di Vittorio C, Baglioni C. Tumour necrosis factor in serum and synovial fluid of patients with active and severe rheumatoid arthritis. *Ann Rheum Dis*. (1990) 49:665–7. doi: 10.1136/ard.49.9.665

108. Kim D, Zeng MY, Núñez G. The interplay between host immune cells and gut microbiota in chronic inflammatory diseases. *Exp Mol Med*. (2017) 49:e339–9. doi: 10.1038/emm.2017.24

109. Mousa WK, Chehadeh F, Husband S. Microbial dysbiosis in the gut drives systemic autoimmune diseases. *Front Immunol*. (2022) 13:906258. doi: 10.3389/fimmu.2022.906258

110. Freuer D, Linseisen J, Meisinger C. Association between inflammatory bowel disease and both psoriasis and psoriatic arthritis. *JAMA Dermatol*. (2022) 158:1262–8. doi: 10.1001/jamadermatol.2022.3682

111. Li Y, Guo J, Cao Z, Wu J. Causal association between inflammatory bowel disease and psoriasis: A two-sample bidirectional mendelian randomization study. *Front Immunol*. (2022) 13:916645. doi: 10.3389/fimmu.2022.916645

112. Fletcher JM, Lalor SJ, Sweeney CM, Tubridy N, Mills KHG. T cells in multiple sclerosis and experimental autoimmune encephalomyelitis. *Clin Exp Immunol*. (2010) 162:1–11. doi: 10.1111/j.1365-2249.2010.04143.x

113. Mitamura M, Nakano N, Yonekawa T, Shan L, Kaise T, Kobayashi T, et al. T cells are involved in the development of arthritis induced by anti-type II collagen antibody. *Int Immunopharmacol*. (2007) 7:1360–8. doi: 10.1016/j.intimp.2007.05.021

114. Keenan JD, Bailey RL, West SK, Arzika AM, Hart J, Weaver J, et al. Azithromycin to reduce childhood mortality in sub-saharan africa. *N Engl J Med*. (2018) 378:1583–92. doi: 10.1056/NEJMoa1715474

115. Anthony WE, Wang B, Sukhum KV, D'Souza AW, Hink T, Cass C, et al. Acute and persistent effects of commonly used antibiotics on the gut microbiome and resistome in healthy adults. *Cell Rep*. (2022) 39:110649. doi: 10.10f16/j.celrep.2022.110649

116. Palleja A, Mikkelsen KH, Forslund SK, Kashani A, Allin KH, Nielsen T, et al. Recovery of gut microbiota of healthy adults following antibiotic exposure. *Nat Microbiol*. (2018) 3:1255–65. doi: 10.1038/s41564-018-0257-9

117. Dessein R, Bauduin M, Grandjean T, Le Guern R, Figeac M, Beury D, et al. Antibiotic-related gut dysbiosis induces lung immunodepression and worsens lung infection in mice. *Crit Care*. (2020) 24:611. doi: 10.1186/s13054-020-03320-8

118. Elkrief A, Méndez-Salazar EO, Maillou J, Vanderbilt CM, Gogia P, Desilets A, et al. Antibiotics are associated with worse outcomes in lung cancer patients treated with chemotherapy and immunotherapy. *NPJ Precis. Onc*. (2024) 8:1–9. doi: 10.1038/s41698-024-00630-w

119. McKee AM, Kirkup BM, Madgwick M, Fowler WJ, Price CA, Dreger SA, et al. Antibiotic-induced disturbances of the gut microbiota result in accelerated breast tumor growth. *iScience*. (2021) 24:103012. doi: 10.1016/j.isci.2021.103012

120. Winek K, Engel O, Koduah P, Heimesaat MM, Fischer A, Bereswill S, et al. Depletion of cultivatable gut microbiota by broad-spectrum antibiotic pretreatment worsens outcome after murine stroke. *Stroke*. (2016) 47:1354–63. doi: 10.1161/STROKEAHA.115.011800

121. Zhang X, Borbet TC, Fallegger A, Wipperman MF, Blaser MJ, Müller A. An antibiotic-impacted microbiota compromises the development of colonic regulatory T

cells and predisposes to dysregulated immune responses. *mBio*. (2021) 12:e03335–20. doi: 10.1128/mBio.03335-20

122. Balmer ML, Schürch CM, Saito Y, Geuking MB, Li H, Cuenca M, et al. Microbiota-derived compounds drive steady-state granulopoiesis via MyD88/TICAM signaling. *J Immunol*. (2014) 193:5273–83. doi: 10.4049/jimmunol.1400762

123. Clarke TB, Davis KM, Lysenko ES, Zhou AY, Yu Y, Weiser JN. Recognition of peptidoglycan from the microbiota by Nod1 enhances systemic innate immunity. *Nat Med*. (2010) 16:228–31. doi: 10.1038/nm.2087

124. Ganal SC, Sanos SL, Kallfass C, Oberle K, Johner C, Kirschning C, et al. Priming of natural killer cells by nonmucosal mononuclear phagocytes requires instructive signals from commensal microbiota. *Immunity*. (2012) 37:171–86. doi: 10.1016/j.immuni.2012.05.020

125. Thackray LB, Handley SA, Gorman MJ, Poddar S, Bagadia P, Briseño CG, et al. Oral antibiotic treatment of mice exacerbates the disease severity of multiple flavivirus infections. *Cell Rep*. (2018) 22:3440–3453.e6. doi: 10.1016/j.celrep.2018.03.001

126. Vanderkerken M, Baptista AP, De Giovanni M, Fukuyama S, Browaeys R, Scott CL, et al. ILC3s control splenic cDC homeostasis via lymphotoxin signaling. *J Exp Med*. (2021) 218:e20190835. doi: 10.1084/jem.20190835

127. Sikder MAA, Rashid RB, Ahmed T, Sebina I, Howard DR, Ullah MA, et al. Maternal diet modulates the infant microbiome and intestinal Flt3L necessary for dendritic cell development and immunity to respiratory infection. *Immunity*. (2023) 56:1098–1114.e10. doi: 10.1016/j.immuni.2023.03.002

128. Diehl GE, Longman RS, Zhang J-X, Breart B, Galan C, Cuesta A, et al. Microbiota restricts trafficking of bacteria to mesenteric lymph nodes by CX3CR1hi cells. *Nature*. (2013) 494:116–20. doi: 10.1038/nature11809

129. Lynn DJ, Benson SC, Lynn MA, Pulendran B. Modulation of immune responses to vaccination by the microbiota: implications and potential mechanisms. *Nat Rev Immunol*. (2022) 22:33–46. doi: 10.1038/s41577-021-00554-7

130. Lamousé-Smith ES, Tzeng A, Starnbach MN. The intestinal flora is required to support antibody responses to systemic immunization in infant and germ free mice. *PloS One*. (2011) 6:e27662. doi: 10.1371/journal.pone.0027662

131. Oh JZ, Ravindran R, Chassaing B, Carvalho FA, Maddur MS, Bower M, et al. TLR5-mediated sensing of gut microbiota is necessary for antibody responses to seasonal influenza vaccination. *Immunity*. (2014) 41:478–92. doi: 10.1016/j.immuni.2014.08.009

132. Hong S-H. Influence of microbiota on vaccine effectiveness: "Is the microbiota the key to vaccine-induced responses? *J Microbiol*. (2023) 61:483–94. doi: 10.1007/s12275-023-00044-6

133. Lee-Sarwar KA, Kelly RS, Lasky-Su J, Zeiger RS, O'Connor GT, Sandel MT, et al. Fecal short-chain fatty acids in pregnancy and offspring asthma and allergic outcomes. *J Allergy Clin Immunol Pract*. (2020) 8:1100–1102.e13. doi: 10.1016/j.jaip.2019.08.036

134. Thorburn AN, McKenzie CI, Shen S, Stanley D, Macia L, Mason LJ, et al. Evidence that asthma is a developmental origin disease influenced by maternal diet and bacterial metabolites. *Nat Commun*. (2015) 6:7320. doi: 10.1038/ncomms8320

135. Nastasi C, Candela M, Bonefeld CM, Geisler C, Hansen M, Krejsgaard T, et al. The effect of short-chain fatty acids on human monocyte-derived dendritic cells. *Sci Rep*. (2015) 5:16148. doi: 10.1038/srep16148

136. Uribe-Herranz M, Rafail S, Beghi S, Gil-de-Gómez L, Verginadis I, Bittinger K, et al. Gut microbiota modulate dendritic cell antigen presentation and radiotherapy-induced antitumor immune response. *J Clin Invest*. (2020) 130:466–79. doi: 10.1172/JCI124332

Supplementary Material

Supplementary Material

1 Supplementary Tables and Figures

Supplementary Tables

Table S1-2 are GAM estimates and statistical outputs. The model estimates and related standard errors (Std.Error) were shown for parametric terms. For non-parametric smooth terms, their estimated and reference degrees of freedom (i.e. edf, sumEDF, Ref.df) and their test statistics were shown.

Table S1. Relative fit of GAM analyzing the predictors for age-standardized inflammatory bowel disease (IBD) incidence rate (IBD%) globally. AIC = Akaike information criterion. sumEDF indicates the degrees of freedom of the models. Model 16 was selected as the best model because of the lowest AIC. (related to Figure 6)

GAM	AIC	sumEDF	Formula
0	5535.093	164.91	gam(IBD% ~ 1 + s(Country, bs = "re"))
1	5484.476	169.33	gam(IBD% ~ s(Country, bs = "re") + s(GDP))
2	5483.403	167.47	gam(IBD% ~ s(Country, bs = "re") + s(Year))
3	5466.237	171.63	gam(IBD% ~ s(Year) + s(GDP) + s(Country, bs = "re"))
4	5352.781	175.84	gam(IBD% ~ te(Year, GDP) + s(Country, bs = "re"))
5	5481.126	172.77	gam(IBD% ~ s(ANTIBIOTIC.CONSUMPTION) + s(Country, bs = "re"))
6	5449.299	175.51	gam(IBD% ~ s(ANTIBIOTIC.CONSUMPTION) + s(Year) + s(Country, bs = "re"))
7	5461.934	177.17	gam(IBD% ~ s(ANTIBIOTIC.CONSUMPTION) + s(GDP) + s(Country, bs = "re"))
8	5436.978	179.59	gam(IBD% ~ s(ANTIBIOTIC.CONSUMPTION) + s(Year) + s(GDP) + s(Country, bs = "re"))
9	5354.420	176.85	gam(IBD% ~ s(ANTIBIOTIC.CONSUMPTION) + te(Year, GDP) + s(Country, bs = "re"))
10	5444.488	180.15	gam(IBD% ~ te(ANTIBIOTIC.CONSUMPTION, GDP) + s(Year) + s(Country, bs = "re"))
11	5433.675	191.48	gam(IBD% ~ te(ANTIBIOTIC.CONSUMPTION, Year) + s(GDP) + s(Country, bs = "re"))
12	5071.345	221.43	gam(IBD% ~ te(ANTIBIOTIC.CONSUMPTION, Year, GDP) + s(Country, bs = "re"))
13	5445.612	186.89	gam(IBD% ~ te(ANTIBIOTIC.CONSUMPTION, Year) + s(Country, bs = "re"))
14	5471.002	176.61	gam(IBD% ~ te(ANTIBIOTIC.CONSUMPTION, GDP) + s(Country, bs = "re"))
15	5096.472	232.23	gam(IBD% ~ s(ANTIBIOTIC.CONSUMPTION) + s(Year) + s(GDP) + ti(ANTIBIOTIC.CONSUMPTION, Year, GDP) + s(Country, bs = "re"), data = complete
16	4966.310	252.65	gam(IBD% ~ s(ANTIBIOTIC.CONSUMPTION) + s(Year) + s(GDP) + ti(ANTIBIOTIC.CONSUMPTION, Year, GDP) + ti(ANTIBIOTIC.CONSUMPTION, Year) + ti(ANTIBIOTIC.CONSUMPTION, GDP) + ti(GDP, Year) + s(Country, bs = "re"))

Table S2. Estimated effects of antibiotic consumption (ANTIBIOTIC.CONSUMPTION), GDP per capita and year on IBD% globally. (related to Figure 6)

Parametric coefficients				
	Estimate	**Std.Error**	**t value**	**Pr(>|t|)**
(Intercept)	4.467	285.901	0.016	0.988
Approximate significance of smooth terms				
	edf	**Ref.df**	**F**	**P value**
s(ANTIBIOTIC.CONSUMPTION)	7.952	8.660	8.925	<2e-16
s(Year)	3.899	4.979	7.317	1.03e-06
s(GDP)	8.456	8.900	8.553	<2e-16
ti(ANTIBIOTIC.CONSUMPTION, Year, GDP)	38.034	42.235	7.547	<2e-16
ti(ANTIBIOTIC.CONSUMPTION, Year)	10.113	11.277	5.086	<2e-16
ti(ANTIBIOTIC.CONSUMPTION, GDP)	9.508	10.727	8.478	<2e-16
ti(Year, GDP)	9.685	11.106	8.920	<2e-16
s(Country)	164.000	35.000	4326.229	<2e-16
R-sq.(adj) = 0.991 Deviance explained = 99.2%				
GCV = 0.28722 Scale est. = 0.26408 n = 3135				

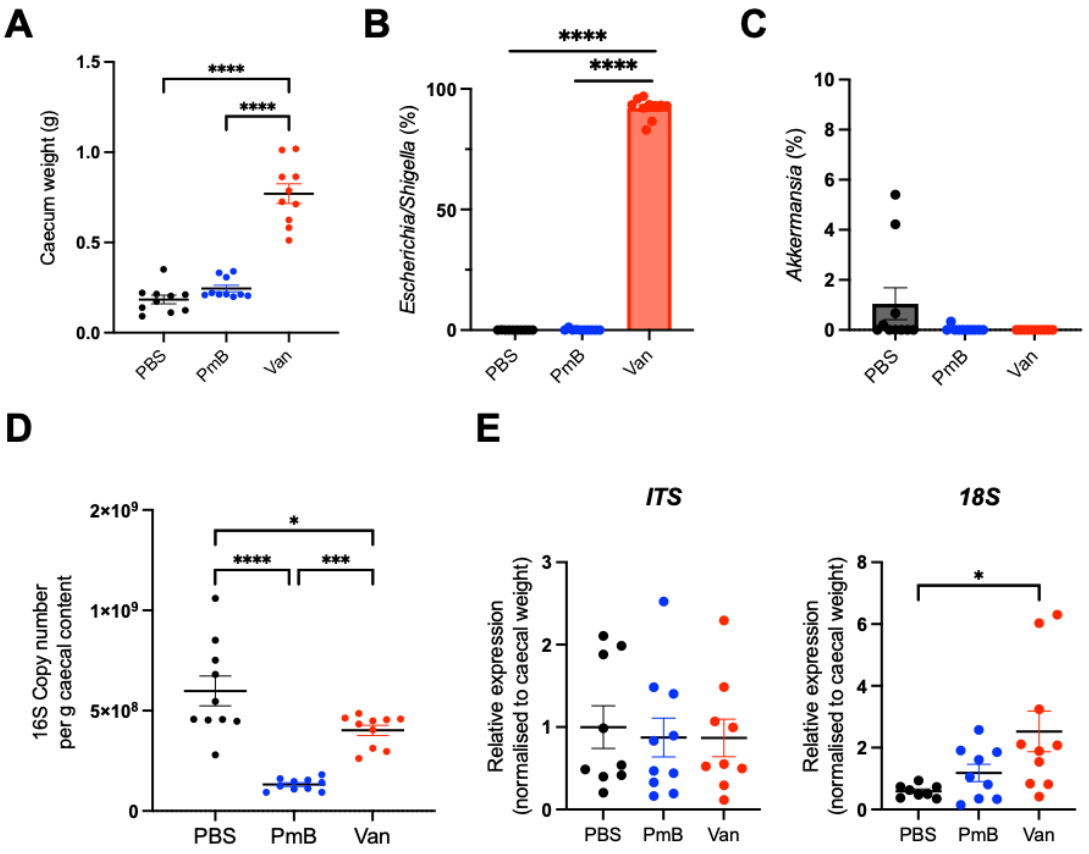

Supplementary Figure 1.

(**A**) Total weight of caecum. (**B-C**) Differential abundance analysis of *Escherichia/Shigella* and *Akkermansia*, as assessed using ALDEx2, with expected Benjamini-Hochberg corrected p-value of Wilxocon test, with ****p<0.0001 (**D**) 16S copy number per g caecal conent, as determined by qPCR. (**E**) Relative expression of *ITS* and *18S* rRNA sequences per g caecal content, as determined by qPCR. Data are represented as mean ± SEM with *p<0.05, **<0.01, ***0.001, ****<0.0001 by ordinary one-way ANOVA followed by Tukey's multiple comparisons test.

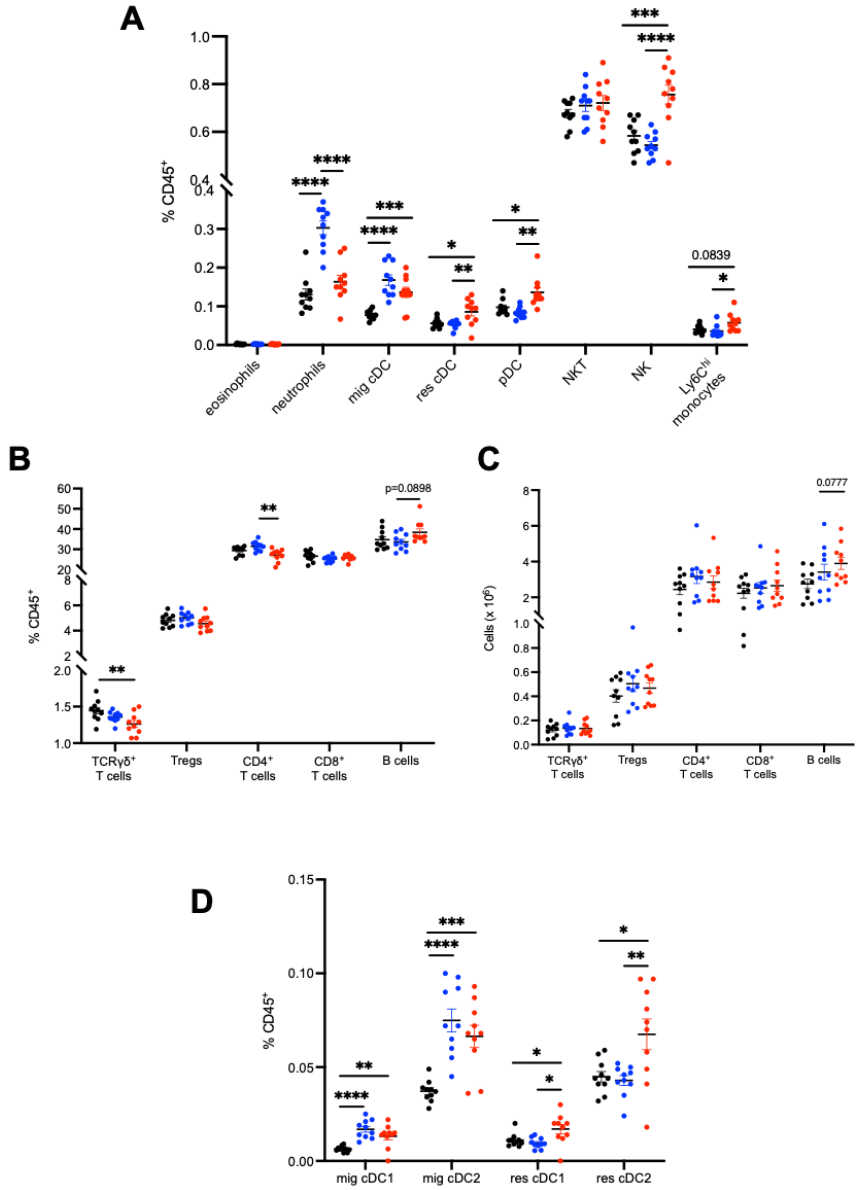

Supplementary Figure 2.

(**A**) Proportion of eosinophils, neutrophils, migratory conventional dendritic cells (mig cDC), resident cDCs (res cDC), plasmacytoid dendritic cells (pDC), natural killer T (NKT) cells, natural killer (NK) cells and LyC6^{hi} monocytes as quantified by flow cytometry (**B**) Proportions of TCRγδ^{+} T cells, regulatory T cells (Tregs), CD4^{+} and CD8^{+} T cells, and B cells in the MLNs as well as (**C**) total numbers of these cells. (**D**) Proportions of cDC1 and cDC2 subsets.

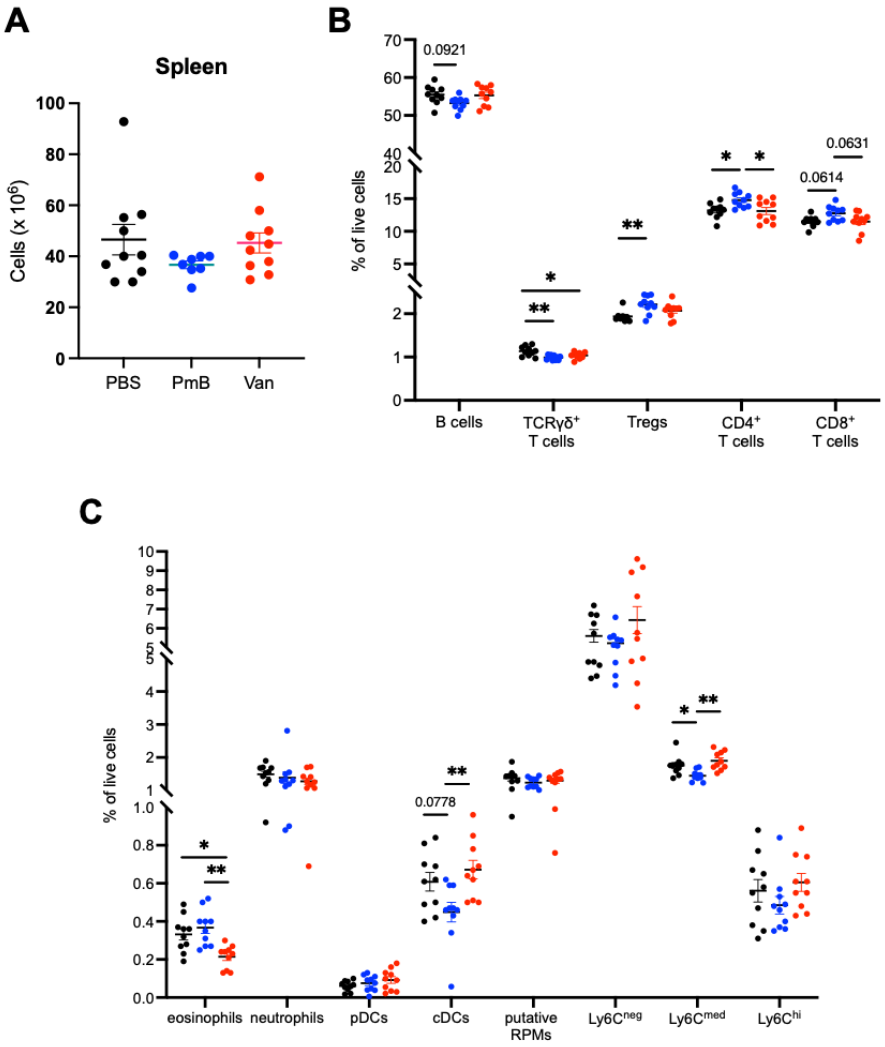

Supplementary Figure 3.

(**A**) Total cellularity in spleen. (**B**) Proportion (of live cells) of B cells, TCRγδ^{+} T cells, regulatory T cells (Tregs), CD4^{+} and CD8^{+} T cells. (**C**) Proportion of live cells of eosinophils, neutrophils, plasmacytoid dendritic cells (pDCs), conventional dendritic cells (cDCs), putative red pulp macrophages (RPMs), and monocyte subsets (Ly6C^{hi,} Ly6C^{mid} Ly6C^{neg}) as quantified by flow cytometry.

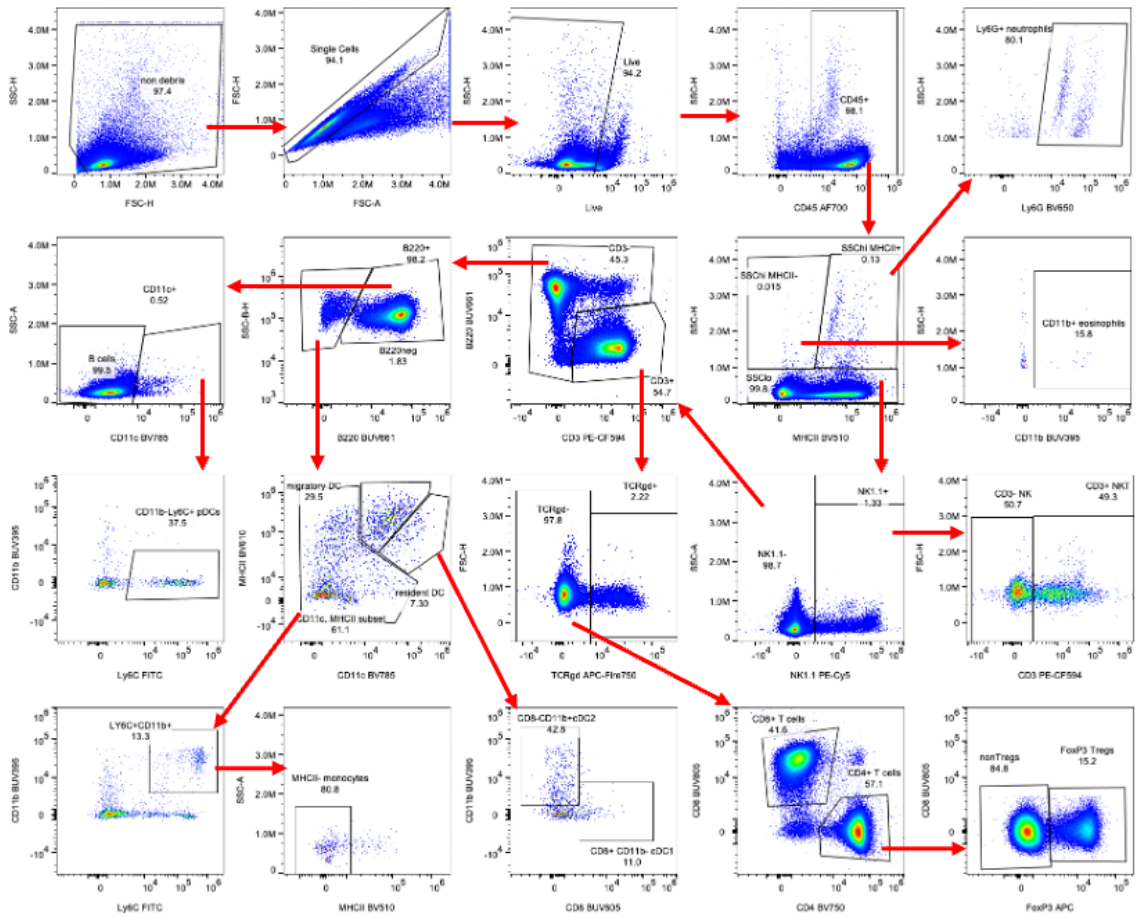

Supplementary Figure 4. Gating strategy for analysis of MLN immune cell profile, as in Figure 3.

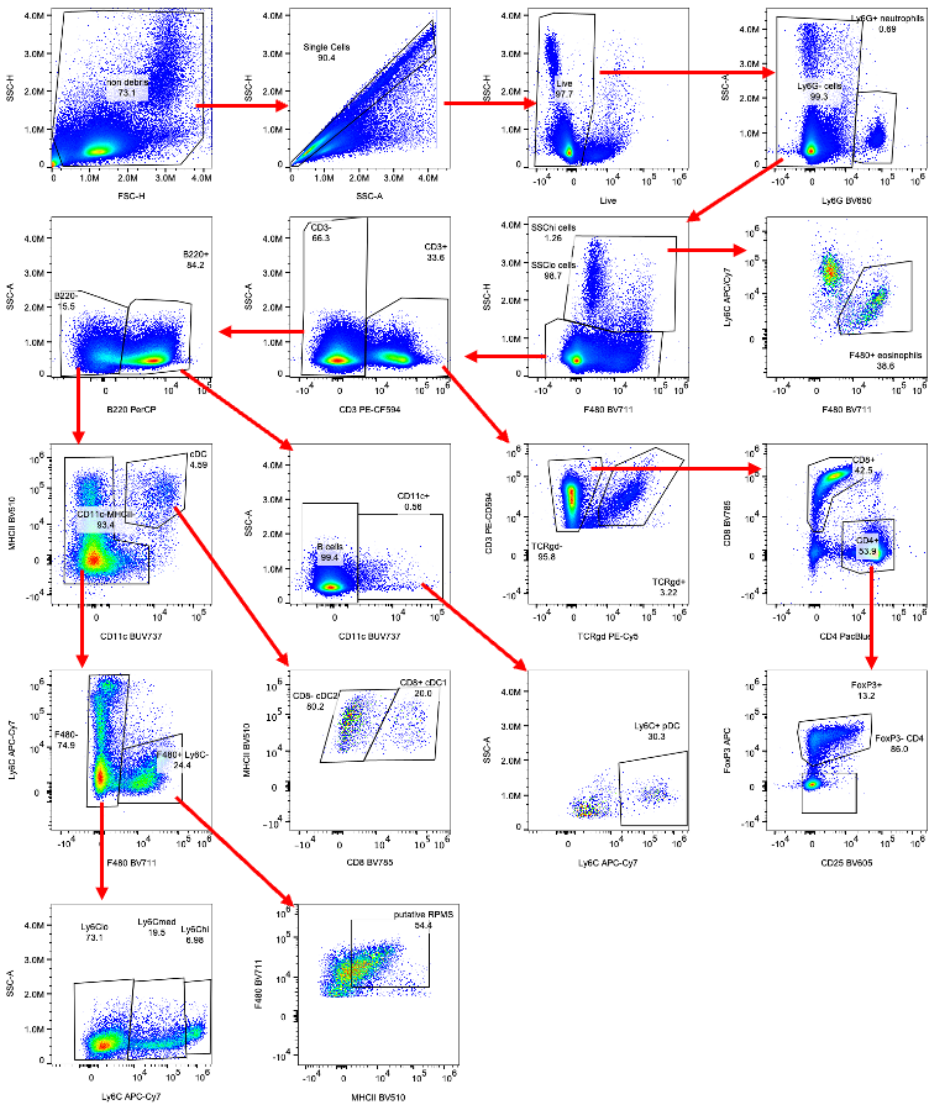

Supplementary Figure 5. Gating strategy for analysis of spleen immune cell profile, as in Figure 4

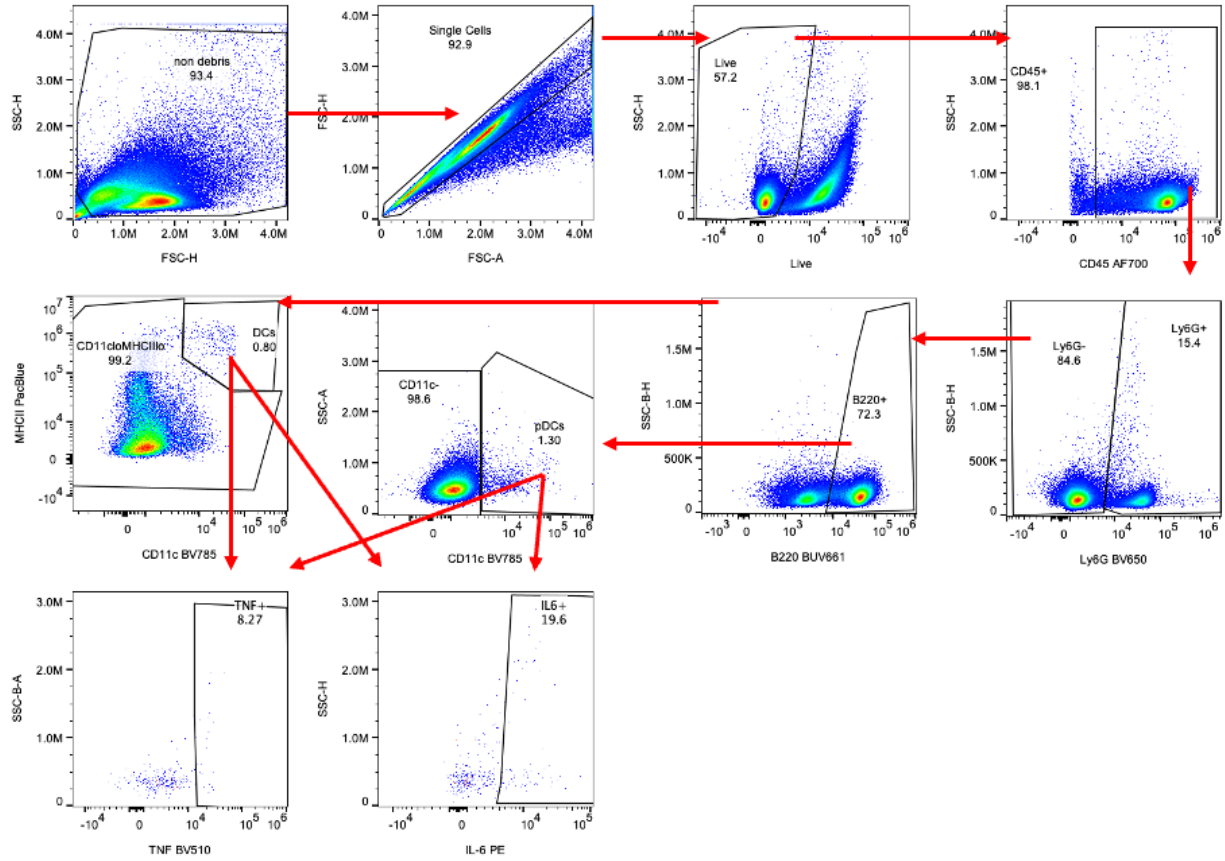

Supplementary Figure 6. Gating strategy for analysis of LPS stimulated splenocytes, as in Figure 4

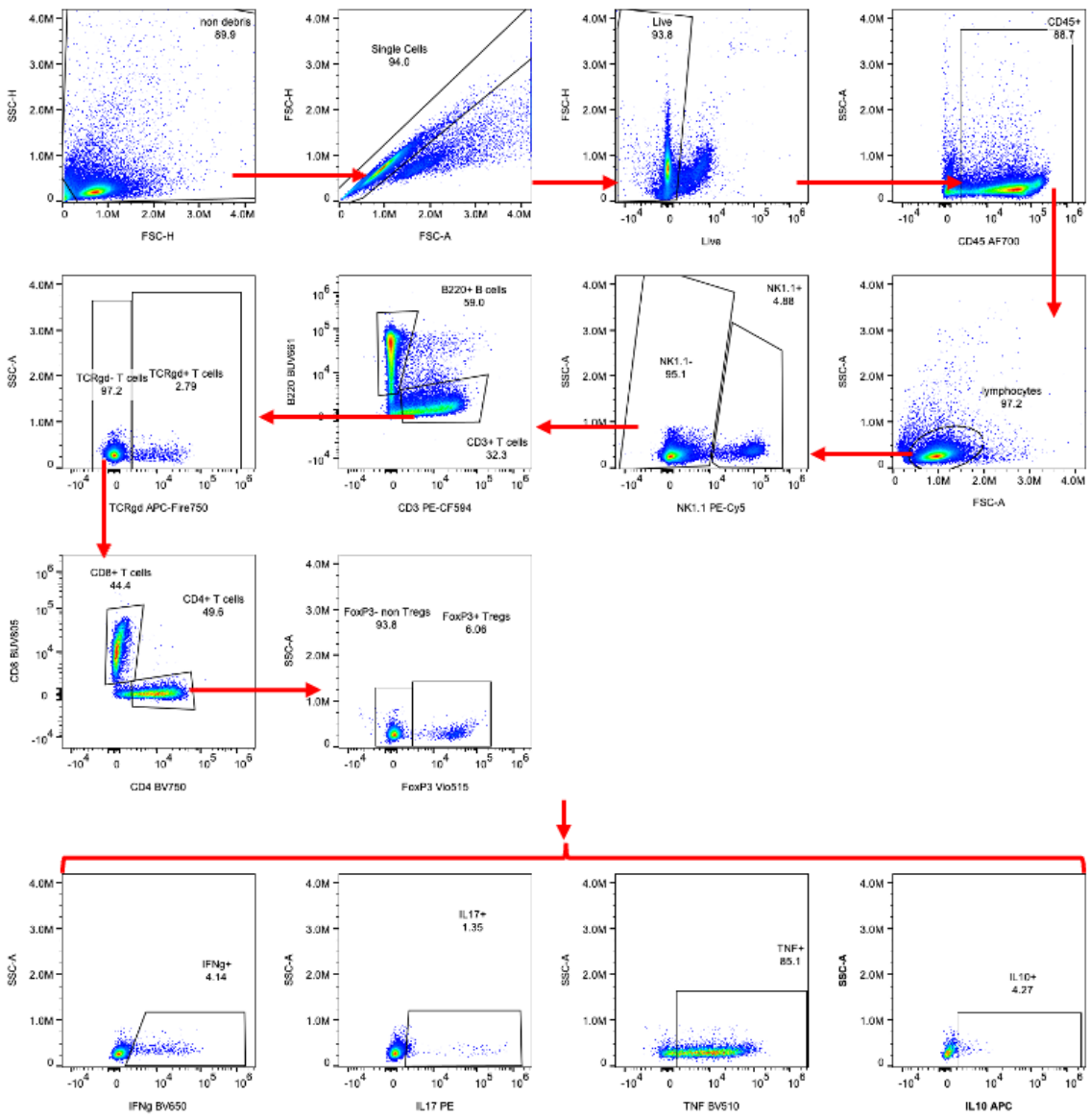

Supplementary Figure 7. Gating strategy for analysis of PMA/ionomycin stimulated splenocytes, as in Figure 5.

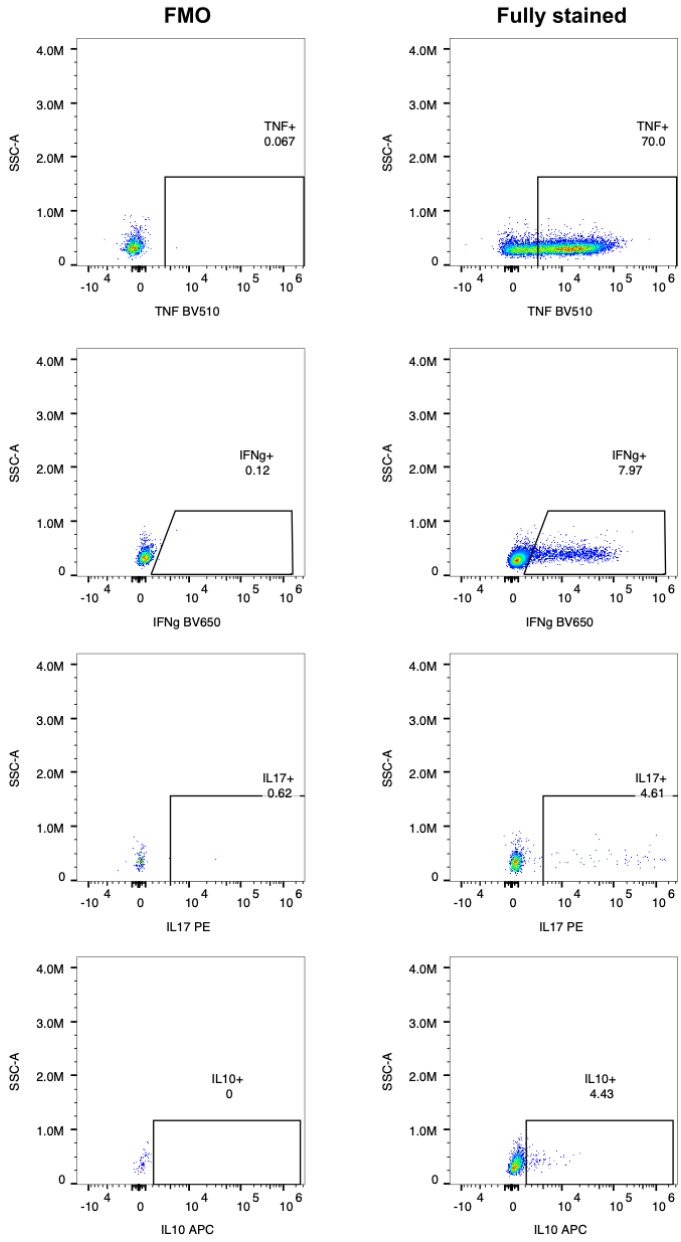

Supplementary Figure 8: Representative flow cytometry plots showing fluorescence minus one (FMO) controls and fully stained samples used to define the gating strategy in Supplementary Figure 7, for Figure 5 of Results section.

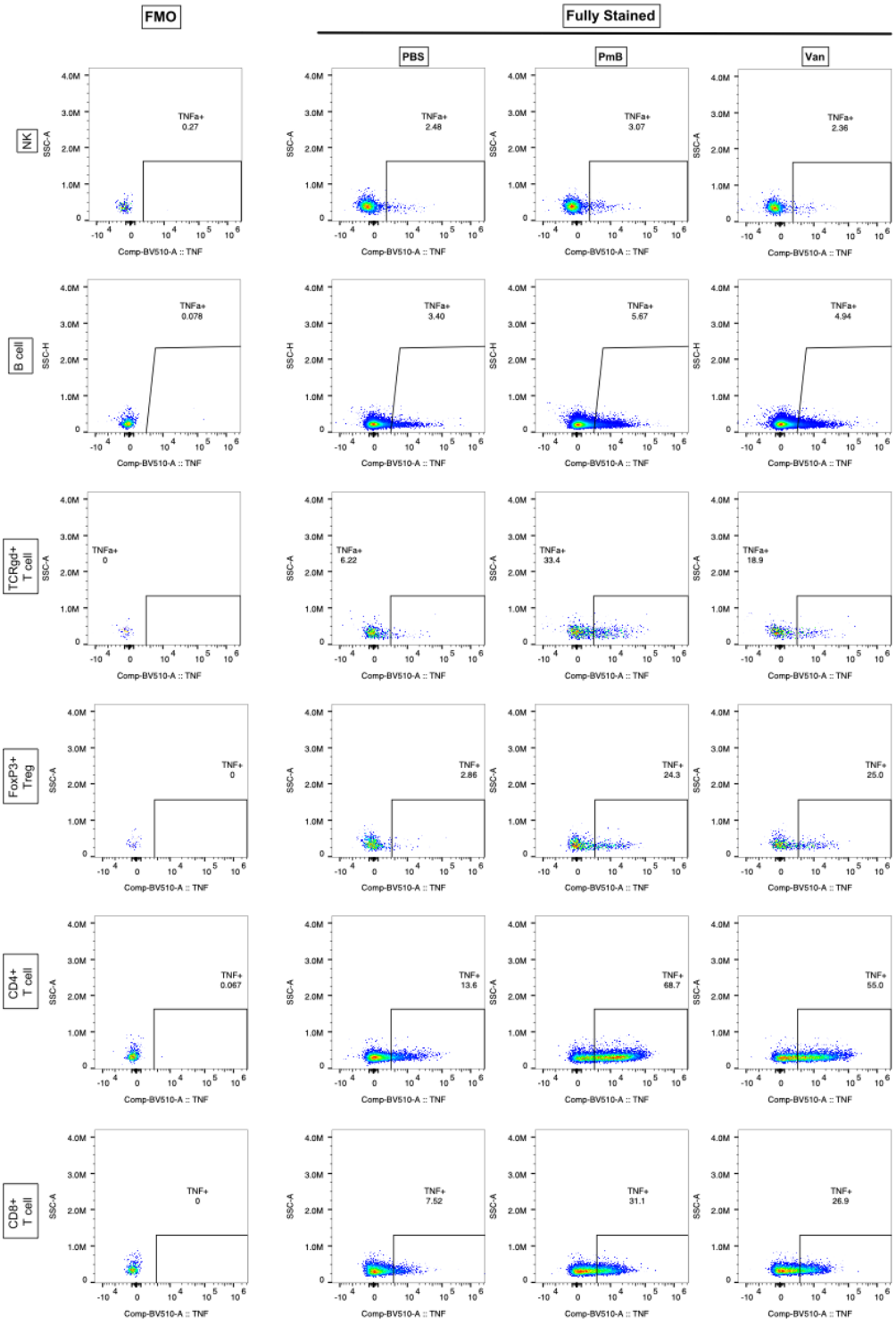
FMO
Fully Stained
PBS
PmB
Van
NK
B cell
TCRgd+ T cell
FoxP3+ Treg
CD4+ T cell
CD8+ T cell
SSC-A
SSC-H
Comp-BV510-A :: TNF
TNFa+ 0.27
TNFa+ 2.48
TNFa+ 3.07
TNFa+ 2.36
TNFa+ 0.078
TNFa+ 3.40
TNFa+ 5.67
TNFa+ 4.94
TNFa+ 0
TNFa+ 6.22
TNFa+ 33.4
TNFa+ 18.9
TNF+ 0
TNF+ 2.86
TNF+ 24.3
TNF+ 25.0
TNF+ 0.067
TNF+ 13.6
TNF+ 68.7
TNF+ 55.0
TNF+ 0
TNF+ 7.52
TNF+ 31.1
TNF+ 26.9

Supplementary Figure 9: Representative flow cytometry plots showing FMO control and fully stained samples for TNF^+ cells in subsets presented in Figure 5 of Results.

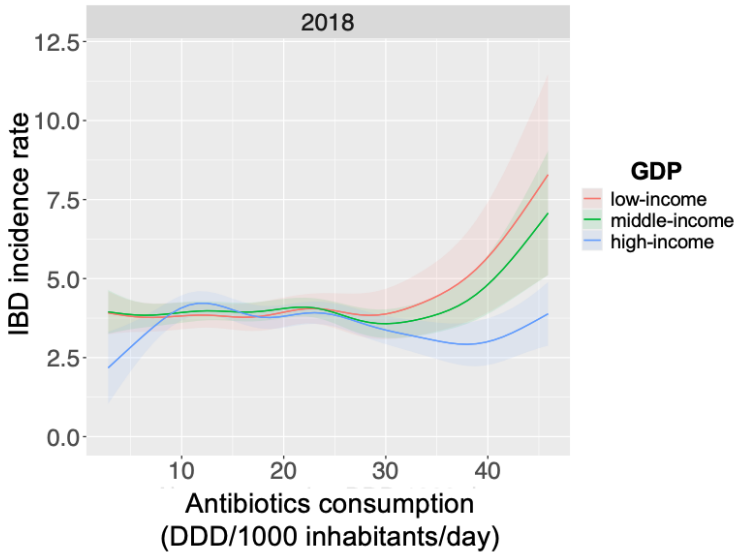

Supplementary Figure 10. Modelled effects of antibiotic consumption on global inflammatory bowel disease (IBD) disease burden (incidence rate) stratified by 25% (red, low-income), 50% (green, median-income) and 75% (blue, high-income) quantiles of gross domestic product (GDP).

Chapter 3 Dietary Protein Increases T-Cell-Independent sIgA Production through Changes in Gut Microbiota-Derived Extracellular Vesicles

This chapter has been published as:
Tan J, Ni D, **Taitz J**, Pinget GV, Read M, Senior A, Wali JA, Elnour R, Shanahan E, Wu H, Chadban SJ, Nanan R, King NJC, Grau GE, Simpson SJ, Macia L. "Dietary Protein Increases T-Cell-Independent sIgA Production through Changes in Gut Microbiota-Derived Extracellular Vesicles" *Nature Communications*. 2022;**13**:4336.

I optimised protocols for EV isolation and analysis which formed the basis of this study. I acquired and analysed IVIS imaging data, and worked jointly on animal experiments (dissections, tissue processing, flow cytometry and flow analysis). I helped develop the study design and collaborated with co-authors in drafting and revising the manuscript. All co-authors contributed to data interpretation and manuscript preparation.

This work in the context of this thesis:

Building on the findings of **Chapter 2**, this chapter explores diet as another key modulator of gut microbiota composition and its downstream effects on host physiology. Alterations in the ratio of dietary macronutrients (protein, carbohydrates, and fats) shape the gut microbiota and have been linked to the rise of NCDs in industrialised nations. Understanding how these macronutrients influence the host immune system via gut microbiota is pivotal for deciphering host-microbiota interactions and identifying potential disease interventions.

Using isocaloric diets with varying macronutrient composition, we identified dietary protein as a key driver of host sIgA, a vital component of the mucosal immune response

that maintains microbiota segregation and fosters host-microbiota mutualism. While different diets significantly altered gut bacterial composition, the protein-driven increase in sIgA was linked to a shift in gut microbial metabolism rather than a compositional change. High-protein feeding increased microbial succinate production which triggered bacterial reactive oxygen species (ROS)-mediated release of BEVs. These BEVs activated TLR4 in the SI epithelium, increasing expression of key regulators of sIgA production, including the cytokines APRIL and BAFF, the chemokine CCL28, and the IgA transporter, pIgR, thereby inducing sIgA through a T-cell independent pathway.

This chapter uses the term BEVs, which reflects the terminology used at the time of publication. These vesicles are referred to as MEVs elsewhere in this thesis, but in this chapter the term BEVs refers to vesicles isolated from the complex microbial community of the gut (i.e. equivalent to MEVs). BEVs and MEVs refer to the same biological entity, unless otherwise specified.

This chapter establishes a novel link between dietary macronutrient content and the host mucosal immune response, demonstrating for the first time that BEVs serve as critical mediators of this signalling. Overall, this chapter highlights how dietary modulation of gut bacterial metabolism influences host immunity via gut microbiota-derived BEVs, positioning BEVs as central intermediaries in the gut-host axis.

nature COMMUNICATIONS

ARTICLE

https://doi.org/10.1038/s41467-022-31761-y OPEN

Dietary protein increases T-cell-independent sIgA production through changes in gut microbiota-derived extracellular vesicles

Jian Tan[1,2], Duan Ni[1,2], Jemma Taitz[1,2], Gabriela Veronica Pinget[1,2], Mark Read[1,3], Alistair Senior[1,4], Jibran Abdul Wali[1,4], Reem Elnour[1,4], Erin Shanahan[1,4], Huiling Wu[1,5,6], Steven J. Chadban[1,5,6], Ralph Nanan[1,7], Nicholas Jonathan Cole King[1,2,8], Georges Emile Grau[2,9], Stephen J. Simpson[1,4] & Laurence Macia[1,2,8]✉

Secretory IgA is a key mucosal component ensuring host-microbiota mutualism. Here we use nutritional geometry modelling in mice fed 10 different macronutrient-defined, isocaloric diets, and identify dietary protein as the major driver of secretory IgA production. Protein-driven secretory IgA induction is not mediated by T-cell-dependent pathways or changes in gut microbiota composition. Instead, the microbiota of high protein fed mice produces significantly higher quantities of extracellular vesicles, compared to those of mice fed high-carbohydrate or high-fat diets. These extracellular vesicles activate Toll-like receptor 4 to increase the epithelial expression of IgA-inducing cytokine, APRIL, B cell chemokine, CCL28, and the IgA transporter, PIGR. We show that succinate, produced in high concentrations by microbiota of high protein fed animals, increases generation of reactive oxygen species by bacteria, which in turn promotes extracellular vesicles production. Here we establish a link between dietary macronutrient composition, gut microbial extracellular vesicles release and host secretory IgA response.

[1] Charles Perkins Centre, The University of Sydney, Sydney, NSW, Australia. [2] School of Medical Sciences, Faculty of Medicine and Health, University of Sydney, Sydney, NSW, Australia. [3] School of Computer Science, Faculty of Engineering, University of Sydney, Sydney, NSW, Australia. [4] School of Life and Environmental Sciences, Faculty of Science, University of Sydney, Sydney, NSW, Australia. [5] Kidney Node Laboratory, The Charles Perkins Centre, University of Sydney, Sydney, NSW, Australia. [6] Renal Medicine, Royal Prince Alfred Hospital, Sydney, NSW, Australia. [7] Sydney Medical School Nepean, University of Sydney, Sydney, NSW, Australia. [8] Sydney Cytometry, The University of Sydney and The Centenary Institute, Sydney, NSW, Australia. [9] Vascular Immunology Unit, The University of Sydney, Sydney, NSW, Australia. ✉email: Laurence.macia@sydney.edu.au

The gut microbiota, defined by the trillions of bacteria that inhabit the gut, play a critical role in the physiology and immunity of the host[1]. To maintain a symbiotic relationship, strategies have been developed by the host to regulate its interaction with the gut microbiota. Mucosal secretory IgA (sIgA) plays a key role in this host-microbiota mutualism by excluding pathobionts and pathogens and limiting bacterial attachment to the epithelium[2]. While patients with selective IgA deficiency appear healthy, they are more susceptible to various diseases, including gastrointestinal disorders and allergies[3], highlighting the importance of IgA in mucosal homoeostasis.

Under homoeostatic conditions, IgA is primarily produced by plasma cells local to the small intestine lamina propria through a T cell-independent pathway[4,5]. The majority of commensal bacteria induce T-cell-independent IgA responses[6], and sIgA generated via this pathway is of low affinity and polyreactive towards common bacterial antigens, limiting the attachment of a diverse range of bacteria to the host epithelium[7]. The induction of sIgA is regulated by the local cytokine environment, with the increase in class switch recombination (CSR) cytokines, APRIL and BAFF, produced by epithelial cells, promoting the differentiation of IgM^+ B cells into IgA-producing plasma cells[5,8]. These cytokines are produced as a result of toll-like receptor (TLR) activation, particularly TLR4, which recognises bacterial lipopolysaccharide (LPS)[9].

TLR activation by commensal bacteria is critical both for the recruitment of IgM^+ B cells in the lamina propria, by increasing the expression of the gut homing chemokine CCL28[9], and for the induction IgA CSR by upregulating APRIL[10]. TLR4 is the major TLR expressed on the epithelium and its overstimulation in TLR4 transgenic mice has been shown to promote CCL28 and APRIL production and accumulation of IgA in the lamina propria and gut lumen[9]. The majority of IgA produced in the gut is in dimeric form, which can be transported through the epithelium into the lumen by binding the polymeric immunoglobulin receptor (pIgR)[11]. Similarly, pIgR expression can be upregulated by several inflammatory cytokines such as IFN-γ, IL-1, IL-17, TNF, and IL-4, following TLR4/NFκB signalling[12]. Of note, IL-4 can have a dual role by also promoting IgA CSR.

Seminal work utilising germ-free mice has established that the presence of gut bacteria is the main driver of sIgA response, and transient colonisation of germ-free animals with *E. coli* leads to transient sIgA production[13]. However, how dynamic changes to the gut microbiota composition affect sIgA is less clear. Diet composition is a major driver of the microbiota composition with most studies focusing on microbiota profiling in the caecum and the colon[14], where IgA production is minimal, compared to the small intestine. How dietary macronutrient composition (i.e., protein, fat and carbohydrate) affects the dynamic interplay between the small intestine microbiota and mucosal IgA remains unknown. This knowledge could establish which diet compositions are beneficial for restoring gut homoeostasis and which diets are detrimental.

In our approach, we fed mice on one of 10 different isocaloric diets varying in their macronutrient composition, which identified an association between dietary protein and sIgA levels using mixture modelling. We validated and explored these results further using a subset of the 10 diets, representing a high-protein, high-carbohydrate or high-fat diet. We found that the high-protein diet had the highest intestinal sIgA levels, and this was associated with increased expression of CCL28 and APRIL in the small intestine. These changes were correlated with the increased capacity of the microbiota to stimulate TLR4 directly or indirectly via increased production of gut microbiota-derived extracellular vesicles (EV). We also established that EV derived from high-protein diet microbiota could directly promote the expression of CCL28. Our work highlights the key role of dietary protein on sIgA production and identifies bacterial-derived EV as a mediator of gut microbiota-host mutualism.

Results

High protein feeding promotes high lamina propria IgA production and higher secretion of luminal sIgA. To determine how dietary macronutrients might affect sIgA and thus host-microbiota mutualism, we fed mice on one of 10 isocaloric diets with defined ratios of macronutrients in the ranges 5–60% protein, 20–75% fat, and 20–75% carbohydrate, for at least 6 weeks (Fig. 1a and Supplementary Table 1).

The impact of macronutrient composition on gut luminal concentrations of sIgA was visualised using a proportion-based nutritional geometry approach, as described previously[15,16]. Mixture models were used to determine the effects of diet composition on luminal sIgA concentration, as quantified by ELISA ($n = 8$ per diet). Predicted effects of diet on sIgA were mapped onto a right-angled mixture triangle plot, where protein concentration in the diet is represented on the x axis, fat on the y axis and carbohydrate on the hypotenuse (Fig. 1b). Regions of the nutrient mixture space appearing in red demonstrate high levels of sIgA while areas in deep blue represent low levels of sIgA, and values on the isolines indicate the modelled concentration of sIgA (ng/ml). Of the 4 models fitted to sIgA concentration (relating to the first to fourth-order of the Scheffé polynomials, described by Lawson and Wilden[17]), model 1 was the most appropriate as indicated by the lowest Akaike Information Criterion (AIC) value (Supplementary Table 2), which reveal that dietary protein concentration was the principal predictor of sIgA, there being a clearly graded increase in sIgA with increasing protein concentration, irrespective of fat or carbohydrate content ($R^2 = 0.8076$). Linear regression revealed that this effect was driven significantly by protein, but not by carbohydrate or fat intake, and was independent of total caloric intake (Supplementary Fig. 1a–d). Accordingly, when the three diets located at the apices of the mixture space in Fig. 1a were compared, the highest concentrations of gut luminal sIgA were observed in mice fed on the highest protein diet (HP; P60 C20 F20), compared to those fed on a diet high in fat (HF; P5 C20 F75) or high in carbohydrate (HC; P5 C75 F20) (Fig. 1c).

The shape of the response surface for plasma IgA was markedly different from that of sIgA, with plasma IgA being lowest on diets containing high-protein coupled with both low fat and low carbohydrate (Fig. 1d, e and Supplementary Table 3, $R^2 = 0.7243$). Macronutrient composition was not a predictor of plasma IgM concentrations, as the null model was determined to be most favourable by AIC (Supplementary Table 4). This suggests that high luminal sIgA under high-protein feeding conditions was not linked to a systemic increase in basal B cell activity and that this effect was, therefore, mucosa-specific.

To determine whether elevated sIgA levels in the gut lumen of HP-fed mice were due to higher local production of IgA in the lamina propria, we performed immunofluorescence staining with anti-IgA on frozen sections of small intestine isolated from mice fed on HP, HC, or HP diets. Immunofluorescence analysis showed that HP feeding led to the highest expression of IgA in the lamina propria, compared to HC or HF feeding (Fig. 1f). Consistent with this, mice fed on an HP diet had a significantly greater number of $B220^-IgA^+$ plasma cells in the small intestinal lamina propria (Fig. 1g), as determined by flow cytometry (gating strategy presented in Supplementary Fig. 1e). Prior to differentiation into IgA-producing plasma B cells, B cells are recruited to the gut by the gut epithelial chemokine CCL28. By qPCR analysis, we found that mice fed on HP diet had significantly higher intestinal gene expression of the B cell gut homing chemokine, CCL28

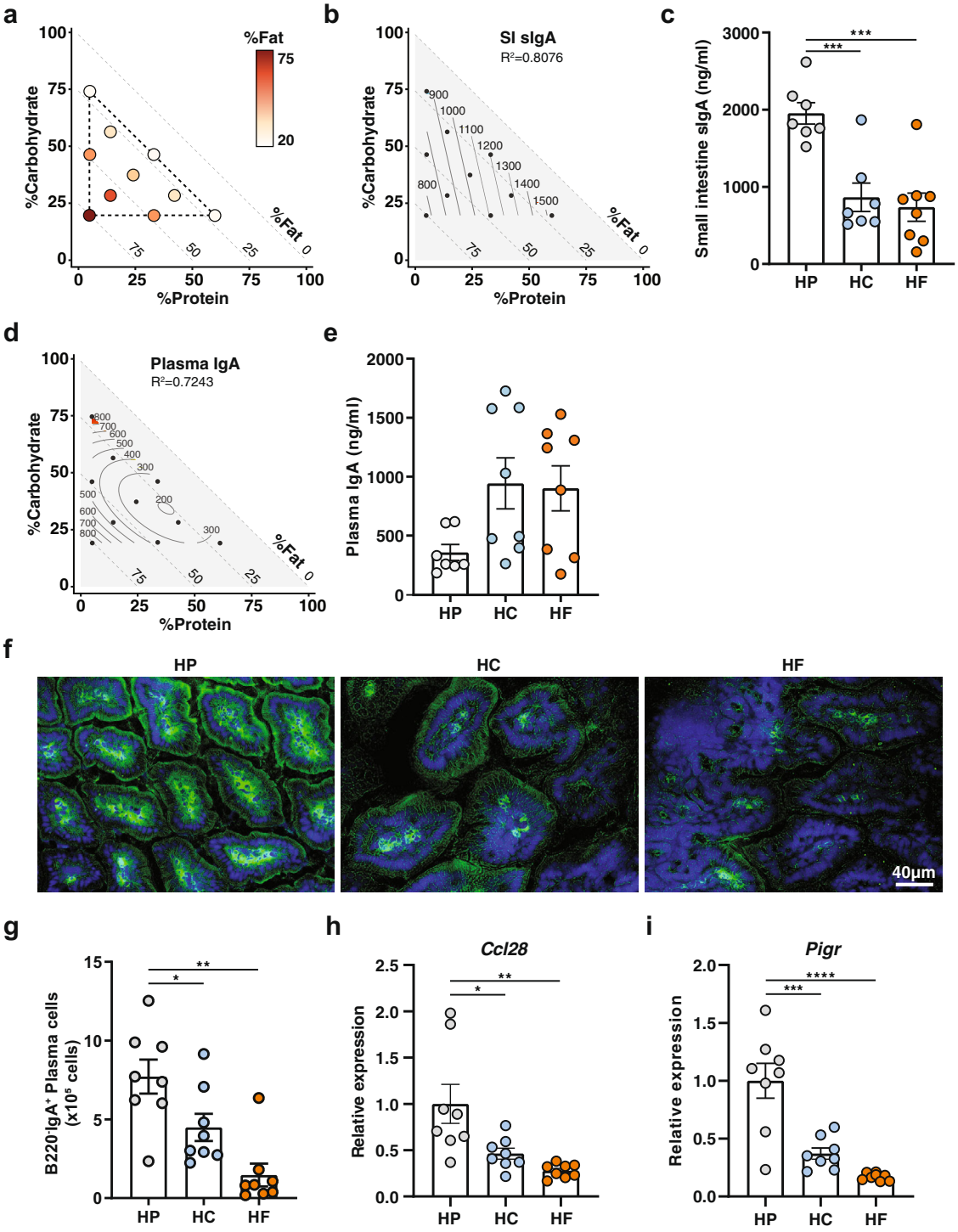

(Fig. 1h). Additionally, the expression of the gene encoding for pIgR, involved in the transport of sIgA to the lumen via the epithelium, was significantly increased under HP feeding conditions (Fig. 1i).

Finally, we observed that a minimum of 5 weeks on HP feeding was necessary to stably increase sIgA levels (Supplementary Fig. 1f) and that this effect was a reversible process, as sIgA levels in HP-fed animals decreased when switched to an HF diet (Supplementary Fig. 1g).

Together, these data show that protein is the major macronutrient driving sIgA production in the gut lumen and that this is reversible. An HP diet promotes the expression of the B cell gut homing chemokine, CCL28, and accordingly, a higher presence of IgA in the small intestine lamina propria. Finally, an HP diet also promotes increased expression of pIgR, the transporter of IgA in the gut lumen, consistent with the highest concentration of luminal sIgA.

High protein feeding promotes IgA production through T-cell-independent mechanisms. IgA-producing plasma cells in the lamina propria either originate from IgM-producing B cells that differentiate locally in the lamina propria, or from IgA-expressing plasmablasts induced in gut-associated lymphoid structures such as the Peyer's patches or the mesenteric lymph nodes, which

Fig. 1 High protein feeding promotes high lamina propria IgA production and higher luminal sIgA. Animals were fed one of ten isocaloric diets encompassing a macronutrient range of protein (5–60%), carbohydrate (20–75%), and fat (20–75%) for 6 weeks. **a** Visual representation of the composition of the diets used in this study. Each diet is represented by one circle each and their localisation on the *x* axis and on the *y* axis define their proportion of protein and of carbohydrate, respectively. The proportion of fat is indicated by the colour range as illustrated in the legend. **b** Contribution of macronutrient composition to small intestinal luminal sIgA ($n = 7$–8 per diet, quantified by ELISA) was modelled by mixture model and represented on a right-angled mixture triangle comprising of carbohydrate (*y* axis), protein (*x* axis) and fat (hypotenuse) with small intestinal content IgA concentration (ng/ml, numbers on isolines) as the response variable. Red represents high levels of sIgA while blue represents low levels of sIgA in the nutrient mixture space. Each dot represents one of the 10 diets used for modelling response surface. **c** Scatter bar plot of sIgA from mice fed on a high-protein (HP), high-carbohydrate (HC) or high-fat (HF) diet as determined by ELISA ($n = 7$ or $n = 8$ mice per diet for HP/HC and HF diet respectively; HP vs. HC $p = 0.0009$, HP vs. HF $p = 0.0002$). **d** Mixture model of plasma IgA represented on a right-angled mixture triangle and (**e**) corresponding scatter bar plot ($n = 7$ or $n = 8$ mice per diet for HP, and HC/HF diet respectively). **f** Representative immunofluorescence staining of IgA (green) in the small intestine counterstained with DAPI (blue) from mice fed on an HP, HC, or HF diet for 5 weeks. The scale bar represents 40 µm. **g** Total number of $B220^{-}IgA^{+}$ IgA plasma cells in the small intestine lamina propria as determined by flow cytometry ($n = 8$ mice per group; HP vs. HC $p = 0.0489$, HP vs. HF $p = 0.0002$). **h**, **i** Gene expression of (**h**) *Ccl28* (HP vs. HC $p = 0.0187$, HP vs. HF $p = 0.0017$) and (**i**) *Pigr* (HP vs. HC $p = 0.0002$, HP vs. HF $p = <0.0001$) in whole small intestine tissue was determined by qPCR from mice fed on either a HP, HC, or HF diet ($n = 8$ mice per group). Data are represented as mean ± SEM. Results represent $n = 2$ (**e**–**i**) and $n = 3$ independent experiments (**c**). *p < 0.05, **<0.01, ***<0.001, ****<0.0001 by ordinary one-way ANOVA followed by Tukey's multiple comparisons test.

migrates back into the lamina propria to differentiate into mature plasma cells. To identify the origin of the IgA^{+} plasma cells that are increased under HP feeding conditions, we assessed by flow cytometry the proportion of total B cells, as well as IgA plasmablasts in both Peyer's patches, the main site of T-cell-dependent IgA plasma cell induction, and mesenteric lymph nodes of mice fed on HP, HC or HF diets. We found that proportions of total B cells in both the Peyer's patches (Fig. 2a) and mesenteric lymph nodes (Fig. 2b) were similar between groups. Likewise, no changes in the proportion of $IgA^{+}B220^{+}$ plasmablast were observed between groups in both the Peyer's patches (Fig. 2c, d) and the mesenteric lymph nodes (Supplementary Fig. 2a). This suggests that HP feeding does not increase T-cell-dependent IgA production, as confirmed by the similar proportions of $GL7^{+}CD95^{+}$ germinal centre B cells in both the Peyer's patches (Fig. 2e, f) and the mesenteric lymph nodes (Supplementary Fig. 2b). To confirm this, we depleted $CD4^{+}$ T cells in mice fed on an HP diet from the start of the dietary intervention and found that mice treated with isotype or anti-CD4 depleting antibodies had comparable levels of sIgA (Supplementary Fig. 2c, d). Mice fed on a control diet had lower sIgA than HP-fed mice regardless of the depletion of $CD4^{+}$ T cells. Together, our results show that HP feeding promotes high levels of small intestine sIgA via a T cell-independent pathway.

High-protein feeding modulates the lamina propria cytokine environment, specifically APRIL, to favour IgA production. T-cell-independent induction of IgA CSR results from the complex interaction between gut microbes, host gut epithelial cells, immune cells and the stromal cells of the lamina propria. TLR activation in epithelial cells leads to the production of A Proliferation-inducing Ligand (APRIL) and B cell-activating factor (BAFF), the major cytokines in B cell IgA CSR, as well as thymic stromal lymphopoietin (TSLP). TSLP further amplifies this signal by inducing APRIL and BAFF production by dendritic cells[18].

To determine whether diet composition affects these cytokines, we quantified their expression levels in the small intestines of mice fed on HP, HC and HF diets by qPCR. The expression of *April* was significantly higher under HP feeding conditions, approximately twofold greater than HC- and HF-fed mice (Fig. 3a). Similarly, *Baff* was highly expressed under HP feeding conditions, compared to HF feeding conditions but HC-fed mice had levels of *Baff* expression similar to HP-fed mice (Fig. 3b). This suggests that increased expression of *April* might account for elevated sIgA levels under HP feeding conditions. Like *Baff*, *Tslp* expression was significantly lower in HF-fed mice, whilst HP- and HC-fed mice had similar higher levels of expression (Fig. 3c). TSLP biases T-cell differentiation towards Th2 T cells which are characterised by their production of the cytokine IL-4. IL-4 has been shown to promote IgA CSR as well as pIgR expression. Indeed, mice fed on an HP diet had significantly elevated expression of *Il4*, while HF-fed mice had the lowest expression (Fig. 3d). Among other key cytokines involved in IgA CSR induction, IL-10 and TGF-beta produced by epithelial cells or dendritic cells are co-signals necessary for BAFF and APRIL to mediate their effects. We found that the expression of *Tgfb* was significantly higher in HP-fed mice and *Il10* was significantly lower in HF-fed mice compared to HC groups (Fig. 3e, f).

These data demonstrate that HP feeding induces the highest expression of cytokines involved in IgA CSR, and that these key cytokines are lowest under HF feeding.

Dietary intervention significantly affects the small intestine microbiota composition. Diet is one of the most influential factors driving gut microbiota composition[19], which in turn modulates host IgA responses. To characterise the impact of HP, HC and HF diet feeding on the small intestinal gut microbiota composition, we performed 16 S rRNA DNA sequencing of small intestine luminal samples. The analysis demonstrated equal sequencing reads between samples (raw data presented in Supplementary Table 5 and corresponding graphs in Supplementary Fig. 3a, b). Furthermore, rarefaction analysis revealed adequate sequencing depth (total number of sequencing reads), with a horizontal asymptote evident for all samples (Supplementary Fig. 3c), demonstrating that our sequencing depth far exceeded what is required to uncover all observations (number of unique taxa, or ASV) present in each sample.

The diversity of the gut microbiota is often used as a marker of a "healthy microbiome". We found that bacterial richness was similar across all diets (Fig. 4a). However, HF-fed animals had lower diversity measures such as evenness and Inverse Simpson index, where Inverse Simpson index was significantly lower when compared to the HP group (Fig. 4a). By principal component analysis (PCA) of Aitchison distance, a compositionally appropriate between-sample distance metric, mice fed on the different diets had significantly distinct gut microbiota composition (Fig. 4b) as determined by PERMANOVA analysis (Supplementary Table 6). Likewise, principal coordinates analysis (PCoA) of UniFrac distances, a between-sample distance metric that considers phylogenetic relatedness, showed similar results, with HF feeding having the most distinct bacterial communities in

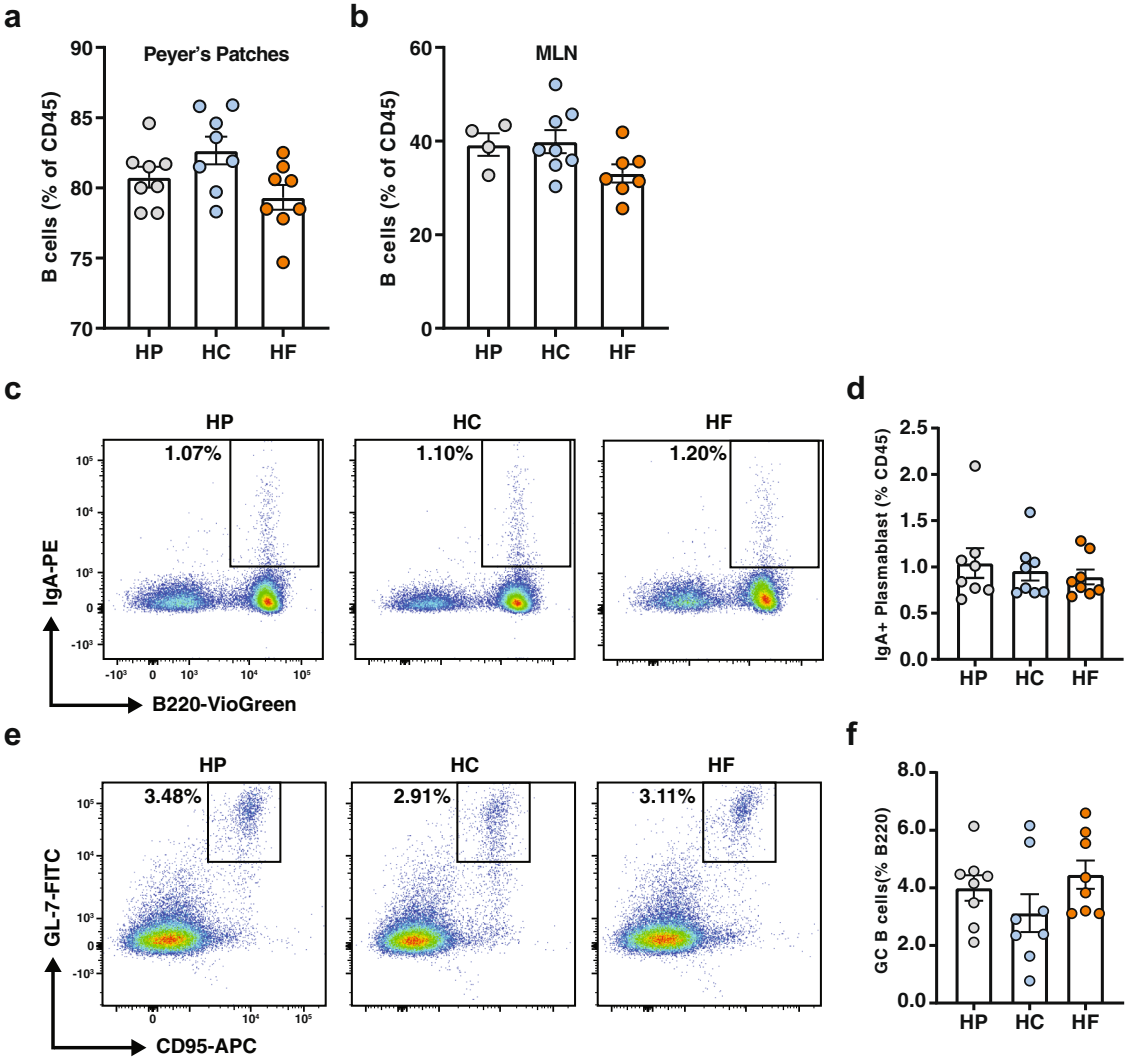

Fig. 2 High protein feeding promotes IgA production through T-cell-independent mechanisms. Mice were fed on either a high-protein (HP), high-carbohydrate (HC) or high-fat (HF) diet for 6 weeks. **a** Proportion of B220$^+$ B cells in the Peyer's patches ($n = 8$ mice per diet) and in the (**b**) mesenteric lymph nodes (MLN; $n = 4$, $n = 8$, and $n = 7$ mice per diet for HP, HC and diet, respectively) were determined by flow cytometry. **c** Representative flow cytometry plots representing the proportion of B220$^+$IgA$^+$ plasmablasts in the Peyer's patches and (**d**) corresponding scatter bar graph ($n = 8$ mice per diet). **e** Representative flow cytometry plots and graph representing the proportions of CD95$^+$GL7$^+$ germinal centre B cells in the Peyer's patches and (**f**) corresponding scatter bar graph ($n = 8$ mice per diet). Data are represented as mean ± SEM. Results represent $n = 2$ independent experiments.

both unweighted and weighted UniFrac PCoA analyses (Supplemental Fig. 3d, e and Supplementary Table 6).

At the phylum level, HF feeding was associated with a higher ratio of *Firmicutes:Bacteroidetes*, as well as increased representation of *Verrucomicrobia*, compared to the microbiota of HP- and HC-fed mice (Fig. 4c). On the other hand, Proteobacteria was underrepresented in the microbiome of HP-fed mice (Fig. 4c). To investigate this further, we applied the ALDEx2 statistical test at the genus level (Fig. 4d) to identify differentially abundant genera (Supplementary Tables 7-9). Consistent with the over-representation of bacteria from the phylum Verrucomicrobia in HF-fed mice (Fig. 4c), *Akkermansia*, which can utilise host mucus as a carbon source[20], was significantly higher compared to both HP- and HC- fed mice (Fig. 4e). The microbiota of the HP-fed mice was characterised by the increased abundance of bacteria from the phylum *Actinobacteria* (Fig. 4c) with the over-representation of bacteria from the genus *Bifidobacterium* (Fig. 4f). Finally, HC feeding was characterised by the over-representation of bacteria from the genus *Allobacullum* (Fig. 4g). Of note, we did not identify segmented filamentous bacteria or *Mucispirillum* in our animals (Supplementary Tables 7-9), which are two genera known to induce strong T-cell-dependent sIgA responses[6].

Overall, macronutrient composition significantly impacts both the alpha and beta diversity of the small intestine microbiome, with fat appearing to be the dominant driver.

EV derived from high-protein-fed microbiota activate epithelial TLR4 and promote the expression of PIGR and APRIL. While we identified that each diet had an impact on the gut microbiota, we then investigated the mechanisms through which the HP microbiota promote the host sIgA response. TLR4 is one of the main TLRs expressed by the small intestinal enterocytes and TLR4 signalling is the major pathway promoting T-cell-independent IgA responses[9]. To determine whether TLR4 signalling was linked to the effect of HP in vivo, we fed wild type (WT) versus *Tlr4*$^{-/-}$ mice on HP diets for 6 weeks and measured sIgA levels in the small intestine. The absence of TLR4 abrogated the effects of HP on sIgA levels (Supplementary

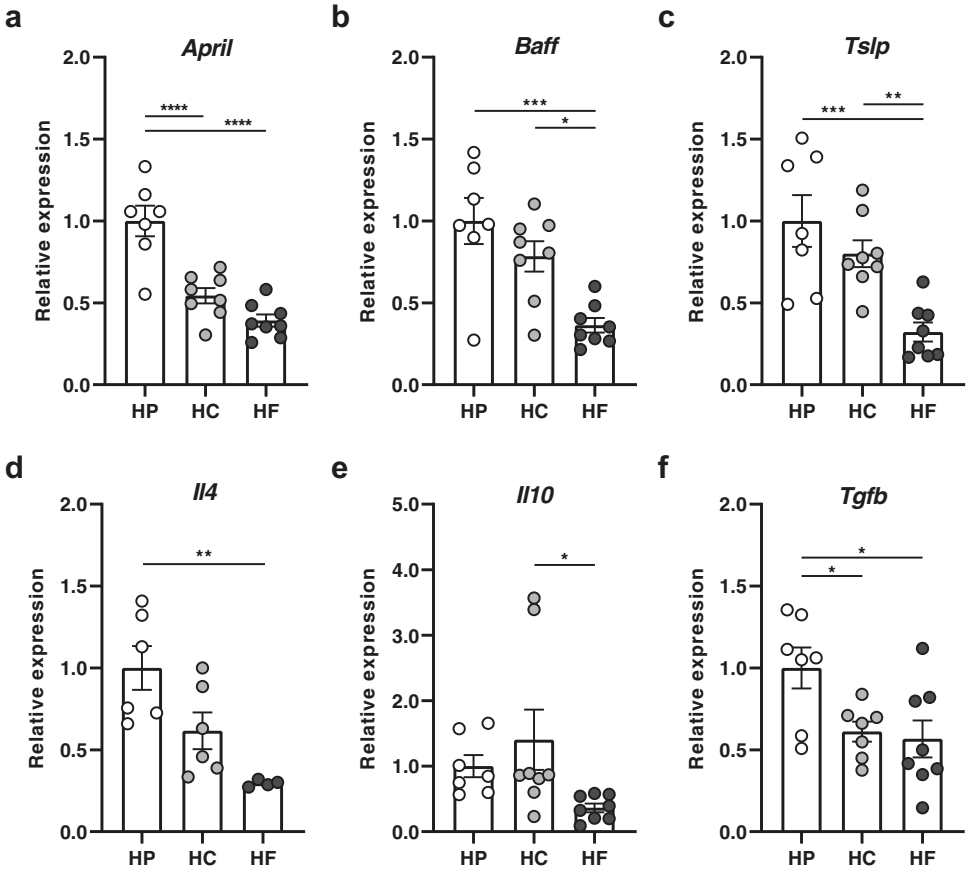

Fig. 3 High protein feeding promotes a pro-IgA cytokine environment, specifically APRIL in the lamina propria. Mice were fed on either a high-protein (HP), high-carbohydrate (HC), or high-fat (HF) diet for 6 weeks and intestinal ileal gene expression of **a** *April* (HP vs. HC $p = <0.0001$, HP vs. HF $p = <0.0001$), **b** *Baff* (HP vs. HF $p = 0.0005$, HC vs. HF $p = <0.0135$), **c** *Tslp* (HP vs. HF $p = 0.0005$, HC vs. HF $p = 0.0082$), **d** *Il4* (HP vs. HF $p = 0.0033$), **e** *Il10* (HC vs. HF $p = 0.0481$) and **f** *Tgfb* (HP vs. HC $p = 0.0481$, HP vs. HF $p = 0.0214$) was determined by qPCR (**a**–**c**, **e** $n = 7$ and $n = 8$ mice per diet for HP and HC/HF diet respectively, **d** $n = 6$ and $n = 4$ mice per diet for HP/HC and HF diet respectively, **f**; $n = 7$ and $n = 8$ mice per diet for HP/HC and HF diet respectively). Data are represented as mean ± SEM. Results represent $n = 2$ independent experiments. *$p < 0.05$, **<0.01, ***<0.001, ****<0.0001 by ordinary one-way ANOVA followed by Tukey's multiple comparisons test.

Fig. 4a), confirming that an HP diet promotes sIgA production via TLR4-dependent mechanisms.

Increased TLR4 signalling may be attributable to either higher expression of TLR4, increased concentration of its ligand, or increased exposure to its ligand through defects in the mucus layer or tight junction proteins. Mice fed on an HP, HC or HF diet had similar expression of TLR4 in the small intestine (Supplementary Fig. 4b), as well as comparable bacterial loads as determined by DNA concentration and total 16 S copy number (Supplementary Fig. 4c, d). We also quantified the levels of endotoxin in each diet and found low levels of endotoxin, which were comparable between the different diets (EU/ml of 0.0137, 0.053 and below the detection limit for HP, HC and HF diet, respectively). Furthermore, the expression of gut barrier-related markers *Tjp1* (tight junction protein 1) and *Ocln* (occludin) were similar between groups (Supplementary Fig. 4e), as was the integrity of the mucus layer (Supplementary Fig. 4f) and *Muc2* (mucin 2) expression (Supplementary Fig. 4g). These results indicate that increased activation of TLR4 and sIgA production under HP-feeding conditions are not linked to impaired gut integrity, higher bacterial load or higher *Tlr4* expression.

Typically, the mucus layer mediates an efficient physical separation of microbes from the gut epithelium. We, therefore, hypothesised that in vivo activation of TLR4 might be mediated by smaller structures containing PAMPs, rather than through physical interaction with whole bacteria. Bacterial extracellular vesicles (EV) are small spherical structures less than 300 nm in diameter, produced by the budding of the membrane and consequently contain PAMPs. EV can contain nucleic acid, protein, metabolites and other molecules as cargo and are a key component of bacterial communication[21]. EV derived from *Bacteroides fragilis* has been shown to promote regulatory T-cell differentiation through the stimulation of TLR[22], highlighting the ability of EV to traverse the mucus layer to reach the host. As such, we investigated whether EV derived from the microbiota of HP-fed mice might activate TLR and promote cytokines involved in IgA CSR.

To determine whether the small intestinal environment of HP-fed mice could differentially activate TLR4 signalling, we used the reporter cell line, HEK-Blue mTLR4, in which the intensity of TLR4 activation is assessed through a colorimetric assay. These cells were incubated with the non-bacterial fraction of small intestine luminal contents isolated from mice fed on HP, HC or HF diets. HEK cells stimulated with HP small intestine content had significantly higher levels of TLR4 activation than those stimulated with either HC or HF small intestine content (Fig. 5a), suggesting the highest potential for HP-fed mice to activate host cells.

The luminal environment contains bacterial metabolites, food derivatives and bacterial EV, but bacterial EV are the only candidates containing bacterial motifs able to activate TLR4. Thus, we characterised the number and size distribution of microbiota-derived EV from mice fed on different diets by nanoparticle tracking analysis (NTA). While microbiota-derived

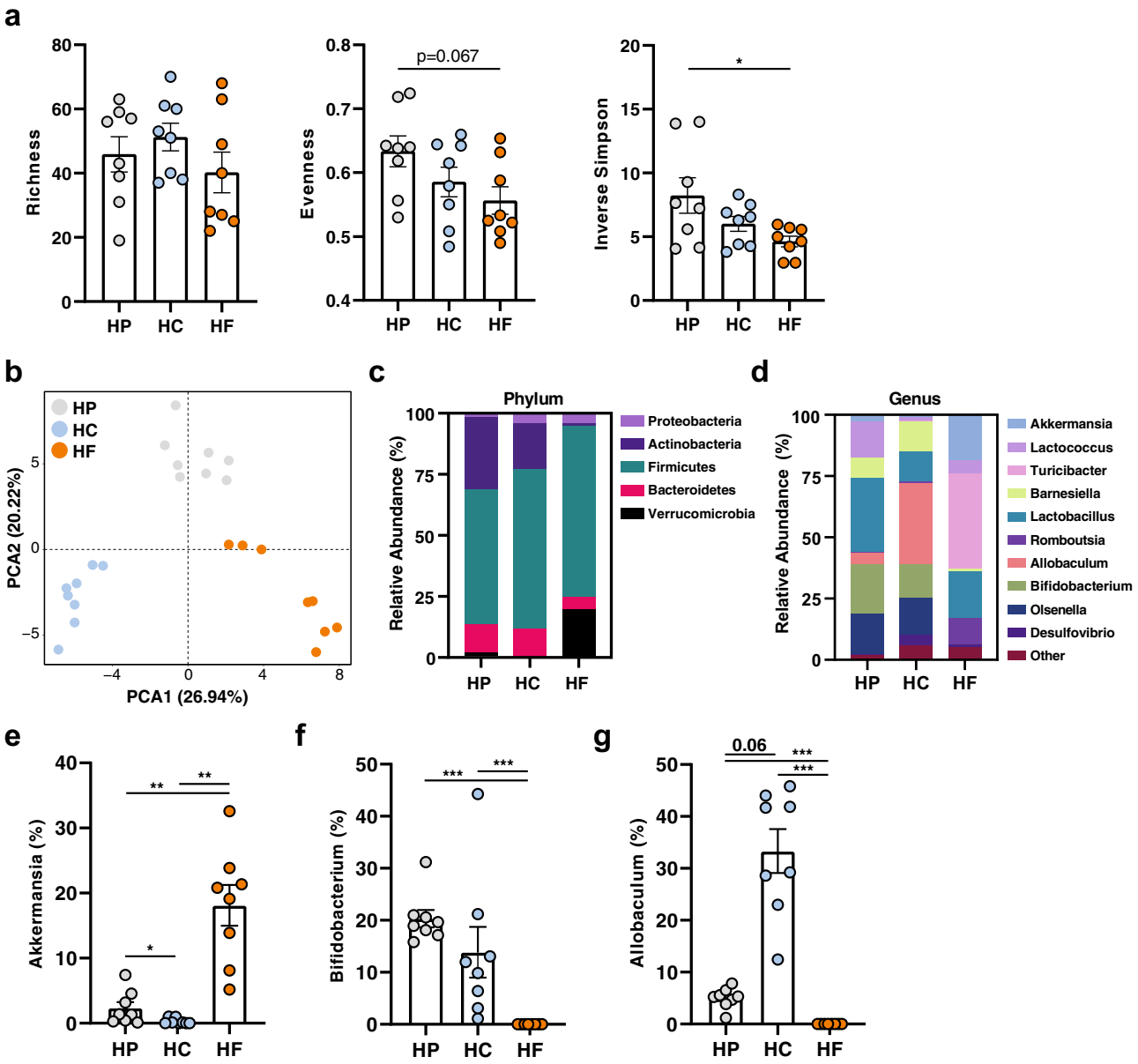

Fig. 4 Dietary intervention significantly affects the small intestine microbiota composition. Mice were fed on either a high-protein (HP), high-carbohydrate (HC), or high-fat (HF) diet for 6 weeks and DNA was extracted from small intestinal content for 16 S rRNA gene sequencing ($n = 8$ mice per diet). Diversity of the small intestinal microbiome was determined by **a** Richness, Evenness and Inverse Simpson Index (HP vs. HF $p = 0.0269$) with $^*p < 0.05$ by ordinary one-way ANOVA followed by Tukey's multiple comparisons test. **b** Differences in the structure of the small intestinal microbiota communities were determined by principal component analysis (PCA) of Aitchison's distance (Euclidean distance of centre-log transformed counts). Relative abundance of bacteria in the small intestine is represented at the **c** phylum and **d** genus level (showing only the top 10 genera). Relative abundance of (**e**) *Akkermansia* (HP vs. HC $p = 0.032/p = 0.013$, HP vs. HF $p = 0.002/p = 0.003$, HC vs. HF $p = 0.002/p = 0.003$), **f** *Bifidobacterium* (HP vs. HF $p = <0.0001/p = 0.001$, HC vs. HF $p = <0.0001/p = 0.001$), and (**g**) *Allobaculum* (HP vs. HF $p = <0.0001/p = 0.001$, HC vs. HF $p = <0.0001/p = 0.001$) with, $^{**}<0.01$, $^{***}<0.001$ by Aldex2 test (Welch's *t* test/Wilcoxon test with Benjamini–Hochberg corrected false discovery rate). Data are represented as mean ± SEM.

EV isolated from the small intestine luminal content had a similar size distribution across the diets (Fig. 5b), we found a 2-fold increase in concentration under HP feeding conditions (Fig. 5b). To determine whether microbiota-EV isolated from mice fed on the different diets differentially activated TLR4, we incubated HEK-Blue mTLR4 cells with similar doses of small intestine microbiota-derived EV relative to those observed in vivo (2:1:1 ratio of HP:HC:HF). Consistent with previous results showing the highest potential of small intestine content to activate TLR4, we found that purified EV derived from HP microbiota stimulated TLR4 and to the highest extent (Fig. 5c). However, when the HEK-Blue mTLR4 cells were incubated with the same concentration of EV from each group, the activation of TLR4 was similar (Fig. 5c). Thus, the higher activation of TLR4 by microbiota-derived EV under HP feeding conditions was due to a quantitative rather than a qualitative effect.

To determine the impact of microbiota-derived EV on host sIgA production and translocation, we quantified the gene expression of *CCL28*, *APRIL* and *PIGR* in HT-29 cells incubated with vehicle control (PBS) or with small intestine microbiota-derived EV from mice fed on HP, HF and HC at physiological levels (HP > HC = HF). EV derived from HP small intestine

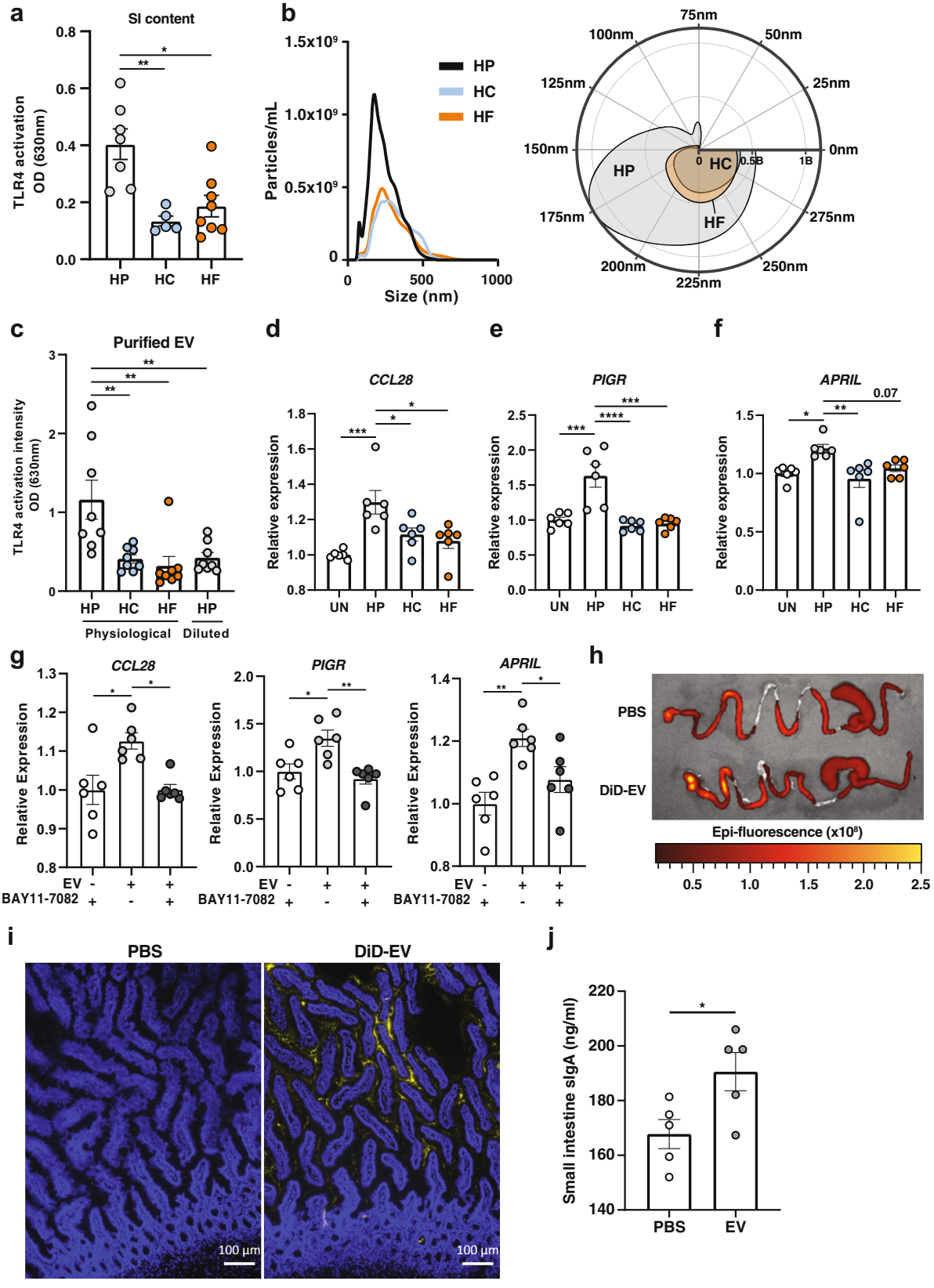

microbiota significantly upregulated *CCL28, PIGR and APRIL*, compared to cells treated with PBS or EV derived from HC and HF microbiota, and close to significance for APRIL when compared to EV derived from HC microbiota (Fig. 5d–f). To confirm whether HP-derived EV mediated these effects via TLR signalling, we cultured HT-29 cells with EV in the presence of BAY11-7082, an inhibitor of NF-κB, the transcription factor involved in TLR signalling[12]. The addition of BAY11-7082 abrogated the effect of HP-EV on the expression of *PIGR*, *APRIL* and *CCL28* (Fig. 5g), suggesting that EV mediated their effects via

Fig. 5 EV derived from high protein-fed microbiota activate epithelial TLR4 and promote the expression of PIGR and APRIL. Mice were fed on either a high-protein (HP), high-carbohydrate (HC) or high-fat (HF) diet for 6 weeks. **a** Small intestinal content (diluted at 1:200) ($n = 5$ and $n = 8$ mice per diet for HP/HC and HF diet, respectively) was incubated overnight with HEK-TLR4 cell line and TLR4 activation was quantified at 630 nm. (HP vs. HC $p = 0.0017$, HP vs. HF $p = 0.0038$). **b** Small intestine microbiota-derived EV were characterised by Nanoparticle Tracking Analysis ($n = 2$ per diet pooled from $n = 4$ mice each) and represented as an XY plot (left): 0–500 nm vs. particle number/mL), or polar plot (right): angular axis represents particle size between 0 and 300 nm and radial axis represents particle number/mL). **c** Small intestine microbiota-derived extracellular vesicles (EV) were incubated at physiological ratio (~2:1:1 of HP:HC:HF), or at 1:1:1 ratio (HP diluted) overnight with the HEK-Blue TLR4 cell line and TLR activation measured at 630 nm ($n = 8$ mice per condition; HP vs. HC $p = 0.0058$, HP vs. HF $p = 0.0019$, HP vs. HP diluted $p = 0.007$). **d**–**f** HT-29 were stimulated with small intestine microbiota-derived EV isolated from HP (2×10^9 EV per well) or HC/HF (1×10^9 EV per well) fed animals for 16 h and expression of **d** *CCL28* (Un vs. HP $p = 0.0006$, HP vs. HC $p = 0.0372$, HP vs. HF $p = 0.0105$), **e** *PIGR* (Un vs. HP $p = 0.0003$, HP vs. HC $p = <0.0001$, HP vs. HF $p = 0.0001$) and **f** *APRIL* (Un vs. HP $p = 0.0165$, HP vs. HF $p = 0.0036$) were quantified by qPCR ($n = 6$ wells per condition). **g** HT-29 cells were incubated with 2×10^9 small intestine microbiota-derived EV from HP-fed animals for 16 hours in the presence or absence of 10 μM of NF-κB inhibitor BAY11-7082, or BAY11-7082 alone and expression of *CCL28* (−EV + BAY11-7082 vs. +EV-BAY11-7082 $p = 0.0103$, +EV-BAY11-7082 vs. +EV + BAY11-7082 $p = 0.0106$), *PIGR* (−EV + BAY11-7082 vs. +EV-BAY11-7082 $p = 0.0131$, +EV-BAY11-7082 vs. +EV + BAY11-7082 $p = 0.0032$) and *APRIL* (−EV + BAY11-7082 vs. +EV-BAY11-7082 $p = 0.0021$, +EV-BAY11-7082 vs. +EV + BAY11-7082 $p = 0.0443$) were quantified by qPCR ($n = 6$ wells per condition). **h** Representative ex vivo epi-fluorescence imaging of gastrointestinal tract 6 hours post-oral administration of DiD-stained EV or PBS. **i** Presence of DiD-EV (yellow) and DAPI (blue) were assessed by fluorescent microscopy from sections of small intestine isolated from mice 6 hours after oral administration, with PBS as control. Scale bar represents 100 μm. **j** Mice were intragastrically administered with $1–3 \times 10^{10}$ EV daily for 5 weeks and small intestine sIgA quantified by ELISA ($n = 5$ mice per group; $p = 0.0319$ by two-tailed unpaired *t* test). Data are represented as mean ± SEM. Results represent $n = 2$ independent (**a**–**h**) and $n = 1$ independent experiment (**i**, **j**). *$p < 0.05$, **<0.01, ***<0.001, ****<0.0001 by ordinary one-way ANOVA followed by Tukey's multiple comparisons test unless otherwise stated.

TLR signalling. We confirmed these in vitro findings using caecum microbiota-derived EV (Supplementary Fig. 4h–k), a site containing a higher density and purity of bacteria.

To determine whether microbiota-derived EV could reach the host small intestine epithelium in vivo, we isolated microbiota-EV from mice fed on normal chow, fluorescently labelled them with DiD, and administered them by gavage to another set of mice. Ex vivo imaging of gut tissue by IVIS revealed higher epi-fluorescence intensity in the gastrointestinal tract of mice receiving DiD-EV, compared to the PBS control, showing that DiD-EV readily reached the small intestine (Fig. 5h). There was also a presence of DiD-EV in both the lumen and mucosa of these mice, as determined by fluorescence microscopy (Fig. 5i). Finally, we showed that daily administration of purified microbiota-derived EV for 5 weeks in vivo could increase sIgA levels (Fig. 5j).

Together, these data highlight a close interaction between bacterial EV and host cells in vivo as well as a role for gut microbiota-derived EV on the regulation of host genes involved in sIgA regulation via TLR activation.

Succinate promotes bacterial ROS and bacterial EV production. In addition to TLR activation, the gut microbiota can also modulate host sIgA production through the generation of metabolites, such as short-chain fatty acids[23–25]. To determine whether such mechanisms are involved, we quantified microbiota-derived metabolites by NMR and focused on metabolites that are significantly increased under HP feeding conditions (Supplementary Tables 10-11). Of the major bacterial metabolites detected, we found that succinate was significantly elevated in both the small intestine luminal content (Fig. 6a), and caecal content (Supplementary Fig. 5a) in HP-fed mice, compared to mice fed on HC and HF diets. Of note, succinate was not detectable in the diets used in this study (Supplementary Fig. 5b). We incubated HT-29 cells with succinate to determine whether it could directly affect *CCL28, APRIL and PIGR* expression. We found that, unlike EV-stimulated HT-29, succinate could not directly induce the expression of *CCL28, APRIL or PIGR* expression (Supplementary Fig. 5c). As such, we hypothesised that changes to the gut metabolite environment would affect the gut microbiota, rather than the host directly to elicit host sIgA response.

Like any cell types, bacteria can produce EV in response to stress signals such as reactive oxygen species (ROS)[21]. Succinate, which we found to be highly upregulated in HP-fed mice, has been shown to increase ROS in host cells such as macrophages[26]. High levels of microbiota-produced succinate under HP-feeding conditions might promote bacterial ROS, which would, in turn, stimulate the release of EV. To test this hypothesis, we incubated *E. coli* with increasing concentrations of succinate and quantified ROS. Strikingly, succinate increased ROS production in a dose-dependent manner (Fig. 6b) without affecting bacterial growth (Supplementary Fig. 5d). To determine the impact of succinate on EV production, we cultured *E. coli* with succinate for 16 h and found that succinate significantly increased EV production by NTA at the high concentrations (Fig. 6c). These results uncover a mechanism through which gut bacterial vesiculation is regulated by the metabolites in the environment, particularly succinate.

High bacterial EV and high succinate production under HP feeding correlates with worse DSS-induced colitis. Increased succinate has also been reported in human inflammatory bowel disease (IBD), as well as in DSS-induced colitis in mice[27,28]. Accordingly, we found that mice treated with DSS had higher gut bacterial EV production with similar size distribution (Fig. 6d, e). As observed under HP feeding conditions, IBD is not only characterised by high gut succinate levels[27] but also increased TLR activation by gut microbial PAMPs[29]. We found that DSS colitis was exacerbated under conditions of high succinate, either through HP feeding (Fig. 6f–h) or direct administration of succinate in drinking water (Fig. 6i–k). Our results suggest succinate is a key mediator that can contribute to an inflammatory intestinal environment by promoting the production of microbiota EV that can activate TLR4. This model is summarised in Fig. 7.

Together, these results highlight a potential pathway involved in IBD severity through the increased production of the bacterial metabolite, succinate, in the induction of bacterial EV that can in turn activate TLR signalling and modulate host gene expression and inflammatory responses.

Discussion

In the present study, we have identified a key role for dietary macronutrient composition in the dynamic regulation of IgA production and sIgA release in the small intestinal lumen. Dietary

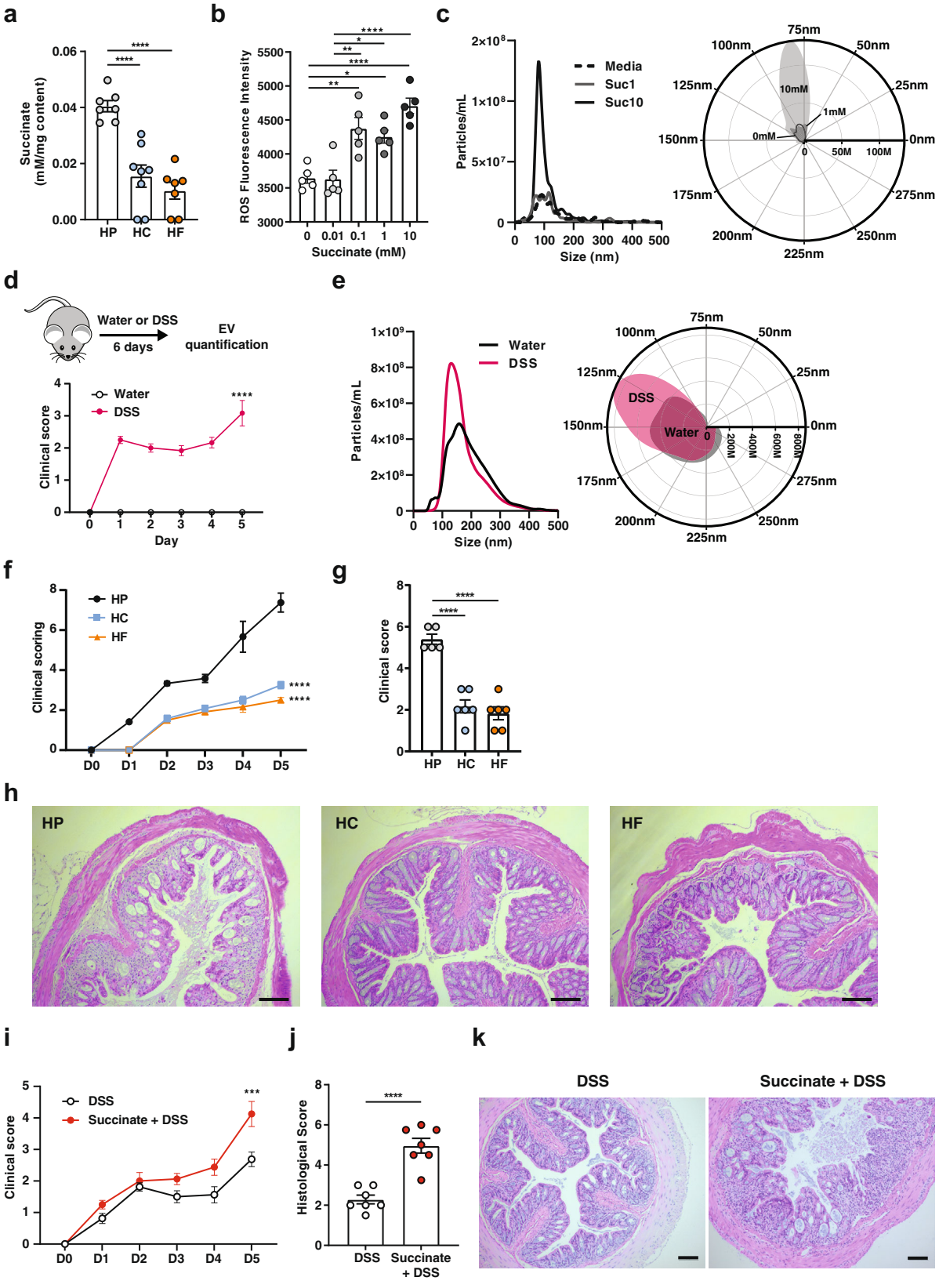

protein was the major driver of T-cell-independent sIgA response, associated with increased expression of the CSR-promoting cytokines APRIL and BAFF. Increased luminal sIgA was associated with elevated expression of the transporter *pIgR* that was correlated with the highest expression of IL-4, a cytokine involved in both IgA induction and pIgR expression. These changes are commonly observed under pro-inflammatory conditions linked to increased activation of host pattern-recognition receptors by gut bacterial products. Accordingly, we found that intestinal luminal content from HP-fed mice activated the TLR4-NFκB pathway to a greater extent than contents obtained from either HC or HF-fed mice. This was attributed to the greater

Fig. 6 Succinate promote bacterial ROS and bacterial EV production and is associated with worse DSS-induced colitis. a The concentration of succinate in the small intestine luminal content of mice fed on a high-protein (HP), high-carbohydrate (HC) or high-fat (HF) diet for 6 weeks was quantified by NMR spectroscopy ($n = 7$ and $n = 8$ mice per diet for HP/HF and HC group respectively; HP vs. HC $p = <0.0001$, HP vs. HF $p = <0.0001$). **b** *E. coli* were grown in the presence of increasing concentration of succinate (0–10 mM) for 2 h and ROS production quantified by the conversion of 2′,7′-dichlorofluorescein diacetate to 2′,7′-dichlorofluorescein ($n = 5$ independent culture per condition; 0 vs. 0.1 mM $p = 0.0026$, 0 vs. 1 mM $p = 0.0131$, 0 vs 10 mM $p = <0.0001$, 0.01 vs. 0.1 mM $p = 0.0021$, 0.01 vs. 1 mM $p = 0.0108$, 0.01 vs. 10 mM $p = <0.0001$). **c** *E. coli* was grown in the presence of succinate (0, 1, or 10 mM) for 16 h and extracellular vesicles (EV) isolated and quantified by NTA ($n = 5$–6 per condition) and represented as XY plot (left): 0–500 nm vs. particle number/mL or polar plot (right): angular axis represents particle size between 0 and 300 nm and radial axis represents particle concentration in number/mL. **d** Mice received 3% DSS in drinking water for 6 days (upper) and colitis development was scored daily (lower) ($n = 6$ mice per group; $p = <0.0001$ by two-way ANOVA) and (**e**) at endpoint, faecal EV were isolated and quantified by Nanoparticle Tracking Analysis ($n = 6$ mice per condition) and represented as an XY plot (left): 0–500 nm vs. particle number/mL, or polar plot (right): angular axis represents particle size between 0 and 300 nm and radial axis represents particle concentration in number/mL. **f–h** Mice were mice fed on a HP, HC, or HF diet for 6 weeks before induction of DSS colitis (3% DSS in drinking water for 6 days) and (**f**) clinical colitis development was scored daily (HP vs. HC $p = <0.001$, HP vs. HF $p = <0.0001$) and **g** colonic histological score assessed (HP vs. HC $p = <0.0001$, HP vs. HF $p = <0.0001$) and **h** representative haematoxylin and eosin-stained colonic sections ($n = 6$ mice per group). **i–k** Mice were administered 100 mM pH-adjusted succinate in drinking water for 3 weeks before induction of DSS colitis (3% DSS in drinking water for 6 days) and **i** clinical colitis development was scored daily ($p = 0.0005$ by two-way ANOVA) and **j** histological scores quantified at endpoint on colonic section ($p = <0.0001$ by two-tailed unpaired *t* test) with **k** representative haematoxylin and eosin-stained colonic sections shown. ($n = 7$ mice per group). Scale bar represents 100 µm. Data are represented as mean ± SEM. Results represent $n = 3$ independent (**b**), $n = 2$ (**b–e**) and $n = 1$ independent experiments (**f–k**). *$p < 0.05$, **<0.01, ***<0.001, ****<0.0001 and were analysed by ordinary one-way ANOVA followed by Tukey's multiple comparisons test unless otherwise stated.

production of microbiota-derived EV that could activate the TLR4 signalling pathway under HP feeding conditions. Increased production of EV is likely the result of increased microbial stress, as previously reported in bacteria[21]. Consistent with this, we found that high protein consumption significantly increased microbial succinate production, which we demonstrated to promote bacterial ROS production in a concentration-dependent manner in vitro. This work highlights a mechanism through which the gut microbiota regulates host sIgA response modulated by diet composition.

The majority of sIgA produced under homoeostatic conditions is induced by commensal bacteria via T-cell-independent mechanisms. Indeed, sIgA induced by the monocolonization of germ-free mice with various strains of bacteria were mostly non-specific and polyreactive in nature[4]. This observation highlights that the presence, rather than the composition of the microbiota is important in inducing sIgA and the mechanism likely involves a shared feature of bacteria, such as their capacity to activate host TLR via MAMPs. Our small intestinal microbiome data revealed no obvious dysbiosis associated with HP feeding that could explain the increase of sIgA. Rather, lower microbiota diversity was observed in HF-fed animals, an indicator of dysbiosis commonly observed in patients with allergies or IBD[30–32]. Furthermore, an HP microbiome was associated with a higher abundance of bacteria from the genus *Bifidobacterium*, commonly considered a beneficial bacteria. Additionally, phyla commonly associated with adherent intestinal bacteria, which are typically considered pro-inflammatory[33–35], such as those from *Firmicutes*, *Bacteroidetes* and *Proteobacteria* did not differ between HP- and HC-fed groups. Despite this, an HP microbiome had an exacerbated pro-inflammatory potential via increased production of microbiota EV that can activate TLR4, which was associated with exacerbated colitis compared to both HC- and HF-fed mice. Reduced colitis severity under HC feeding is likely due to increased levels of SCFA, which have been shown to be protective[36]. HF had similarly reduced colitis either due to the macronutrient composition or to the high cellulose content used as filler in this diet. While cellulose is not a functional fibre and does not yield fermentable products such as SCFA, it has been shown to be protective against colitis[37]. Future studies examining qualitative aspects of macronutrients, such as different types of fat and protein (i.e., animal vs. plant-based protein), would be required to fully appreciate the role of macronutrients on gut homoeostasis as well as on the host sIgA responses. For example, soy-derived protein has been associated with lower sIgA, compared to casein-derived protein[38].

How the gut microbiota can adequately activate TLR under homoeostatic conditions remains unclear, as TLR is usually inaccessible to whole bacteria due to the presence of a mucus layer. We highlight that microbiota-derived EV might be the link as they can traverse the mucus and can activate TLR4 to upregulate IgA-related epithelial genes in vitro, revealing a mechanism underpinning host-microbiota mutualism. HT-29, being a human cell line, highlights the translational potential of our finding. Quantification of microbiota-derived EV could prove a useful tool to evaluate the functional characteristics as well as the inflammatory potential of the gut microbiota as an alternative to sequencing.

Our study examined both qualitative and quantitative effects of microbiota-derived EV on the host. TLR4 and CCL28 were modulated by EV in a dose-dependent manner, with HP feeding conditions increasing the activity of the former and gene expression of the latter. This suggests that EV could be a mechanism by which the host perceives changes in the state of the gut microbiota via TLR activation. As a result, the host would mobilise B cells to the gut and increase the translocation of sIgA to control the situation based on the amount of EV sensed. This could have clinical implications in diseases such as food allergy, in which low levels of IgA are commonly reported. We also uncovered a qualitative effect of EV on the host. Significant changes in the gut microbiota composition have been shown to promote the production of different types of EV. Indeed, EV can carry a range of molecules including proteins, metabolites and nucleic acids as cargo, and EV have been shown to mediate the virulence and pro-inflammatory effects of pathogenic bacteria[21]. A complete analysis of the features of EV derived from HP, HC and HF microbiota, although outside the scope of this study, would confirm this.

The high levels of succinate under HP-feeding conditions remain unexplained. We could not identify a specific microbiome signature that would account for greater succinate production in HP-fed mice. One possibility is the disappearance of succinate consumers in the HP microbiota. We find that succinate could modulate ROS production in bacteria and the long-term impact of this on the gut microbiota is yet to be determined. ROS is known to induce bacterial mutation and antibiotic resistance which could thus raise concerns that high protein diet feeding could promote the potential growth of antibiotic-resistant

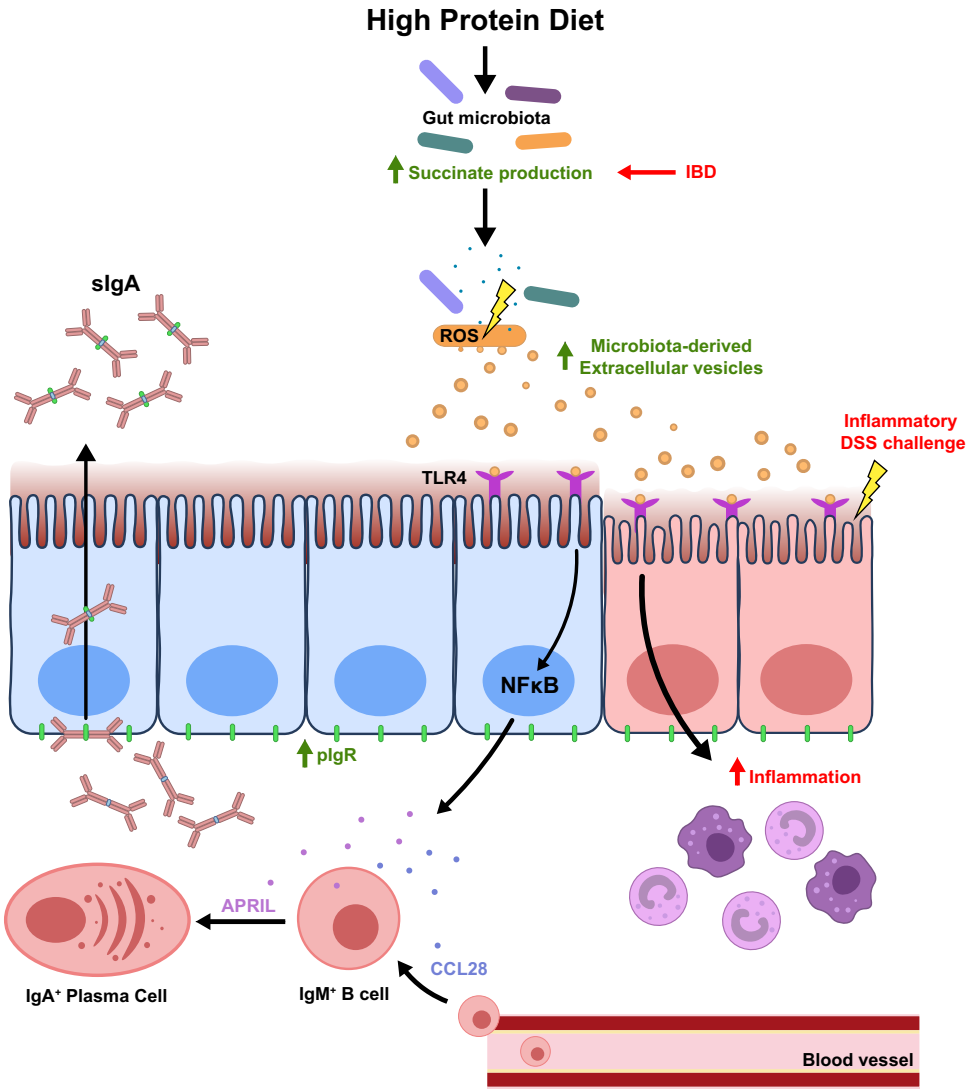

Fig. 7 Model of high protein diet in the induction of sIgA response. High protein diet feeding promotes succinate production by the gut microbiota. High levels of luminal succinate induce gut bacterial cellular stress and reactive oxygen species (ROS) production, which promote vesiculation and increased production of microbiota-derived extracellular vesicles. Microbiota-derived extracellular vesicles can directly activate TLR4 expressed on the gut epithelium, activating downstream NFκB signalling that results in increased expression of APRIL, CCL28 and PIGR, which drives the T-cell-independent sIgA response. Increased TLR4 signalling also potentiates pro-inflammatory responses, resulting in more severe DSS-induced colitis. Increased intestinal succinate observed in IBD patients may contribute to disease pathology by promoting microbiota-derived extracellular vesicle production and the TLR4/NFκB signalling pathway.

bacteria. Moreover, we identified higher levels of bacterial EV in DSS colitis, a disease in which gut bacterial dysbiosis, as well as high succinate levels, were previously reported[27,28]. This result suggests that dysbiosis, in general, could be sensed by the host via EV. However, whether bacterial dysbiosis observed in diseases other than IBD is associated with higher microbiota EV production remains unknown.

In summary, we describe a pathway by which the gut microbiota can regulate T-cell-independent IgA induction via bacteria-derived EV as illustrated in Fig. 7. More broadly, we show a mechanism through which the microbiota impact the host. This opens exciting new prospects for characterising microbiota EV as a biomarker for dysbiosis, as well as the potential use of microbiota EV as a postbiotic to restore gut homoeostasis.

Methods

Animals and housing. Male C57BL/6 mice (6 weeks of age) were purchased from Animal Bioresource (NSW, Australia). Mice were maintained under specific pathogen-free conditions at 22 °C, 50% humidity with a 12 hour light/dark cycle (6PM–6AM) in the animal facility of the Charles Perkins Centre. Animals were housed in cages with non-edible compressed cotton fibre (iso-PADS) bedding. All experiments were performed in accordance with protocols approved by the University of Sydney Animal Ethics Committee (Protocol 2017/1280, 2019/1493, and 2019/1688).

Animal diets and feeding. Animals were fed *ad libitum* on either a high protein, moderately low carbohydrate, moderately low-fat diet (P60, C20, F20; henceforth, HP); a low protein, high carbohydrate, moderately low-fat diet (P5, C75, F20; henceforth, HC), or a low protein, moderately low carbohydrate, high-fat diet (P5, C20, F75; henceforth, HF). These three diets represented the extremes (apices) from a larger set of 10 diet compositions (Supplementary Table 1) that were used in a subset of the experiments, encompassing a macronutrient range of protein (5–60%), carbohydrate (20–75%), and fat (20–75%) chosen using nutritional geometry to comprehensively sample dietary macronutrient mixture space[39]. All diets were isocaloric at 14.5 MJ/kg and based on a modification to the semi-purified AIN93G formulation and purchased from Specialty Feeds, Glenn Forest, Australia (SF17-188-SF17-197) and the HP/HC/HF used for most experiments had very low endotoxin levels as tested with the PyroGene Recombinant Factor C kit (Lonza).

Quantification of immunoglobulins. Small intestinal content was resuspended in PBS (100 mg/ml) containing cOmplete™ Protease Inhibitor Cocktail (Roche), centrifuged at 14,000 × *g* for 10 min to pellet bacteria and debris and supernatant collected. Quantification of IgA and IgM levels was performed using the Mouse IgA or IgM ELISA quantification set (Bethyl Laboratories), or the Mouse IgA ELISA Antibody Pair Kit (STEMCELL Technologies) according to the manufacturer's instruction.

Immunofluorescence. For immunohistochemistry, frozen small intestine sections were fixed with ice-cold methanol, and incubated with goat anti-mouse IgA (1:100, Bethyl Laboratories) followed by AF488-conjugated chicken anti-goat IgG secondary antibody (1:200, Invitrogen). Sections were stained with DAPI and examined with an Olympus BX51 Microscope and images were captured using the cellSens Standard v1.12 software.

Flow cytometry. Single-cell suspensions were prepared by mechanical disruption of tissues through a 100 µm filter. For isolation of intestinal lamina propria cells, mesenteric fat and Peyer's patches were first resected from small intestine tissues, then tissues washed with PBS and cut into 1 cm pieces and incubated in predigestion buffer (HBSS containing 10% FBS, 10 mM HEPES, 5 mM EDTA) for 40 min at 37 °C at 200 rpm in an orbital incubator. Tissues were washed twice with PBS then cut into <1 mm pieces and incubated in digestion buffer (RPMI containing 10% FBS, 10 mM HEPES, 2.5 mg/ml collagenase type IV (Gibco)) for 60 min at 37 °C at 200 rpm in an orbital incubator and lymphocytes were enriched via a 40/80% Percoll gradient (GE Healthcare). Cells were incubated with LIVE/DEAD™ Fixable Blue Dead Cell Stain Kit (ThermoFisher Scientific) for exclusion of non-viable cells and anti-mouse CD16/32 (91; BioLegend) for blocking non-specific binding, then stained with the antibodies described in Supplementary Table 12 and acquired on the LSRII (BD Bioscience) with the BD FACS Diva v8.0.2 software. Data were analysed with the FlowJo v10.4.2 software (FlowJo LLC).

RNA extraction and qPCR. Total RNA was extracted using TRI Reagent (Sigma-Aldrich) following the manufacturer's instructions and cDNA was generated using the High-Capacity cDNA Reverse Transcription Kit (ThermoFisher Scientific). qPCR was conducted using the Power SYBR™ Green PCR Master Mix (ThermoFisher Scientific) on a LightCycler® 480 Instrument II (Roche Life Science) and LightCycler® 480 v1.5.0 software: 1 cycle of 95 °C for 5 min; 45 cycles of 95 °C for 15 s, 60 °C for 60 s followed by dissociation curve: 95 °C for 5 s, 65 °C for 60 s followed by 0.11 °C/s to 97 °C. Expression was normalised to a housekeeping gene as indicated in the Figure legends. Primers were used at a final concentration of 200 nM, and sequences are provided in Supplementary Table 13.

16 S rRNA gene sequencing and bioinformatics. DNA from small intestinal jejunum content was extracted using the FastDNA™ SPIN Kit for Feces (MP Biomedicals). Illumina sequencing of the V4 region (515f-806r) of the 16 S rRNA gene was performed commercially at the Ramaciotti Centre for Genomics (UNSW, Australia). Paired-end reads (2 × 250 bp) were processed with the dada2 package (1.12.1) using R software (3.6.1) with RStudio (1.4.1717) to generate amplicon sequence variant (ASV)[40]. Taxonomic classification of ASV was performed using the Ribosomal Database Project naïve Bayesian classifier (rdp_train_set_16) with species-level taxonomy assignment (doi:10.5281/zenodo.801828). For downstream analysis, ASV with a total abundance of less than 0.01% was first filtered out. For beta diversity analysis, a compositional data analysis approach was used[41]. ASV was centre log-ratio (CLR) transformed after replacement of zeros via count zero multiplicative replacement[42]. Differences in microbiome composition between 2 groups were determined by PERMANOVA of Aitchison distance (Euclidean distance of CLR transformed data), after validation of homogeneity of group dispersions. For differential abundance testing of ASV between two groups, ALDEx2 was used, and taxa were considered differentially abundant when Benjamini–Hochberg corrected the expected *p* value for both Welch's *t* test and Wilcoxon test were <0.05 and magnitude of effect size >1. Analysis was performed with the following R packages phyloseq (1.32.0), vegan (2.5.7), ALDEx2 (1.20.0), zCompositions (1.3.4), ranacapa (0.1.0). DNA sequencing data were deposited in the European Nucleotide Archive under accession number PRJEB39583.

Quantitative assessment of intestinal bacterial load. Intestinal bacterial load was determined by absolute 16 S copy number per mg of intestinal content, determined by qPCR using the following 16 S rDNA universal primers: UniF: GTGSTGCAYGGYYGTCGTCA and UniR: ACGTCRTCCMCNCCTTCCTC with the following cycling protocol: 1 cycle of 95 °C for 5 min; 45 cycles of 95 °C for 30 s, 60 °C for 30 s, 72 °C for 30 s, 1 cycle of 72 °C for 5 min followed by dissociation curve: 95 °C for 5 s, 65 °C for 60 s followed by 0.11 °C/s to 97 °C. Copy number was determined via a standard curve (10^8 to 10^2 copies/µl).

EV isolation and nanoparticle tracking analysis (NTA). In all, 100 mg of caecum content or small intestine luminal content was homogenised in 0.02 µm filtered PBS and EV isolated by differential centrifugation, as described previously[43,44]. Briefly, the homogenate was centrifuged at 340 × *g* for 10 min at 4 °C. Supernatant was then centrifuged at 10,000 × *g* for 20 min at 4 °C followed by 18,000 × *g* for 45 min at 4 °C, filtered through a 0.22 µm filter and centrifuged at 100,000 × *g* for 2 hr at 4 °C. EV pellet was resuspended in 0.02 µm filtered PBS. EV particle size and concentration were assessed by NTA on a Nanosight NS300 (Malvern Instruments Limited). NTA 3.2 software was used to calculate EV concentration and size distribution.

Ex vivo imaging of EV uptake. Fluorescent staining of EV was performed with the Vybrant DiD Cell Labelling Kit (Invitrogen) at a final concentration of 5 µM for 30 min at room temperature and washed with PBS by ultracentrifugation at 100,000 × *g* for 2 h at 4 °C. Animals were intragastrically administered 80 µg of DiD-EV and organs imaged 6 h later with the IVIS Spectrum In Vivo Imaging System (Perkin Elmer) at excitation: 640 nm and emission: 680 nm. Images were analysed using the Living Image 4.5 Software (Perkin Elmer) and fluorescence was quantified as radiant efficiency.

Mucus layer thickness quantification. For quantification of mucus thickness, colon tissues were fixed in Carnoy's solution fixative for 24 hours and then transferred to 70% ethanol prior to paraffin embedding. All samples were transversely sectioned at 7 µm and stained with Alcian blue (pH 2.5) and 0.1% (w/v) acetic safranin solutions for histological characterisation of the mucus layer. All slides were imaged by the Aperio AT2 Slide scanner at ×20 magnification and visualised using Aperio ImageScope v12.3.3 (Leica Biosystems Imaging). Analysis was performed using the image processing software FIJI (v1.52p). The scale bar of each sample was used to determine the known length using the line tool. A total of 10 measurements of the mucus thickness were recorded per sample and values were averaged.

TLR4 activity assay and cell culture. HEK-Blue mTLR4 reporter cell line (InvivoGen) was maintained in complete DMEM (Gibco) containing 10% FBS (Bovogen Biologicals), 100 U/ml Penicillin and 100 µg/ml Streptomycin (Gibco), 2 mM L-glutamine (Sigma-Aldrich) and supplemented with 100 µg/ml Normocin and 1× HEK-Blue selection (InvivoGen). TLR4 activation by bacterial-derived EV or diluted small intestinal content was assessed according to the manufacturer's instructions. HT-29 cells (ATCC) were maintained in complete DMEM media and stimulated with small intestinal content or bacteria-derived EV for 16 h. NF-κB inhibitor BAY11-7082 (Sigma-Aldrich) was used at 10 µM.

Detection of polar metabolites. For detection of polar metabolites by ^{1}H nuclear magnetic resonance spectroscopy (NMR), caecal or small intestinal content was homogenised in deuterium oxide (Sigma-Aldrich) at a concentration of 100 mg/ml and centrifuged at 14,0000 × *g* for 5 min at 4 °C. For dietary metabolite analysis, diet pellets were suspended in 5 ml deuterium oxide per gram diet and allowed to fully dissolve overnight at 4 °C before clarification by centrifugation at 14,000 × *g* for 5 min at 4 °C. Contents were then filtered through a 3 kDa centrifugal filtration unit (Merck Millipore), and polar metabolites were collected from the aqueous phase of a chloroform-D/methanol-D/water extraction. The resulting solution was diluted with sodium triphosphate buffer (pH 7.0) containing 0.5 mM 4,4-dimethyl-4-silapentane-1-sulfonic acid as internal standard (All from Sigma-Aldrich) and samples were run on a Bruker 600 MHz AVANCE III spectrometer. The Chenomx NMR Suite v8.4 software (Chenomx Inc) was used to identify and fit compounds from the acquired sample spectrum against pre-defined spectral reference libraries and concentrations quantified in reference to the internal standard.

Bacterial culture and ROS quantification. *Escherichia coli* (K-12 MG1655) were cultured in Luria-Bertani broth with succinate, propionate or pyruvate at indicated doses and supernatants were collected for EV quantification 16 h later. For quantification of ROS production, *E. coli* were treated with succinate at indicated doses for 2 h, and cells pelleted by centrifugation (5000 rpm for 5 min). Pellet was resuspended in PBS containing 10 µM of 2',7'-dichlorofluorescein diacetate (Sigma-Aldrich) and incubated for 60 min at room temperature. Fluorescence intensity was measured using a TECAN Infinite M1000 microplate reader (Excitation 485 nm, Emission 538 nm, Gain 100) using the Tecan i-control v1.10.4.0 software.

Experimental model of colitis. Murine model of colitis was induced by the administration of 3% dextran sodium sulfate (DSS, MW: 36,000-50,000, MP Biomedicals) in drinking water for 6 days. In some experiments, mice were treated with pH-adjusted sodium succinate (100 mM, Sigma-Aldrich) in drinking water for 3 weeks prior to DSS model induction and throughout the model. Mice were monitored daily and clinical score was assessed as follows: 0-normal faeces; 1-soft faeces; 2-pasty faeces; 3-liquid faeces; 4-moderate rectal bleeding; 5-severe rectal bleeding; 6-haemorrhagia/diarrhoea and 7- signs of morbidity as previously reported[36]. Histological analysis of haematoxylin and eosin-stained colon sections were performed blinded by at least 2 independent researchers for tissue damage: 0, no mucosal damage; 1, lymphoepithelial lesions; 2, surface mucosal erosion and 3, extensive mucosal damage, extension into deeper structure, and for inflammatory cell infiltration: 0, occasional cell infiltrate; 1, increased number of infiltrating cells; 2, confluency of inflammatory cells extending to the submucosa and 3, transmural extension of the inflammatory cells.

Mixture model and statistical analyses. The effects of dietary macronutrient composition on outcomes were analysed using mixture models (also known as Scheffé's polynomials). Analyses were performed on each outcome variable separately. Models were implemented using the *mixexp* package (1.2.5) using R software (3.6.1). For each outcome, four models equivalent to equations described by Lawson and Willden[17] as well as a null model were fitted. Collectively, these models test for no effect, linear effects, and non-linear effects of macronutrient composition on the outcome variable. The most appropriate model was determined by Akaike information criterion (AIC), where the lowest AIC value (where AIC was within two points of difference, the simpler model was selected) was deemed the most appropriate model. Predictions from the best model were represented on a right-angled mixture triangle plot[15]. For comparison between groups, analysis was done with GraphPad Prism v9 using Ordinary one-way ANOVA followed by Tukey's multiple comparisons test. No statistical method was used to predetermine sample size. Differences were considered as significant when $p < 0.05$ where $^{*}p < 0.05$, $^{**}p < 0.01$, $^{***}p < 0.001$, and $^{****}p < 0.0001$.

Reporting summary. Further information on research design is available in the Nature Research Reporting Summary linked to this article.

Data availability

The 16 S rRNA sequencing data generated in this study have been deposited in the European Nucleotide Archive database under accession code PRJEB39583. Source data are provided in this paper.

Received: 12 August 2020; Accepted: 30 June 2022;
Published online: 27 July 2022

References

1. Sommer, F. & Bäckhed, F. The gut microbiota—masters of host development and physiology. *Nat. Rev. Microbiol.* **11**, 227–238 (2013).
2. Mantis, N. J., Rol, N. & Corthésy, B. Secretory IgA's complex roles in immunity and mucosal homeostasis in the gut. *Mucosal Immunol.* **4**, 603–611 (2011).
3. Yel, L. Selective IgA deficiency. *J. Clin. Immunol.* **30**, 10–16 (2010).
4. Pabst, O. & Slack, E. IgA and the intestinal microbiota: the importance of being specific. *Mucosal Immunol.* **13**, 12–21 (2020).
5. Hand, T. W. & Reboldi, A. Production and function of immunoglobulin A. *Annu Rev. Immunol.* **39**, 695–718 (2021).
6. Bunker, J. J. et al. Innate and adaptive humoral responses coat distinct commensal bacteria with immunoglobulin A. *Immunity* **43**, 541–553 (2015).
7. Macpherson, A. J. et al. A primitive T cell-independent mechanism of intestinal mucosal IgA responses to commensal bacteria. *Science* **288**, 2222–2226 (2000).
8. Castigli, E. et al. Impaired IgA class switching in APRIL-deficient mice. *Proc. Natl. Acad. Sci. USA* **101**, 3903–3908 (2004).
9. Shang, L. et al. Toll-like receptor signaling in small intestinal epithelium promotes B-cell recruitment and IgA production in lamina propria. *Gastroenterology* **135**, 529–538 (2008).
10. He, B. et al. Intestinal bacteria trigger T cell-independent immunoglobulin A(2) class switching by inducing epithelial-cell secretion of the cytokine APRIL. *Immunity* **26**, 812–826 (2007).
11. Fagarasan, S., Kawamoto, S., Kanagawa, O. & Suzuki, K. Adaptive immune regulation in the gut: T cell-dependent and T cell-independent IgA synthesis. *Annu. Rev. Immunol.* **28**, 243–273 (2010).
12. Bruno, M. E. C., Frantz, A. L., Rogier, E. W., Johansen, F.-E. & Kaetzel, C. S. Regulation of the polymeric immunoglobulin receptor by the classical and alternative NF-κB pathways in intestinal epithelial cells. *Mucosal Immunol.* **4**, 468–478 (2011).
13. Hapfelmeier, S. et al. Reversible microbial colonization of germ-free mice reveals the dynamics of IgA immune responses. *Science* **328**, 1705–1709 (2010).
14. Lubomski, M. et al. Parkinson's disease and the gastrointestinal microbiome. *J. Neurol.* https://doi.org/10.1007/s00415-019-09320-1 (2019).
15. Raubenheimer, D. Toward a quantitative nutritional ecology: the right-angled mixture triangle. *Ecol. Monogr.* **81**, 407–427 (2011).
16. Saner, C. et al. Evidence for protein leverage in children and adolescents with obesity. *Obesity* **28**, 822–829 (2020).
17. Lawson, J. & Willden, C. Mixture experiments in R using mixexp. *J. Stat. Softw.* **72**, 1–20 (2016).
18. Wells, J. M., Rossi, O., Meijerink, M. & van Baarlen, P. Epithelial crosstalk at the microbiota-mucosal interface. *Proc. Natl. Acad. Sci. USA* **108**, 4607–4614 (2011).
19. Singh, R. K. et al. Influence of diet on the gut microbiome and implications for human health. *J. Transl. Med.* **15**, 73 (2017).
20. Geerlings, S. Y., Kostopoulos, I., de Vos, W. M. & Belzer, C. Akkermansia muciniphila in the human gastrointestinal tract: when, where, and how? *Microorganisms* **6**, 75 (2018).
21. Macia, L., Nanan, R., Hosseini-Beheshti, E. & Grau, G. E. Host- and microbiota-derived extracellular vesicles, immune function, and disease development. *Int. J. Mol. Sci.* **21**, 107 (2019).
22. Shen, Y. et al. Outer membrane vesicles of a human commensal mediate immune regulation and disease protection. *Cell Host Microbe* **12**, 509–520 (2012).
23. Kim, M., Qie, Y., Park, J. & Kim, C. H. Gut microbial metabolites fuel host antibody responses. *Cell Host Microbe* **20**, 202–214 (2016).
24. Tan, J. et al. Dietary fiber and bacterial scfa enhance oral tolerance and protect against food allergy through diverse cellular pathways. *Cell Rep.* **15**, 2809–2824 (2016).
25. Sanchez, H. N. et al. B cell-intrinsic epigenetic modulation of antibody responses by dietary fiber-derived short-chain fatty acids. *Nat. Commun.* **11**, 60 (2020).
26. Mills, E. L. et al. Succinate dehydrogenase supports metabolic repurposing of mitochondria to drive inflammatory macrophages. *Cell* **167**, 457–470.e13 (2016).
27. Connors, J., Dawe, N. & Van Limbergen, J. The role of succinate in the regulation of intestinal inflammation. *Nutrients* **11**, 25 (2018).
28. Fremder, M. et al. A transepithelial pathway delivers succinate to macrophages, thus perpetuating their pro-inflammatory metabolic state. *Cell Rep.* **36**, 109521 (2021).
29. Lu, Y., Li, X., Liu, S., Zhang, Y. & Zhang, D. Toll-like receptors and inflammatory bowel disease. *Front. Immunol.* **9**, 72 (2018).
30. Manichanh, C. et al. Reduced diversity of faecal microbiota in Crohn's disease revealed by a metagenomic approach. *Gut* **55**, 205–211 (2006).
31. Hua, X., Goedert, J. J., Pu, A., Yu, G. & Shi, J. Allergy associations with the adult fecal microbiota: analysis of the american gut project. *EBioMedicine* **3**, 172–179 (2016).
32. Abrahamsson, T. R. et al. Low gut microbiota diversity in early infancy precedes asthma at school age. *Clin. Exp. Allergy* **44**, 842–850 (2014).
33. Lu, Y. et al. Mucosal adherent bacterial dysbiosis in patients with colorectal adenomas. *Sci. Rep.* **6**, 26337 (2016).
34. Sicard, J.-F., Le Bihan, G., Vogeleer, P., Jacques, M. & Harel, J. Interactions of intestinal bacteria with components of the intestinal mucus. *Front. Cell Infect. Microbiol.* **7**, 387 (2017).
35. Yu, L. C.-H. Microbiota dysbiosis and barrier dysfunction in inflammatory bowel disease and colorectal cancers: exploring a common ground hypothesis. *J. Biomed. Sci.* **25**, 79 (2018).
36. Macia, L. et al. Metabolite-sensing receptors GPR43 and GPR109A facilitate dietary fibre-induced gut homeostasis through regulation of the inflammasome. *Nat. Commun.* **6**, 6734 (2015).
37. Kim, Y. et al. Dietary cellulose prevents gut inflammation by modulating lipid metabolism and gut microbiota. *Gut Microbes* **11**, 944–961 (2020).
38. Zeng, B. et al. Dietary soy protein isolate attenuates intestinal immunoglobulin and mucin expression in young mice compared with casein. *Nutrients* **12**, 2739 (2020).
39. Simpson, S. J., Le Couteur, D. G. & Raubenheimer, D. Putting the balance back in diet. *Cell* **161**, 18–23 (2015).
40. Callahan, B. J. et al. DADA2: High-resolution sample inference from Illumina amplicon data. *Nat. Methods* **13**, 581–583 (2016).
41. Gloor, G. B., Macklaim, J. M., Pawlowsky-Glahn, V. & Egozcue, J. J. Microbiome datasets are compositional: and this is not optional. *Front. Microbiol.* **8**, 2224 (2017).
42. Palarea-Albaladejo, J. & Martín-Fernández, J. A. zCompositions — R package for multivariate imputation of left-censored data under a compositional approach. *Chemom. Intell. Lab. Syst.* **143**, 85–96 (2015).
43. Momen-Heravi, F. et al. Current methods for the isolation of extracellular vesicles. *Biol. Chem.* **394**, 1253–1262 (2013).
44. Momen-Heravi, F. Isolation of extracellular vesicles by ultracentrifugation. *Methods Mol. Biol.* **1660**, 25–32 (2017).

Acknowledgements

This project was funded by the Australian Research Council grant APP160100627 and APP210102943 and by the Sydney Medical School MCR BioMed-Connect Grants. We thank Alexandra Angelatos for her help with some aspects of the project. We thank professor Arthur Conigrave for his input and discussion. We acknowledge the Sydney Cytometry facility for providing access to flow cytometer analysers, the Sydney Preclinical Imaging facility for training and access to the IVIS Spectrum Imaging System, and the Laboratory Animal Services at The University of Sydney for animal housing and husbandry.

Author contributions

J.T. performed most of the experiments, participated in the project design and wrote the manuscript, D.N., J.Taitz., G.V.P., R.E., E.S., H.W., and S.J.C. participated in the experiments, A.S. and M.R. helped with the data analysis, J.W., R.N., N.J.C.K., G.E.G.,

and S.J.S. helped with the study design, L.M. participated to the study design, supervised the study, and wrote the manuscript.

Competing interests
The authors declare no competing interests.

Additional information
Supplementary information The online version contains supplementary material available at https://doi.org/10.1038/s41467-022-31761-y.

Correspondence and requests for materials should be addressed to Laurence Macia.

Peer review information *Nature Communications* thanks Maria De Angelis, Stephanie Ganal-Vonarburg and Ruairi Robertson for their contribution to the peer review of this work. Peer reviewer reports are available.

Reprints and permission information is available at http://www.nature.com/reprints

Publisher's note Springer Nature remains neutral with regard to jurisdictional claims in published maps and institutional affiliations.

Supplementary Material

Supplementary Table 1 – Detailed composition of the experimental diets used in the study

Diet formulation provided as gram of ingredients per 100g for each of the 10 diets used in the study. The diets are isocaloric at 14.5 MJ/kg with the following net metabolizable energy (NME) assigned: casein (13.3 kJ/g; 3.2 kCal/g), L-methionine (18 kJ/g; 4.3 kCal/g), Canola oil (36.6 kJ/g; 8.7 kCal/g), Wheat starch (14.13 kJ/g; 3.4 kCal/g), Dextrinized Starch (14.6 kJ/g; 3.49 kCal/g), Sucrose 14.92 kCal/g and cellulose was given a NME of 0 kCal/g.

		Diet 1	**Diet 2**	**Diet 3**	**Diet 4**	**Diet 5**	**Diet 6**	**Diet 7**	**Diet 8**	**Diet 9**	**Diet 10**
	%P	60	5	5	33	33	5	14	14	42	24
	%C	20	75	20	47	20	47	29	57	29	38
	%F	20	20	75	20	47	48	57	29	29	38
INGREDIENTS											
Protein	**Casein**	64.87	5.04	5.04	35.50	35.50	5.04	14.83	14.83	45.29	25.71
	L-Methionine	0.30	0.30	0.30	0.30	0.30	0.30	0.30	0.30	0.30	0.30
Fat	**Canola Oil**	7.91	7.91	29.65	7.91	18.58	18.98	22.53	11.46	11.46	15.03
Carbohydrate	**Wheat Starch**	12.59	47.87	12.60	29.91	12.60	29.91	18.37	36.34	18.37	24.13
	Dextrinized Starch	4.10	15.57	4.10	9.73	4.10	9.73	5.98	11.82	5.98	7.85
	Sucrose	3.11	11.81	3.11	7.38	3.11	7.38	4.54	8.97	4.54	5.96
Minerals	**$CaCO_3$**	1.31	1.31	1.31	1.31	1.31	1.31	1.31	1.31	1.31	1.31
	NaCl	0.26	0.26	0.26	0.26	0.26	0.26	0.26	0.26	0.26	0.26
	AIN93 Trace Minerals	0.14	0.14	0.14	0.14	0.14	0.14	0.14	0.14	0.14	0.14
	KH_2PO_4	0.69	0.69	0.69	0.69	0.69	0.69	0.69	0.69	0.69	0.69
	K_2SO_4	0.16	0.16	0.16	0.16	0.16	0.16	0.16	0.16	0.16	0.16
	KCl	0.25	0.25	0.25	0.25	0.25	0.25	0.25	0.25	0.25	0.25
	$C_5H_{14}ClNO$	0.25	0.25	0.25	0.25	0.25	0.25	0.25	0.25	0.25	0.25
Vitamins	**AIN93 vitamins**	1.00	1.00	1.00	1.00	1.00	1.00	1.00	1.00	1.00	1.00
Cellulose	**Cellulose**	3.06	7.44	41.15	5.21	21.75	24.60	29.39	12.23	10.00	16.97

Supplementary Table 2 – Statistical output for mixture models relating to sIgA

Model (Scheffé Polynomials)	Akaike Information Criterion	Degrees of freedom
1	1168.363	4
2	1168.552	7
3	1156.861	11
4	1170.262	8
Null	1181.324	2

Model 1 Coefficients			
Components	**Estimate (Std. Error)**	**t value**	**P(>|t|)**
Protein	2094.2 (264.7)	7.913	2.05e−11
Fat	517.6 (214.5)	2.413	0.018334
Carbohydrate	868.8 (220.6)	3.939	0.000185
Adjusted R-squared	0.8076		
p-value	< 2.2e−16		

Supplementary Table 3 – Statistical output for mixture models relating to plasma IgA

Model (Scheffé Polynomials)	Akaike Information Criterion	Degrees of freedom
1	1160.604	4
2	1142.835	7
3	1149.336	11
4	1144.762	8
Null	1171.433	2

Model 2 Coefficients			
Components	**Estimate (Std. Error)**	**t value**	**P(>|t|)**
Protein	1244.4 (600.3)	2.073	0.041706
Fat	2042.4 (371.3)	5.501	5.31e−07
Carbohydrate	2110.2 (375.5)	5.619	3.30e−07
Protein:Fat	−3432.3 (1666.8)	−2.059	0.043043
Protein:Carbohydrate	−4738.6 (1667.2)	−2.842	0.005804
Fat:Carbohydrate	−6169.1 (1657.3)	−3.722	0.000385
Adjusted R-squared	0.7243		
p-value	< 2.2e−16		

Supplementary Table 4 – Statistical output for mixture models relating to plasma IgM

Model (Scheffé Polynomials)	Akaike Information Criterion	Degrees of freedom
1	696.561	4
2	700.119	7
3	701.771	11
4	700.027	8
Null	693.555	2

Supplementary Table 5 – 16S rRNA sequencing quality control

	Total reads	Reads post filtering	Reads post merging and chimera filtering	Reads retained
HP 1	135805	119366	97727	71.96%
HP 2	49009	43630	43301	88.35%
HP 3	120743	107426	91056	75.41%
HP 4	59370	51662	50927	85.78%
HP 5	71171	62355	61855	86.91%
HP 6	55324	49431	49288	89.09%
HP 7	24290	21876	21826	89.86%
HP 8	111569	96616	95494	85.59%
HC 1	89660	79158	78435	87.48%
HC 2	133887	119303	102883	76.84%
HC 3	52702	47334	46964	89.11%
HC 4	29954	26904	26437	88.26%
HC 5	121070	100002	94779	78.28%
HC 6	86078	71337	71144	82.65%
HC 7	69380	59366	59010	85.05%
HC 8	136477	117920	101334	74.25%
HF 1	44447	41330	40566	91.27%
HF 2	135418	126495	117867	87.04%
HF 3	13618	12835	12692	93.20%
HF 4	19284	18178	17971	93.19%
HF 5	23368	22069	21948	93.92%
HF 6	19495	18154	18134	93.02%
HF 7	120323	113333	103573	86.08%
HF 8	102020	95906	84963	83.28%

Supplementary Table 6 – Statistical output for the comparison of different dietary groups of different beta diversity distance metric, based on PERMANOVA test (permutation = 9999)

PERMANOVA	HP vs HC	HP vs HF	HC vs HF
Unweighted UniFrac	R^2= 0.18861 P= 0.005	R^2= 0.34924 P= 2e-4	R^2= 0.35927 P= 3e-4
Weighted UniFrac	R^2= 0.45964 P= 2e-4	R^2= 0.67843 P= 2e-4	R^2= 0.81691 P= 2e-4
Atchison's distance	R^2= 0.35152 P= 3e-04	R^2= 0.53433 P= 1e-04	R^2= 0.52121 P= 3e-04

Supplementary Table 7 –Statistical output of ALDEx2 analysis comparing HP and HC at the genera level. CLR, centered log-ratio transformed; FDR, Benjamini–Hochberg corrected false discovery rate. Two-sided tests used.

Genus	Median CLR (HP)	Median CLR (HC)	Effect size	FDR (Welch's t test)	FDR (Wilcoxon test)
Akkermansia	5.230	-1.047	-1.365	0.032	0.013
Lactococcus	7.187	3.426	-1.481	0.024	0.009
Pseudomonas	-4.515	-6.937	-0.439	0.404	0.427
Turicibacter	-5.442	-1.88	0.555	0.317	0.315
Barnesiella	7.097	7.503	0.257	0.628	0.773
Lactobacillus	9.757	7.297	-0.683	0.185	0.278
Romboutsia	-3.655	0.020	0.071	0.815	0.880
Allobaculum	7.151	8.922	1.063	0.061	0.050
Bifidobacterium	9.147	7.640	-0.506	0.275	0.382
Olsenella	8.893	8.177	-0.419	0.362	0.442
Clostridium_XlVa	-2.954	-5.438	-0.439	0.416	0.437
Acetatifactor	1.263	2.133	0.582	0.165	0.194
Desulfovibrio	3.196	5.494	0.794	0.118	0.074
Parabacteroides	-5.583	-5.925	-0.041	0.698	0.771
Coprobacter	-0.637	2.605	0.732	0.145	0.175
Dorea	2.102	3.489	0.531	0.194	0.190
Sporobacter	-6.180	-4.408	0.346	0.440	0.541
Ruminococcus2	-1.070	-3.723	-0.300	0.528	0.567
Clostridium_sensu_st ricto	2.372	-6.863	-1.355	0.047	0.049
Enterorhabdus	1.809	2.222	0.128	0.660	0.833
Clostridium_IV	-0.607	-0.186	0.084	0.801	0.913
Mesorhizobium	-0.669	-0.841	-0.057	0.828	0.905
Intestinimonas	-4.610	-5.968	-0.253	0.609	0.679
Corynebacterium	-6.419	0.715	0.818	0.166	0.228
Murimonas	-2.197	-6.755	-0.743	0.235	0.214
Staphylococcus	-3.963	2.500	0.642	0.211	0.168
Escherichia/Shigella	-5.458	-5.203	0.026	0.697	0.770
Ralstonia	-4.315	-3.492	0.156	0.635	0.743
Burkholderia	-3.611	-3.850	0.031	0.773	0.860
Enterococcus	-6.467	-2.824	0.633	0.276	0.286
Bacillus	-6.061	-2.534	0.627	0.265	0.297
Senegalimassilia	-3.162	-3.831	-0.118	0.694	0.787

Supplementary Table 8 –Statistical output of ALDEx2 analysis comparing HP and HF at the genera level. CLR, centered log-ratio transformed; FDR, Benjamini–Hochberg corrected false discovery rate. Two-sided tests used.

Genus	Median CLR (HP)	Median CLR (HF)	Effect size	FDR (Welch's t test)	FDR (Wilcoxon test)
Akkermansia	5.201	8.460	1.823	0.002	0.003
Lactococcus	7.158	6.614	-0.458	0.244	0.447
Pseudomonas	-4.552	2.817	0.604	0.233	0.434
Turicibacter	-5.315	9.107	4.267	0.000	0.001
Barnesiella	7.137	4.406	-0.925	0.040	0.071
Lactobacillus	9.804	9.049	-0.428	0.276	0.367
Romboutsia	-3.374	7.604	1.943	0.006	0.001
Allobaculum	7.201	-6.456	-3.674	0.000	0.001
Bifidobacterium	9.221	-5.819	-4.804	0.000	0.001
Olsenella	8.948	-6.443	-4.254	0.000	0.001
Clostridium_XlVa	-2.878	1.792	0.587	0.224	0.194
Acetatifactor	1.231	0.101	-0.157	0.616	0.828
Desulfovibrio	3.181	3.842	0.119	0.672	0.671
Parabacteroides	-5.452	-3.252	0.407	0.370	0.395
Rhodococcus	-6.354	0.442	0.699	0.213	0.272
Coprobacter	-0.594	1.230	0.245	0.575	0.612
Dorea	2.128	1.273	-0.194	0.752	0.603
Ruminococcus2	-1.074	-5.474	-0.784	0.136	0.135
Clostridium_sensu_stricto	2.420	-6.603	-1.184	0.041	0.048
Enterorhabdus	1.855	3.425	0.536	0.254	0.347
Clostridium_IV	-0.654	-2.718	-0.290	0.552	0.515
Mesorhizobium	-0.700	0.052	0.298	0.546	0.477
Intestinimonas	-4.387	-5.404	-0.235	0.545	0.557
Murimonas	-2.214	-2.454	0.098	0.657	0.781
Staphylococcus	-3.825	-2.447	0.326	0.500	0.538
Escherichia/Shigella	-5.473	-3.606	0.494	0.249	0.338
Ralstonia	-4.262	0.189	0.518	0.314	0.250
Burkholderia	-3.616	-2.998	0.075	0.701	0.754
Enterococcus	-6.275	-2.906	0.500	0.329	0.310
Senegalimassilia	-3.159	-5.558	-0.427	0.327	0.332

Supplementary Table 9 –Statistical output of ALDEx2 analysis comparing HC and HF at the genera level. CLR, centered log-ratio transformed; FDR, Benjamini–Hochberg corrected false discovery rate. Two-sided tests used.

Genus	Median CLR (HC)	Median CLR (HF)	Effect size	FDR (Welch's t test)	FDR (Wilcoxon test)
Akkermansia	5.201	8.460	1.823	0.002	0.003
Lactococcus	7.158	6.614	-0.458	0.244	0.447
Pseudomonas	-4.552	2.817	0.604	0.233	0.434
Turicibacter	-5.315	9.107	4.267	0.000	0.001
Barnesiella	7.137	4.406	-0.925	0.040	0.071
Lactobacillus	9.804	9.049	-0.428	0.276	0.367
Romboutsia	-3.374	7.604	1.943	0.006	0.001
Allobaculum	7.201	-6.456	-3.674	0.000	0.001
Bifidobacterium	9.221	-5.819	-4.804	0.000	0.001
Olsenella	8.948	-6.443	-4.254	0.000	0.001
Clostridium_XlVa	-2.878	1.792	0.587	0.224	0.194
Acetatifactor	1.231	0.101	-0.157	0.616	0.828
Desulfovibrio	3.181	3.842	0.119	0.672	0.671
Parabacteroides	-5.452	-3.252	0.407	0.370	0.395
Rhodococcus	-6.354	0.442	0.699	0.213	0.272
Coprobacter	-0.594	1.230	0.245	0.575	0.612
Dorea	2.128	1.273	-0.194	0.752	0.603
Ruminococcus2	-1.074	-5.474	-0.784	0.136	0.135
Clostridium_sensu_stricto	2.420	-6.603	-1.184	0.041	0.048
Enterorhabdus	1.855	3.425	0.536	0.254	0.347
Clostridium_IV	-0.654	-2.718	-0.290	0.552	0.515
Mesorhizobium	-0.700	0.052	0.298	0.546	0.477
Intestinimonas	-4.387	-5.404	-0.235	0.545	0.557
Murimonas	-2.214	-2.454	0.098	0.657	0.781
Staphylococcus	-3.825	-2.447	0.326	0.500	0.538
Escherichia/Shigella	-5.473	-3.606	0.494	0.249	0.338
Ralstonia	-4.262	0.189	0.518	0.314	0.250
Burkholderia	-3.616	-2.998	0.075	0.701	0.754
Enterococcus	-6.275	-2.906	0.500	0.329	0.310
Senegalimassilia	-3.159	-5.558	-0.427	0.327	0.332

Supplementary Table 10 – Concentration of small intestine luminal metabolites detected by nuclear magnetic resonance (NMR). Concentrations are expressed as mM per mg of SI content (SD).

	HP	HC	HF
2-Aminobutyrate	1.076 (2.789)	0.753 (0.893)	0.624 (1.205)
Acetate	0.792 (0.199)	0.633 (0.127)	0.330 (0.159)
Alanine	3.981 (1.553)	2.561 (1.291)	0.000 (1.365)
Choline	1.208 (0.357)	1.434 (0.272)	1.068 (0.148)
Fumarate	0.094 (0.009)	0.066 (0.038)	0.000 (0.009)
Glutamate	5.568 (1.792)	3.293 (0.462)	2.850 (1.271)
Glycine	1.335 (0.309)	1.054 (0.553)	1.252 (0.361)
Homoserine	0.000 (1.212)	2.054 (0.877)	1.703 (0.466)
Isoleucine	3.090 (0.571)	2.070 (0.734)	1.408 (0.503)
Lactose	2.468 (0.628)	1.450 (0.295)	0.946 (0.152)
Leucine	9.563 (1.047)	5.229 (1.082)	4.309 (0.857)
Lysine	3.674 (1.803)	3.284 (0.877)	2.852 (0.463)
Malonate	0.366 (0.366)	0.310 (0.310)	0.291 (0.291)
Methionine	2.791 (0.425)	1.393 (0.711)	1.219 (0.468)
Pyruvate	0.133 (0.242)	0.264 (0.129)	0.125 (0.119)
Serine	1.945 (0.942)	1.227 (0.832)	0.000 (0.431)
Succinate	0.039 (0.005)	0.017 (0.011)	0.013 (0.008)
Valine	5.303 (1.046)	3.182 (0.688)	2.429 (0.800)

Supplementary Table 11 – Concentration of cecal content metabolites detected by nuclear magnetic resonance (NMR). Concentrations are expressed as mM per mg of cecal content (SD).

	HP	HC	HF
Acetate	23.21 (4.367)	35.50 (15.36)	14.87 (2.479)
Alanine	0.4942 (0.6841)	0.5355 (0.6802)	0.2778 (0.2390)
Butyrate	3.558 (0.8711)	8.759 (3.395)	2.027 (1.026)
Glutamate	4.083 (1.991)	2.808 (2.193)	1.026 (1.109)
Isoleucine	0.6867 (0.3561)	0.1078 (0.2042)	0 (0)
Lactate	1.457 (0.8441)	1.119 (1.143)	1.909 (1.849)
Leucine	1.597 (0.9185)	0.5091 (0.4334)	0.1735 (0.2790)
Lysine	0.8053 (0.9037)	0.6552 (0.6331)	0 (0)
Malonate	0.3504 (0.1826)	0.3163 (0.1561)	0.1881 (0.1885)
Methionine	0.2958 (0.2621)	0.1782 (0.1760)	0.03506 (0.07632)
Propionate	5.771 (1.606)	2.777 (0.8856)	3.297 (0.6736)
Pyruvate	1.445 (0.6071)	0.6418 (0.2915)	0.4338 (0.1698)
Succinate	0.7279 (0.2722)	0.2428 (0.08354)	0.1241 (0.07370)
Valine	0.8662 (0.4700)	0.4675 (0.3449)	0.03995 (0.1130)

Supplementary Table 12 – Antibodies used for flow cytometry

Target	Conjugate	Clone	Dilution	Manufacturer
CD45	BV785	30-F11	1:400	BioLegend
CD95	APC	SA367H8	1:200	BioLegend
GL-7	FITC	GL7	1:200	BioLegend
B220	VioGreen	REA755	1:50	Miltenyi Biotec
B220	APC	RA3-6B2	1:200	BioLegend
IgA	PE	11-44-2	1:200	eBioscience
CD4	PerCP	RM4-5	1:200	BioLegend

Supplementary Table 13 – Primers used in this study and their sequence

Pre-designed and validated primers used in this study. All primers were purchased from Sigma-Aldrich (KiCqStart SYBR® Green primers).

Gene target	Specie	Forward (5'-3')	Reverse (5'-3')
Pigr	Mouse	AAGAACTCCAGAGATTTGGG	GTGGTAGTCACGATTTCATC
Ccl28	Mouse	GAGGTGTCTCATCATGTTTC	ATACGTTTTCTCTGCCATTC
Tnfsf13	Mouse	TCTATAGTCAGGTCCTGTTTC	GGCATACTTCTGATACATCG
Baff	Mouse	ATCTACAGCCAGGTTCTATAC	AGCTGAATCTCATCTCCTTC
Tgfb	Mouse	GGATACCAACTATTGCTTCAG	TGTCCAGGCTCCAAATATAG
Tslp	Mouse	CCTGAAACTGAGAGAAATGAC	ACACCCTTAGTATTCTGTCC
Il10	Mouse	AAGGGTTACTTGGGTTGCCA	AAATCGATGACAGCGCCTCAG
Il4	Mouse	CTGGATTCATCGATAAGCTG	TTTGCATGATGCTCTTTAGG
Muc2	Mouse	ATTCTGAAGCCTGGGGAGAT	GAAGTCGGGACAGGTGATGT
Tjp1	Mouse	GTCTGCCATTACACGGTCCT	GGCTTAAGTCCAGGGGAGTC
Ocln	Mouse	CGGTACAGCAGCAATGGTAA	CTCCCCACCTGTCGTGTAGT
Tlr4	Mouse	GATCAGAAACTCAGCAAAGTC	TGTTTCAATTTCACACCTGG
Rpl13a	Mouse	ATCCCTCCACCCTATGACAA	GCCCCAGGTAAGCAAACTT
GAPDH	Human	GAAGGTGAAGGTCGGAGTCA	CAGAGTTAAAAGCAGCCCTGG
CCL28	Human	GAGGTGTCTCATCATGTTTC	ATACGTTTTCTCTGCCATTC
APRIL	Human	CAGGTGTCTTCCATTTACAC	TGGAGAGAGGTTAAGTTTCG
PIGR	Human	GACCGAGTTTCAATCAGAAG	TTGTCATTGGCTCCAAATTC

Supplementary Figure 1

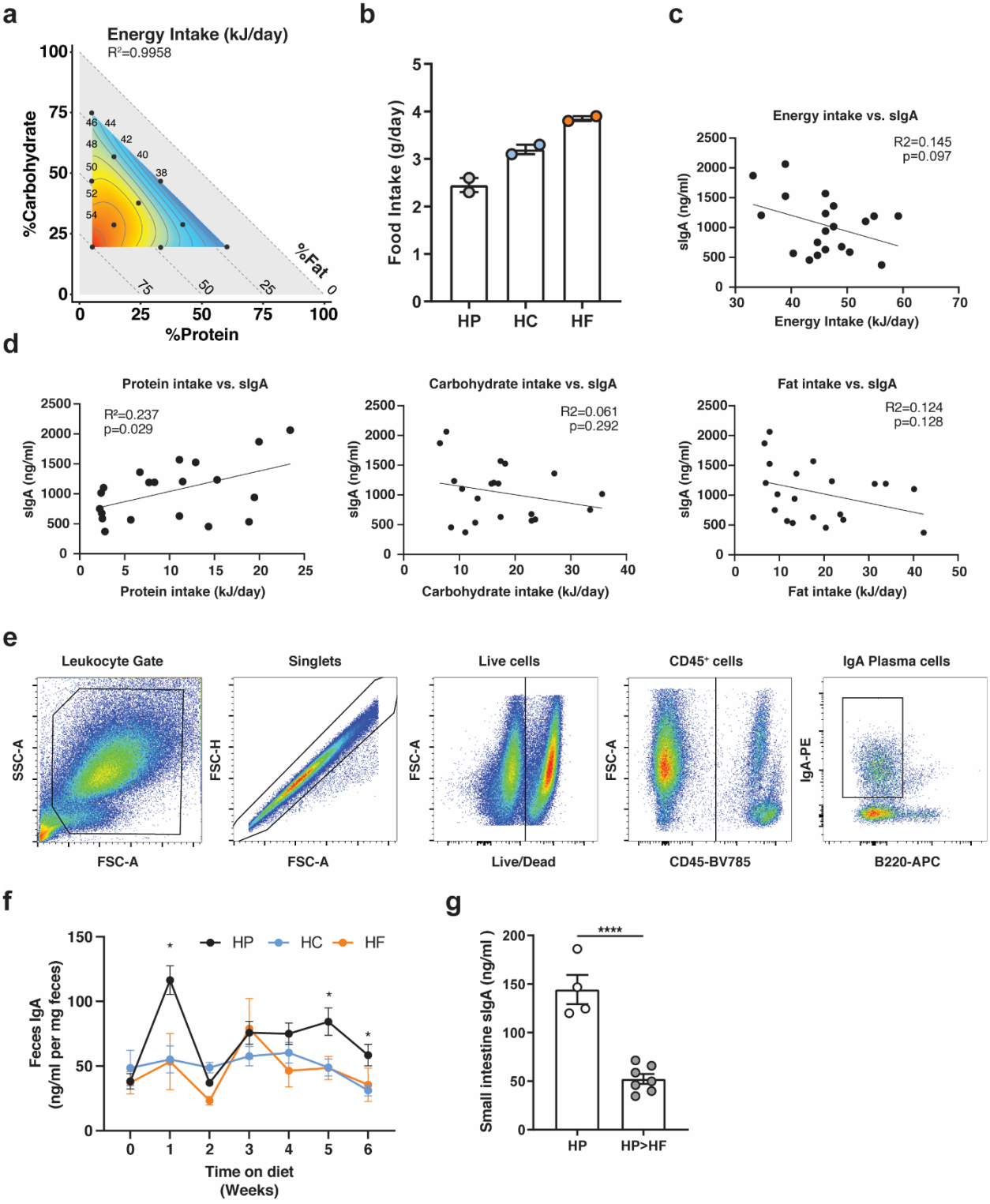

Supplementary Figure 1: Mice were fed on one of 10 diets encompassing a macronutrient range of 5-60% protein, 20-75% carbohydrate, and 20-75% fat for 6 weeks. (a) Contribution of macronutrient composition to average total daily energy intake (kJ/day) (averaged cage data) was modelled by Scheffé mixture model and represented on a right-angled mixture triangle. 3 component mixture model represented on a right-angled mixture triangle comprising of carbohydrate (y-axis), protein (x-axis) and fat (hypotenuse) with average total daily energy intake (kJ/day) as the response variable. Red represents higher average total daily energy intake while blue represents lower average total daily energy intake (kJ/day) in the nutrient mixture space. Each dot represents one of the 10 diets used for modelling response surface. (b) Average food intake (each point represents averaged cage data of n=4 mice per cage) of mice fed on a high-protein (HP), high-carbohydrate (HC) or high-fat (HF) diet. Linear regression of (c) total energy intake vs. sIgA levels as well as (d) protein, carbohydrate and fat eaten vs. sIgA levels were performed by simple linear regression analysis. (e) Gating strategy for the identification of $B220^{-}IgA^{+}$ IgA plasma cells by flow cytometry. (f) Mice were fed on a HP, HC or HF diet for 6 weeks and feces were collected weekly for determination of feces IgA by ELISA (n=6 mice per group for Week 0-2 and n=10 mice per group for Week 3-6). (g) Mice were fed on a HP diet for 6 weeks or fed on a HP diet for 6 weeks then switched to a HF diet for an additional 6 weeks and sIgA determined by ELISA (n=4 mice per group for HP and n=7 mice per group for HP>HF; $p = <0.0001$ by two-tailed unpaired t-test). Data are represented as mean ± SEM. Results represent n=3 independent (a-b), n=2 (c-e) and n=1 experiments (f-g).

Supplementary Figure 2

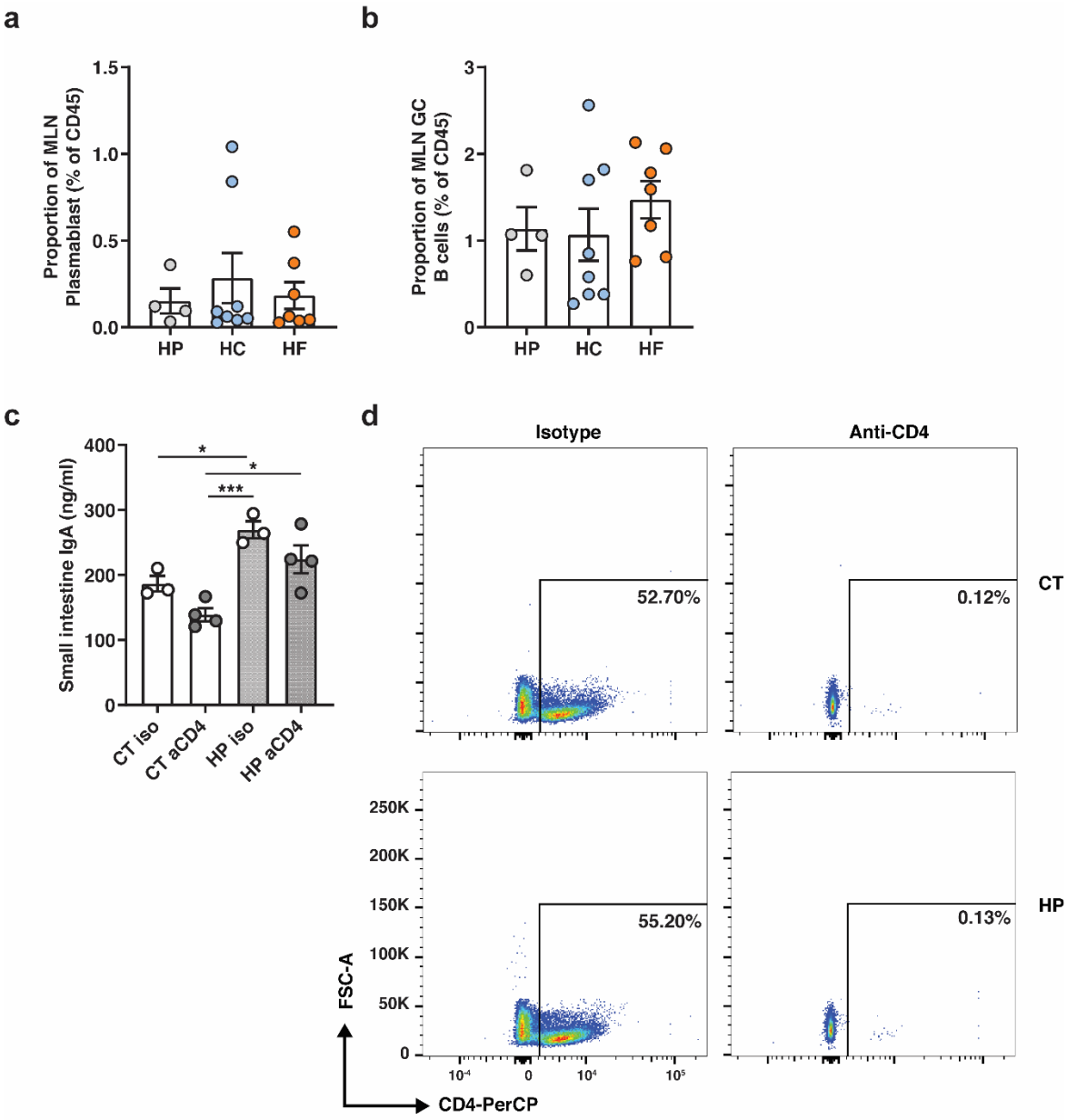

Supplementary Figure 2: (a) Proportion of B220^{+}IgA^{+} plasmablast and (b) CD95^{+}GL7^{+} germinal centre B cells in the mesenteric lymph nodes (n=4, n=7 and n=8 mice per diet for HP, HC and HF diet respectively) were determined by flow cytometry from mice fed on either a high-protein (HP), high-carbohydrate (HC) or high-fat (HF) diet for 6 weeks. (c) Mice were administered 200µg of anti-CD4 (GK1.5) or isotype control (LTF-2) antibody one day prior to either HP or control (AIN93G) diet feeding. Antibody treatment was administered twice weekly and small intestine sIgA determined 6 weeks later (n=3 mice per group for isotype control and n=4 mice per group for anti-CD4 treated groups; CT iso vs. HP iso p=0.0276, CT aCD4 vs HP iso p=0.0008, CT aCD4 vs. HP aCD4 p=0.01 by ordinary one-way ANOVA followed by Tukey's multiple comparisons test). Data are represented as mean ± SEM. (d) Representative flow cytometry plot demonstrating the successful systemic depletion of CD4^{+} lymphocytes by flow cytometry. Results represent n=2 independent (a-b) and n=1 independent experiment (c-d).

Supplementary Figure 3

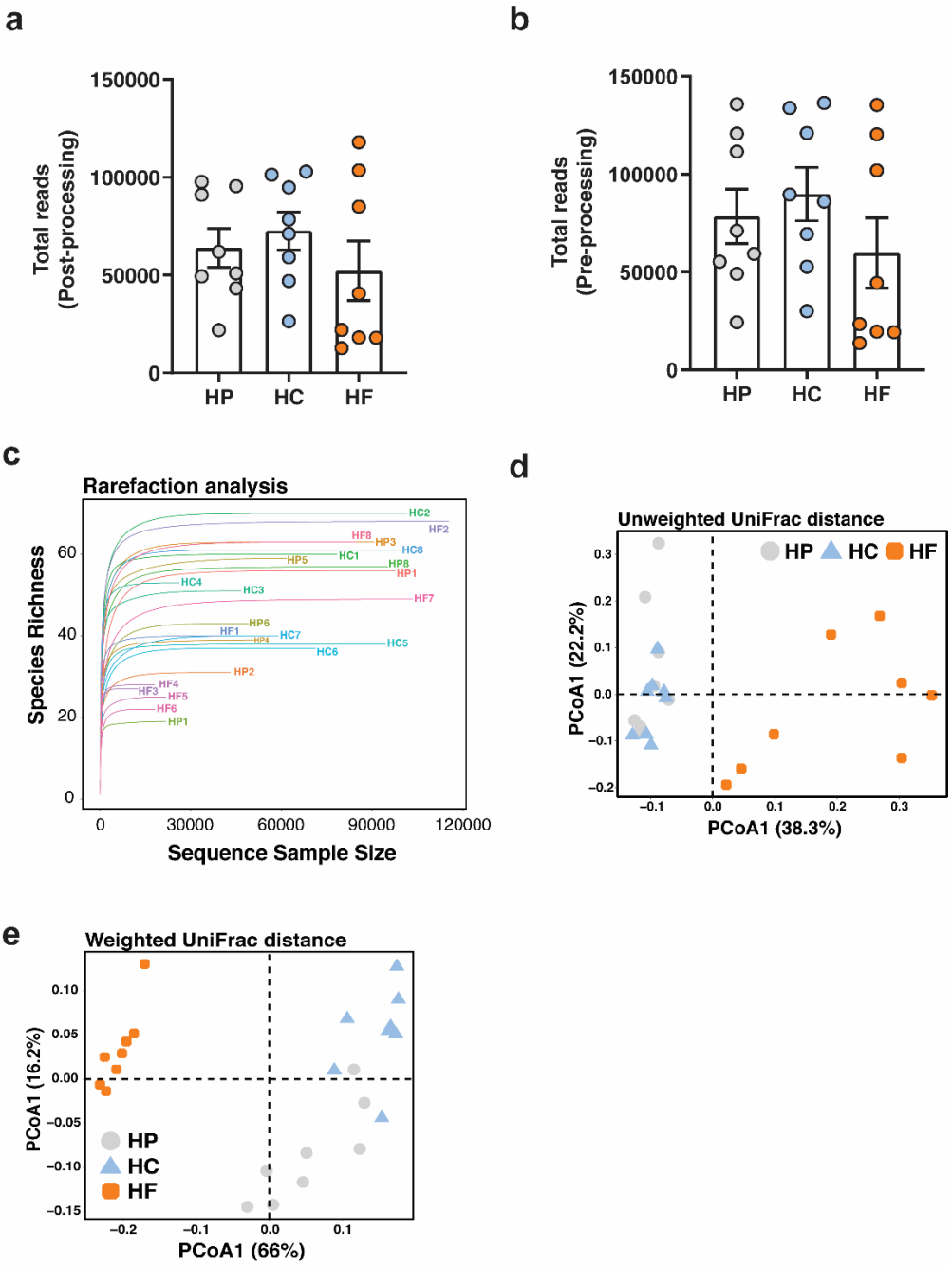

Supplementary Figure 3: DNA from luminal content was extracted for 16S rRNA DNA sequencing from mice fed on a high-protein (HP), high-carbohydrate (HC) or high-fat (HF) diet for 6 weeks (n=8 per group). The total number of reads per samples (a) post and (b) pre-processing were quantified and no statistical significance between groups were found (Kruskal-Wallis test). Data are represented as mean ± SEM. (c) Rarefaction analysis was performed for each sample demonstrating that sequencing depth was sufficient to uncover all unique taxa (ASV) present in each sample. (d-e) Differences in the structure of the small intestinal microbiota communities were determined by principal coordinate analysis (PCoA) of both (d) Unweighted and (e) Weighted UniFrac distances. Results represent n=1 independent experiment.

Supplementary Figure 4

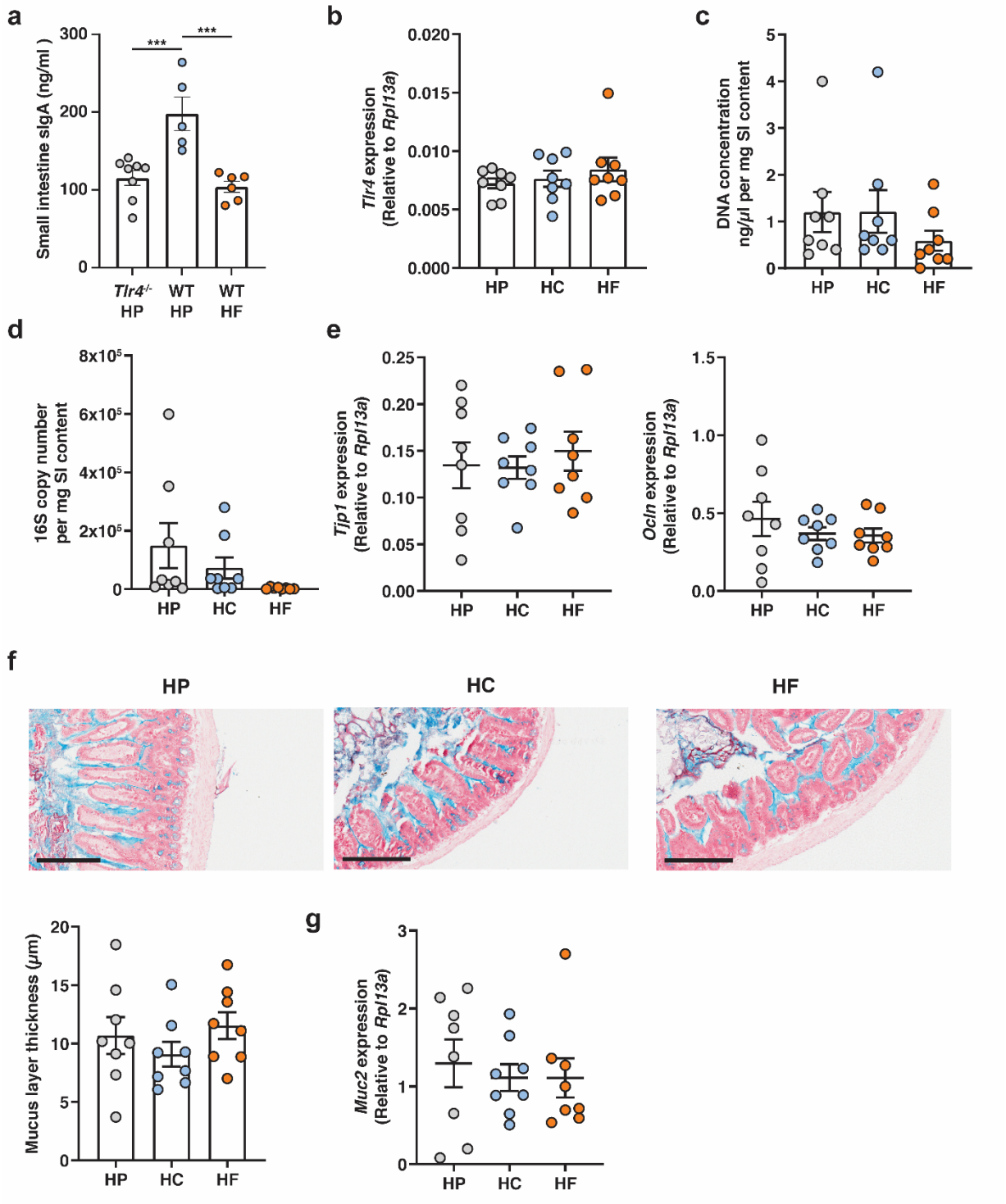

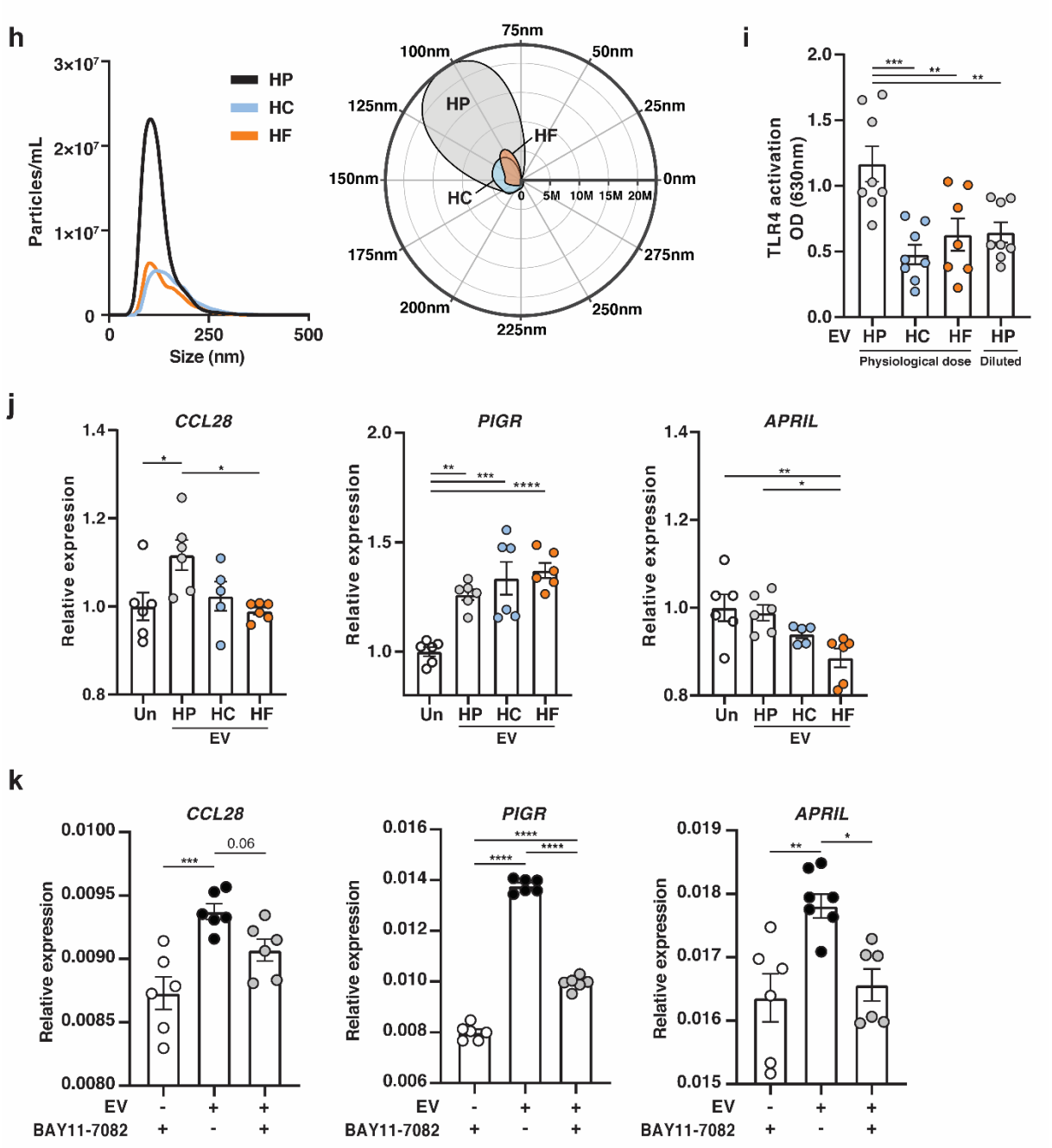

Supplementary Figure 4: (a) *Tlr4*$^{-/-}$ or wild type (WT) mice were fed on a high-protein (HP) diet, or WT mice fed on a high-fat (HF) diet for 6 weeks and sIgA levels were determined by ELISA (n=8, n=5 and n=6 mice per group for *Tlr4*$^{-/-}$ HP, WT HP and WT HF respectively; *Tlr4*$^{-/-}$ HP vs. WT HP p=0.008, WT HP vs. WT HF p=0.0004). Wild type mice were fed on either a high-protein (HP), high-carbohydrate (HC) or high-fat (HF) diet for 6 weeks and small intestine gene expression of (b) *Tlr4*, (e) *Tjp1* and *Ocln* and (g) *Muc2* was determined by qPCR (n=8 mice per group). Their small intestine contents were collected for DNA extraction and (c) DNA concentration was quantified by the Qubit™ dsDNA HS Assay Kit and (d) total 16S copy number by qPCR (n=8 mice per group). Wild type mice were fed on either a high-protein (HP), high-carbohydrate (HC) or high-fat (HF) diet for 6 weeks and (f) average mucus layer thickness was determined by histological analysis of Alcian blue-stained small intestine sections with the scale bar representing

100µm. (n=8 mice per group) (h) Cecum microbiota-derived extracellular vesicles (EV) were characterised by Nanoparticle Tracking Analysis (n=2 per diet pooled from n=4 mice each) and represented as an XY plot (left): 0-500nm vs. particle number/mL, or polar plot (right): angular axis represents particle size between 0-300nm and radial axis represents particle concentration in number/mL). (i) Cecum microbiota-derived EV were incubated at physiological ratio (approximately 3:1:1 of HP:HC:HF; n=8,n=8 and n=7 mice per group respectively), or at 1:1:1 ratio (HP diluted, n=8 mice per group) overnight with HEK-Blue TLR4 cell line and TLR activation measured at 630nm (HP vs. HC p=0.0004, HP vs. HF p=0.0072, HP vs. HP diluted p=0.007). (j) HT-29 were stimulated with cecum microbiota-derived EV isolated from HP ($3x10^9$ EV per well) or HC/HF ($1x10^9$ EV per well) fed animals for 16 hours and expression of CCL28 (Un vs. HP p=0.0372, HP vs. HF p=0.0213), PIGR (Un vs. HP p=0.0027, Un vs. HC p=0.0002, Un vs. HF p=<0.0001) and APRIL (Un vs. HF p=0.0067, HP vs. HF p=0.0156) were quantified by qPCR (n=6 wells per condition) and as well as (k) in the presence or absence of 10µM of NF-κB inhibitor BAY 11-7082, or with BAY 11-7082 alone and expression of CCL28 (-EV+Bay11-7082 vs. +EV-BAY11-7082 p=0.008), PIGR (-EV+Bay11-7082 vs. +EV-BAY11-7082 p=<0.0001, -EV+Bay11-7082 vs. +EV+Bay11-7082 p=<0.0001, +EV-BAY11-7082 vs. +EV+Bay11-7082 p=<0.0001) and APRIL (-EV+Bay11-7082 vs. +EV-BAY11-7082 p=0.0069, +EV-BAY11-7082 vs. +EV+BAY11-7082 p=0.0188) were quantified by qPCR (n=6 wells per condition). Data are represented as mean ± SEM. Results represent n=2 (b-e, g-k) and n=1 independent experiment(s) (a, f). *p<0.05, **<0.01, ***<0.001, ****<0.0001 by ordinary one-way ANOVA followed by Tukey's multiple comparisons test.

Supplementary Figure 5

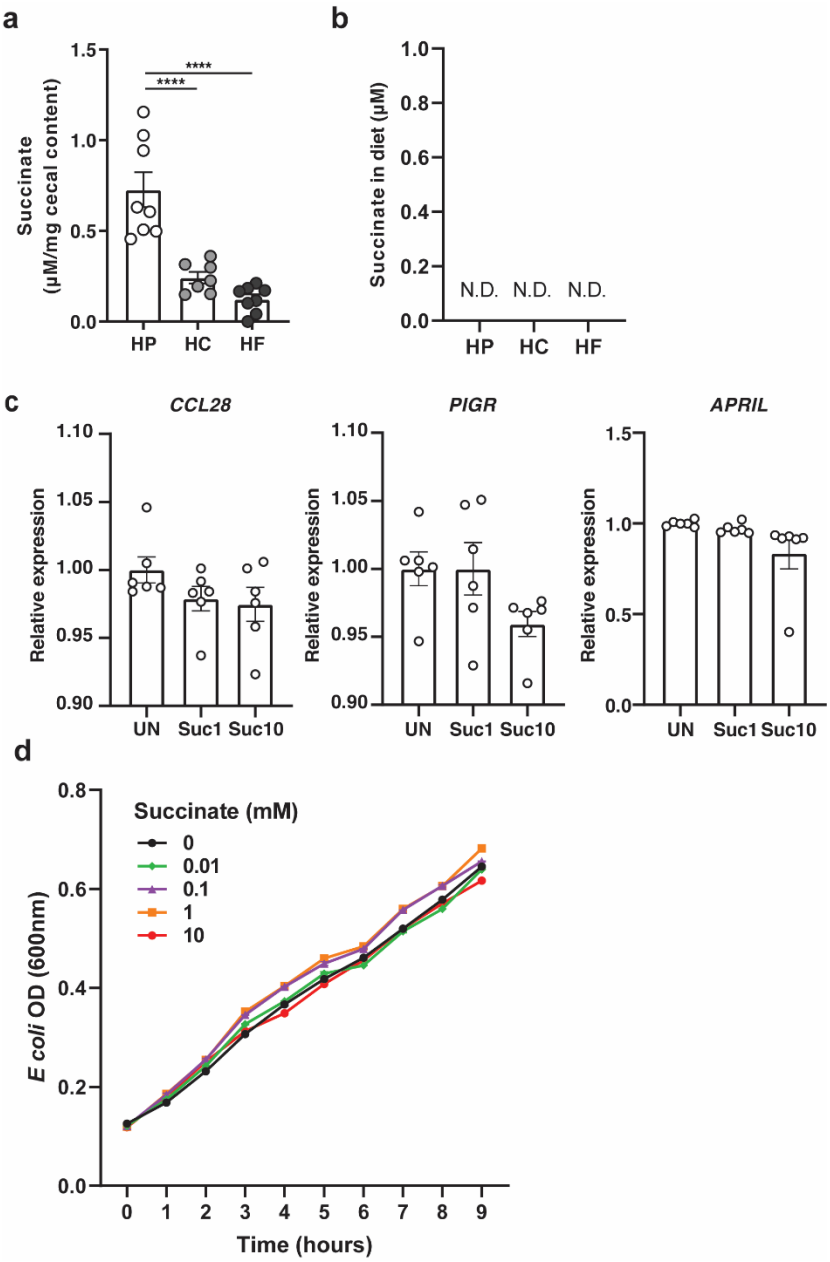

Supplementary Figure 5: (a) Levels of succinate in the cecum were quantified by NMR spectroscopy from mice fed on a high-protein (HP), high-carbohydrate (HC) or high-fat (HF) diet for 6 weeks (n=7 and n=8 mice per diet for HC and HP/HF diet respectively; HP vs. HC p=<0.0001, HP vs. HF p= p=<0.0001). (b) Levels of succinate in food pellet of the HP, HC or HF diet was quantified by NMR spectroscopy (n=2 pellet from each diet were analyzed to confirm undetectable levels of succinate). (c) HT29 were stimulated overnight with vehicle control (PBS), or 1mM or 10mM of succinate and gene expression levels of CCL28, PIGR and APRIL quantified by qPCR (n=6 wells per condition). (d) Growth of *E coli,* cultured with the indicated concentrations of succinate, was quantified by spectrophotometry (OD 600nm). Data are represented as mean ± SEM. Results represent n=2 (d) and n=1 independent experiments (a-c). ****p<0.0001 by ordinary one-way ANOVA followed by Tukey's multiple comparisons test.

Chapter 4 Gut microbiota-derived extracellular vesicles promote hepatic gluconeogenesis via the activation of hepatic circadian

This chapter is formatted as a manuscript that has been submitted for publication:
Tan J, **Taitz J**, Ni D, Potier-Villette C, Pulpitel T, Stanley D, Nanan R, Macia L. "Gut microbiota-derived extracellular vesicles promote hepatic gluconeogenesis via the activation of hepatic circadian", Since the thesis submission this has been published in Molecular Metabolism (doi:10.1016/j.molmet.2025.102180)

I optimised protocols for EV isolation and analysis, contributed to EV experiments, and generated and analysed the data presented in Figure 1A-E, G; Figure 2C, D; Figure 3E; and Supplementary Figure 1A, C, D. I performed animal experiment including dissections, tissue processing and sample staining and acquisition. I worked with co-authors on the study design and drafting and editing of the manuscript. All co-authors contributed to data interpretation and manuscript preparation.

This work in the context of this thesis:

As identified in **Chapter 3**, BEVs serve as key intermediaries in the gut microbiota's influence on host immunity. In this chapter, we investigate whether BEVs also regulate host metabolic health. Gut microbiota metabolites and membrane components have been found to influence glucose homeostasis and insulin sensitivity through various pathways. While BEVs from specific bacterial strains have been linked to metabolic disease, the role of the total gut BEV pool (referred to as microbiota EVs or MEVs from this chapter onwards) in regulating baseline host metabolism has not been explored. Host metabolic processes are partly regulated by circadian rhythms, and their disruption contributes to metabolic dysregulation. The gut microbiota also exhibits diurnal patterns of activity, yet these interact with host rhythms and how disturbances in this interplay affect host metabolism, remains poorly understood.

Using GF mice which are devoid of endogenous MEVs, we demonstrate that MEVs translocate from the intestines to systemic circulation and accumulate significantly in the liver. Intermittent MEV administration to GF mice (twice weekly for three weeks) upregulated hepatic gluconeogenesis, a key pathway in the maintenance of glucose homeostasis. In SPF mice, chronic daily MEV administration upregulated hepatic gluconeogenesis, and induced liver inflammation, mild insulin resistance and glucose intolerance. We identified that MEVs follow a diurnal pattern of production aligning with host glucose demands, driven by host feeding patterns and peaking during fasting. MEVs regulate hepatic gluconeogenesis by modulating the hepatic circadian clock pathway, increasing the expression of clock-controlled genes. This suggests that MEVs function as an environmental cue for the host to fine-tune glucose production, supporting glucose homeostasis during periods of increased energy demand.

Overall, this chapter reveals a novel role for MEVs in host metabolic regulation and highlights a synchrony between microbial and host metabolic rhythms. Furthermore, our findings suggest that disruptions in MEV production (driven by diet, feeding patterns, or antibiotics) may represent a potential mechanism linking the gut microbiota to glucose-associated metabolic disorders, such as type 2 diabetes and obesity.

Gut microbiota-derived extracellular vesicles promote hepatic gluconeogenesis via the activation of hepatic circadian

Authors

Jian K. Tan,[1,2] **Jemma J. Taitz,**[1,2] Duan Ni,[1,2,3] Camille Potier-Villette,[1,2] Tamara Pulpitel,[1,4] Dragana Stanley,[5] Ralph Nanan,[1,3] Laurence Macia[1,2]

Affiliations

[1]Charles Perkins Centre, The University of Sydney, Sydney, NSW, Australia.

[2]School of Medical Sciences, Faculty of Medicine and Health, The University of Sydney, Sydney, NSW, Australia.

[3]Sydney Medical School Nepean, The University of Sydney, Sydney, NSW, Australia.

[4]School of Life and Environmental Sciences, Faculty of Medicine and Health, The University of Sydney, Sydney, NSW, Australia.

[5]School of Health, Medical and Applied Science, Central Queensland University, Rockhampton, QLD, Australia.

Abstract

The circadian clock regulates tissue-specific homeostasis, and its disruption is associated with metabolic disorders. Both host metabolic processes and the gut microbiota exhibit diurnal regulation, and both contribute to the maintenance of glucose homeostasis. However, how the gut microbiota and circadian rhythm interplay to control host glucose homeostasis is poorly understood. We identified gut microbiota-derived extracellular vesicles (MEVs) as a peripheral Zeitgeber (time cue) for hepatic circadian, controlling hepatic gluconeogenesis. Host feeding patterns influence the gut microbiota, driving the diurnal production of MEVs. MEVs directly activate hepatic gluconeogenesis and elevated MEV exposure impairs glucose homeostasis *in vivo*. Our findings reveal a novel

mechanism by which the gut microbiota supports host glucose needs during periods of energy demand, such as fasting. On the contrary, an abnormal increase in MEV production, leading to dysregulated gluconeogenesis, may underlie glucose-associated disorders like type 2 or gestational diabetes. Together, our data reconciles the gut microbiota and circadian rhythm in the control of host glucose homeostasis and metabolic health.

4.1 Introduction

Glucose is a major energy source critical for the optimal function and survival of most cellular organisms. However, the availability of glucose fluctuates constantly, influenced by factors like nutrient availability and the organism's feeding state. Gluconeogenesis is a critical metabolic process evolved to maintain euglycemia during periods of low glucose availability. In mammals, it occurs predominantly in the liver and is activated in response to low blood glucose levels, such as during fasting. This process is hormonally regulated and is primarily stimulated by cortisol and glucagon produced by the adrenal glands and the pancreas, respectively. The secretion of these hormones is also regulated by circadian rhythm (Petrenko et al., 2017), anticipatory to the rhythmic transition between feeding and fasting states. Indeed, gluconeogenic genes like phosphoenolpyruvate carboxykinase (PEPCK) and glucose-6-phosphatase (G6P) exhibit diurnal regulation, aligning with the activity of the master transcription factors CLOCK and BMAL1 (Rudic et al., 2004), which govern the mammalian circadian clock. Recent evidence has highlighted a role for the gut microbiota in regulating host metabolism and metabolic health (Fan and Pedersen, 2021). Notably, the absence of a gut microbiota led to lower blood glucose levels under both fed and fasted states (Krisko et al., 2020), while microbial-derived metabolites like

butyrate can directly stimulate hepatic gluconeogenesis (Ji et al., 2019). Dysregulation of blood glucose levels is associated with metabolic disorders like type 2 diabetes (Galicia-Garcia et al., 2020) and gestational diabetes (Choudhury and Devi Rajeswari, 2021). Modern lifestyle factors are linked to detrimental shifts in gut microbiota composition and their function (Tan et al., 2023a; Tan et al., 2023b). This underscores the importance of understanding how gut microbes can influence host glucose homeostasis, and ultimately, metabolic health. Furthermore, despite the well-established consequence of circadian disruption to the development of metabolic disorders, little is known about how the gut microbiota regulates peripheral clocks (Kishman et al., 2024; Schrader et al., 2024; Shimizu et al., 2016). So far, microbial factors identified to influence gluconeogenesis act indirectly by optimising intracellular hepatic metabolism (Krisko et al., 2020), or directly by acting as substrates for gluconeogenesis (Ji et al., 2019). While many of these pathways are rhythmically regulated due to host dietary behaviours, they do not directly affect circadian *per se*, with no reported effects on the mammalian clock system. Emerging evidence indicates that gut microbiota-derived extracellular vesicles (MEVs) play a significant role in the host-gut microbiota axis (Macia et al., 2019; Taitz et al., 2023; Liang et al., 2022). MEVs are nanosized membrane structures produced primarily from the budding of the plasma membrane and can carry a wide range of products including DNA, protein, and lipids. There is evidence that bacterial-derived extracellular vesicles (EV) can influence host metabolic outcomes. For example, orally administered *Pseudomonas panacis*-derived EVs induce insulin resistance and impairs glucose metabolism in skeletal muscles (Choi et al., 2015) while *Akkermansia muciniphila* EVs improved the metabolic profile of high-fat induced diabetic mice (Chelakkot et al., 2018). It is unclear what role EVs produced by resident gut microbiota play on host gluconeogenesis and hence glucose homeostasis.

4.2 Materials and Methods

4.2.1 Animals

Male C57BL/6 mice (6-8 weeks of age) were purchased commercially from Animal BioResources and housed at the Charles Perkins Centre animal facility. Animals were maintained under specific-pathogen-free (SPF) conditions, with a standard 12hour light-dark cycle, at 25°C and 50% humidity. Animals were fed ad libitum on AIN93G control diet, with free access to drinking water. Germ-free (GF) animals were purchased commercially from the Walter and Eliza Hall Institute of Medical Research and were housed at the Charles Perkins Centre germ-free animal facility. The administration of MEV were performed in the late afternoon, and faeces and caecal content were collected in the morning, unless otherwise stated. All animal experiments were performed under protocols approved by the University of Sydney Animal Ethics Committee (AEC).

4.2.2 Extracellular vesicle isolation

For the isolation of microbiota extracellular vesicles, caecum content or faecal pellets were homogenised in 0.02μm filtered PBS and EVs isolated by differential centrifugation, as described previously with slight modifications (Tan et al., 2022). Briefly, the homogenates or bacterial culture broth were centrifuged at 10,000xg for 20min at 4°C followed by 18,000xg for 45min at 4°C, before filtration through a 0.22μm filter and centrifuged at 100,000xg for 2hr at 4°C. The EV pellet was resuspended in 0.02μm filtered PBS. EV particle size and concentration were assessed by Nanoparticle Tracking Analysis using the Particle Metrix Zetaview and analysed with the Zetaview software (8.05.16 SP3) or the Nanosight NS300 (Malvern Instruments Limited) and analysed with the NTA 3.2 software.

4.2.3 RNA sequencing and data analysis

Total RNA was extracted from snap-frozen liver tissues using TRI Reagent (Sigma Aldrich) following the manufacturer's instructions, and RNA was purified using the RNeasy MinElute Cleanup Kit (Qiagen). Library preparation and Illumina HiSeq sequencing was done commercially (Azenta Life Sciences, previously Genewiz). Raw data had an average of 22232315 reads per sample with 94.02% of reads with quality of Q30 or above. Sequences were aligned to the GRCm38 mouse reference genome using STAR v2.7.3a with two-pass mapping (Dobin et al., 2013). Gene count was quantified using HTSeq and genes with less than 20 counts across all samples were filtered out prior to analysis. DESeq2 (1.42.0) was used for differential expression analysis (Love et al., 2014) using R software (4.3.1). DESeq2 normalized counts and statistical outputs were used for downstream pathway analysis using Gene Set Enrichment Analysis (Subramanian et al., 2005) and Ingenuity Pathway Analysis (Qiagen).

4.2.4 Quantitative PCR

Total RNA was extracted using TRI Reagent (Sigma Aldrich) following the manufacturer's instructions and cDNA generated using the High-Capacity cDNA Reverse Transcription Kit (ThermoFisher Scientific). qPCR was conducted using the Power SYBR™ Green PCR Master Mix (ThermoFisher Scientific) on a LightCycler® 480 Instrument II (Roche Life Science) and LightCycler® 480 v1.5.0 software. A list of primers used and their sequences are provided in Table S4.1.

4.2.5 Cell culture

HEPG2 cells were cultured in DMEM supplemented with 10% FBS, 10mM HEPES, 2mM L-glutamine, 1mM sodium pyruvate, 100units/ml penicillin and 100µg/ml streptomycin. For experiments, HEPG2 cells were seeded into 6-well plate and grown until ~80% confluence. For siRNA experiments, knockdown of CLOCK was performed using Silencer pre-designed siRNA (GGAACAAUAGACCCAAAGGtt and CCUUUGGGUCUAUUGUUCCtc) from Ambion (Life technologies) with Lipofectamine RNAiMAX (ThermoFisher) via reverse transfection, and experiments performed 48 hours later. C57BL/6 mouse primary hepatocytes were isolated as previously described (Son et al., 2023). Briefly, liver was perfused with 25ml of HBSS containing 5mM calcium chloride and 0.05% collagenase IV maintained at 37°C, and then hepatocytes teased out by gentle shaking on a petri dish. Hepatocytes were then centrifuged at 50xg for 30min at 22°C, then resuspended in 37.5% Percoll solution and centrifuged for 500xg for 15min at 22°C with minimal brake. RBC lysis was then performed, and hepatocytes resuspended in DMEM/F12 supplemented with 10% FBS, 5mM HEPES, 2mM L-glutamine, 2mM sodium pyruvate, 1µM dexamethasone, 100units/ml penicillin and 100µg/ml streptomycin, and allowed to rest for 4 hours on collagen coated plates (5µg/cm^2) before media removed and cell resuspended in fresh media without FBS and dexamethasone for experiments.

4.2.6 Metabolic assessments

For glucose tolerance test, mice were fasted for 6 hours and then given an oral bolus of glucose at a dose of 2g/kg body weight. For insulin tolerance test, mice were fasted for 4 hours, then 0.5 U/kg insulin was given by intraperitoneal injection. For pyruvate tolerance test, mice were fasted overnight, then given sodium pyruvate at a dose of

2.5g/kg body weight. Blood glucose level was measured using a glucometer (AccuChek Advantage).

4.2.7 Bacterial cell culture

Frozen glycerol scraping of *Enterococcus faecalis* (NCTC 775) was first inoculated in Brain Heart Infusion (BHI) broth and allowed to rest overnight, 37°C shaking 200rpm. The culture was then diluted to OD0.1 in BHI broth and grown for 18 or 24 hours as indicated. *Escherichia coli* (K-12 MG1655) was grown in Luria-Bertani (LB) broth instead. For some experiments, *E. faecalis* was grown in BHI broth diluted with salt solution (4.5g/L NaCl and 2.5g/L sodium phosphate dibasic).

4.2.8 Western blots

Samples were lysed by probe sonication (15sec) in RIPA buffer supplemented with protease (Roche Mini Protease Inhibitor Cocktail) and phosphatase (Roche PhosSTOP) inhibitors before centrifuging (4°C, 10min, 16,000xg). Protein concentration was quantified with bicinchoninic acid (BCA) assay (Sigma-Aldrich). Lysates were prepared for polyacrylamide gel electrophoresis under reduced conditions. Proteins were resolved by western blot using 4-12% Bis-Tris gels (BioRAD) and transferred to a nitrocellulose membrane (BioRAD). After blocking with 5% BSA in TBST, protein expression was detected using specific primary antibodies by incubating overnight at 4°C (Cell Signalling Technology: phospho-AKT #4058; AKT #4685; β-actin #4970). All antibodies were detected using secondary rabbit IgG-horse radish peroxidase (Cell Signalling Technology #7074) and visualized by enhanced chemiluminescence using the Pierce ECL Western Blotting Substrate (Thermo Fisher Scientific).

4.2.9 Statistical analysis

For comparison of two independent groups, the Mann-Whitney tests were used. For comparison of three or more groups, a one-way ANOVA with Tukey's multiple comparison test was used. For comparison of differences among group means over time, two-way ANOVA was used. For comparison of paired samples, non-parametric paired t-test was used. Mixture modelling was performed as previously reported (Tan et al., 2022, 2021). P value <0.05 were considered statistically significant with *p<0.05; **p<0.01; ***p<0.005; ****p<0.001.

4.3 Results

4.3.1 Gut microbiota-derived extracellular vesicles directly activate hepatic gluconeogenesis

To elucidate the potential role of MEVs in host glucose homeostasis, we first determined whether MEVs produced by gut bacteria can cross the intestinal barrier and translocate systemically. Germ-free (GF) mice were orally administered fluorescently-tagged MEV (**Figure S4.1A-B**) derived from caecal content of specific-pathogen-free (SPF) mice and translocation was tracked by *ex vivo* tissue imaging 12 hours later. We found that MEVs predominantly concentrated in the liver (**Figure 4.1A**), and to a lesser extent in the kidneys (**Figure S4.1C**). To understand the impact of MEVs on the liver, we administered MEVs to GF mice orally twice weekly for 3 weeks and performed transcriptomic analysis on the liver (**Figure 4.1B**). Genes related to gluconeogenesis including *Pck1*, *G6pc*, *Foxo1* and *Ppargc1a* were differentially upregulated in MEV-treated animals, compared to PBS-treated animals (**Figure 4.1C**). This was confirmed by pathway enrichment analysis, with the FOXO-mediated transcription pathway significantly enriched (**Figure 4.1D**). FOXO1

is a key transcription factor that induces the expression of the key gluconeogenic enzymes PEPCK and G6P. Indeed, the gluconeogenesis pathway was also enriched in MEV-treated mice (**Figure 4.1D**), corresponding to higher *Pck1* and *G6pc* expression (**Figure S4.1D**). Differentially expressed genes are provided (**Table S4.2**, Excel attachment). To validate this phenotype, we orally administered $1x10^{10}$ MEV to SPF mice daily for 5 weeks, and then quantified liver gene expression of *Pck1* and *G6pc*. Compared to PBS-treated animals, MEV-treated mice had increased liver expression of both *Pck1* and *G6pc* (**Figure 4.1E**). We further verified that MEVs induced hepatic gluconeogenesis, upregulating the expression of genes encoding for PEPCK and G6P, under both *ex vivo* conditions with mouse primary hepatocytes (**Figure 4.1F**), and under *in vitro* conditions with the human hepatocyte cell line HEPG2 (**Figure 4.1G**). These results indicate that MEVs act directly on hepatocytes to induce gluconeogenesis. We also found that the effect of MEVs on the expression of gluconeogenic genes in HEPG2 cells occurred in a dose-dependent manner (**Figure S4.1E**). Finally, to determine the physiological significance of MEVs on the host, SPF mice were administered PBS or MEVs for 5 weeks, as described above. Pyruvate tolerance test was then performed, a gold standard method to assess the conversion of exogenous pyruvate to glucose *in vivo*, as a readout of gluconeogenesis. Indeed, MEV-treated mice had higher blood glucose levels following fasting and administration of the gluconeogenic substrate pyruvate (**Figure 4.1H**). Together, these results demonstrate that MEV exposure increases liver gluconeogenesis both *in vivo* and *in vitro*, and that MEV act directly on hepatocytes to induce gluconeogenesis.

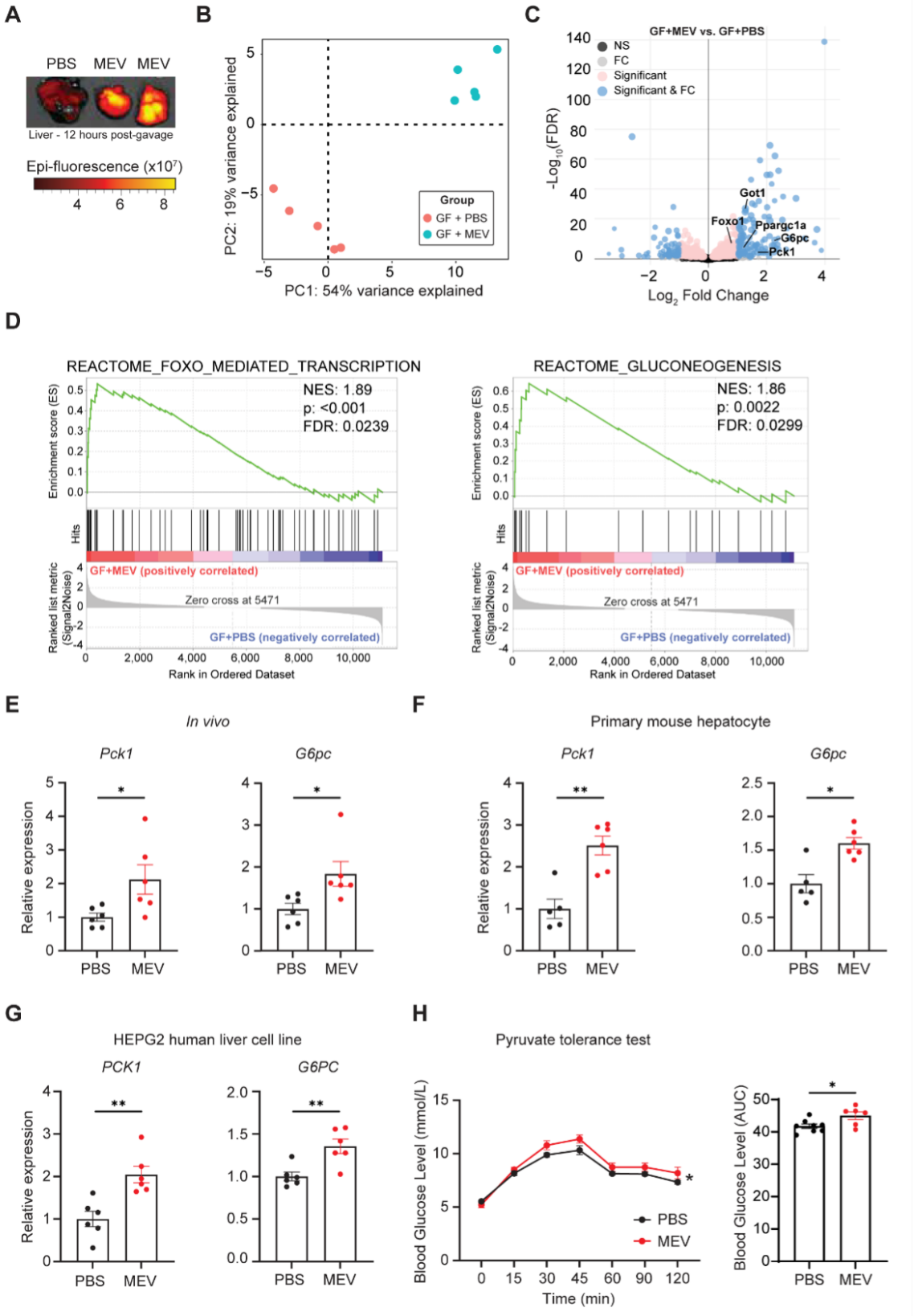
A
PBS MEV MEV
Liver - 12 hours post-gavage
Epi-fluorescence (x10⁷)
4 6 8
B
PC2: 19% variance explained
PC1: 54% variance explained
Group
GF + PBS
GF + MEV
C
GF+MEV vs. GF+PBS
NS
FC
Significant
Significant & FC
-Log10(FDR)
Log2 Fold Change
Got1
Foxo1
Ppargc1a
G6pc
Pck1
D
REACTOME_FOXO_MEDIATED_TRANSCRIPTION
NES: 1.89
p: <0.001
FDR: 0.0239
REACTOME_GLUCONEOGENESIS
NES: 1.86
p: 0.0022
FDR: 0.0299
Enrichment score (ES)
Hits
Ranked list metric (Signal2Noise)
GF+MEV (positively correlated)
Zero cross at 5471
GF+PBS (negatively correlated)
Rank in Ordered Dataset
E
In vivo
Pck1
G6pc
Relative expression
PBS MEV
F
Primary mouse hepatocyte
Pck1
G6pc
Relative expression
PBS MEV
G
HEPG2 human liver cell line
PCK1
G6PC
Relative expression
PBS MEV
H
Pyruvate tolerance test
Blood Glucose Level (mmol/L)
Time (min)
PBS
MEV
Blood Glucose Level (AUC)
PBS MEV

Figure 4.1 Gut microbiota-derived extracellular vesicles induce hepatic gluconeogenesis *in vivo* and *in vitro*

(**A**) Germ-free animals were orally administered 80µg of DiD-labelled microbiota-derived extracellular vesicles (MEV) (n=2) or PBS as control (n=1). 12 hours later, liver tissue was collected and fluorescence quantified *ex vivo* using the IVIS (in vivo imaging system). Fluorescence represented as Epi-fluorescence. (**B**) Germ-free animals were orally administered 80µg MEVs in PBS (GF+MEV), or PBS alone (GF+PBS), twice-weekly for 3 weeks. Whole liver was then collected and RNAseq performed and differences in individual transcriptome represented on a principal component analysis (PCA) plot (n=5 per group). (**C**) Volcano plot illustrating differentially down- and up-regulated genes in GF+MEV vs. GF+PBS mice. (**D**) Enrichment plot for GSEA Reactome pathway analysis of liver RNA transcriptome data, with significant enrichment in pathway associated with 'FOXO mediated transcription' and 'Gluconeogenesis' in GF+MEV livers (**E**) Specific-pathogen free (SPF) mice were administered $1x10^{10}$ MEVs (MEV), or PBS as control (PBS) daily for 5 weeks, and liver gene expression of Pck1 and G6pc quantified by qPCR (n=6 per group). (**F**) Primary hepatocyte cells isolated from control C57BL/6 male mice were cultured for 18 hours in the absence (PBS) or presence of $3x10^{9}$ MEVs (MEV), and gene expression level of Pck1 and G6pc quantified by qPCR (n=5 PBS, n=6 MEV). (**G**) HEPG2 human hepatocyte cell line was cultured for 18 hours in the absence (PBS) or presence of $3x10^{9}$ MEVs (MEV), and gene expression level of PCK1 and G6PC quantified by qPCR (n=6 per condition). (**H**) SPF mice were administered $1x10^{10}$ MEVs (MEV), or PBS as control (PBS) daily for 5 weeks, and then pyruvate tolerance test performed, with blood glucose level measured over 2 hours following intraperitoneal injection of pyruvate at a dose of 2.5g/kg body weight following overnight fasting (n=8 PBS and n=6 MEV). Results represent n=5 independent experiments (**G**), n=2 independent experiments (**A, E-F**) and n=1 independent experiment (**B-D, H**). All data are presented as mean±SEM. *$p < 0.05$ and **$p<0.01$ by Mann-Whitney test. For PTT experiment, overall difference was determined by two-way ANOVA.

4.3.2 Gut microbiota-derived extracellular vesicles promote hepatic inflammation and metabolic syndrome

Next, we sought to determine how increased exposure to MEVs affects host metabolic health. Treatment with MEVs for 5 weeks did not alter food intake (**Figure S4.2A**), nor affect body weight gain (**Figure 4.2A**). MEV treatment did not affect inguinal white adipose tissue (WATi) weight but increased epididymal white adipose tissue (WATe) weight (**Figure S4.2B**). Notably, it significantly increased liver weight (**Figure 4.2B**), a change often associated with inflammation (Wang et al., 2023). As liver weight and hepatocyte size fluctuate diurnally with variation in lipid, glycogen, protein and RNA storage and synthesis (Weger et al., 2022), this may also reflect alterations in the circadian-regulation of these hepatic processes. This was confirmed by Ingenuity pathway analysis of our transcriptomic data (**Figure 4.2C**), revealing enrichment of pro-inflammatory pathways relating to IL-6 and acute phase response signalling, as well as HMGB1 signalling pathways. Genes common to these pathways like *Jun*, *Cebpb* and *Tnfrsf1b* are generally considered pro-inflammatory and were significantly upregulated in MEV treated animals (**Figure 4.2D**). Excessive gluconeogenesis is a feature of obesity, and chronic low-grade inflammation is a feature of metabolic syndrome. To determine the physiological implications of increased hepatic gluconeogenesis and hepatic inflammatory state, we tested the impacts of MEVs on glucose metabolism. We performed glucose tolerance and insulin tolerance tests on mice treated with PBS or MEVs for 5 weeks, which revealed that MEV administration induced mild but significant insulin resistance (**Figure 4.2E**) and glucose intolerance (**Figure 4.2F**). Indeed, mouse primary hepatocytes that were pre-treated overnight with MEVs had decreased Akt phosphorylation following stimulation with insulin, highlighting that MEVs can directly induce insulin resistance (**Figure 4.2G**). Altogether, these results demonstrate that

increased MEV exposure can lead to a mild but significant disruption to metabolic health, by promoting glucose intolerance and insulin resistance.

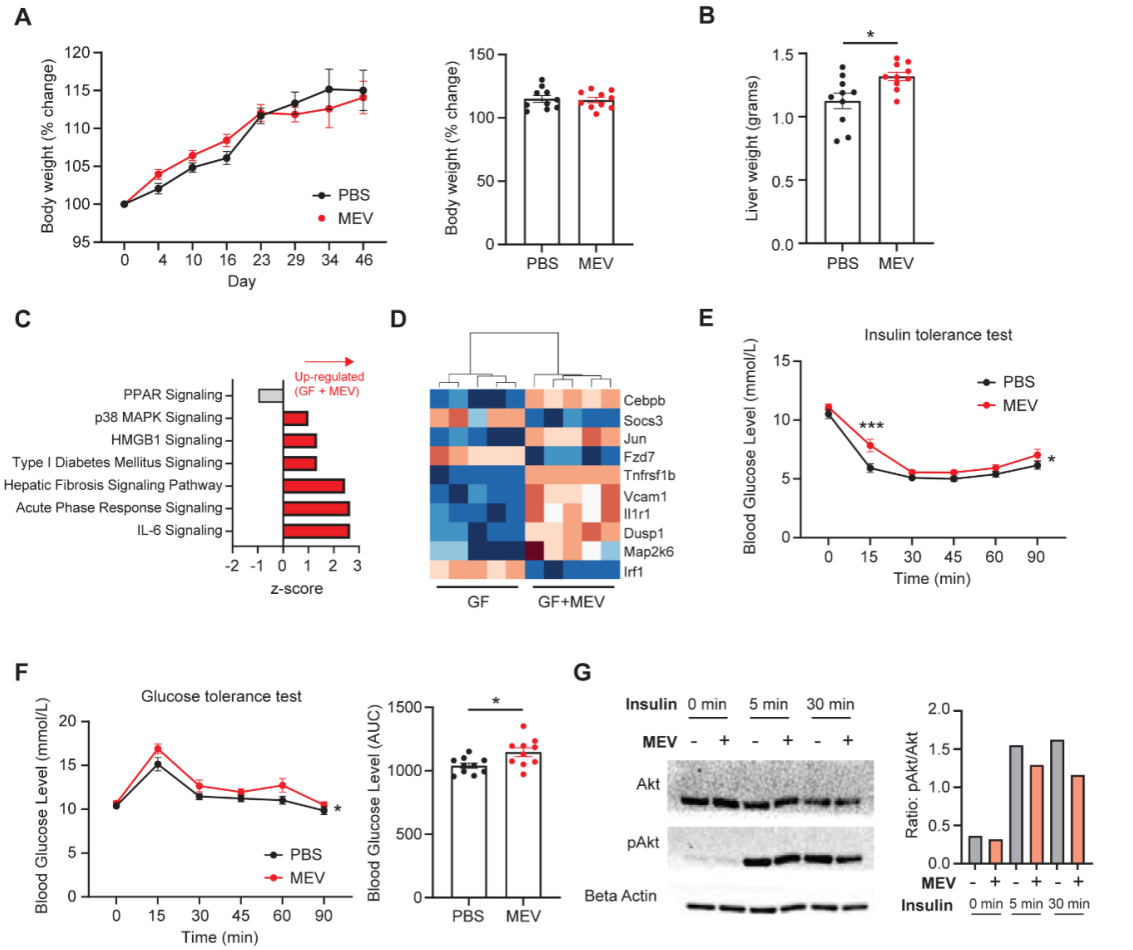

Figure 4.2 Gut microbiota-derived extracellular vesicles promote low-grade hepatic inflammation and insulin resistance

(**A**) SPF mice were administered 1x10^{10} MEVs (MEV), or PBS as control (PBS) daily for 5 weeks. Graph represents % body weight change over the 5 week period (left) and scatter plot showing the percentage change at endpoint (right) (n=10 mice per group). (**B**) Scatter plot showing whole liver weight following 5 weeks oral administration of MEV or PBS (n=10 mice per group). (**C**) Germ-free animals were orally administered 80µg MEV in PBS (GF+MEV), or PBS alone (GF+PBS), twice-weekly for 3 weeks. Whole liver was then collected and RNAseq performed, and Qiagen Ingenuity pathway analysis performed, with (**D**) heatmap with key genes involved in the pathways shown. (n=5 per group). (**E**) SPF mice were administered 1x10^{10} MEVs (MEV), or PBS as control (PBS) daily for 5 weeks, and then oral glucose tolerance test performed, with blood glucose level measured to 90min following oral administration of glucose at a dose of 2g/kg body weight following 6 hours of fasting (n=10 mice per group). (**F**) SPF mice were administered 1x10^{10} MEV (MEV), or PBS as control (PBS) daily for 5 weeks, and then insulin tolerance test performed, with blood glucose level measured to 90min following intraperitoneal administration of insulin at a dose of 0.5U/kg body weight following 4 hours of fasting (n=10 mice per group). (**G**) Primary hepatocytes isolated from control C57BL/6 male mice were cultured for 18 hours in the absence (PBS) or presence of 3x10^{9} MEVs (MEV), and then stimulated with 10nM insulin for 0, 5 or 30min and protein levels of Akt and p-Akt quantified by Western blot (each condition pooled from n=3 replicates of n=1 mice). Results represent n=3 independent experiments (**A**), n=2 independent experiments (**B, G**) and n=1 independent experiment (**C-F**). All data are presented as mean±SEM. *p < 0.05 by Mann-Whitney test. For oral glucose tolerance test and insulin tolerance test experiments, overall difference was determined by two-way ANOVA.

4.3.3 Host feeding patterns control the diurnal production of MEV to activate hepatic circadian and gluconeogenesis

MEVs can promote hepatic gluconeogenesis via numerous pathways. We previously found that MEV modulated host immunity through the activation of toll-like receptors (TLRs), such as TLR4, via lipopolysaccharide (LPS) present on the MEV surface (Tan et al., 2022). LPS has also been shown to promote hepatic gluconeogenesis via the activation of the transcriptional regulator P300 (He et al., 2013; Cao et al., 2017). To test whether LPS-mediated signalling was involved, we found that MEV were still able to upregulate *PCK1* and *G6PC* expression in the presence of the NF-κB inhibitor BAY11-7082 (**Figure S4.3A**), and the P300 inhibitor C646 (**Figure S4.3B**), suggesting that these signalling pathways may not be required for MEV-induced hepatic gluconeogenesis.

Supporting this, EVs derived from both *Escherichia coli* (Gram-negative, enriched in LPS) and *Enterococcus faecalis* (Gram-positive, lacking LPS) could induce *PCK1* and/or *G6PC* expression in the HEPG2 cell line (**Figure 4.3A**), suggesting that MEV-associated LPS was not involved in the induction of hepatic gluconeogenesis.

MEV-induced gluconeogenesis also appeared to be independent of JNK signalling, a key mediator of hepatic proinflammatory pathways in response to a range of stimuli (**Figure S4.3C**). Using a range of inhibitors, we also tested other pathways known to induce gluconeogenesis, including reactive oxygen species activation (**Figure S4.3D-F**) and the enzyme SIRT1 (**Figure S4.3G**). MEVs continued to upregulate *PCK1* and *G6PC* despite the presence of these inhibitors, suggesting these pathways are not essential for MEV-induced gluconeogenic activity, though inhibitor efficacy was not directly assessed in this system.

We hypothesised that MEVs may control hepatic gluconeogenesis by regulating the circadian clock, given the rhythmic expression of *PEPCK* and *G6P* observed in hepatocytes (Rudic et al., 2004). This hypothesis was supported by several observations. Firstly, we found that the quantities of MEVs produced by the gut microbiota (particles per mL of faecal homogenate) correlated with the reported diurnal expression pattern of *PEPCK* and *G6P* in the liver (**Figure 4.3B**). Notably, MEV concentration was lowest during the feeding phase (dark phase of light-dark cycle, Zeitgeber time 12), when host cellular glucose demand is lowest, whereas it was highest during the fasting phase (light phase of light-dark cycle, Zeitgeber time 0), when glucose demand is at its peak. This demonstrates that MEV are produced in a diurnal pattern, and this directly aligns with host cellular glucose requirements. To further demonstrate the relationship between host nutritional status and MEV production, we subjected mice to starvation via overnight fasting. Starvation was linked to a dramatic increase in MEV concentrations in the gut, with approximately 3 times more MEV produced by the gut microbiota following overnight fasting, compared to *ad libitum* fed animals (**Figure 4.3C**). Next, to directly test the relationship between nutrient availability and bacterial EV production, we cultured *E. faecalis*, a common gut commensal microbe, at a decreasing concentration of nutrients in growth media. We found that the quantities of EVs produced increased with decreasing nutrient concentration (**Figure 4.3D**), highlighting that nutrient depletion is associated with increased EV production. Interestingly, we also found that Gram-positive bacteria generally produced higher levels of EVs than Gram-negative bacteria, at least under *in vitro* conditions (**Figure S4.4E**), contrary to dominant hypotheses about EV biogenesis in the literature (Briaud and Carroll, 2020; Xu et al., 2023). Additionally, changes to diet composition, which alters gut microbiota composition and is associated with differences in MEV production (Tan et al., 2022), also correlate with liver *Pck1* in a similar manner

(**Figure S4.4F**). To explore the concept of gut microbes supporting host energy demands in a different physiological setting, we also identified that pregnant mice had increased MEV concentrations during the third trimester of gestation (**Figure S4.4A**), the period where energy demands (Butte et al., 2004) and maternal gluconeogenesis (Kalhan et al., 1997) are both reported to be at their highest. Additionally, our hepatic transcriptome data revealed enrichment in the circadian clock pathway in MEV-treated animals (**Figure 4.3E**). The activation of circadian (via CLOCK/BMAL1) drives the expression of clock-controlled genes, which include the protein regulators Period (PER) and Cryptochrome (CRY) that negatively regulate CLOCK/BMAL1 activity (Takahashi, 2017). It also induces the expression of other regulators such as *Rora* and *Ciart1*. Accordingly, we found that the expression of these genes was differentially upregulated in MEV-treated mice in our transcriptomic dataset (**Table S4.2**). Consistent with this, SPF mice treated with MEVs for 5 weeks also had upregulation of *Per1*, *Rora* and *Ciart1* compared to PBS-treated animals (**Figure 4.3F**), and this phenotype was replicated in the HEPG2 cell line treated with MEVs *in vitro* (**Figure S4.4B**). Interestingly, MEV administration did not induce gluconeogenesis in the kidneys (**Figure S4.4C**), another major site of gluconeogenesis, suggesting that this effect is specific to the liver. This aligns with a previous report indicating that kidney gluconeogenesis is not regulated by circadian rhythm, unlike the liver (Rudic et al., 2004). Finally, to confirm that MEVs promoted gluconeogenesis by activating circadian pathways, we performed siRNA knockdown of CLOCK in HEPG2 cell line (**Figure S4.4D**). Under these conditions, we found that the ability for MEV to upregulate *G6PC* expression was abrogated (**Figure 4.3G**).

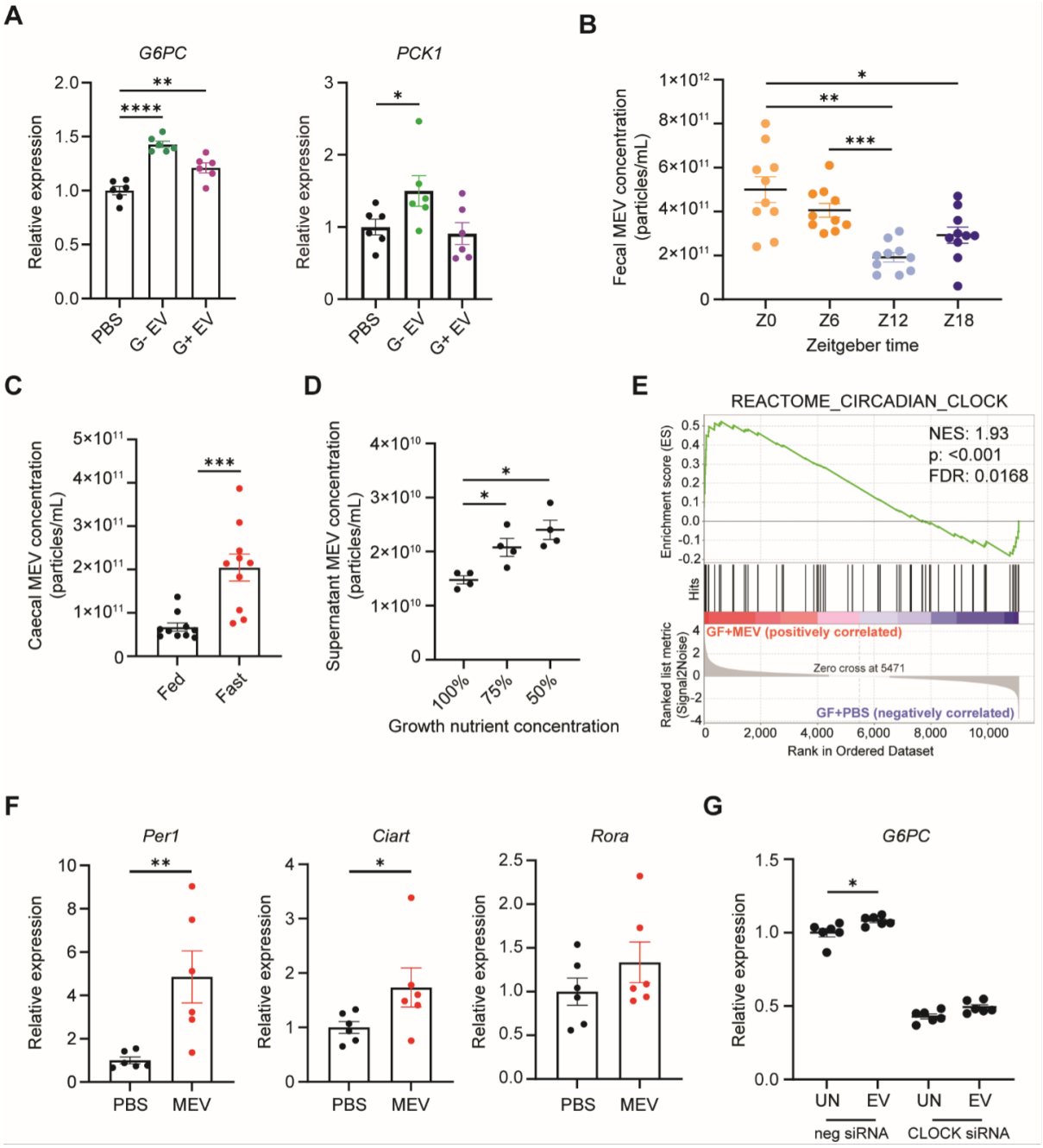
A
G6PC
PCK1
Relative expression
PBS
G- EV
G+ EV
B
Fecal MEV concentration (particles/mL)
Z0
Z6
Z12
Z18
Zeitgeber time
C
Caecal MEV concentration (particles/mL)
Fed
Fast
D
Supernatant MEV concentration (particles/mL)
100%
75%
50%
Growth nutrient concentration
E
REACTOME_CIRCADIAN_CLOCK
NES: 1.93
p: <0.001
FDR: 0.0168
Enrichment score (ES)
Hits
GF+MEV (positively correlated)
Zero cross at 5471
GF+PBS (negatively correlated)
Ranked list metric (Signal2Noise)
Rank in Ordered Dataset
F
Per1
Ciart
Rora
PBS
MEV
G
G6PC
UN
EV
neg siRNA
CLOCK siRNA

Figure 4.3 Gut microbiota-derived vesicles are produced rhythmically in response to host nutritional status and activate the circadian clock to promote gluconeogenesis

(**A**) HEPG2 hepatocyte cell line was cultured for 18 hours in the absence (PBS) or presence of $3x10^9$ Gram-negative EVs (G- EV) from *Escherichia coli* or Gram-positive EVs (G+ EV) from *Enterococcus faecalis*, and gene expression level of *PCK1* and *G6PC* quantified by qPCR (n=6 per condition). (**B**) Faeces MEV concentration was quantified by Nanoparticle tracking analysis from the faeces of SPF control mice collected at Zeitgeber time 0 (start of light cycle), 6, 12 (start of dark cycle) and 18. (**C**) Faecal MEV concentration was quantified by Nanoparticle tracking analysis from the faeces of control mice that were fed *ad libitum* or fasted overnight (18 hours). (**D**) *E. faecalis* was grown *in vitro* at decreasing concentration of nutrients and EVs were isolated and quantified by Nanoparticle tracking analysis. (**E**) Germ-free animals were orally administered 80µg MEV in PBS (GF+MEV), or PBS alone (GF+PBS), twice-weekly for 3 weeks. Whole liver was then collected and RNAseq performed, and enrichment plot for the GSEA Reactome 'Circadian Clock' pathway analysis shown. (**F**) SPF mice were administered $1x10^{10}$ MEVs (MEV), or PBS as control (PBS) daily for 5 weeks, and liver expression of *Per1*, *Ciart1* and *Rora* was quantified by qPCR. (**G**) HEPG2 hepatocyte cell line was reverse transfected with CLOCK-siRNA or control negative-siRNA and cultured for 18 hours in the absence (PBS) or presence of $3x10^9$ MEVs (MEV), and gene expression level of *PCK1* and *G6PC* quantified by qPCR (n=6 per condition). Results represent n=3 independent experiments (**G**), n=2 independent experiments (**A, D**) and n=1 independent experiment (**B-C, E**). All data are presented as mean±SEM. *$p < 0.05$, **$p<0.01$, ***$p<0.001$, ****$p<0.0001$ by Mann-Whitney test or ordinary one-way ANOVA followed by Tukey's multiple comparisons test (**A, B, D**).

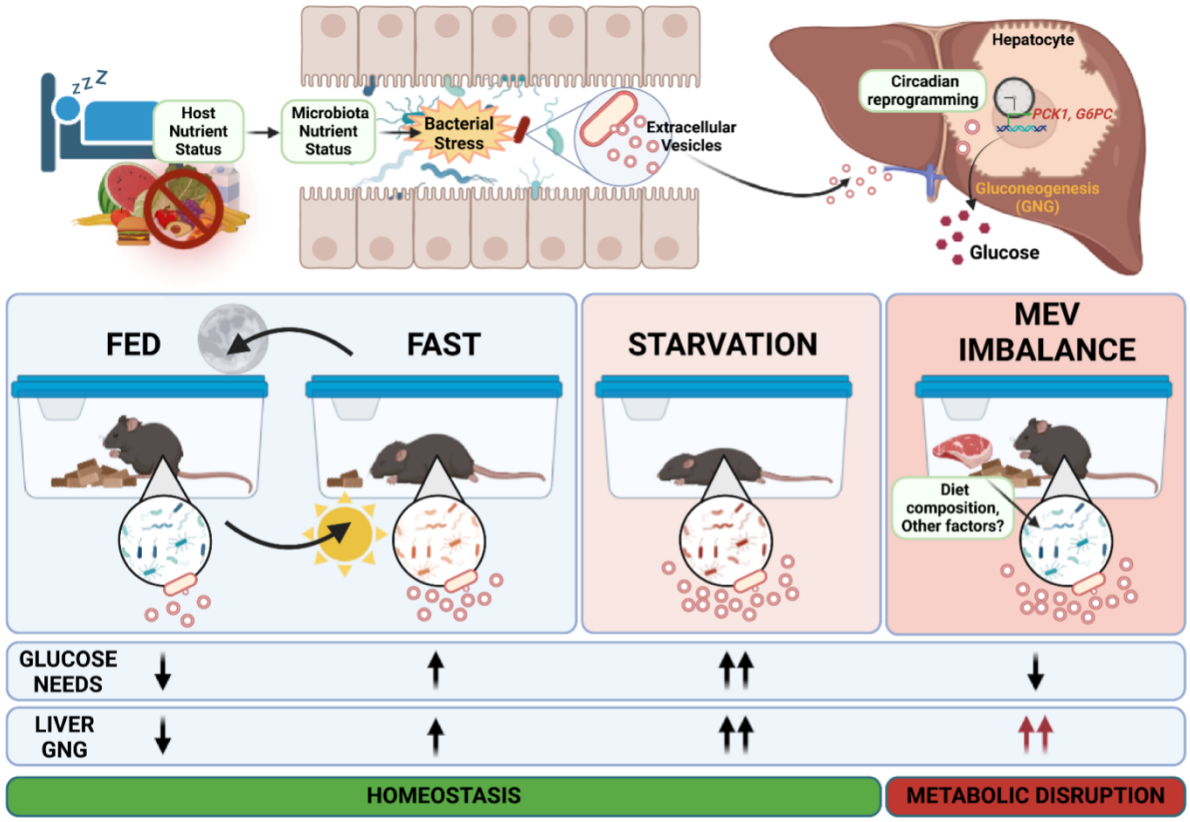

Figure 4.4 Model of gut microbiota-derived extracellular vesicles induction of host hepatic gluconeogenesis.

Schematic of the interplay between host nutritional status, gut microbiota production of extracellular vesicles, and host hepatic gluconeogenesis. Host nutrient status mediates gut microbial stress, with fasting leading to bacterial stress and increased production of microbiota-derived extracellular vesicles (MEVs). MEVs can translocate to the liver, where they tune hepatic circadian rhythm by activating the circadian clock, leading to the expression of *PCK1* and *G6PC*, and the upregulation of hepatic gluconeogenesis (GNG). Under normal conditions, the diurnal regulation of MEV correlates with host glucose requirements, leading to homeostasis. However, the disruption of MEV production, such as improper diet or other factors, can stimulate gluconeogenesis despite the host being euglycemic, which may lead to metabolic disruption and predisposition to metabolic disorders. Figure created using BioRender.com.

4.4 Discussion

In conclusion, we show for the first time that the gut microbiota, via its EVs, can act as a peripheral Zeitgeber for the hepatic circadian system, establishing new fundamental knowledge towards host-gut microbe interactions. MEVs tune hepatic peripheral circadian programming, to control gluconeogenesis under normal physiological conditions. This pathway appears to have evolved to support host glucose demands, linking host nutritional status to gut MEV production (**Figure 4**). Indeed, greater quantities of MEV were found to be produced during periods of high glucose demands (i.e. fasting and pregnancy). This peripheral mode of regulation is likely conserved across mammalian species, regardless of whether they are nocturnal or diurnal, unlike central clock signalling which is governed by the suprachiasmatic nucleus in the hypothalamus in response to light.

Our finding carries several implications. Firstly, does different gut microbiota composition have different capacity for MEV production, and does this contribute, in part, to interindividual differences in baseline and fasting glucose levels? A minor increase in blood glucose level, along with other factors like genetics and dietary habits, might be sufficient to predispose to metabolic disorders. Our finding that Gram-positive bacteria produced greater quantities of EVs compared to Gram-negative bacteria is intriguing, suggesting that the ratio of these bacterial classes in the gut microbiota could influence hepatic circadian rhythm. This could also explain the observation found in some studies that obese individuals have a higher ratio of *Firmicutes* (mostly Gram-positive) to *Bacteroidetes* (Gram-negative) (Magne et al., 2020), with high *Firmicutes* levels possibly associated with dysregulated gluconeogenesis and the increased glucose levels typically

observed in metabolic syndrome. Host dietary composition can also affect MEV production. For example, we have previously shown that a high-protein diet was linked to greater quantities of gut MEVs (Tan et al., 2022). This may partly explain the established effects of a high-protein diet on host gluconeogenesis, with a high-protein, carbohydrate-free diet linked to increased gluconeogenesis in humans (Veldhorst et al., 2009). We also validated this observation in mice, utilising 10 diets with different ratios of macronutrient composition, which revealed a positive association between liver *Pck1* expression and dietary protein content, with a minor interaction with carbohydrate content (**Figure S4.4F**).

As well as diet composition, irregular patterns of food intake which is common in modern lifestyles, may also impair the normal control of host glucose homeostasis by disrupting natural rhythms of MEV production. While MEVs act as a cue to support host glucose demands under normal conditions, it is possible that physiological disruption to MEV production (such as altered diet composition, irregular feeding and possibly medication etc.) may partly underlie the increased metabolic disorders associated with a Western lifestyle.

Secondly, the fact that MEVs directly activate gluconeogenesis *in vitro* indicates that MEVs act independently of the diurnal actions of cortisol and glucagon on hepatic gluconeogenesis. This feature probably allows for the fine-tuning of hepatic gluconeogenesis, allowing the organism to adapt to different degrees of hypoglycaemia. Indeed, the relative production of MEV quantities was much greater in mice that were fasted overnight (**Figure 4.3C**) compared to the difference observed during normal rhythmic oscillation (**Figure 4.3B**). Consistent with this, we found that MEVs act on the

expression of *PCK1* and *G6PC* in a dose-dependent fashion (**Figure S4.1E**). The production of MEVs was related to the nutritional status of the gut microbiota, and thus directly linked to the host's nutritional intake. Stress (such as antibiotics) has been shown to promote bacterial EV production (Kim et al., 2020), and in this study, we provide evidence that nutrient availability is another factor regulating bacterial EV production.

In conclusion, our study provides new fundamental insights into the regulation of host glucose homeostasis. Assessing gut MEV profiles holds significant clinical potential as a biomarker or risk factor for metabolic disorders, including gestational diabetes. Additionally, our study provides a mechanism for the control of host glucose homeostasis, via the alteration of MEV production. Inhibition of hepatic gluconeogenesis has been effective in ameliorating type 2 diabetes (Sharabi et al., 2017). Thus, developing strategies aimed at reducing gut MEV production, i.e. by shaping dietary composition, have incredible potential to possibly alleviate hyperglycaemia. This could form part of a strategy for the control or treatment of metabolic disorders like type 2 diabetes, by reducing hepatic gluconeogenesis.

Acknowledgments

We acknowledge the Sydney Preclinical Imaging facility for training and access to the IVIS Spectrum Imaging System, Sydney Analytical for access to the ZetaView and NS300 for Nanoparticle tracking analysis, and the Laboratory Animal Services at The University of Sydney for animal housing and husbandry.

Funding:

Australian Research Council grant APP210102943 (LM)

Author contributions:

Conceptualization: J.T. and L.M. Validation: J.J.T., D.N. and C.P.V. Investigation: J.T., J.J.T., D.N., C.P.V. T.P., D.S., R.N. Data Curation: J.T. J.J.T, D.N., C.P.V. T.P. Writing – Original Draft: J.T. Writing – Review & Editing: J.J.T., D.N., C.P.V., T.P., D.S., R.N., L.M. Visualization: J.T. Supervision: L.M. Funding Acquisition: L.M.

Competing interests:

L.M. is a current employee of the Translational Science Hub Global Sanofi Vaccines R&D Brisbane, Australia. Her contribution to this work was done when she was an employee of the University of Sydney. All other authors declare they have no competing interests.

Data and materials availability: All data are available in the main text or the supplementary materials.

4.5 Supplementary Material

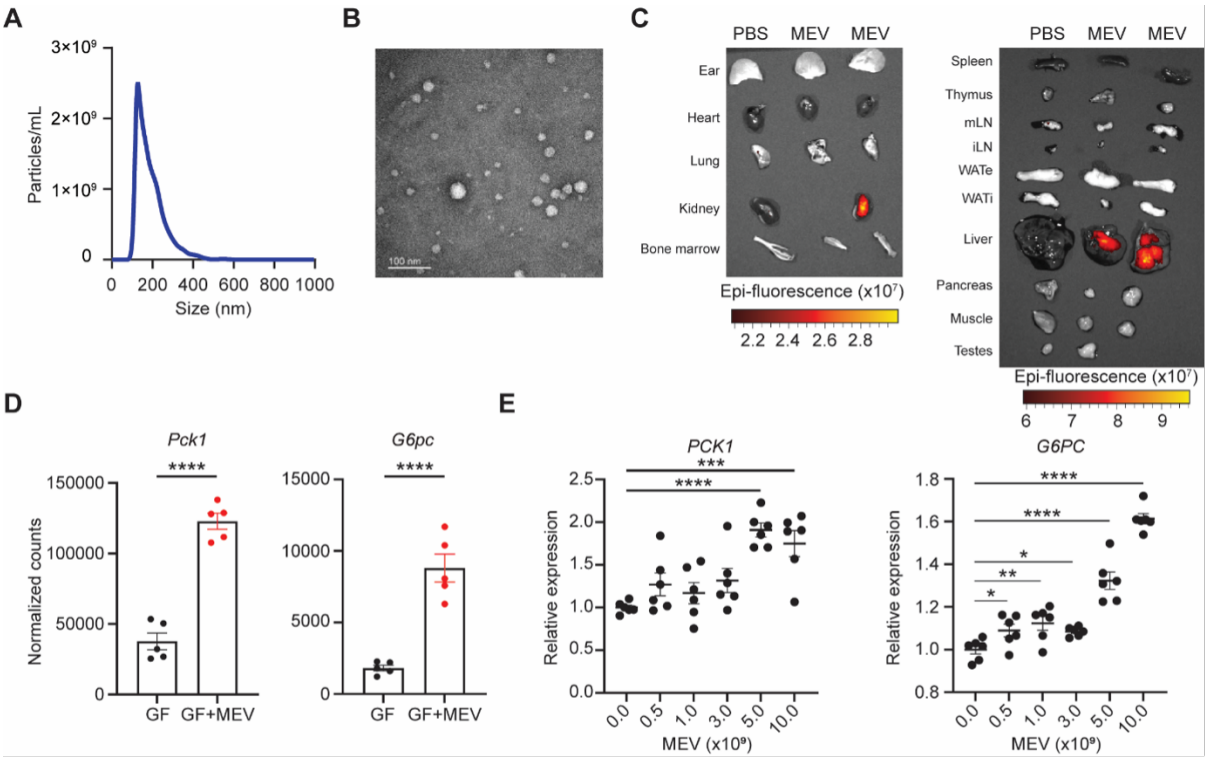

Figure S4.1 Gut microbiota-derived extracellular vesicles induce hepatic gluconeogenesis in vivo and in vitro.

(A) Representative plot of nanoparticle tracking analysis of microbiota-derived extracellular vesicles (MEV) isolated from control mice and **(B)** representative transmission electron microscopy image of isolated MEV. **(C)** Germ-free animals were orally administered 80µg of DiD-labelled microbiota-derived extracellular vesicles (MEV) (n=2) or PBS as control (n=1). 12 hours later, skin (ear), heart, lung, kidney, bone marrow, spleen, thymus, mesenteric lymph nodes (mLN), inguinal lymph nodes (iLN), epididymal white adipose tissue (WATe), inguinal white adipose tissue (WATi), liver. Pancreas, muscle and testes were collected and fluorescence quantified *ex vivo* using the IVIS (In vivo imaging system). Relative fluorescence represented as Epi-fluorescence. **(D)** Germ-free animals were orally administered 80µg MEV in PBS (GF+MEV), or PBS alone (GF), twice-weekly for 3 weeks. Whole liver was then collected and RNAseq performed and DESeq2 normalized counts of PEPCK and G6P presented. **(E)** HEPG2 hepatocyte cell line was cultured for 18 hours in the presence of 0.0, 0.5, 1.0, 3.0, 5.0 or 10.0 x10^9 MEV, and gene expression level of *PCK1* and *G6PC* quantified by qPCR (n=6 per condition). Results represent n=2 independent experiments, and n=1 independent experiments (B-C). All data are presented as mean±SEM. *p<0.05, **p<0.01, ***p<0.001 and ****p<0.0001 by Mann-Whitney test when compared to untreated (E), or FDR corrected p value based on DESeq2 analysis (D).

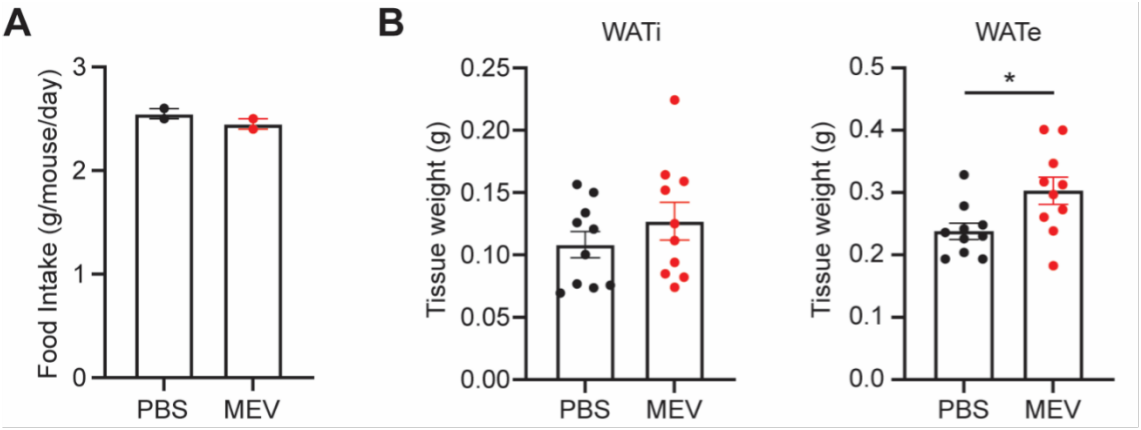

Figure S4.2 Gut microbiota-derived extracellular vesicles promote low-grade hepatic inflammation and insulin resistance.

(A) SPF mice were administered 1x10[10] MEV (MEV), or PBS as control (PBS) daily for 5 weeks. Graph represents average food intake (g/mouse/day). Each dot represents the average intake of one cage with n=5 animals per cage and **(B)** Scatter plot showing the weight of inguinal white adipose tissue (WATi) and epididymal white adipose tissue (WATe) weight. (n=10 mice per group). All data are presented as mean±SEM. *$p < 0.05$ by Mann-Whitney test.

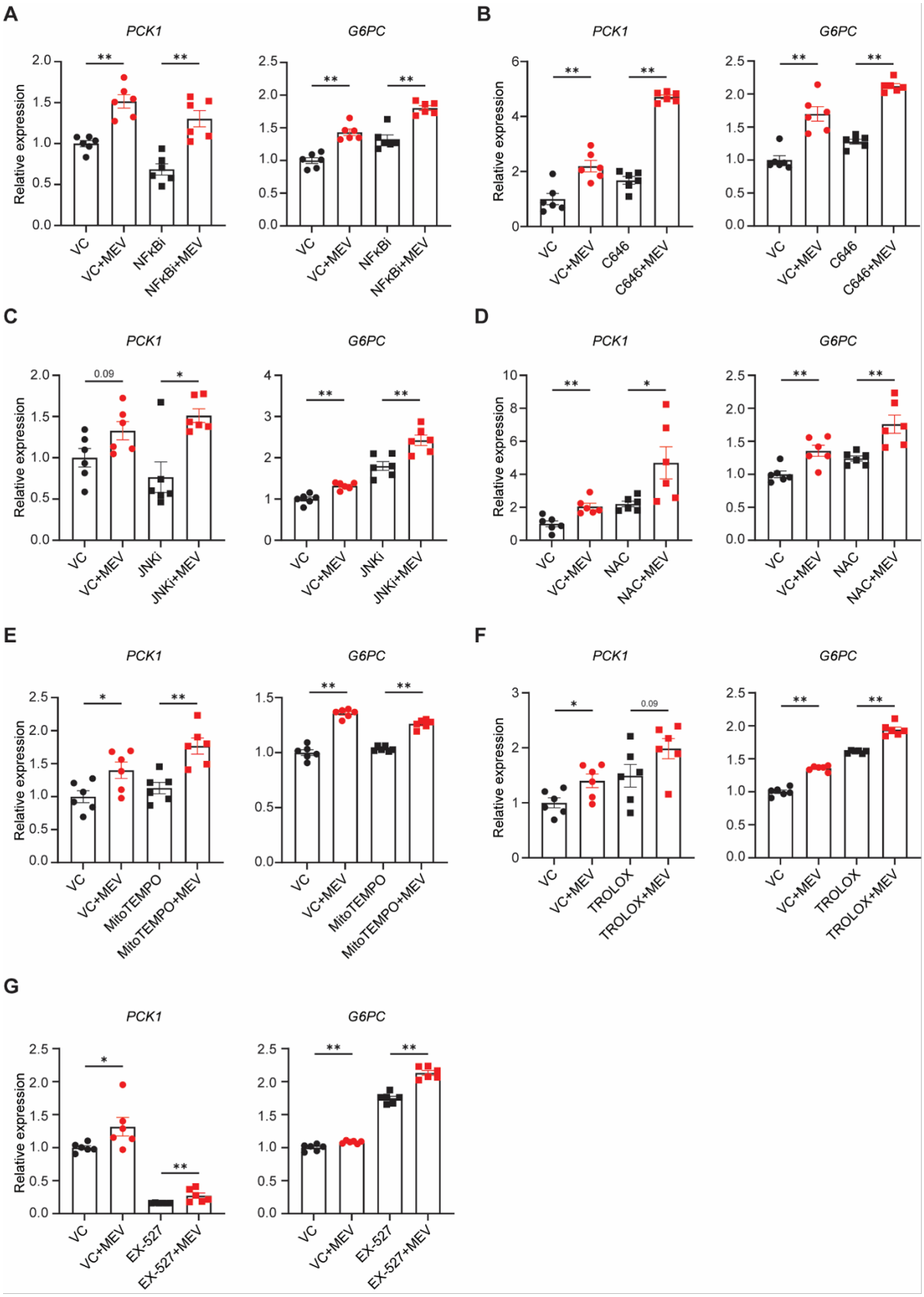
A
PCK1
G6PC
Relative expression
VC
VC+MEV
NFκBi
NFκBi+MEV
B
C646
C646+MEV
C
JNKi
JNKi+MEV
D
NAC
NAC+MEV
E
MitoTEMPO
MitoTEMPO+MEV
F
TROLOX
TROLOX+MEV
G
EX-527
EX-527+MEV

Figure S4.3 Gut microbiota-derived vesicles do not promote hepatic gluconeogenesis through activation of inflammatory and cellular-stress related pathways.

HEPG2 hepatocyte cell line was cultured for 18 hours in the absence (vehicle control; VC) or in the presence of $3x10^9$ MEV (VC+MEV), in the absence or presence of (**A**) 10μM NFkB inhibitor BAY11-7082, (**B**) 20μM p300 inhibitor C646, (**C**) 20μM JNK inhibitor SP600125, the antioxidants (**D**) 10mM N-acetyl cysteine, (**E**) 10μM MitoTEMPO and (**F**) 10μM TROLOX, (**G**) 10μM SIRT1 inhibitor EX-527, and gene expression level of *PCK1* and *G6PC* quantified by qPCR (n=6 per condition). Cells were pre-treated with the inhibitor for at least 30min prior to the addition of MEV. Results represent n=2 independent experiments. All data are presented as mean±SEM. *$p < 0.05$ and **<0.01 by Mann-Whitney test between untreated and MEV-treated samples for each condition.

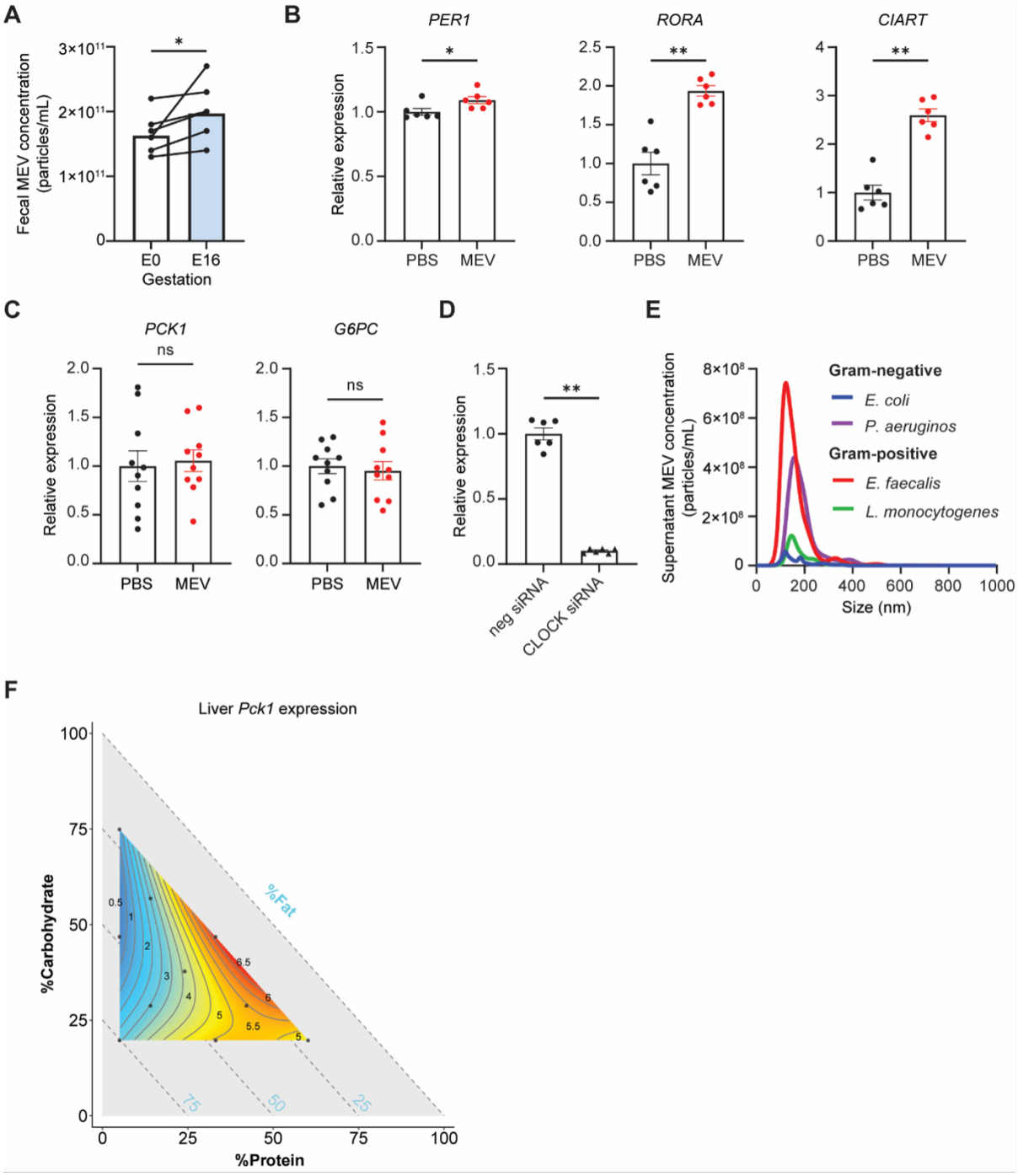
A
Fecal MEV concentration (particles/mL)
3×10¹¹
2×10¹¹
1×10¹¹
0
*
E0
E16
Gestation
B
PER1
RORA
CIART
Relative expression
*
**
**
PBS
MEV
C
PCK1
G6PC
ns
ns
D
**
neg siRNA
CLOCK siRNA
E
Supernatant MEV concentration (particles/mL)
8×10⁸
6×10⁸
4×10⁸
2×10⁸
Gram-negative
E. coli
P. aeruginos
Gram-positive
E. faecalis
L. monocytogenes
Size (nm)
F
Liver Pck1 expression
%Carbohydrate
%Protein
%Fat

Figure S4.4 Gut microbiota-derived vesicles are produced rhythmically in response to host nutritional status and activate the circadian clock to promote gluconeogenesis.

(**A**) MEV was quantified by Nanoparticle tracking analysis from feces collected from pregnant mice prior to gestation (E0) or at the third trimester of gestation (E16) (n=5 per group). (**B**) HEPG2 hepatocyte cell line was cultured for 18 hours in the absence (PBS) or presence of $3x10^9$ MEV (MEV), and gene expression level of *PER1*, *RORA* and *CIART* quantified by qPCR (n=6 per condition). (**C**) Specific-pathogen free (SPF) mice were administered $1x10^{10}$ MEV (MEV), or PBS as control (PBS) daily for 5 weeks, and kidney gene expression of *Pck1* and *G6pc* quantified by qPCR (n=10 per group). (**D**) HEPG2 hepatocyte cell line was reverse transfected with CLOCK-siRNA or control negative-siRNA and cultured for 18 hours in the absence (PBS) and gene expression level of CLOCK quantified by qPCR (n=6 per condition). (**E**) Representative relative production of EV produced in culture *in vitro* by *Escherichia coli*, *Pseudomonas aeruginosa*, *Enterococcus faecalis* and *Listeria monocytogenes* following 18 hours of culture. (**F**) Contribution of macronutrient composition to liver *Pck1* expression (n = 7–8 per diet) was modelled by mixture model and represented on a right-angled mixture triangle comprising of carbohydrate (y axis), protein (x axis) and fat (hypotenuse) with liver *Pck1* expression (expression relative to the housekeeping gene *Rpl13a*, numbers on isolines) as the response variable. Red represents higher levels of *Pck1* expression while blue represents lower levels of *Pck1* expression in the nutrient mixture space. Each dot represents one of the 10 diets used for modelling response surface. Results represent n=3 independent experiments (**D**), n=2 independent experiments (**B, E-F**) and n=1 independent experiment (**A, C**). All data are presented as mean±SEM. *$p < 0.05$ and **<0.01, by non-parametric paired t-test (**A**) or Mann-Whitney test (B-D).

Table S4.1 List of primers and their sequences used in this study

Gene	Species	Forward (5'-3')	Reverse (5'-3')
GAPDH	Human	GAAGGTGAAGGTCGGAGTCA	CAGAGTTAAAAGCAGCCCTGG
ACTB	Human	GACGACATGGAGAAAATCTG	ATGATCTGGGTCATCTTCTC
PCK1	Human	ATTCTGGGTATAACCAACCC	GTTGATGGCCCTTAAATGAC
G6PC	Human	ACTGTGCATACATGTTCATC	TGAATGTTTTGACCTAGTGC
CLOCK	Human	ACTACAAGACGAAAACGTAG	CATCTCTGTCAACAATCGAG
PER1	Human	ACACTTCAGAACCAGGATAC	AGTGGAACCATAGAAGACTC
CIART1	Human	AAGGATTTATACCTCCTCTCAC	TCTTTAACATCCCTTCTACCTG
RORA	Human	GCCATCAAAATTACAGAAGC	ATAAACACCACCTCTAGAGAAC
Rpl13a	Mouse	ATCCCTCCACCCTATGACAA	GCCCCAGGTAAGCAAACTT
Pck1	Mouse	AATATGACAACTGTTGGCTG	AATGCTTTCTCAAAGTCCTC
G6pc	Mouse	TTCAAGTGGATTCTGTTTGG	AGATAGCAAGAGTAGAAGTGAC
Clock	Mouse	AAGTGACTCATTAACCCCTG	CTATGTGTGCGTTGTATAGTTC
Per1	Mouse	GTTCTCATAGTTCCTCTTCTG	GTGAGTTTGTACTCTTGCTG
Ciart	Mouse	AGTCAAGAGATCAAGAGACG	GAAGCTACTTAATCCTCTGTC
Rora	Mouse	GAGTTTGTGTTCTATGCACC	CCTTGCATATTAGCTTGGTTAG

Table S4.2 Transcriptomic dataset of differentially upregulated genes

This dataset is provided as an Excel file attached to this PDF

References

Briaud, P., Carroll, R.K., 2020. Extracellular Vesicle Biogenesis and Functions in Gram-Positive Bacteria. Infection and Immunity 88, 10.1128/iai.00433-20. https://doi.org/10.1128/iai.00433-20

Butte, N.F., Wong, W.W., Treuth, M.S., Ellis, K.J., O'Brian Smith, E., 2004. Energy requirements during pregnancy based on total energy expenditure and energy deposition. Am J Clin Nutr 79, 1078–1087. https://doi.org/10.1093/ajcn/79.6.1078

Cao, J., Peng, J., An, H., He, Q., Boronina, T., Guo, S., White, M.F., Cole, P.A., He, L., 2017. Endotoxemia-mediated activation of acetyltransferase P300 impairs insulin signaling in obesity. Nat Commun 8, 131. https://doi.org/10.1038/s41467-017-00163-w

Chelakkot, C., Choi, Y., Kim, D.-K., Park, H.T., Ghim, J., Kwon, Y., Jeon, J., Kim, M.-S., Jee, Y.-K., Gho, Y.S., Park, H.-S., Kim, Y.-K., Ryu, S.H., 2018. Akkermansia muciniphila-derived extracellular vesicles influence gut permeability through the regulation of tight junctions. Exp Mol Med 50, e450. https://doi.org/10.1038/emm.2017.282

Choi, Y., Kwon, Y., Kim, D.-K., Jeon, J., Jang, S.C., Wang, T., Ban, M., Kim, M.-H., Jeon, S.G., Kim, M.-S., Choi, C.S., Jee, Y.-K., Gho, Y.S., Ryu, S.H., Kim, Y.-K., 2015. Gut microbe-derived extracellular vesicles induce insulin resistance, thereby impairing glucose metabolism in skeletal muscle. Sci Rep 5, 15878. https://doi.org/10.1038/srep15878

Choudhury, A.A., Devi Rajeswari, V., 2021. Gestational diabetes mellitus - A metabolic and reproductive disorder. Biomed Pharmacother 143, 112183. https://doi.org/10.1016/j.biopha.2021.112183

Dobin, A., Davis, C.A., Schlesinger, F., Drenkow, J., Zaleski, C., Jha, S., Batut, P., Chaisson, M., Gingeras, T.R., 2013. STAR: ultrafast universal RNA-seq aligner. Bioinformatics 29, 15–21. https://doi.org/10.1093/bioinformatics/bts635

Fan, Y., Pedersen, O., 2021. Gut microbiota in human metabolic health and disease. Nat Rev Microbiol 19, 55–71. https://doi.org/10.1038/s41579-020-0433-9

Galicia-Garcia, U., Benito-Vicente, A., Jebari, S., Larrea-Sebal, A., Siddiqi, H., Uribe, K.B., Ostolaza, H., Martín, C., 2020. Pathophysiology of Type 2 Diabetes Mellitus. Int J Mol Sci 21, 6275. https://doi.org/10.3390/ijms21176275

He, L., Cao, J., Meng, S., Ma, A., Radovick, S., Wondisford, F.E., 2013. Activation of Basal Gluconeogenesis by Coactivator p300 Maintains Hepatic Glycogen Storage. Mol Endocrinol 27, 1322–1332. https://doi.org/10.1210/me.2012-1413

Ji, X., Zhou, F., Zhang, Y., Deng, R., Xu, W., Bai, M., Liu, Y., Shao, L., Wang, X., Zhou, L., 2019. Butyrate stimulates hepatic gluconeogenesis in mouse primary hepatocytes. Exp Ther Med 17, 1677–1687. https://doi.org/10.3892/etm.2018.7136

Kalhan, S., Rossi, K., Gruca, L., Burkett, E., O'Brien, A., 1997. Glucose turnover and gluconeogenesis in human pregnancy. J Clin Invest 100, 1775–1781.

Kim, S.W., Seo, J.-S., Park, S.B., Lee, A.R., Lee, J.S., Jung, J.W., Chun, J.H., Lazarte, J.M.S., Kim, J., Kim, J.-H., Song, J.-W., Franco, C., Zhang, W., Ha, M.W., Paek, S.-M., Jung, M., Jung, T.S., 2020. Significant increase in the secretion of extracellular vesicles and antibiotics resistance from methicillin-resistant Staphylococcus aureus induced by ampicillin stress. Sci Rep 10, 21066. https://doi.org/10.1038/s41598-020-78121-8

Kishman, E.E., Reutrakul, S., Broussard, J.L., 2024. Metabolic consequences of sleep and circadian disruption during pregnancy and postpartum. Trends Endocrinol Metab S1043-2760(24)00243–1. https://doi.org/10.1016/j.tem.2024.08.008

Krisko, T.I., Nicholls, H.T., Bare, C.J., Holman, C.D., Putzel, G.G., Jansen, R.S., Sun, N., Rhee, K.Y., Banks, A.S., Cohen, D.E., 2020. Dissociation of Adaptive Thermogenesis from Glucose Homeostasis in

Microbiome-Deficient Mice. Cell Metab 31, 592-604.e9. https://doi.org/10.1016/j.cmet.2020.01.012

Liang, X., Dai, N., Sheng, K., Lu, H., Wang, J., Chen, L., Wang, Y., 2022. Gut bacterial extracellular vesicles: important players in regulating intestinal microenvironment. Gut Microbes 14, 2134689. https://doi.org/10.1080/19490976.2022.2134689

Love, M.I., Huber, W., Anders, S., 2014. Moderated estimation of fold change and dispersion for RNA-seq data with DESeq2. Genome Biol 15, 550. https://doi.org/10.1186/s13059-014-0550-8

Macia, L., Nanan, R., Hosseini-Beheshti, E., Grau, G.E., 2019. Host- and Microbiota-Derived Extracellular Vesicles, Immune Function, and Disease Development. Int J Mol Sci 21, 107. https://doi.org/10.3390/ijms21010107

Magne, F., Gotteland, M., Gauthier, L., Zazueta, A., Pesoa, S., Navarrete, P., Balamurugan, R., 2020. The Firmicutes/Bacteroidetes Ratio: A Relevant Marker of Gut Dysbiosis in Obese Patients? Nutrients 12, 1474. https://doi.org/10.3390/nu12051474

Petrenko, V., Saini, C., Giovannoni, L., Gobet, C., Sage, D., Unser, M., Heddad Masson, M., Gu, G., Bosco, D., Gachon, F., Philippe, J., Dibner, C., 2017. Pancreatic α- and β-cellular clocks have distinct molecular properties and impact on islet hormone secretion and gene expression. Genes Dev 31, 383–398. https://doi.org/10.1101/gad.290379.116

Rudic, R.D., McNamara, P., Curtis, A.-M., Boston, R.C., Panda, S., Hogenesch, J.B., FitzGerald, G.A., 2004. BMAL1 and CLOCK, Two Essential Components of the Circadian Clock, Are Involved in Glucose Homeostasis. PLoS Biol 2, e377. https://doi.org/10.1371/journal.pbio.0020377

Schrader, L.A., Ronnekleiv-Kelly, S.M., Hogenesch, J.B., Bradfield, C.A., Malecki, K.M., 2024. Circadian disruption, clock genes, and metabolic health. J Clin Invest 134, e170998. https://doi.org/10.1172/JCI170998

Sharabi, K., Lin, H., Tavares, C.D.J., Dominy, J.E., Camporez, J.P., Perry, R.J., Schilling, R., Rines, A.K., Lee, J., Hickey, M., Bennion, M., Palmer, M., Nag, P.P., Bittker, J.A., Perez, J., Jedrychowski, M.P., Ozcan, U., Gygi, S.P., Kamenecka, T.M., Shulman, G.I., Schreiber, S.L., Griffin, P.R., Puigserver, P., 2017. Selective Chemical Inhibition of PGC-1α Gluconeogenic Activity Ameliorates Type 2 Diabetes. Cell 169, 148-160.e15. https://doi.org/10.1016/j.cell.2017.03.001

Shimizu, I., Yoshida, Y., Minamino, T., 2016. A role for circadian clock in metabolic disease. Hypertens Res 39, 483–491. https://doi.org/10.1038/hr.2016.12

Son, E.T., Paul-Heng, M., Leong, M., Wang, C., Hill, A.E., Denkova, M., Purcell, A.W., Mifsud, N.A., Sharland, A.F., 2023. Screening self-peptides for recognition by mouse alloreactive CD8+ T cells using direct ex vivo multimer staining. STAR Protoc 4, 101943. https://doi.org/10.1016/j.xpro.2022.101943

Subramanian, A., Tamayo, P., Mootha, V.K., Mukherjee, S., Ebert, B.L., Gillette, M.A., Paulovich, A., Pomeroy, S.L., Golub, T.R., Lander, E.S., Mesirov, J.P., 2005. Gene set enrichment analysis: a knowledge-based approach for interpreting genome-wide expression profiles. Proc Natl Acad Sci U S A 102, 15545–15550. https://doi.org/10.1073/pnas.0506580102

Taitz, J.J., Tan, J.K., Potier-Villette, C., Ni, D., King, N.J., Nanan, R., Macia, L., 2023. Diet, commensal microbiota-derived extracellular vesicles, and host immunity. Eur J Immunol 53, e2250163. https://doi.org/10.1002/eji.202250163

Takahashi, J.S., 2017. Transcriptional architecture of the mammalian circadian clock. Nat Rev Genet 18, 164–179. https://doi.org/10.1038/nrg.2016.150

Tan, J., Ni, D., Taitz, J., Pinget, G.V., Read, M., Senior, A., Wali, J.A., Elnour, R., Shanahan, E., Wu, H., Chadban, S.J., Nanan, R., King, N.J.C., Grau, G.E., Simpson, S.J., Macia, L., 2022. Dietary protein increases T-cell-independent sIgA production through changes in gut microbiota-derived extracellular vesicles. Nat Commun 13, 4336. https://doi.org/10.1038/s41467-022-31761-y

Tan, J., Ni, D., Wali, J.A., Cox, D.A., Pinget, G.V., Taitz, J., Daïen, C.I., Senior, A., Read, M.N., Simpson, S.J., King, N.J.C., Macia, L., 2021. Dietary carbohydrate, particularly glucose, drives B cell lymphopoiesis and function. iScience 24, 102835. https://doi.org/10.1016/j.isci.2021.102835

Tan, J., Macia, L., Mackay, C.R., 2023a. Dietary fiber and SCFAs in the regulation of mucosal immunity. J Allergy Clin Immunol 151, 361–370. https://doi.org/10.1016/j.jaci.2022.11.007

Tan, J., Taitz, J., Nanan, R., Grau, G., Macia, L., 2023b. Dysbiotic Gut Microbiota-Derived Metabolites and Their Role in Non-Communicable Diseases. Int J Mol Sci 24, 15256. https://doi.org/10.3390/ijms242015256

Veldhorst, M.A.B., Westerterp-Plantenga, M.S., Westerterp, K.R., 2009. Gluconeogenesis and energy expenditure after a high-protein, carbohydrate-free diet. Am J Clin Nutr 90, 519–526. https://doi.org/10.3945/ajcn.2009.27834

Wang, Z., Zhu, S., Jia, Y., Wang, Y., Kubota, N., Fujiwara, N., Gordillo, R., Lewis, C., Zhu, M., Sharma, T., Li, L., Zeng, Q., Lin, Y.-H., Hsieh, M.-H., Gopal, P., Wang, T., Hoare, M., Campbell, P., Hoshida, Y., Zhu, H., 2023. Positive selection of somatically mutated clones identifies adaptive pathways in metabolic liver disease. Cell 186, 1968-1984.e20. https://doi.org/10.1016/j.cell.2023.03.014

Weger, M., Weger, B.D., Gachon, F., 2022. The Mechanisms and Physiological Consequences of Diurnal Hepatic Cell Size Fluctuations: A Brief Review. Cell Physiol Biochem 56, 1–11. https://doi.org/10.33594/000000489

Xu, Y., Xie, C., Liu, Y., Qin, X., Liu, J., 2023. An update on our understanding of Gram-positive bacterial membrane vesicles: discovery, functions, and applications. Front Cell Infect Microbiol 13, 1273813. https://doi.org/10.3389/fcimb.2023.1273813

Chapter 5 Gut microbial extracellular vesicles regulate gut microbiota composition and maternal programming of the offspring

This chapter is formatted as a manuscript to be submitted for publication:
Taitz J, Tan J, Ni D, Potier-Villette C, Pinget G, King NJC, Grau G, Nanan R, Macia L. "Gut microbial extracellular vesicles regulate gut microbiota composition and maternal programming of the offspring", to be submitted in 2025
I took the lead in designing and carrying out the majority of the experiments, with assistance from co-authors. I analysed the data, and wrote the original manuscript. All co-authors contributed to data interpretation and manuscript preparation.

This work in the context of this thesis:

Expanding on our findings in **Chapters 3 and 4** that MEVs modulate host mucosal immunity and glucose homeostasis, this chapter explores their role in shaping gut microbiota composition in adulthood, and their influence on fetal development during gestation. While alterations in the bacterial origins of MEVs have been observed in disease and are increasingly studied alongside overall microbiota changes, whether MEVs actively regulate gut bacterial composition under homeostatic conditions remains unclear. Similarly, while maternal gut-derived metabolites and MAMPs influence fetal development with long-term consequences for offspring health, whether maternally derived MEVs contribute to this process is unknown. Emerging evidence suggests maternal gut MEVs can cross the placenta and are detectable in amniotic fluid and fetal tissues, yet specific effects on fetal physiology have not been investigated.

We identified that MEVs constitute a distinct and functionally active component of a healthy gut microbiota, with specific bacterial taxa enriched in the MEV fraction despite their low abundance in the overall microbiota. Daily MEV administration to adult male

mice altered microbiota composition, reducing overall diversity, and shifting taxonomic profiles, suggesting that MEVs actively regulate bacterial composition even under homeostatic conditions.

When administered during gestation, MEVs did not alter overall gut microbiota diversity at three weeks postnatally but led to significant compositional shifts, despite efforts to normalise microbiota composition by fostering to control dams. Notably, MEVs induced changes to offspring colonic gene expression, upregulating genes related to gut barrier integrity, bacterial recognition, epithelial differentiation, and cytokine expression, which may collectively have shaped early-life colonisation patterns. Beyond the gut, gestational MEV exposure expanded immune populations in peripheral, but not primary, lymphoid organs and primed splenic T cell towards IFNγ expression. However, this immune modulation did not alter susceptibility to allergic airway inflammation later in life.

Collectively, this chapter establishes MEVs as an intrinsic component of a healthy gut microbiota, with a composition that is likely always distinct, pointing to a significant but underexplored role in microbiota-host interactions. Furthermore, this chapter provides the first evidence that maternally derived gut MEVs represent a novel pathway through which the maternal gut microbiota influences fetal physiology. These findings expand our current knowledge of MEVs as underappreciated but important intermediaries in gut microbiota-host interactions and highlights their potential as therapeutics tools that can modulate composition in adulthood and influence fetal development for long-term health benefits to the offspring.

Gut microbial extracellular vesicles regulate gut microbiota composition and maternal programming of the offspring

Authors

Jemma J. Taitz[1,2], Jian K. Tan[1,2], Duan Ni[1,2,3,4], Camille Potier-Villette[1,2], Gabriela Pinget[1,3,4], Ralph Nanan[1,3,4], Laurence Macia[1,2]

Affiliations

[1]Charles Perkins Centre, The University of Sydney, Sydney, NSW, Australia.

[2]School of Medical Sciences, Faculty of Medicine and Health, The University of Sydney, Sydney, NSW, Australia.

[3]Sydney Medical School Nepean, The University of Sydney, Sydney, NSW, Australia.

[4]Nepean Hospital, Nepean Blue Mountains Local Health District, Sydney, NSW, Australia

Abstract

Bacterial extracellular vesicles are emerging as key mediators of gut-microbiota host communication, but their role in gut homeostasis and fetal development remains poorly understood. In this project, we demonstrate that gut microbiota derived extracellular vesicles (MEVs) represent a distinct component of healthy gut microbiota, with specific taxa markedly enriched in the vesicle secretome. Oral administration of MEVs to adult mice altered gut microbiota composition, reducing overall diversity, and impacting specific taxa. When administered during gestation (E0-E19), MEV exposure resulted in alterations in offspring gut microbiota composition, despite postnatal normalisation. Gestational MEVs programmed colonic gene expression, enhancing genes related to barrier integrity, bacterial recognition, epithelial differentiation, and cytokine signalling. Beyond the gut, gestational MEVs also expanded immune cell populations in peripheral lymphoid organs and enhanced T cell IFNγ expression *ex vivo*. However, MEV-exposed

offspring showed no altered susceptibility to house dust mite-induced allergic airway inflammation. Collectively, our findings highlight MEVs as fundamental regulators of gut microbiota composition and reveal a novel mechanism through which maternal gut bacteria may condition offspring immunity during gestation. This work highlights the therapeutic potential for MEVs to alleviate dysbiosis and promote healthy immune programming during pregnancy.

5.1 Introduction

Trillions of microorganisms, predominantly bacteria, inhabit the gastrointestinal tract and form the gut microbiota. This community of microbes profoundly influences host physiology, regulating immunity, metabolism, and tissue development (Marchesi et al., 2016; Rooks and Garrett, 2016). Gut bacteria impact the host via multiple molecular mechanisms, with metabolite and microbe-associated molecular pattern (MAMP)-based signalling pathways being the most well-characterised. Metabolites, including short-chain fatty acids (SCFAs), indoles and secondary bile acids, diffuse through the gastrointestinal barrier to influence both local and systemic host cells (Liu et al., 2022). Similarly, MAMPs engage host pattern recognition receptors (PRRs) to shape development and function of the immune system, such as Polysaccharide A from *Bacteroides fragilis* which drives regulatory T cell (Treg) differentiation (Mazmanian et al., 2005), and induction of intestinal T-helper 17 (Th17) cells by segmented filamentous bacteria (Ivanov et al., 2009).

More recently, bacterial extracellular vesicles have emerged as novel players in microbiota-host communication (Macia et al., 2019; Taitz et al., 2023). These nanosized

structures, produced by both Gram-positive and Gram-negative species, can carry a diverse array of molecules including proteins, lipids, and nucleic acids (Macia et al., 2019; McMillan and Kuehn, 2021). The collective vesicles produced by the gut microbiota, here referred to as microbiota extracellular vesicles (MEVs), transport metabolites, MAMPs and other biologically active molecules across the intestinal barrier under homeostatic conditions. MEVs have been detected in various body fluids in both healthy and pathological conditions (Chang et al., 2024; Park et al., 2021), which has generated significant interest in their potential as diagnostic and predictive biomarkers, and as therapeutics (Xie et al., 2022). However, research on their immunomodulatory effects has primarily focused on vesicles from single bacterial strains, whether commensal or pathogenic (Bitto and Kaparakis-Liaskos, 2017; Molina-Tijeras et al., 2019). As such, the broader role of MEVs in microbiota-host communication during homeostasis remains poorly understood and is a critical gap in advancing their therapeutic potential.

Gestation represents a crucial window in immune development where the maternal gut microbiota significantly influences fetal programming, with long-term consequences for offspring health (Koren et al., 2024). Microbial metabolites directly cross the placenta to fine-tune the fetus, demonstrated by SCFA-mediated induction of Tregs via upregulation of the transcription factors AIRE and Foxp3 (Hu et al., 2019; Thorburn et al., 2015). Bacterial antigens also impact fetal development (Koren et al., 2024) and can even be delivered across the placenta via active transport mechanisms, such as in complex with maternal IgG (Gomez de Agüero et al., 2016). These pathways reflect how host-microbiota co-evolution has shaped adaptations that facilitate beneficial microbiota signalling during fetal development, while maintaining a protected environment *in utero*. Despite their capacity to carry diverse microbial signals, the role of maternal MEVs on the

fetus remains unexplored. Recent evidence supports that maternal MEVs cross the placenta and are detectable in amniotic fluid and placental tissue (Kaisanlahti et al., 2023; Menon et al., 2023; Turunen et al., 2023), suggesting MEVs may represent an underappreciated mechanism of maternal gut microbiota-fetal communication.

In this study we aimed to characterise MEV composition in healthy mouse gut microbiota and examine their functional influence on gut bacterial structure. We also aimed to explore whether MEVs may modulate the gut-host axis during early development, by investigating the impact of gestational MEV exposure on offspring immune development and disease susceptibility. Our study highlights MEVs as having a fundamental role in modulating the gut microbiota as well as fetal programming during pregnancy.

5.2 Materials and Methods

5.2.1 Animals and housing

6-8 week-old C57BL/6 mice (Australian BioResources, NSW, Australia) were housed under specific-pathogen-free conditions at the Charles Perkins Centre animal facility at the University of Sydney. All experimental procedures were approved by USYD Animal Ethics committee (Protocol Numbers 2019/1579, 2021/1950, 2023/2308). During all experiments, mice were given *ad libitum* access to the rodent diet AIN-93G (Specialty Feeds, Glen Forrest, Australia) and water.

5.2.2 MEV gavages and breeding

For all gavage experiments, mice were administered MEVs derived from either faeces or caecal content, daily, in 200µL of 0.02µm filtered PBS. For Figure 5.2, male mice were

administered $1x10^{10}$ MEVs extracted from faeces, or PBS (control) for 5 weeks and euthanised using CO_2 asphyxiation. For the gestational MEV experiments, female mice were gavaged PBS (control) or 60µg (protein content) faecal MEVs daily during gestation from E0 - E19. From E19 mice were left to give birth naturally with no intervention. Within 48 hours of birth, litters of similar size were fostered to PBS-treated dams. Offspring and dams were left untouched throughout the weaning period. In the first gestational MEV experiment (Figures 5.3-5), male and female offspring were euthanised using CO_2 asphyxiation at postnatal day 21 (PN21) for tissue collection and analysis. For the second gestational MEV experiment (Figure 5.6), female offspring were retained and left undisturbed until 9 weeks of age, at which point were used in an allergic airway model.

5.2.3 House dust mite model

9-week-old female offspring exposed to MEVs or PBS *in utero* were sensitised via intranasal administration with 50µg house dust mite (HDM) extract (Citek, Netherlands) in 50µL PBS on days 0, 1, 2 (MEV and PBS groups, n=10 per group) as previously described (Thorburn et al., 2015). A non-sensitised control group (PBS offspring, n=10) received PBS intranasally. All mice were challenged intranasally with 5µg HDM extract in 50µL PBS, daily from days 12-15. At D16, mice were euthanised by gradual CO_2 asphyxiation, and serum, bronchioalveolar lavage fluid (BALF), and mediastinal lymph nodes were collected. BALF was collected by inserting a blunt 18-gauge needle into the trachea and instilling with two 0.8 mL volumes of PBS (0.5M EDTA). Lavage volume was recorded and centrifuged 500xg for 10mins at 4℃. The cell pellet was resuspended in 500µL flow cytometry buffer (2% FBS in PBS) and total cells counted using trypan blue

(0.4%) and a haemocytometer and normalised to original lavage volume. Cells were then stained for flow cytometry as below in Section 5.3.8.

Mediastinal lymph nodes were processed into single-cell suspensions via mechanical disruption, under sterile conditions. Cells were filtered using 100μm mesh and 10^3 cells were incubated with HDM extract (20μg/mL) in complete media for 72 hours at 37℃ 5% CO_2. Supernatant was then collected and frozen at -30℃ for subsequent cytokine measurement by ELISA.

5.2.4 MEV Isolation and characterisation

MEVs were extracted from either caecal content or faeces where indicated. MEVs were isolated as previously described (Tan et al., 2020). Briefly, caecal content or faeces was homogenised in 0.02μm filtered, sterile PBS (100mg/mL). Homogenate was spun at 500xg for 5 mins at 4°C. Supernatant was collected and subsequently spun at 10 000xg for 20 mins, and then at 18 000xg for 45 mins at 4°C, to exclude cells and larger vesicle populations (including host epithelial microvesicles). Supernatant was filtered with 0.22μm syringe filter (Millipore). Filtrate was spun on an ultracentrifuge (Hitachi CP100NX, P50A3 rotor) at 100 000xg for 2h at 4°C to pellet the extracellular particle fraction. Pellets were resuspended in 0.02μm filtered PBS, aliquoted and frozen at -80℃ before use. MEV doses were either characterised by protein content, using by bicinchoninic (BCA) assay (Sigma Aldrich) or by particle number. MEVs were characterised for particle concentration and size distribution using the NanoSight NS300 (Malvern, UK) and analysed with the NTA 3.2 software.

For transmission electron microscopy (TEM), 4μL of MEVs (10^8-10^{10} particles/mL) in 0.22μm-filtered sterile HEPES were adsorbed on freshly glow-discharged carbon-film

coated 300 mesh copper grids (Ted Pella) for 20min. Grids were fixed with 2% glutaraldehyde for 20min then washed twice in ultrapure water. Samples were stained 2% uranyl acetate for 1min at 4°C in the dark, and excess liquid was blotted with filter paper (Grade 1, Whatman). Grids were air-dried for 10min then visualised on a FEI Tecnai 12 transmission electron microscope (Thermo Fisher) with an accelerating voltage of 120kV. Images were recorded using the Digital Micrograph software with a Gatan Rio 9 camera.

5.2.5 DNA extraction and 16S sequencing

DNA was extracted from either caecal content or faeces using the FastDNA SPIN Kit for Feces (MP Biomedical) according to instructions. MEV DNA was extracted using QIAamp DNA Mini kit (Qiagen). DNA from caecum cellular content and MEV fractions obtained in Figure 5.1 were sent to Genewiz (Suzhou, China) for 16S rRNA library preparation and sequencing of the 16S V3-V4 rRNA gene. Other DNA samples were processed and sequenced at Central Queensland University. The V3–V4 region of the 16S rRNA gene was amplified with Q5® High-Fidelity 2X Master Mix (New England Biolabs) using the Pro341F (5′- CCTACGGGNBGCASCAG -3′) and Pro805R (5′- GACTACNVGGGTATCTAATCC -3′) primers as previously described (Joat et al., 2023). Following amplification, library cleanup was performed using AMPure XP reagent (Beckman Coulter). Amplicon sequencing was done on the Illumina MiSeq system (2x250 bp PE). Data analysis was performed at the Charles Perkins Centre using the dada2 package (1.30.0) in R software (4.3.1) to generate amplicon sequence variants. Downstream analysis was performed with the phyloseq (1.46.0), vegan (2.6-4) and microbiome (1.24.0) R packages.

5.2.6 ELISA

5.2.6.1 Small intestinal secretory Immunoglobulin A

Small intestinal content was collected and stored at -80°C. Content was homogenised (100mg/mL) in PBS with Complete Protease Inhibitor cocktail (Roche). Homogenate was spun 14 000xg for 10mins at 4°C and supernatant collected. Secretory Immunoglobulin A (sIgA) was determined using the Mouse IgA quantitation Set (Bethyl Laboratories), according to manufacturer's instructions.

5.2.6.2 HDM model

Serum total IgE levels were measured, and HDM-restimulated mediastinal lymph node supernatants were analysed for IL-4, IL-5, IL-13 and IFNγ. The antibodies used for coating, detection and standards are listed below in Table 5.1. HRP-Avidin (Biolegend, 405103) was used as the detection antibody and colour development was carried out using TMB Liquid Substrate System (Sigma). Absorbance was measured at 450nm using the Tecan-HP plate reader.

Table 5.1: List of antibodies used for HDM ELISAs

Assay	Antibody	Manufacturer	Cat #
IgE	Purified rat anti-mouse IgE	BD	553413
	Biotin rat anti-mouse IgE	BD	553419
	Purified Mouse IgE κ Isotype Control	BD	557079
IL-4	Purified anti-mouse IL-4	Biolegend	504102
	Biotin anti-mouse IL-4	Biolegend	504202
IL-5	Purified anti-mouse/human IL-5	Biolegend	504302
	Biotin anti-mouse IL-5	Biolegend	504402
IL-13	Purified anti-mouse IL-13	Invitrogen	14-7133-85
	Biotin anti-mouse IL-13	Invitrogen	13-7135-85
IFNγ	Mouse IFN-γ ELISA MAX™ Capture Antibody	Biolegend	79062
	Mouse IFN-γ ELISA MAX™ Detection Antibody	Biolegend	79063

5.2.7 RNA extraction and qPCR analysis

Distal colon tissue was snap frozen at -80°C. Samples were homogenised using a handheld homogeniser (IKA) in TRIzol Reagent (Sigma Aldrich) to extract RNA as per manufacturer's instructions. cDNA was transcribed using 1µg of RNA, with the High-Capacity cDNA Reverse Transcription Kit (ThermoFisher Scientific) according to manufacturer's directions. RT-qPCR was performed on a LightCycler 480 (Roche) using PowerUp™ SYBR™ Green Master Mix (ThermoFisher Scientific) with the primers listed below in Table 5.2, using *Eef2* as housekeeping gene.

Table 5.2: List of primers used in RT-qPCR

Gene	Forward Primer	Reverse Primer
Eef2	TGTCAGTCATCGCCCATGTG	CATCCTTGCGAGTGTCAGTGA
Ocln	AGCGCTATCCTGGGCATCAT	ATCCATCTTTCTTCGGGTTTTCAC
Cldn	CCACTAATGTCGCCAGACCTGAA	CTGGAGATGATGAGGTGCAGAAGA
Tjp1	TCTGAGGGGAAGGCGGATGGTGCT	TTGTGGCTGCGCTTGTGGTGAGTAA
Cramp	CGGTCACTATCACTGCTGCT	TCCAGGTCCAGGAGACGGTA
Muc2	ATTCTGAAGCCTGGGGAGAT	GAAGTCGGGACAGGTGATGT
Spdef	CTATGGCCGCTTCATCCGCT	GTTCTTGCGCACACCCCAC
Klf4	CACACCTGCGAACTCACAC	GGTAGTGCCTGGTCAGTTCA
Tlr2	ACAGCAAGGTCTTCCTGGTTCC	ATCCCTCCACCCTATGACAA
Tlr4	GATCAGAAACTCAGCAAAGTC	TGTTTCAATTTCACACCTGG
Tlr9	TCTCCCAACATGGTTCTC	CTTCAGCTCACAGGGTAG
Ifnγ	GCAAAAGGATGGTGACATGA	TTCGCCTTGCTGTTGCTGA
Il6	CCTCTCTGCAAGAGACTTCCAT	AGTCTCCTCTCCGGACTTGT
Tnf	ATGGCCTCCCTCTCATCAGT	GTTTGCTACGACGTGGGCTA
Il10	AAGGGTTACTTGGGTTGCCA	AAATCGATGACAGCGCCTCAG
Il17	CTGGAGGATAACACTGTGAGAGT	TGCTGAATGGCGACGGAGTTC

5.2.8 Flow cytometry

5.2.8.1 Tissue processing

Spleen, MLN and thymus were collected into flow cytometry buffer (2% FBS, 0.5M EDTA, PBS) and mechanically disrupted using the blunt end of a syringe. Bone marrow cells were isolated by flushing mouse femurs with cold PBS. Erythrocytes were removed from spleen and bone marrow suspensions using 1X RBC Lysis Buffer (Australian Biosearch). Single-cell suspensions were passed through a 100μm mesh filter and resuspended in flow cytometry buffer. Dead cells were excluded by counting with trypan blue (0.4%) on a haemocytometer.

5.2.8.2 Stimulation and staining

For cytokine analysis, 10^6 splenocytes were stimulated with phorbol 12-myristate 13-acetate (PMA) (50ng/mL) (Sigma Aldrich), ionomycin (500ng/mL) (Sigma Aldrich), and brefeldin A (BFA) (5µg/mL) (Sigma Aldrich) in complete media for 4 hours at 37°C 5% CO_2, then washed and stained for surface markers and intracellular cytokines.

Cells were incubated with anti-mouse CD16/32 (Biolegend) to limit non-specific binding and stained for viability using LIVE/DEAD™ fixable Blue Dead Cell Stain (ThermoFisher Scientific), in PBS on ice for 30 minutes. Surface staining was performed for 30 mins in flow cytometry buffer on ice. For intracellular staining of cytokines and FoxP3, cells were fixed and permeabilised using the Foxp3/Transcription Factor Staining Buffer Set (eBioscience), according to manufacturer's instructions. The list of antibodies used for surface and intracellular staining is listed below in Table 5.3.

Samples were run on either LSRII (BD Biosciences) or Aurora (Cytek). Data analysis was conducted using FlowJo software (Treestar Inc. Ashland, OR, USA), following the gating strategies in Supplementary Figures S5.4-10.

Table 5.3: List of antibodies used in flow cytometry

Target	Fluorophore	Manufacturer (Cat#)	Clone	RRID
B220	PE	Biolegend (103208)	RA3-6B2	AB_312993
B220	BUV661	BD (612972)	RA3-6B2	AB_2870244
B220	BUV737	BD (612838)	RA3-6B2	AB_2870160
B220	BV785	Biolegend (103245)	RA3-6B2	AB_11218795
CD117	FITC	Biolegend (105806	2B8	AB_313215
CD117	PE-Cy5	Biolegend (105810)	2B8	AB_313219
CD11b	BUV395	BD (563553)	M1/70	AB_2738276
CD11b	PerCP	Biolegend (101230)	M1/70	AB_2129374
CD11c	APC-Cy7	Biolegend (117324)	N418	AB_830649
CD11c	BV786	BD (563735)	HL3	AB_2738394
CD122	PE-CY7	Biolegend (123216)	TM-β1	AB_2562895
CD127	PE	Biolegend (121112)	SB/199	AB_493509
CD135	PE-CF594	BD (562537)	A2F10.1	AB_2737639
CD150	BV650	Biolegend (115931)	TC15-12F12.2	AB_2562402
CD16/32	FITC	BD (553144)	2.4G2	AB_394659
CD24	Pacific Blue	Biolegend (101820)	M1/69	AB_572011
CD25	BV605	Biolegend (102036)	PC61	AB_2563059
CD3	AF488	Biolegend (100210	17A2	AB_389301
CD3	PerCP	Biolegend (100325)	145-2C11	AB_893319
CD34	BV421	BD (562608)	RAM34	AB_11154576
CD3e	BV711	BD (563123)	145-2C11	AB_2687954
CD4	PerCP	Biolegend (100538)	RM4-5	AB_893325
CD4	BV570	Biolegend (100542)	RM4-5	AB_2563051
CD44	APC-Cy7	Biolegend (103028)	IM7	AB_830785
CD45	BV785	Biolegend (103149)	30-F11	AB_2564590
CD45	AF700	Biolegend (103128)	30-F11	AB_493715
CD5	BV510	Biolegend (100627)	53-7.4	AB_2563930
CD62L	BV421	Biolegend (104436)	MEL-14	AB_2562560
CD64	PE-Cy7	Biolegend 139314)	X54-5/7.1	AB_2563904
CD8	BUV805	BD (612898)	53-6.7	AB_2870186
CD8	BV650	Biolegend (100742)	53-6.7	AB_2563056
CD8	BV711	Biolegend (100759)	53-6.7	AB_2563510
CD8a	BV785	Biolegend (100750)	53-6.7	AB_2562610
F4/80	PE-Cy7	Biolegend (123114)	BM8	AB_893478
FoxP3	APC	Miltenyi (130-111-601)	REA788	AB_2651768
IFNγ	BV650	Biolegend (505832)	XMG1.2	AB_2734492
IL10	PE	Biolegend (505008)	JES5-16E3	AB_315362
IL17	PE-CY7	Biolegend (506922)	TC11-18H10.1	AB_2125010
Ly6C	BV605	Biolegend (128036)	HK1.4	AB_2562353
Ly6G	APC	Miltenyi (130-120-803)	REA526	AB_2752201
Ly6G	BV650	Biolegend (127641)	1A8	AB_2565881
MHCII	BV510	Biolegend (107636)	M5/114.15.2	AB_2734168
MHCII	Pacific Blue	Biolegend (107620)	M5/114.15.2	AB_493527
NK1.1	PE-Cy7	Biolegend (108714)	Pk136	AB_389364
SCA-1	BV711	BD (744326)	E13-161.7	AB_2742154
Siglec-F	PE	Biolegend (155506)	S17007L	AB_2750235
TCRγδ	PE-Cy5	eBioscience (15-5711-82)	GL3	AB_468804

5.2.9 Statistics

Comparison between two groups was performed using GraphPad Prism software (La Jolla, CA, USA), using either Mann-Whitney U-test or Unpaired t-test. For comparisons involving three groups, one-way ANOVA was used with Tukey's multiple comparison test. Values with $p<0.05$ were considered statistically significant, with *$p<0.05$; **$p<0.01$; ***$p<0.005$; ****$p<0.001$.

5.3 Results

5.3.1 MEVs represent a distinct component of the gut microbiota

While the bacterial composition of the gut microbiota and its influence on host physiology has been well-studied, the contribution of MEVs to the gut-host signalling axis is less understood. To investigate the role of MEVs in the gut microbiota, we isolated MEVs from caecal content of specific-pathogen-free mice (n=6), by differential centrifugation and filtration as previously described (Tan et al., 2020). We first characterised the MEV fraction using nanoparticle tracking analysis and transmission electron microscopy (TEM) (**Figure 5.1A, B**) to confirm their size distribution, concentration, and morphology. We observed that MEVs primarily ranged in size from 100 - 300nm, with a peak size of 141 nm (**Figure 5.1A**), in accordance with typically reported characteristics (Toyofuku et al., 2023, 2019). TEM confirmed the presence of spherical vesicular structures in our isolate, consistent with MEV morphology (**Figure 5.1B**).

Previous studies have demonstrated that gut MEVs possess a distinct composition to the gut microbiota itself (Chelakkot et al., 2018; Choi et al., 2015; Li et al., 2023). Hence, to

compare bacterial composition we performed 16S rRNA sequencing on caecal content samples to compare the cellular and the isolated MEV fraction. Principal component analysis (PCA) revealed distinct clustering between caecal cellular and MEV fractions (**Figure 5.1C**), indicating the two indeed have distinct bacterial signatures. We then examined measures of alpha diversity, including richness, evenness, and Shannon's Diversity Index and Inverse Simpson Index (**Figure 5.1D**). MEV samples had significantly reduced species richness compared to caecal content, suggesting that fewer unique species contribute to the composition of MEVs in the gut. While Shannon's Diversity Index ($p=0.0649$) and Inverse Simpson's Index ($p=0.0931$) trended towards a decrease in the MEV fraction, species evenness was comparable between fractions. Together, this suggests that while not all bacteria in the gut microbiota produce MEVs, those that do, contribute evenly to the overall MEV fraction.

To assess the taxa contributing to the release of MEV, we then compared bacterial composition at the phyla and genus level (**Figure 5.1E**). At the phyla level, both the cellular fraction and MEVs were primarily composed of *Bacteroidetes* and *Firmicutes*, however, MEVs had significantly increased *Firmicutes* to *Bacteroidetes* ratio and a greater enrichment in *Proteobacteria,* which could reflect a differing capacity of the major bacterial phyla to produce MEVs. At the genus level we observed more striking compositional differences (**Figure 5.1E**). The cellular fraction comprised mostly of *Barnesiella* followed by *Alistipes*. In contrast, MEVs showed dramatically reduced abundance of *Barnesiella*, and an enrichment in several genera including *Clostridium IV, Bacteroides, Oscilobacter, Pseudoflavonifractor* and *Alloprevotella*. Notably, some genera that were of very low abundance in the cellular fraction, such as *Clostridium XIVb* and

Anaerotruncus (both *Firmicutes* phyla), were enriched in MEVs, suggesting increased vesicle production by these genera.

Interestingly, when genera were classified by Gram-positive or Gram-negative status, we identified that while the cellular fraction of the microbiota was predominantly Gram-negative, MEVs showed a more balanced representation with approximately equal representation between Gram-negative and Gram-positive genera (**Figure 5.1F**). Although vesiculogenesis in Gram-negative bacteria is well-characterised and more widely studied than in Gram-positives, there is a general assumption that Gram-negative bacteria produce vesicles more readily than Gram-positives, as they lack a thick outer peptidoglycan layer (Briaud and Carroll, 2020; Xu et al., 2023). Our results suggest that within the gut environment, both Gram-positives and Gram-negatives contribute significantly to the MEV pool. A range of environment factors in the gut, such as fluctuations in nutrients, host defense factors, and exposure to antimicrobials (e.g. antibiotics or food additives), may trigger different vesiculation responses across bacterial species (Taitz et al., 2023), highlighting the need for further investigation into how MEVs are regulated *in vivo*.

Altogether, these findings confirm that under homeostatic conditions, the gut microbiota contains an MEV component which has a distinct bacterial signature to the cellular fraction, consistent with recent findings (Kaisanlahti et al., 2025)**.** Altogether, this data highlights that the abundance of taxa at the cellular level may not reflect the "secretome" of gut microbiota, as some taxa may be more prolific producers of immunomodulatory particles such as MEVs.

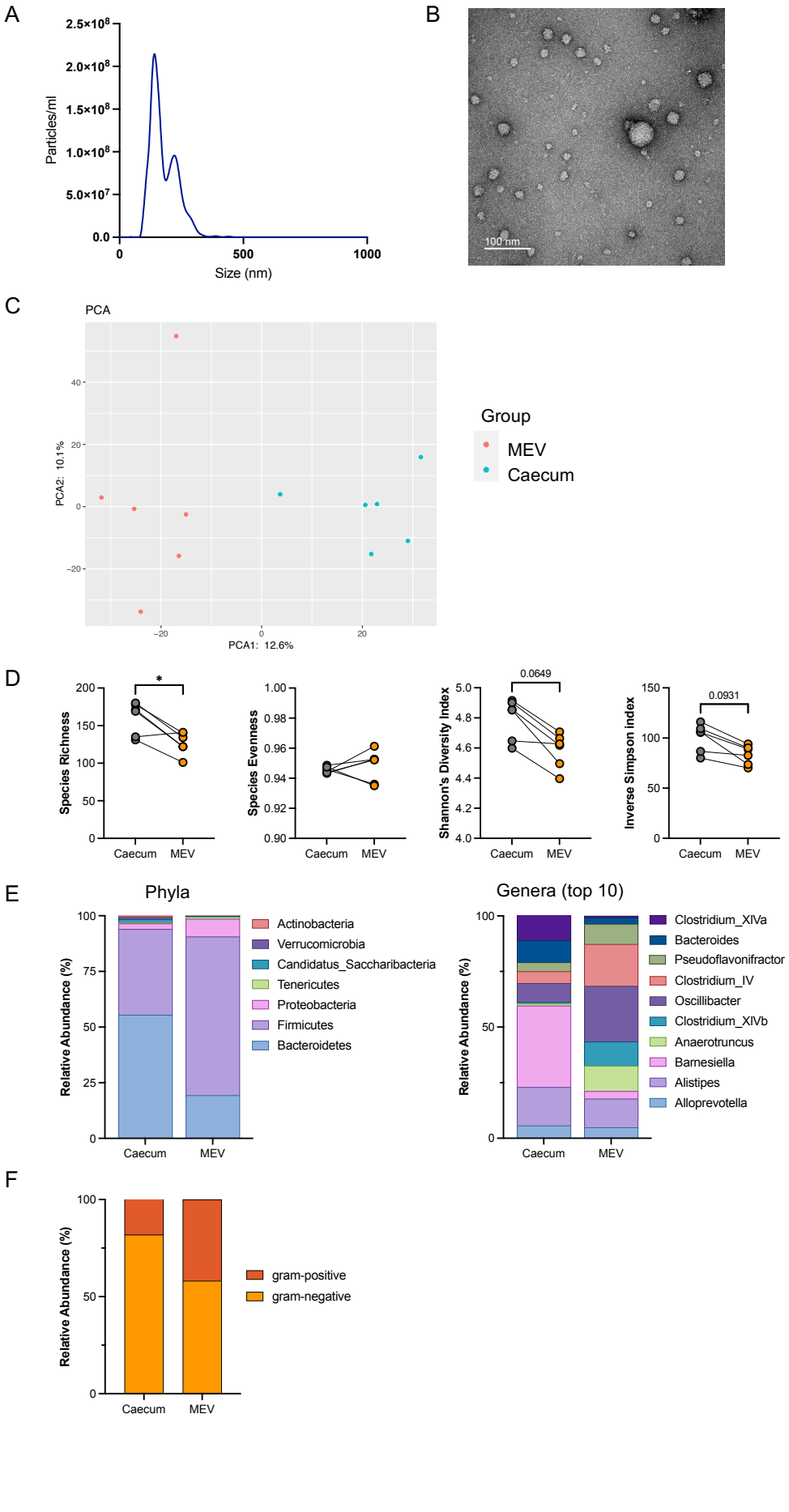
A
Particles/ml
Size (nm)
B
100 nm
C
PCA
PCA2: 10.1%
PCA1: 12.6%
Group
MEV
Caecum
D
Species Richness
Species Evenness
Shannon's Diversity Index
Inverse Simpson index
0.0649
0.0931
Caecum
MEV
E
Phyla
Relative Abundance (%)
Actinobacteria
Verrucomicrobia
Candidatus_Saccharibacteria
Tenericutes
Proteobacteria
Firmicutes
Bacteroidetes
Genera (top 10)
Clostridium_XlVa
Bacteroides
Pseudoflavonifractor
Clostridium_IV
Oscillibacter
Clostridium_XlVb
Anaerotruncus
Barnesiella
Alistipes
Alloprevotella
F
gram-positive
gram-negative

Figure 5.1 The caecum possesses an MEV fraction with a distinct 16S bacterial signature

Caecal content from specific-pathogen-free mice (n=6) was separated into a cellular and MEV fraction via differential centrifugation and filtration, and each fraction was subsequently characterised. (**A**) Representative size and concentration profile of caecal MEVs, as characterised by Nanosight NS300. (**B**) Representative TEM image of caecal MEVs showing presence of vesicular structures. (**C**) DNA was extracted from cellular and MEV fraction for bacterial 16S rRNA analysis. Principal component analysis (PCA) plots of caecum cellular and MEV fractions. (**D**) Alpha diversity measures of observed species richness, evenness, Shannon's Diversity Index, and Inverse Simpsons index, of caecal cellular vs the corresponding MEV fraction. (**E**) Relative abundance of phyla (left) and top 10 genera (right) between cellular and MEV fractions. (**F**) Relative abundance of Gram-positive and Gram-negative genera in cellular or MEV fraction of caecum. Data are shown as mean $\pm$ SEM, with n=6 caecal and MEV samples. *p<0.05, by Mann-Whitney U test.

5.3.2 Exogenous MEV administration modulates gut microbiota composition

Having established that MEVs represent a distinct taxonomic fraction of the gut microbiota, we next investigated whether exogenously administered MEVs could modulate gut microbiota composition. Bacterial composition of the gut microbiota is shaped by various factors, including host secretory defences (such as secretory IgA (sIgA) and antimicrobial peptides), female sex hormones (Kaliannan et al., 2018), and bacterial-derived components (such as metabolites and defence mechanisms) which mediate the competitive interactions between species. MEVs play a critical role in bacteria-to-bacteria interactions and have been shown to facilitate specific functions such as the dissemination of nutrient-digesting enzymes that support cross-feeding (Elhenawy et al., 2014). However, whether they have a role in directly modulating gut bacterial composition under homeostatic conditions is unknown.

To investigate this, we gavaged isolated MEVs or PBS to male C57BL/6 mice daily for 5 weeks (**Figure 5.2A**). We then collected faeces and analysed the gut microbiota composition by 16S rRNA sequencing between PBS and MEV-exposed mice.

PCA revealed PBS- and MEV-treated mice clustered separately, indicating that MEV administration significantly alters the structure of the gut microbiota (**Figure 5.2B**). MEVs also led to a significant reduction across alpha diversity measures (**Figure 5.2C**). Richness was significantly decreased in MEV-treated mice, suggesting that MEVs can reduce the unique number of species present. Evenness showed a trend towards reduction ($p=0.0571$), while Shannon's Diversity and Inverse Simpson indices were significantly reduced in MEV-treated mice (**Figure 5.2C**). Overall, these results suggests

that MEV treatment substantially alters gut microbiota composition, reducing overall bacterial diversity in adult mice.

We further assessed composition at the phylum and genus level (**Figure 5.2D**). At the phylum level, MEV administration increased the *Firmicutes/Bacteroidetes* ratio, reflecting the composition of the MEV fraction itself. Although controversial, the *Firmicutes* to *Bacteroidetes* ratio has been proposed as a marker of gut microbiota "health", with an increased ratio often associated with obesity and other metabolic diseases (Magne et al., 2020). The abundance of the other major phyla, *Actinobacteria* and *Verrucomicrobia* were comparable between groups, suggesting that MEV treatment influences specific phyla while leaving others unaffected. Examination of the top 10 genera showed that MEV mice had enrichment in *Bifidobacterium* and decreased abundance of *Olsenella*. Several other genera, such as *Acetatifactor, Akkermansia, Lactococcus*, as well as low-abundant genera such as *Parabacteroides, Dorea* and *Sporobacter* maintained similar abundance with PBS mice, again suggesting that the impact of MEVs is taxa-specific. Finally, we identified MEV administration had no impact on the proportions of Gram-negative or Gram-positive genera (**Figure 5.2E**).

Overall, these findings demonstrate that administration of MEVs, a taxonomically distinct component of the gut microbiota, can actively modulate the gut microbiota composition in adult mice at steady-state, reducing overall diversity and selectively impacting particular taxa.

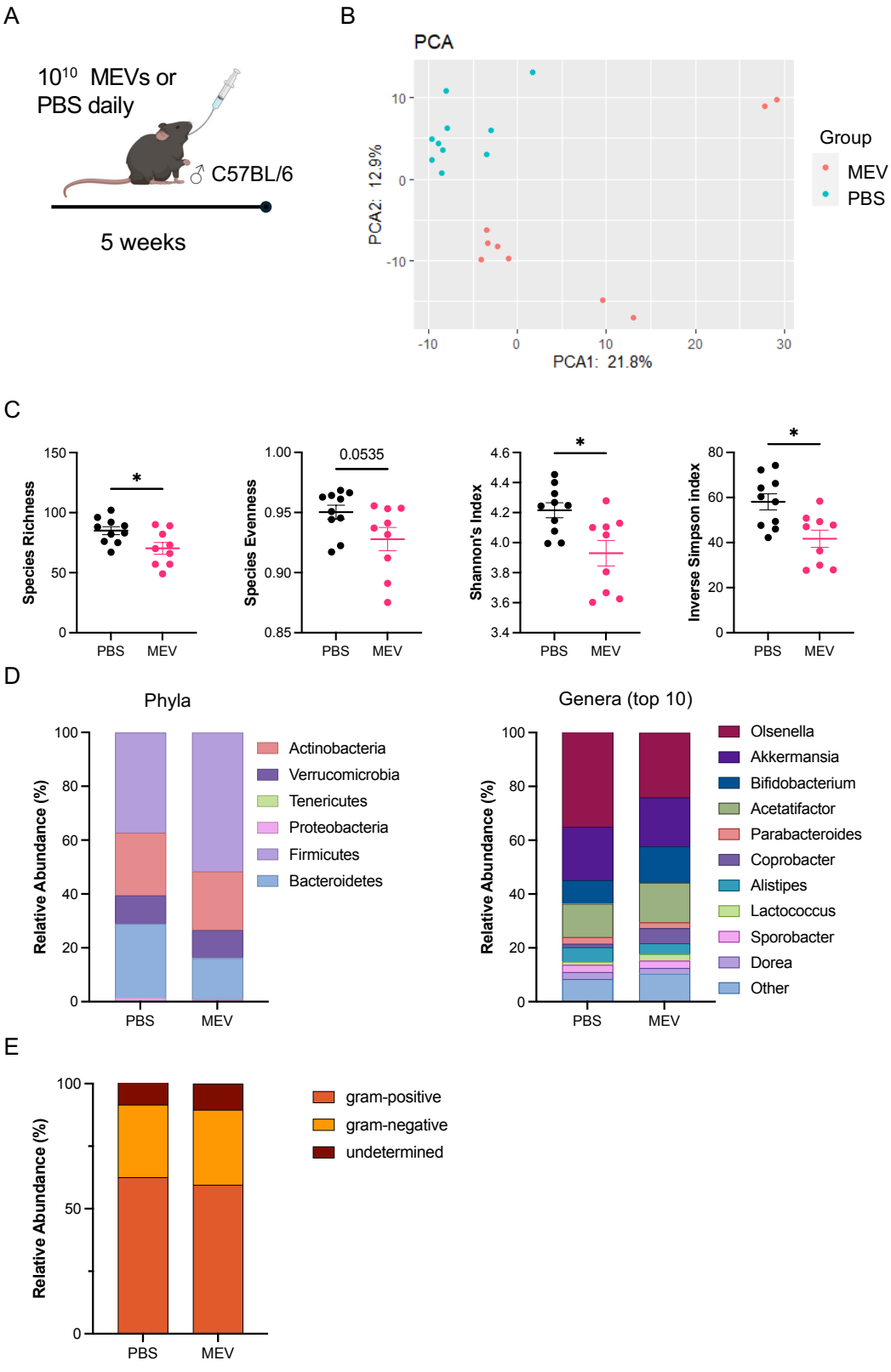
A
10^{10} MEVs or PBS daily
C57BL/6
5 weeks
B
PCA
PCA2: 12.9%
PCA1: 21.8%
Group
MEV
PBS
C
Species Richness
Species Evenness
0.0535
Shannon's Index
Inverse Simpson index
PBS
MEV
D
Phyla
Relative Abundance (%)
Actinobacteria
Verrucomicrobia
Tenericutes
Proteobacteria
Firmicutes
Bacteroidetes
Genera (top 10)
Olsenella
Akkermansia
Bifidobacterium
Acetatifactor
Parabacteroides
Coprobacter
Alistipes
Lactococcus
Sporobacter
Dorea
Other
E
gram-positive
gram-negative
undetermined

Figure 5.2 MEV administration alters microbiota profile in healthy mice

(**A**) Experimental design: C57BL/6 (n=10/group) male mice were orally gavaged 10^{10} MEVs (or PBS control) daily for 5 weeks. Faeces was collected and 16S rRNA sequencing was performed to assess changes in microbiota composition. (**B**) Principal component analysis (PCA) plot showing faeces from PBS- and MEV- gavaged mice. (**C**) Alpha diversity measures of observed species richness, evenness, Shannon's Diversity Index, and Inverse Simpsons index, of PBS or MEV-gavaged mice. (**D**) Relative abundance of phyla (left) and top 10 genera (right). (**E**) Relative abundance of Gram-positive and Gram-negative genera. Data are shown as mean $\pm$ SEM. *p<0.05, by Mann-Whitney U test.

5.3.3 Exogenous MEV exposure in gestation influences offspring microbiota composition

Having demonstrated that MEVs can modulate gut bacterial composition in adult mice, we next investigated whether MEV exposure during gestation, a critical developmental window, could have a measurable effect on offspring's gut bacterial composition. Although diet and environmental factors predominantly shape gut microbiota composition, research indicates that it is also influenced by heritable factors, which include maternal effects (including vertical transmission of the microbiota) and the host's genetic background (Grieneisen et al., 2021; Knoop et al., 2018). To investigate whether MEV-mediated modulation of gut bacterial composition could have a transgenerational effect, we orally administered 60μg of faeces-derived MEVs (or PBS) to female C57BL/6 mice during gestation (E0-E19) (**Figure 5.3A**). Pregnancies were timed to ensure litters were born within a 48-72 hour period. To control for postnatal influences, such as breastfeeding and early-life maternal impacts, all offspring litters were fostered to PBS-treated dams within 48 hours of birth, to normalise microbial exposure and composition. To determine how gestational MEV exposure may shape early-life microbiota development, gut bacterial composition was then examined immediately prior to weaning (postnatal day 21, PN21), which represents a milestone of significant increase in gut microbiota complexity and immune maturation (Nabhani et al., 2019).

PCA demonstrated distinct clustering between MEV- and PBS-exposed offspring (**Figure 5.3B**), suggesting that gestational MEV exposure has a fundamental impact on offspring gut bacteria composition. While MEVs resulted in a distinct composition, we observed no significant differences in alpha diversity measures between MEV and PBS offspring

(**Figure 5.3C**). This suggests that while gestational MEV exposure shapes bacterial composition, it does not appear to influence overall diversity.

At the phylum and genus level, however, we observed significant differences between PBS and MEV offspring (**Figure 5.3D**). Gestational MEV exposure resulted in offspring with a significant reduction in *Firmicutes*/*Bacteroides* ratio compared to PBS offspring, and in contrast with MEV exposure in adulthood. There was also a notable enrichment in *Verrucomicrobia* in MEV offspring, suggesting MEVs may have distinct effects on bacterial composition at different stages of life. At the genus level, MEV offspring were enriched in *Parabacteorides* and *Akkermansia*, both considered to have beneficial effects on host and intestinal health (Cui et al., 2022; Ezeji et al., 2021; Pellegrino et al., 2023). PBS offspring had a microbiota predominantly comprising the genera *Lactobacillus*, also associated with beneficial health effects (Huang et al., 2022)**.** Finally, we found that while PBS offspring had a microbiota predominantly comprising Gram-positive taxa, gestational MEV exposure resulted in a dramatic shift towards Gram-negatives (**Figure 5.3E**).

Altogether these data demonstrate that gestational MEV exposure may shape microbiota composition of the offspring independently of post-natal factors such as breastfeeding or environmental exposure. This highlights a potential novel role of maternally-derived MEVs in influencing the early-life gut microbiota colonisation of the offspring.

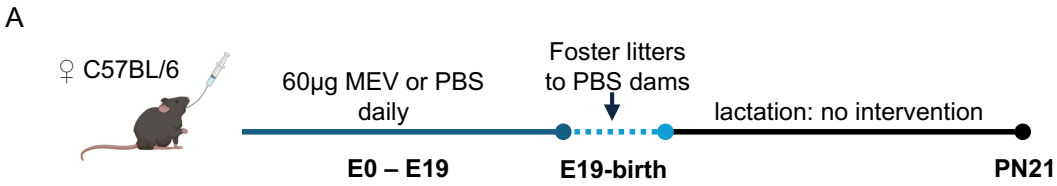
A
♀ C57BL/6
60µg MEV or PBS daily
Foster litters to PBS dams
lactation: no intervention
E0 – E19
E19-birth
PN21

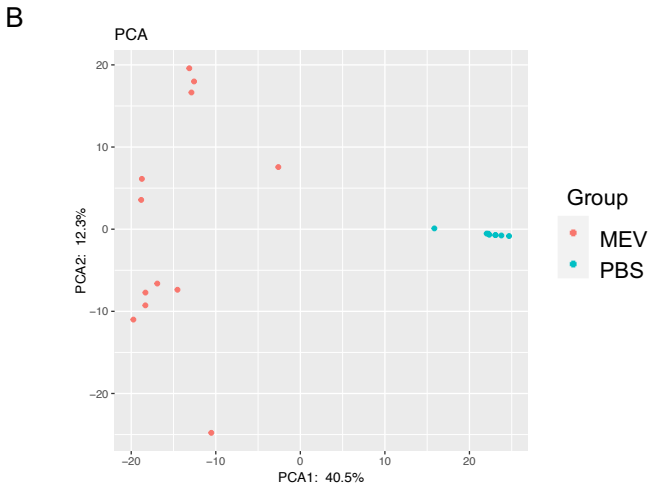
B
PCA
PCA2: 12.3%
PCA1: 40.5%
Group
MEV
PBS

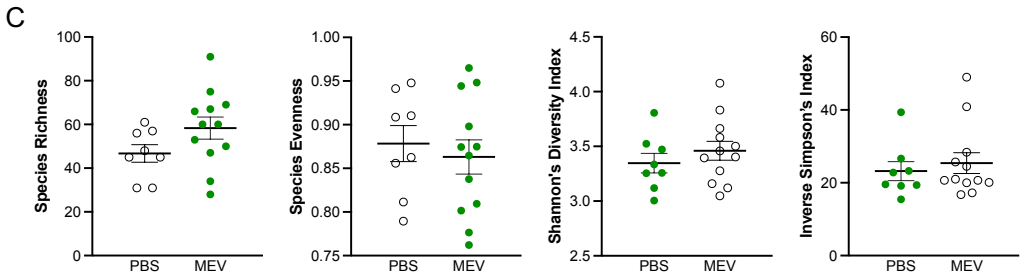
C
Species Richness
Species Evenness
Shannon's Diversity Index
Inverse Simpson's Index
PBS
MEV

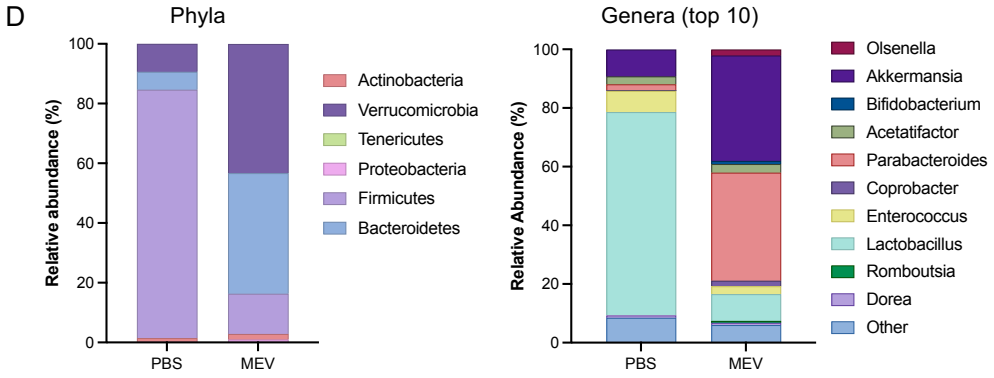
D
Phyla
Relative abundance (%)
Actinobacteria
Verrucomicrobia
Tenericutes
Proteobacteria
Firmicutes
Bacteroidetes
Genera (top 10)
Relative Abundance (%)
Olsenella
Akkermansia
Bifidobacterium
Acetatifactor
Parabacteroides
Coprobacter
Enterococcus
Lactobacillus
Romboutsia
Dorea
Other
PBS
MEV

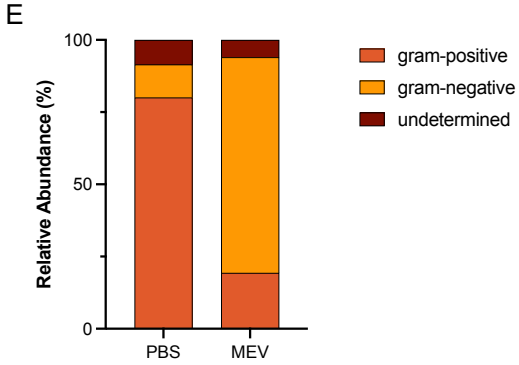
E
Relative Abundance (%)
gram-positive
gram-negative
undetermined
PBS
MEV

Figure 5.3 Gestational MEV exposure alters microbiota profile in healthy offspring

(**A**) Experimental design. Pregnant C57/BL6 mice were gavaged 60μg of MEVs, or PBS control, daily during E0-E19 of gestation. Within 48 hours of birth, offspring litters were fostered to PBS-treated dams and left untreated throughout the lactation period. At PN21, offspring were euthanised, and faeces were collected for 16S rRNA sequencing. (**B**) Principal component analysis (PCA) plot showing MEV- and PBS-exposed offspring. (**C**) Alpha diversity measures of observed species richness, evenness, Shannon's Diversity Index, and Inverse Simpsons index. (**D**) Relative abundance of phyla (left) and top 10 genera (right) between PBS and MEV-exposed mice. (**E**) Relative abundance of Gram-positive and Gram-negative genera. Data are shown as mean ± SEM

5.3.4 Gestational MEV exposure programs intestinal barrier gene expression

Since gestational MEV exposure resulted in dramatically altered offspring microbiota composition despite postnatal normalisation by cross-fostering, we investigated potential underlying mechanisms behind this. Diet, a major regulator of composition, was consistent across groups. MEVs present in amniotic fluid may make direct contact with the developing fetal gut (Kaisanlahti et al., 2023), therefore we focused on internal characteristics of the offspring's gut microenvironment that could influence colonisation patterns in early life.

sIgA is a key host factor that can regulate microbiota composition and diversity, and previously we found increased gut MEV levels boost host sIgA secretion in adult male mice (Tan et al., 2020). However, analysis revealed no differences in small intestinal sIgA levels between offspring groups (**Figure 5.4A**). However, as our analysis was conducted immediately before weaning (PN21), when infant mice begin producing endogenous sIgA, the low levels detected likely reflect maternally-derived antibodies from milk (Guo et al., 2021).

Next, to assess whether gut barrier properties may have influenced colonisation, we examined colonic gene expression via RT-qPCR as a readout for potential changes in the gut microenvironment. Gestational MEV exposure significantly enhanced genes related to intestinal barrier integrity, upregulating tight junction proteins *Tjp1* and *Ocln*, with *Cldn1* showing a similar trend (p=0.0977) (**Figure 5.4B**). *Klf4*, a key transcriptional regulator of intestinal epithelial differentiation was also significantly upregulated

(**Figure 5.4B**). Altogether this suggests MEV exposure enhances colonic epithelial barrier integrity, which may contribute to preferential colonisation of specific bacterial taxa.

Despite the enrichment of the mucus-dwelling and mucolytic *Akkermansia* spp. in MEV offspring, surprisingly, we observed no change in genes associated with mucus production (*Muc2*) or goblet cell differentiation (*Spdef*) (**Figure 5.4C**), suggesting factors beyond mucin-related genes regulate *Akkermansia* abundance. Similarly, we found no change in the expression of *Cramp* (**Figure 5.4C**), which encodes the mouse homolog of human cathelicidin, a major colonic antimicrobial peptide important for controlling bacteria near the epithelial surface (Iimura et al., 2005).

We next examined expression of toll-like receptors (TLRs), a subset of PRRs that, along with other PRRs, contribute to shaping gut bacterial composition through feedback mechanisms and genetic variations in signalling cascades (Chu and Mazmanian, 2013; Kubinak and Round, 2012). In humans, TLR dysregulation is associated with inflammatory bowel disease (IBD), and loss-of-function mutations in the PRR *NOD2* lead to dysbiosis that drives a severe Crohn's disease phenotype (Kordjazy et al., 2018; Lauro et al., 2016). We observed inverse regulation of *Tlr2* and *Tlr4*, which recognise the major cell wall components of Gram-positive and Gram-negative bacteria, respectively. While *Tlr2* expression was significantly decreased in MEV offspring, *Tlr4* was upregulated (**Figure 5.4D**). This expression level also correlated with taxonomic composition, as MEV offspring were enriched in Gram-negatives (*Akkermansia* and *Parabacteroides*) while PBS offspring were enriched with the Gram-positive taxon *Lactobacillus*. Additionally, *Tlr9*, which senses bacterially-derived DNA was dramatically upregulated in MEV offspring, showing a 2-fold increase. Whether these alterations to TLR expression drove the distinct

colonisation patterns observed between MEV and PBS offspring, or resulted from them, remains unclear. However, these processes likely exist in a dynamic and complex feedback relationship, warranting further investigation.

Finally, we examined expression of key cytokines IL-6, IFNγ, TNF and IL-17, which serve multifaceted roles in regulating intestinal homeostasis and immune responses, as well as the cytokine IL-10, which is a critical mediator of anti-inflammatory pathways. We observed all genes encoding for these cytokines were significantly upregulated in MEV offspring, except IL-10, which was unchanged (**Figure 5.4E**). These findings suggest enhanced activation of mucosal immunity, with a potential pro-inflammatory bias, which could shape microbiota composition by regulation of the intestinal barrier and the recruitment and activation of gut immune cells.

Altogether, these data demonstrate that gestational MEV exposure programs colonic gene expression across pathways involved in barrier integrity, bacterial recognition, and cytokine signalling. Although individual gene fold-changes were modest (<2 fold) and protein-level validation was not performed in this experiment, the alterations in multiple genes across these pathways suggests a cohesive biological response to MEV exposure *in utero*. Collectively, these changes may drive differences in colonisation patterns, highlighting a novel mechanism through which maternal MEVs may condition the fetal gut microenvironment.

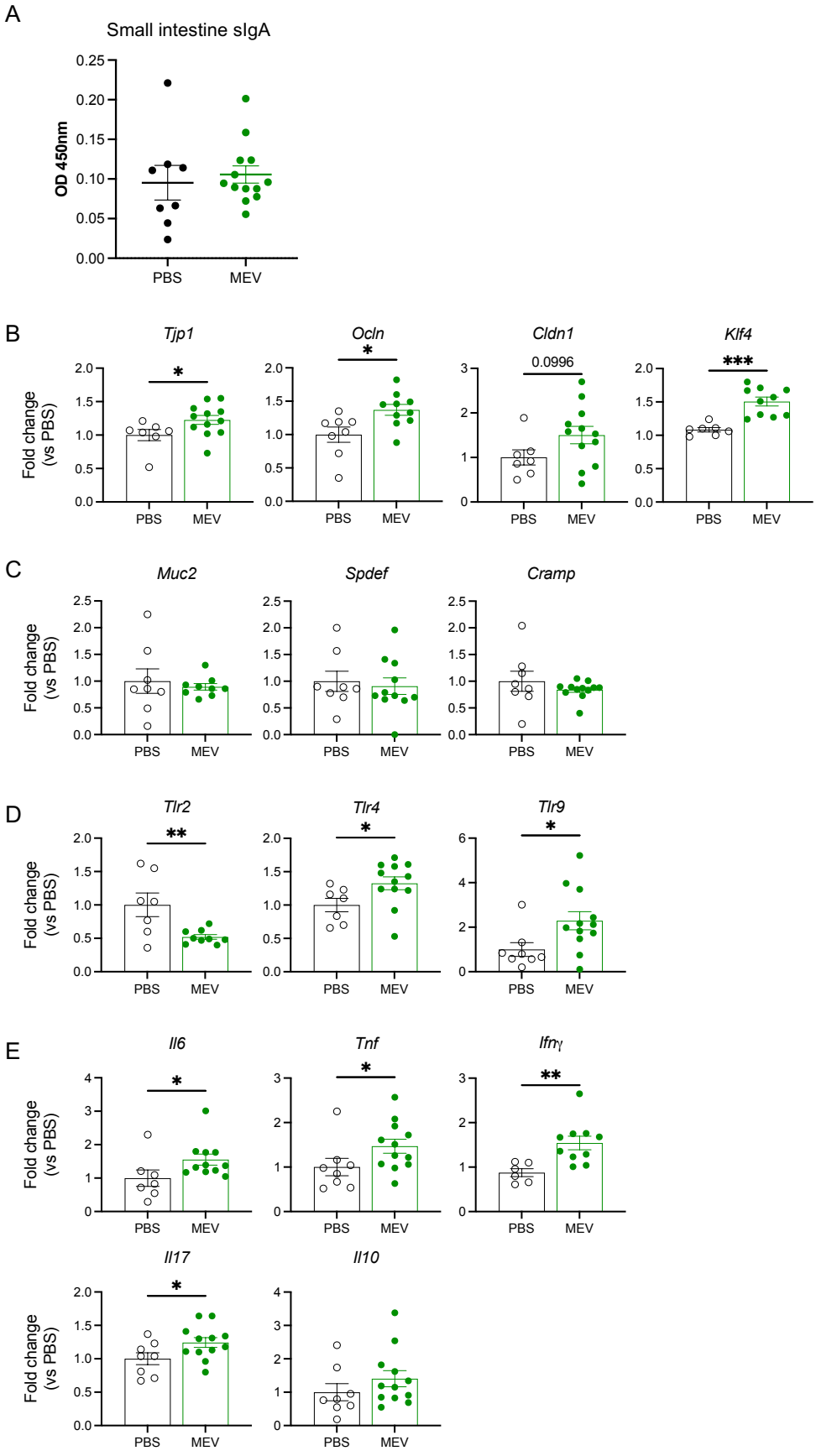
A
Small intestine sIgA
OD 450nm
0.25
0.20
0.15
0.10
0.05
0.00
PBS
MEV
B
Tjp1
Ocln
Cldn1
Klf4
0.0996
***
Fold change (vs PBS)
C
Muc2
Spdef
Cramp
D
Tlr2
Tlr4
Tlr9
E
Il6
Tnf
Ifnγ
Il17
Il10

Figure 5.4 Gestational MEV exposure alters colonic gene expression

Pregnant C57/BL6 mice were gavaged 60μg of MEVs, or PBS control, daily during E0-E19 of gestation. Within 48 hours of birth, offspring litters were fostered to PBS-treated dams and left untreated throughout the lactation period. At PN21, offspring were euthanised for tissue collection. (**A**) Levels of small intestinal secretory Immunoglobulin A (sIgA) as determined by ELISA. Distal colonic tissue was assessed for gene expression for (**B**) *Tjp1*, *Ocln, Cldn1, Klf4*, (**C**) *Muc2, Spdef, Cramp*, (**D**) *Tlr2, Tlr4, Tlr9*, E *Il6, Tnf, IFNγ, Il17, Il10*, as measured by RT-qPCR. Data are shown as mean ± SEM. *p<0.05, **p<0.01, ***p<0.001, ****p<0.0001 by Mann-Whitney U test or Unpaired t-test

5.3.5 Gestational MEVs influence offspring spleen and MLN immune profile

Given our findings of MEV-mediated programming within the gut, we next investigated whether gestational MEV exposure could have a broader impact on offspring immune development. To do this, we examined the immune cell profiles of four major lymphoid compartments: spleen, thymus, bone marrow, and gut-draining mesenteric lymph nodes (MLNs), using flow cytometry (**Figure 5.5**) according to the gating strategies in Supplementary Figures 4 - 9.

Analysis of the total cellularity among these compartments revealed MEV offspring had significantly increased cell numbers in the spleen and MLNs, while thymus and bone marrow cellularity were unchanged (**Figure 5.5A**). Examining the spleen in further detail, we found increased proportions of red pulp macrophages, plasmacytoid DCs (pDCs) and conventional DCs (cDCs), $CD8^+$ T cells and Tregs in MEV offspring, while proportions of $Ly6C^{int}$ monocytes and neutrophils showed a decrease (**Figure S5.1A, B**). For absolute numbers, we observed MEV offspring had a significant increase in multiple innate and adaptive populations including B cells, T cells, natural killer (NK) cells, red pulp macrophages, $Ly6C^+$ monocytes, cDCs and pDCs (**Figure 5.5B**). We also observed a non-significant increase in $Ly6C^-$ monocytes ($p=0.0506$), however, $Ly6C^{int}$ monocytes and neutrophils were unchanged (**Figure 5.5B**). Closer examination of T cell lineages revealed significant increases in $CD4^+$ $CD8^+$, Tregs and $TCR\gamma\delta^+$ subset numbers (**Figure 5.5C**).

In the MLNs, we observed minor changes in proportions, with an increase in B cells and decrease in $CD4^+$ T cells in MEV offspring (**Figure S5.2A, B**). Cell numbers, however, were

globally increased, across B cells, NK cells, natural killer T (NKT) cells and T cell subsets (**Figure 5.5D, E**). While analysis of bone marrow and thymus revealed several changes in cell frequencies, there were no significant differences in the absolute numbers of differentiated cells or progenitor populations (**Figure S5.3A-D**).

Altogether, these findings reveal that gestational MEV exposure selectively enhances innate and adaptive immune cell populations in the spleen and MLNs, while leaving primary lymphoid organs unaffected. This suggests that maternal MEVs may influence immune system development potentially through a post-lymphopoiesis-acting mechanism, rather than one that shapes haematopoiesis or thymopoiesis.

We next characterised peripheral T cell subsets further using markers for naïve, activated and memory cells. Across all T cell lineages, MEV-offspring had increased absolute numbers of these cells in both the spleen and MLNs, with only activated $CD8^+$ T cells in the MLNs remaining unchanged (**Figure 5.5F, G**).

Analysis of T cell subset frequencies revealed distinct distribution patterns across peripheral lymphoid organs. In the spleen, MEV offspring maintained similar proportions of naïve cells across all subsets, while showing increased frequencies of activated and memory $CD8^+$ cells and activated $CD4^+$ cells (**Figure S5.1C**). This expansion of activated and memory cells without alterations to the naïve cell pool, suggests MEVs may induce greater immune competence in this organ, rather than a pathological activation.

The MLNs showed varied changes to T cell frequencies for MEV offspring. $CD4^+$ T cells were decreased for naïve cells and trended towards decreased for activated cells

(p=0.0847) (**Figure S5.2C**). $CD8^+$ T cells and $TCR\gamma\delta^+$ cells showed decreased frequencies of activated cells but increased memory cells, while naïve cells were also increased in $TCR\gamma\delta^+$ cells (**Figure S5.2C**).

These findings reveal that gestational MEV exposure globally expands T cell populations in both the spleen and MLNs, while inducing distinct effects on T cell composition between the two organs examined. This selectivity suggests that maternal MEVs may modulate offspring immune development in a tissue-specific manner.

Finally, we assessed the functional consequences of gestational MEV exposure on offspring T cells, by stimulating splenocytes *ex vivo* with PMA/ionomycin and analysing cytokine expression using flow cytometry (**Figure 5.5H, I**). MEV exposed offspring showed enhanced IFNγ production across multiple T cell subsets, with significant increases in $TCR\gamma\delta^+$, $CD8^+$ and $CD8^-CD25^+$ (putative $CD4^+$ T cells) populations (**Figure 5.5H**). We also observed IL-17 expression was slightly decreased in $TCR\gamma\delta^+$ cells, while IL-10 trended towards increase in $CD8^-CD25^+$ (putative $CD4^+$ T cells) (p=0.0853) (**Figure 5.5I**). This data suggests that gestational MEV exposure primes offspring T cells towards greater IFNγ production across multiple lineages, which may suggest development of an enhanced Type 1 (Th1) immune response.

Collectively, this data demonstrates that gestational MEV exposure not only expands innate and adaptive cell populations in secondary lymphoid organs, but also enhances their functional capacity, particularly through increased IFNγ production. This reveals a novel mechanism through which the maternal gut microbiota can shape offspring immunity via MEVs, which may influence long-term offspring health.

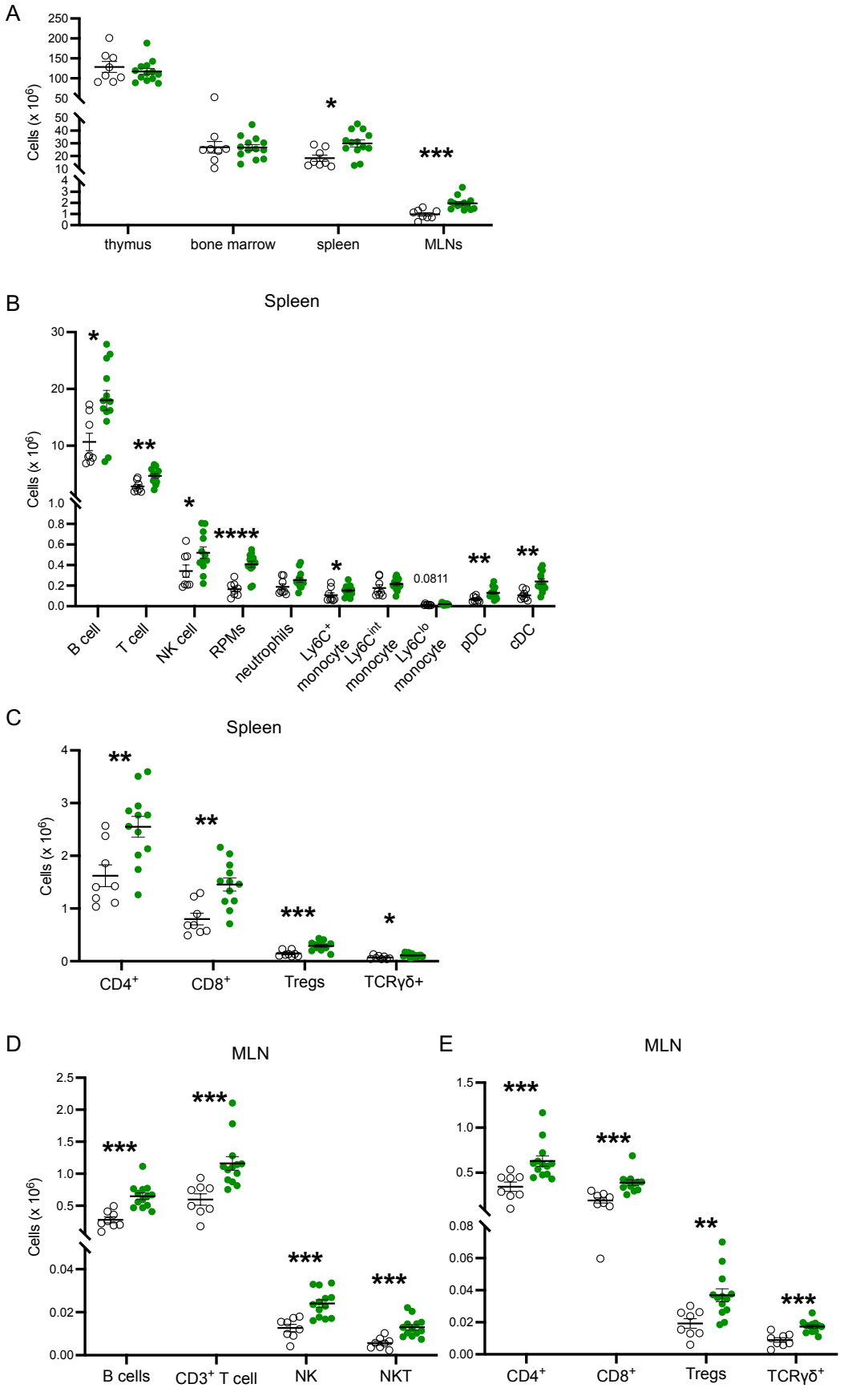
A
Cells (x 10^6)
thymus
bone marrow
spleen
MLNs
B
Spleen
Cells (x 10^6)
B cell
T cell
NK cell
RPMs
neutrophils
Ly6C+ monocyte
Ly6Cint monocyte
Ly6Clo monocyte
pDC
cDC
0.0811
C
Spleen
Cells (x 10^6)
CD4+
CD8+
Tregs
TCRγδ+
D
MLN
Cells (x 10^6)
B cells
CD3+ T cell
NK
NKT
E
MLN
CD4+
CD8+
Tregs
TCRγδ+

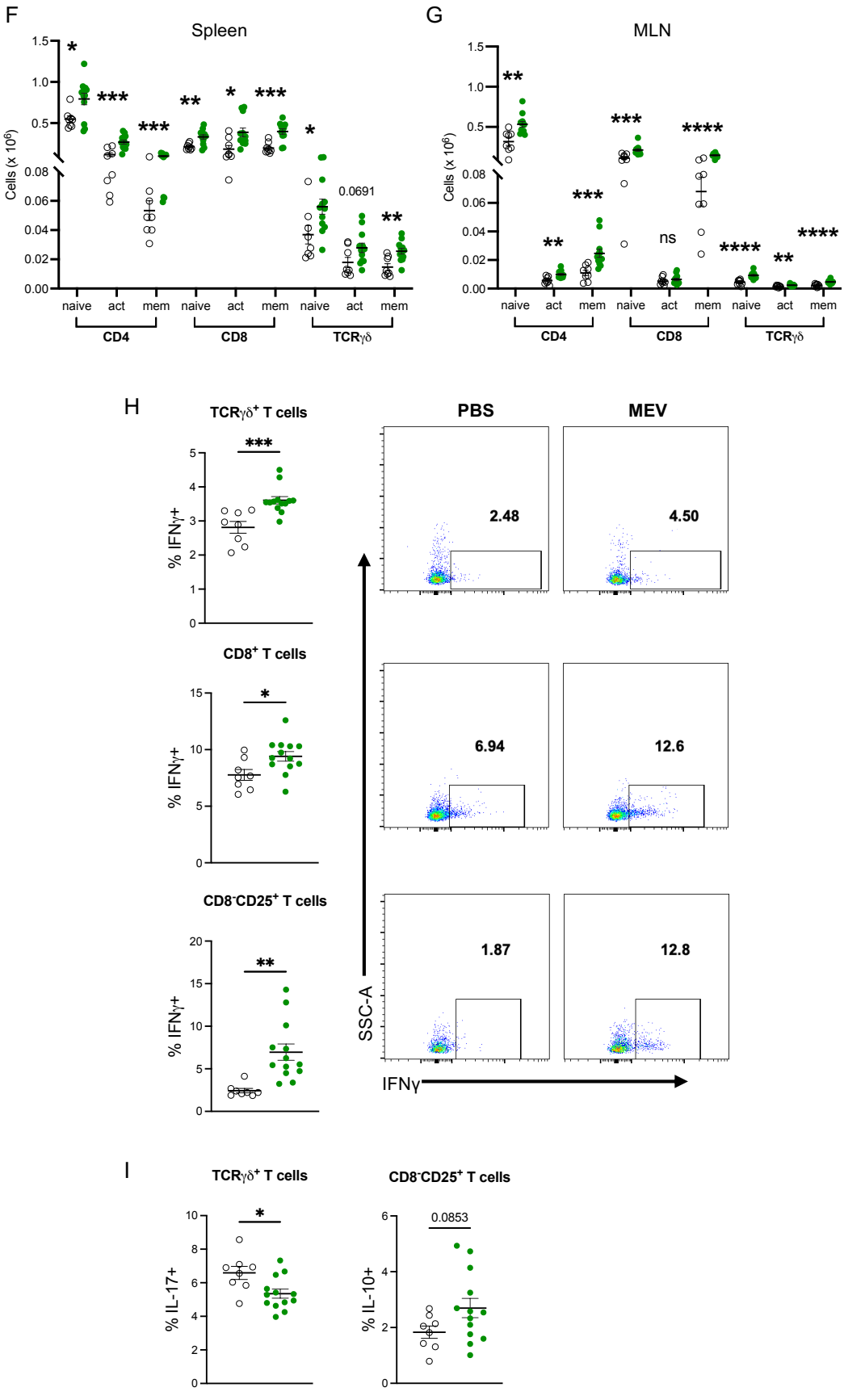
F
Spleen
Cells (x 10^6)
naive
act
mem
CD4
CD8
TCRγδ
0.0691
G
MLN
ns
H
TCRγδ+ T cells
CD8+ T cells
CD8-CD25+ T cells
% IFNγ+
PBS
MEV
2.48
4.50
6.94
12.6
1.87
12.8
SSC-A
IFNγ
I
TCRγδ+ T cells
CD8-CD25+ T cells
% IL-17+
% IL-10+
0.0853

Figure 5.5 Gestational MEV exposure alters cell profiles of secondary lymphoid organs

Pregnant C57/BL6 mice were gavaged 60μg of MEVs, or PBS control, daily during E0-E19 of gestation. Within 48 hours of birth, offspring litters were fostered to PBS-treated dams and left untreated throughout the lactation period. At PN21, offspring were euthanised for immunoprofiling using flow cytometry using gating strategies in Supplementary Figures S5.4-7. (**A**) Total cellularity of thymus, bone marrow, spleen and mesenteric lymph nodes (MLN). (**B**) Absolute number of splenic B cells, T cells, natural killer (NK) cells, red pulp macrophages, neutrophils, Ly6C^{+}, Ly6C^{int}, Ly6C$^{-/lo}$ monocytes, plasmacytoid DCs (pDCs) and conventional DCs (cDCs). (**C**) Absolute numbers of CD4^{+}, CD8^{+}, regulatory T cells (Tregs), and TCRγδ^{+} cells in spleen. (**D**) Absolute numbers of B cells, total T cells, NK and natural killer T (NKT) cells in MLNs. (**E**) Numbers of CD4^{+}, CD8^{+}, Tregs, and TCRγδ^{+} subsets in MLNs. (**F**) Absolute numbers of naïve, activated and memory subsets across CD4^{+}, CD8^{+}and TCRγδ^{+} lineages in spleen and (**G**) in MLNs. (**H**) IFNγ expression in splenocytes stimulated *ex vivo*, for TCRγδ^{+}, CD8^{+} and CD4^{+} (CD8^{-}CD25^{+}) subsets and representative flow cytometry plots (right). (**I**) Expression of IL17 in TCRγδ^{+} cells and IL-10 in CD4^{+} (CD8^{-}CD25^{+}) cells from splenocytes stimulated *ex vivo*. Data are shown as mean ± SEM. *p<0.05, **p<0.01, ***p<0.001, ****p<0.0001 by Mann-Whitney U test or Unpaired t-test

5.3.6 Gestational MEV exposure does not influence susceptibility to allergic airway inflammation

Given our observation that gestational MEV exposure enhanced T cell IFNγ production, we investigated whether this Th1-biased immune programming would influence susceptibility towards a Type-2 (Th2) mediated immune response. As gestational MEVs induced significant changes in the gut, we examined whether the lungs, another mucosal organ influenced by maternal gut microbiota *in utero*, would also be affected. Maternal microbial exposures, in part mediated by the gut microbiota, are strongly linked to shaping offspring susceptibility to allergic diseases such as asthma, which has gestational origins (Thorburn et al., 2015). Hence, we challenged 9-week old female offspring exposed to MEVs or PBS *in utero*, with house dust mite antigen (HDM) in an acute model of allergic airway inflammation (**Figure 5.6A**).

Analysis of bronchoalveolar lavage fluid (BALF) revealed that both PBS and MEV offspring mounted a similar inflammatory response to HDM challenge, compared to non-sensitised controls, although MEV mice had a significant increase in total cell numbers (**Figure 5.6C**). Using flow cytometry gating (**Figure S5.10**), detailed analysis of the BALF populations showed a similar increase in eosinophils, alveolar macrophages, T cells, and B cells, in both groups compared to non-sensitised controls, and with no significant differences between PBS and MEV offspring (**Figure 5.6D**). Serum total IgE levels showed a trend towards increase in MEV and PBS offspring compared to non-sensitised controls (**Figure 5.6E**), however, previous research suggest that HDM-induced allergic airway disease can develop independently of IgE (McKnight et al., 2017).

To assess the functional immune response, we analysed lung-draining mediastinal nodes for *ex vivo* cytokine production after restimulation with HDM antigen (**Figure 5.6FG**). Lymph node cellularity was unchanged across groups (**Figure 5.6F**), however, both PBS and MEV offspring showed elevated production of Th2 cytokines (IL-4, IL-5, IL-13, IFNγ) compared to non-sensitised controls, but with no significant differences between PBS and MEV offspring (**Figure 5.6G**).

Together, these data indicate that despite programming enhanced peripheral immune cell responses and Th1-biased phenotype, gestational MEV exposure does not significantly impact the development or response to HDM-induced allergic airway inflammation.

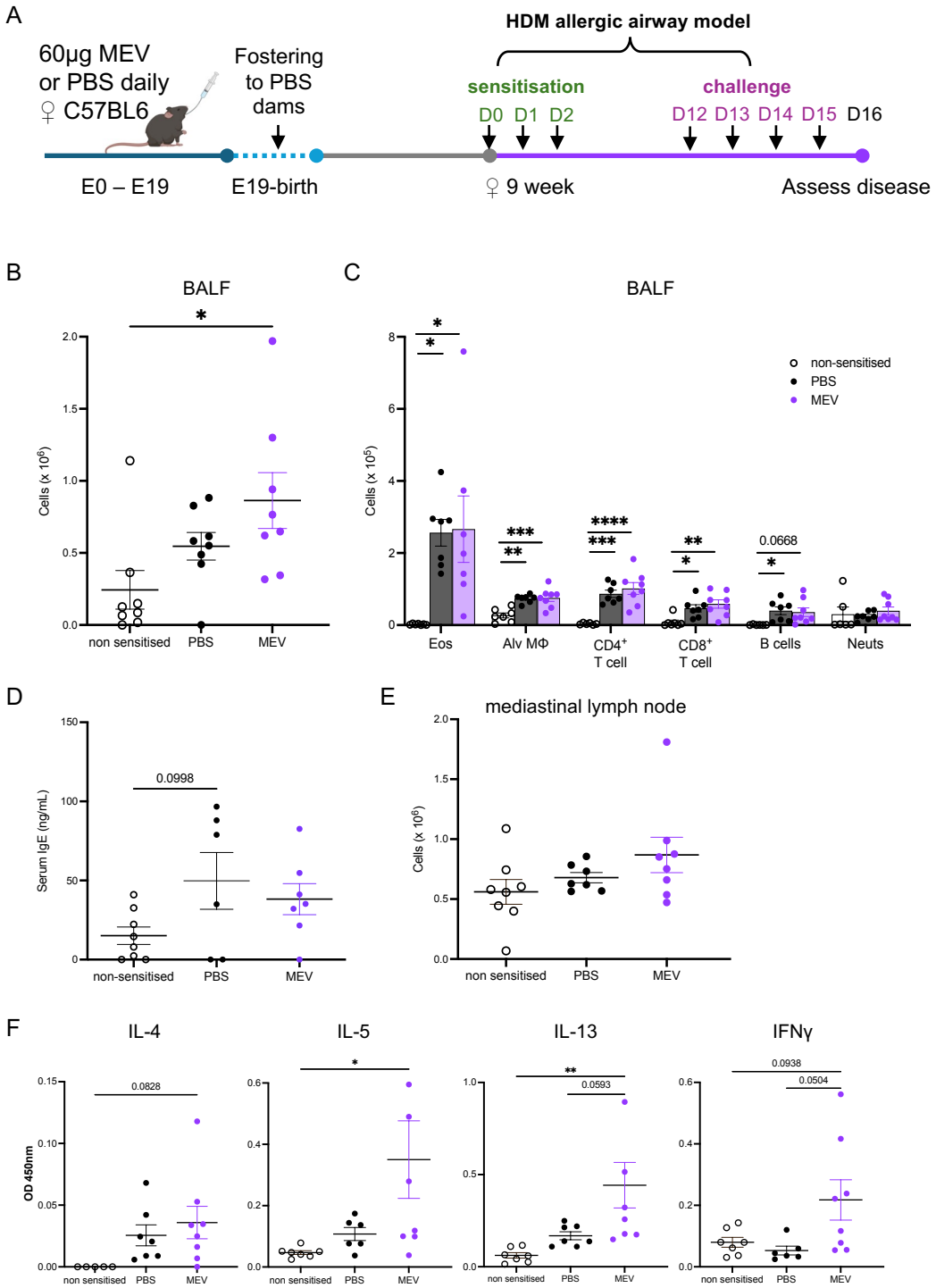
A
60µg MEV
or PBS daily
♀ C57BL6
Fostering
to PBS
dams
HDM allergic airway model
sensitisation
D0 D1 D2
challenge
D12 D13 D14 D15 D16
E0 – E19
E19-birth
♀ 9 week
Assess disease
B
BALF
Cells (x 10^6)
non sensitised
PBS
MEV
C
BALF
Cells (x 10^5)
non-sensitised
PBS
MEV
Eos
Alv MΦ
CD4+ T cell
CD8+ T cell
B cells
Neuts
0.0668
D
Serum IgE (ng/mL)
0.0998
non-sensitised
PBS
MEV
E
mediastinal lymph node
Cells (x 10^6)
non sensitised
PBS
MEV
F
IL-4
IL-5
IL-13
IFNγ
OD 450nm
0.0828
0.0593
0.0938
0.0504
non sensitised
PBS
MEV

Figure 5.6 Gestational MEV exposure does not impact susceptibility to allergic airway disease

(**A**) Experimental design: Pregnant C57/BL6 mice were gavaged 60μg of MEVs, or PBS control, daily during E0-E19 of gestation. Within 48 hours of birth, offspring litters were fostered to PBS-treated dams and left untreated throughout lactation, weaning and adulthood. At 9-weeks of age, female offspring were sensitised and challenged with HDM extract in a model of allergic airway disease. (**B**) Total cellularity of bronchoalveolar lavage fluid (BALF). (**C**) Differential counts of eosinophils (Eos), alveolar macrophages (Alv MΦ), $CD4^+$ T cells, $CD8^+$ T cells, B cells and neutrophils (Neuts) in BALF as determined by flow cytometry using the gating strategy in Supplementary Figure S5.10. (**D**) Serum total IgE as determined by ELISA. (**E**) Cellularity of mediastinal lymph nodes. F Mediastinal lymph node cells were restimulated with HDM extract (20 μg/mL) for 72 hours and supernatant was assessed for levels of Th2 (IL-4, IL-5, IL13) and Th1 (IFNγ) cytokines by ELISA. Data are shown as mean ± SEM. *p<0.05, **p<0.01, ***p<0.001, ****p<0.0001 by one-way ANOVA followed by Tukey's multiple comparisons test

5.4 Discussion

In this study, we have demonstrated MEVs are novel regulators of gut microbiota composition. We confirmed that MEVs are a distinct compositional fraction of the gut microbiota, and that administration of exogenous MEVs actively modifies gut bacterial communities. Importantly, we found this effect is transgenerational if MEVs are administered during gestation. Mechanistically, gestational MEV exposure programmed colonic gene expression, enhancing barrier integrity, bacterial recognition, and cytokine expression, which may have driven changes the postnatal differences in gut bacterial composition. Beyond local effects in the colon, gestational MEVs also expanded immune cells in peripheral lymphoid organs and enhanced T cell IFNγ responses *ex vivo*. Despite this Th1 bias, gestational MEVs did not alter susceptibility to Th2 mediated allergic airway disease in the lungs.

We identified that healthy gut microbiota contains an MEV fraction with a distinct bacterial signature which has a significantly reduced species richness compared to the cellular fraction. This suggests that MEV production is not uniform across gut bacterial species but may be more characteristic of specific taxa. This also aligns with previous studies comparing MEV composition in healthy and diseased mouse models (Chelakkot et al., 2018; Choi et al., 2015; Li et al., 2023), suggesting selective MEV production may be an inherent feature of a healthy gut microbiota. Notably, specific taxa enriched in the MEV fraction were of low abundance in the cellular fraction, particularly *Clostridium XIVb* and *Anaerotruncus*. While *Clostridium XIVb* is a known SCFA-producer whose abundance is decreased in IBD (Wan et al., 2022), *Anaerotruncus* is a newly described genus, belonging to the *Clostridia* family, whose role in health and disease remains unclear (Ma et al., 2024;

Togo et al., 2019). These findings highlight that MEVs may represent an overlooked mechanism of bacterial effects on the host, where some genera may exert a disproportionate effect on the host via MEVs, despite their low abundance at the cellular level.

While vesicle production is constitutive in Gram-negative and Gram-positive bacteria, environmental factors significantly influence their release. Environmental stress can differentially impact MEV production across bacterial taxa, which may also explain the distinct MEV composition we observed and suggests that MEV profiles could serve as an indicator of microbiota status. Indeed, we previously demonstrated that dietary protein promotes expansion of succinate-producing taxa, triggering increased MEV production and subsequent sIgA production in the small intestine (Tan et al., 2020). Thus, quantification of MEV levels, or analysis of their composition may serve as a valuable readout of microbiota stress responses. Recent studies have begun exploring MEVs from bodily fluids as biomarkers for various conditions including diabetes, allergy, IBD, and cancer (Chang et al., 2024; Heo et al., 2023; Jones et al., 2021; Park et al., 2021; Yang et al., 2020). However, more research is needed to understand how environmental factors influence MEV production and the functional consequences on host health, to advance their potential in precision medicine.

We identified MEVs as novel modulator of gut bacterial composition. While the precise mechanisms remain to be elucidated, it is likely that modulation occurs through a combination of direct bacteria to bacteria interactions, and through indirect host-mediated effects, such as sIgA (Tan et al., 2020). Importantly, our findings establish MEVs as key regulators of microbiota homeostasis, whereas previous research has primarily

focused on their role in disease or effects of specific bacterial species. Our study is particularly relevant for therapeutic strategies aimed at altering microbiota composition. While dietary interventions and probiotic supplements show limited efficacy in stably modulating composition to improve disease (Khalesi et al., 2019; Sheflin et al., 2016; Wu et al., 2011), faecal microbiota transplantation (FMT) is highly effective but restricted in use due to risks of infection. Recently, sterile faecal filtrates, which lack whole bacterial cells, have shown comparable efficacy to FMT in treating *Clostridium difficile* infection and promise in improving dysbiosis associated with hepatic encephalopathy and ulcerative colitis (Chechushkov et al., 2024; Gedgaudas et al., 2023; Ott et al., 2017). While the mechanisms behind the efficacy of these filtrates are still being uncovered, MEVs are likely key therapeutic components, highlighting their potency in modulating gut microbiota.

A key finding in our study is that MEV-mediated effects on gut microbiota composition are heritable, as offspring exposed to MEV during gestation show persistent compositional changes despite attempts to normalise microbiota postnatally. We identified this likely occurs through MEV-mediated programming of the fetal gut environment, such as alterations to colonic gene expression. In addition, we found MEV exposure specifically impacted secondary lymphoid organs, enhancing expansion of both innate and adaptive populations in MLNs and spleen while primary organs were unaffected. This tissue-specific effect in the organs we examined may suggest a targeted effect on immune development or may reflect a direct exposure route, as fetal swallowing of amniotic fluid could introduce MEVs into systemic circulation. Mechanistically, MEVs may act directly through fetal interactions, or indirectly via MEV-mediated changes to maternal physiology.

MEVs present in amniotic fluid may contact the fetus externally and internally (through ingestion), potentially influencing the developing skin, lungs and gastrointestinal tract (Kaisanlahti et al., 2023). In humans, T cell development commences in the first trimester, and strong evidence indicates that T cell priming and memory cell formation begins *in utero*, although identification of specific cognate antigens is rare (Koren et al., 2024). Recently, it was demonstrated that fetal memory T cells are responsive to gut microbiota antigens highlighting there is early recognition of microbiota signals (Mishra et al., 2021). Given that MEVs cross the placenta, they likely represent a key pathway through which maternal gut microbiota may condition the developing fetus for subsequent microbial colonisation and exposure. However, as murine T cell development occurs predominantly from late gestation (E15) and postnatally, we were unable to determine if gestational MEVs directly induced formation of antigen-specific memory T cells. Beyond adaptive immunity, MEVs may also contribute to training innate immune cells by providing a source of antigenic signals, although this requires further investigation.

Additionally, the MEVs in our study may have acted indirectly, by regulating the composition of maternal gut microbiota to alter gut metabolic profiles and/or maternal physiology, thereby indirectly influencing the fetal environment. However, our study was not designed to assess potential maternal changes and this pathway requires further investigation.

Beyond the global expansion of peripheral immune cells, we also found MEV exposure programmed offspring T cells towards enhanced IFNγ expression across multiple lineages. Despite their enhanced peripheral immunity and a Th1 bias, MEV-exposed offspring showed no altered susceptibility to Th2-mediated allergic airway inflammation.

This suggests MEV-mediated immune programming may have highly specific effects rather than broadly altering immune responses. Thus, maternally derived MEVs could represent a mechanism through which the maternal gut microbiota may fine-tune offspring immunity while preserving baseline normal development.

The findings of this study also have broader therapeutic implications, particularly in the context of globally increasing rates of obesity and non-communicable diseases (Tan et al., 2023). Gut microbiota dysbiosis is frequently a component of chronic disease, and gut bacteria contribute to chronic disease pathology through production of dysbiotic metabolites and translocation of inflammatory components (Cani et al., 2007; Martel et al., 2022). MEVs could offer a novel therapeutic strategy to modulate a dysbiotic microbiota towards a less inflammatory state. For example, a preparation enriched in MEVs from beneficial taxa, such as SCFA-producers, may directly mitigate inflammation by enhancing anti-inflammatory mucosal responses (Tan et al., 2014). Moreover, as increasing rates of maternal metabolic and non-communicable diseases pose significant risks to long-term offspring health (Li et al., 2011), MEVs may be utilised as a means to promote healthy immune programming during pregnancy.

In conclusion, our study establishes MEVs as a fundamental regulator of the gut microbiota. Notably, we have shown that gestational MEV exposure profoundly impacts offspring microbiota composition and immune development, revealing a novel mechanism of maternal programming of the fetus *in utero*. These findings suggest MEV could serve as promising therapeutic tools to ameliorate dysbiosis and promote healthy immune programming during pregnancy, potentially benefiting life-long health.

Acknowledgements

We acknowledge the Sydney Cytometry Core Research Facility, a joint initiative of Centenary Institute and the University of Sydney. The authors acknowledge Sydney Analytical for access to the ZetaView and NS300 for Nanoparticle tracking analysis, and the Laboratory Animal Services at The University of Sydney for animal housing and husbandry We thank Dr. Dragana Stanley and Dr. Yagav Bajagai for performing 16S Amplicon sequencing at Central Queensland University.

Funding

This project was funded by the Australian Research Council grant APP160100627 and APP210102943. JJT and CPV are recipients of the Australian Government Research Training Program Scholarship.

Author contributions

LM and RN conceived the project and secured funding. JJT contributed to study design, performed the majority of the experiments, data analysis, and wrote the original draft. JT and DN assisted with experiments and data analysis, and CPV and GP assisted with experiments. All authors reviewed and edited the manuscript.

5.5 Supplementary Material

A

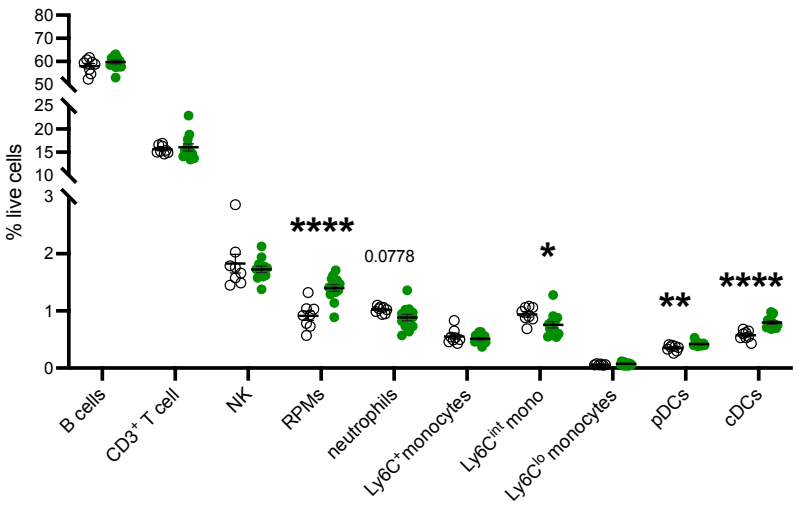
% live cells
80
70
60
50
25
20
15
10
3
2
1
0
****
0.0778
*
**
****
B cells
CD3+ T cell
NK
RPMs
neutrophils
Ly6C+ monocytes
Ly6Cint mono
Ly6Clo monocytes
pDCs
cDCs

B

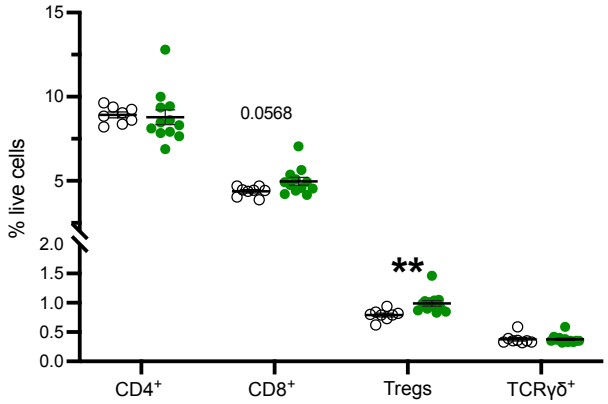
% live cells
15
10
5
2.0
1.5
1.0
0.5
0.0
0.0568
**
CD4+
CD8+
Tregs
TCRγδ+

C

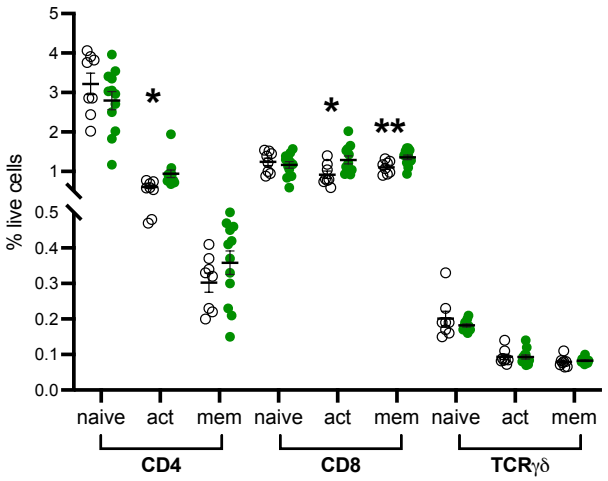
% live cells
5
4
3
2
1
0.5
0.4
0.3
0.2
0.1
0.0
*
*
**
naive
act
mem
naive
act
mem
naive
act
mem
CD4
CD8
TCRγδ

Figure S5.1 Spleen immunoprofiling of offspring exposed to MEVs or PBs *in utero*

Pregnant C57/BL6 mice were gavaged 60μg of MEVs, or PBS control, daily during E0-E19 of gestation. Within 48 hours of birth, offspring litters of similar sizes were cross-fostered to PBS-treated dams and left untreated throughout the lactation period. At PN21, offspring were euthanised for spleen immunoprofiling using flow cytometry according to the gating strategy in Supplementary Figures S5.5, 6. (**A**) Proportion of live cells for splenic B cells, T cells, NK cells, red pulp macrophages, neutrophils, $Ly6C^{+}$, $Ly6C^{int}$, $Ly6C^{-/lo}$ monocytes, plasmacytoid DCs (pDCs) and conventional DCs (cDCs). (**B**) Proportion of live cells for splenic $CD4^{+}$, $CD8^{+}$, Treg, and $TCR\gamma\delta^{+}$T cell subsets. (**C**) Proportion of live cells of naïve, activated and memory subsets across T cell lineages for spleen

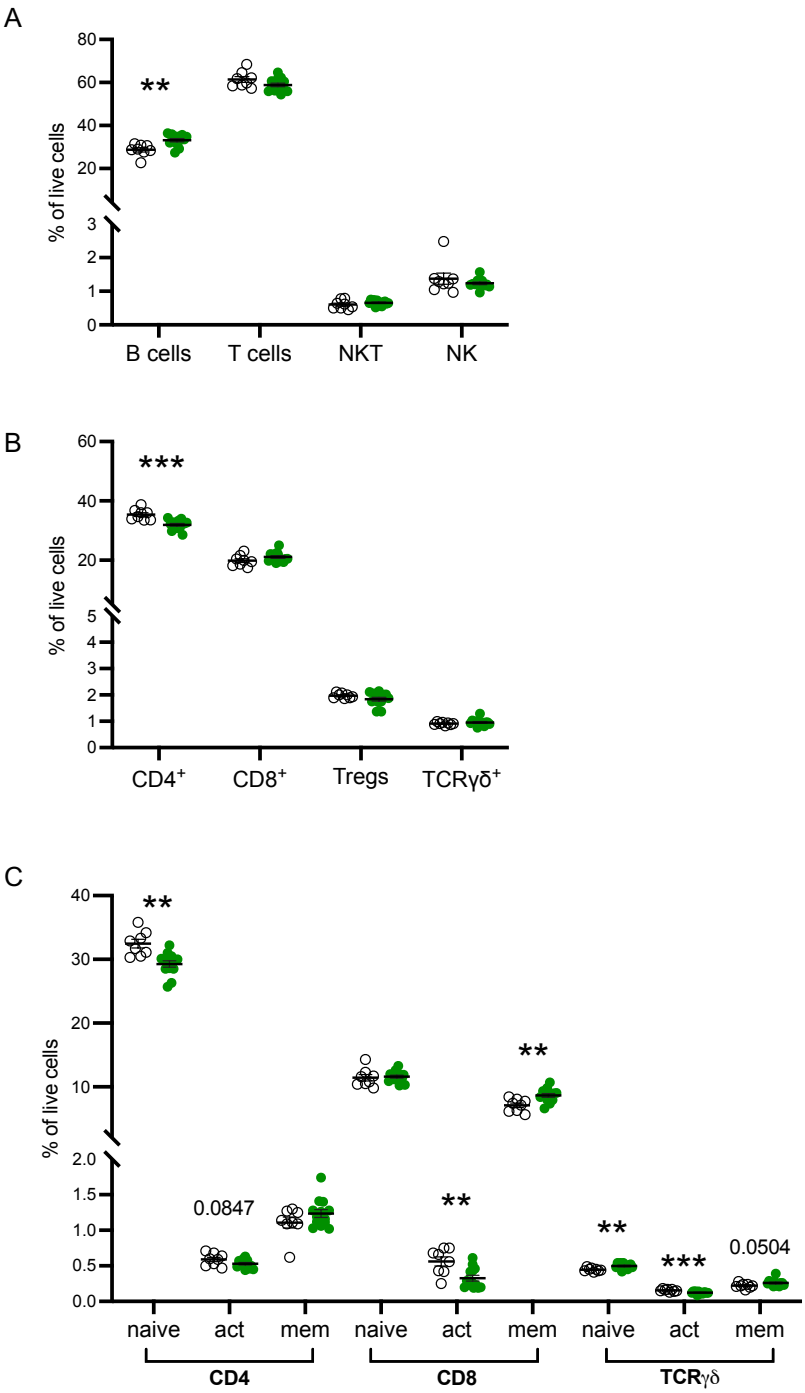
A
% of live cells
80
60
40
20
3
2
1
0
**
B cells
T cells
NKT
NK
B
% of live cells
60
40
20
5
4
3
2
1
0
***
CD4+
CD8+
Tregs
TCRγδ+
C
% of live cells
40
30
20
10
2.0
1.5
1.0
0.5
0.0
**
0.0847
**
**
**
***
0.0504
naive
act
mem
naive
act
mem
naive
act
mem
CD4
CD8
TCRγδ

Figure S5.2 MLN immunoprofiling of offspring exposed to MEVs or PBs *in utero*

Pregnant C57/BL6 mice were gavaged 60μg of MEVs, or PBS control, daily during E0-E19 of gestation. Within 48 hours of birth, offspring litters of similar sizes were cross-fostered to PBS-treated dams and left untreated throughout the lactation period. At PN21, offspring were euthanised for MLN immunoprofiling using flow cytometry according to the gating strategy in Supplementary Figure S5.4. (**A**) Proportion of live cells in MLNs for B cells, T cells, NKT and NK cells, and (**B**) $CD4^+$, $CD8^+$, regulatory T cells (Tregs), and $TCR\gamma\delta^+$ subsets. (**C**) Proportion of live cells of naïve, activated and memory subsets across T cell lineages in the MLNs.

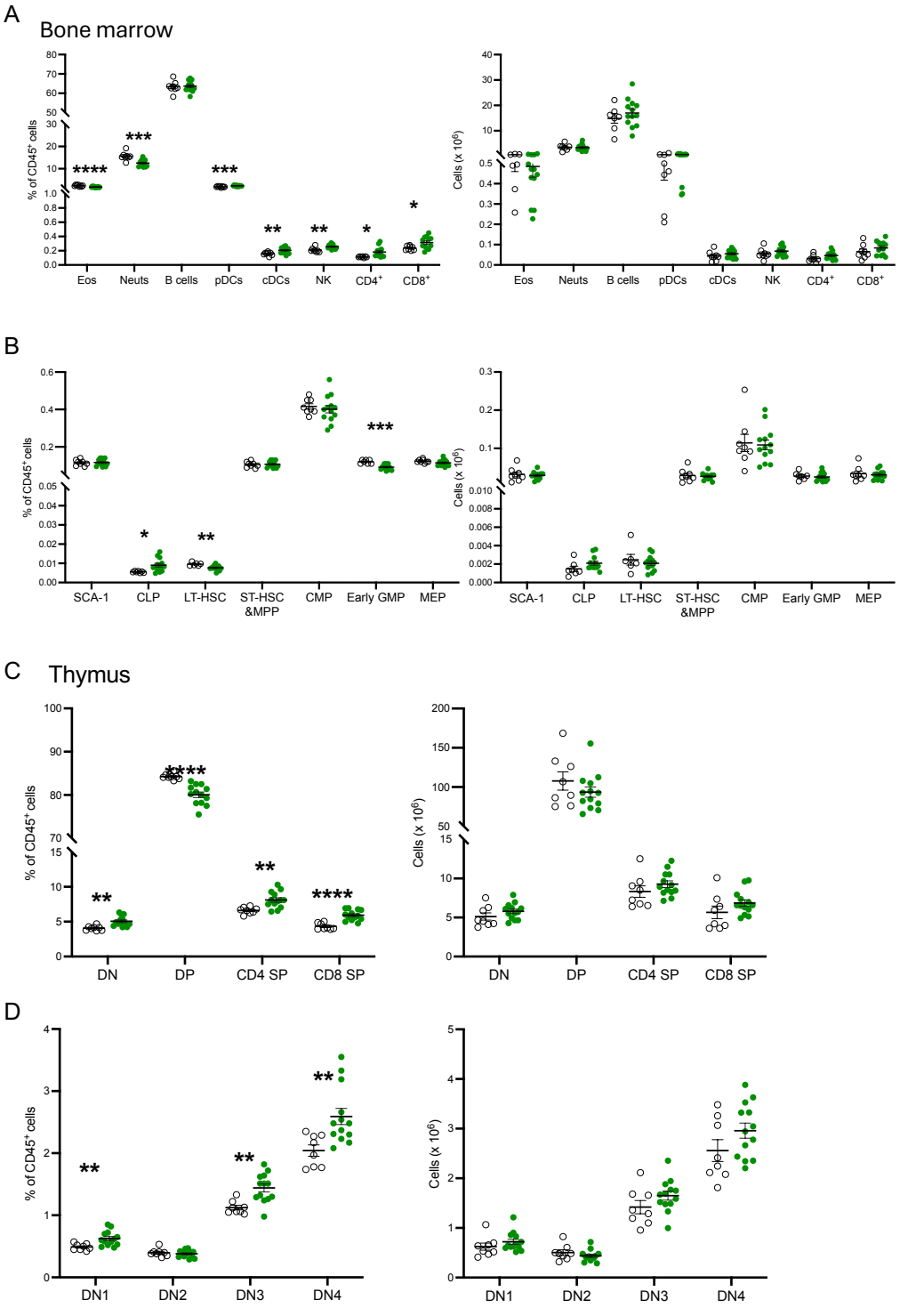
A
Bone marrow
% of CD45+ cells
Cells (x 10^6)
Eos
Neuts
B cells
pDCs
cDCs
NK
CD4+
CD8+
B
SCA-1
CLP
LT-HSC
ST-HSC &MPP
CMP
Early GMP
MEP
C
Thymus
DN
DP
CD4 SP
CD8 SP
D
DN1
DN2
DN3
DN4

Figure S5.3 Bone marrow and thymus immunoprofiling of offspring exposed to MEVs or PBs *in utero*

Pregnant C57/BL6 mice were gavaged 60μg of MEVs, or PBS control, daily during E0-E19 of gestation. Within 48 hours of birth, offspring litters of similar sizes were cross-fostered to PBS-treated dams and left untreated throughout the lactation period. At PN21, offspring were euthanised for immunoprofiling using flow cytometry according to the gating strategies in Figures SF5.8, 9. (**A**) Proportions (left) of $CD45^+$ leukocytes of eosinophils (Eos), neutrophils (Neuts), B cells, pDCs, cDCs, NK cells, $CD4^+$ and $CD8^+$ T cells, and absolute numbers (right) of these subsets in bone marrow. (**B**) Proportions (left) of $CD45^+$ leukocytes of progenitor populations including $SCA\text{-}1^+$ cells, common lymphoid progenitors (CLP), long-term hematopoietic stem cells (LT-HSC), short-term hematopoietic stem cell and multipotent progenitor (ST-HSC & MPP), common myeloid progenitor (CMP), early granulocyte-macrophage progenitor (GMP) and megakaryocyte-erythroid progenitor (MEP), and absolute numbers (right) of these subsets in bone marrow. (**C**) Proportion (left) of $CD45^+$ thymocytes for double negative (DN), double positive (DP), and CD4 and CD8 single positive (CD4 SP and CD8 SP) cells, and absolute numbers (right) of these subsets. (**D**) Proportion (left) of $CD45^+$ thymocytes for double negative (DN) 1-4 subsets, and absolute numbers (right) of these subsets. Data are shown as mean $\pm$ SEM. *p<0.05, **p<0.01, ***p<0.001, ****p<0.0001 by Mann-Whitney U test or Unpaired t-test.

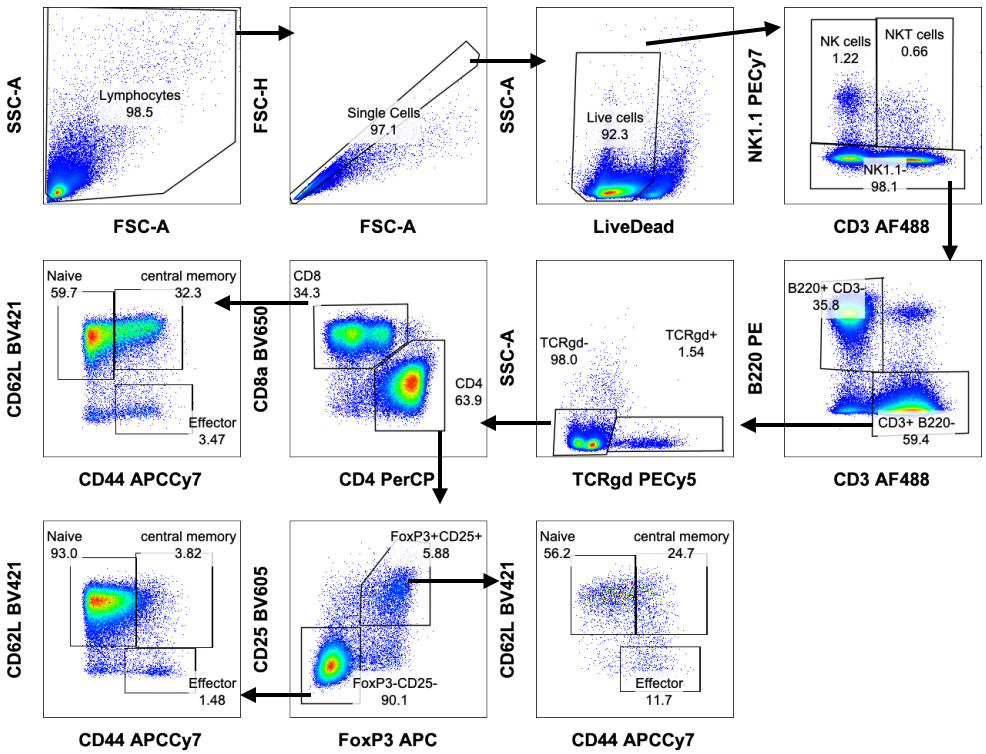
SSC-A
Lymphocytes
98.5
FSC-A
FSC-H
Single Cells
97.1
FSC-A
SSC-A
Live cells
92.3
LiveDead
NK1.1 PECy7
NK cells
1.22
NKT cells
0.66
NK1.1-
98.1
CD3 AF488
B220 PE
B220+ CD3-
35.8
CD3+ B220-
59.4
CD3 AF488
SSC-A
TCRgd-
98.0
TCRgd+
1.54
TCRgd PECy5
CD8a BV650
CD8
34.3
CD4
63.9
CD4 PerCP
CD62L BV421
Naive
59.7
central memory
32.3
Effector
3.47
CD44 APCCy7
CD25 BV605
FoxP3+CD25+
5.88
FoxP3-CD25-
90.1
FoxP3 APC
CD62L BV421
Naive
56.2
central memory
24.7
Effector
11.7
CD44 APCCy7
CD62L BV421
Naive
93.0
central memory
3.82
Effector
1.48
CD44 APCCy7

Figure S5.4 Gating strategy to analyse cells in the mesenteric lymph nodes

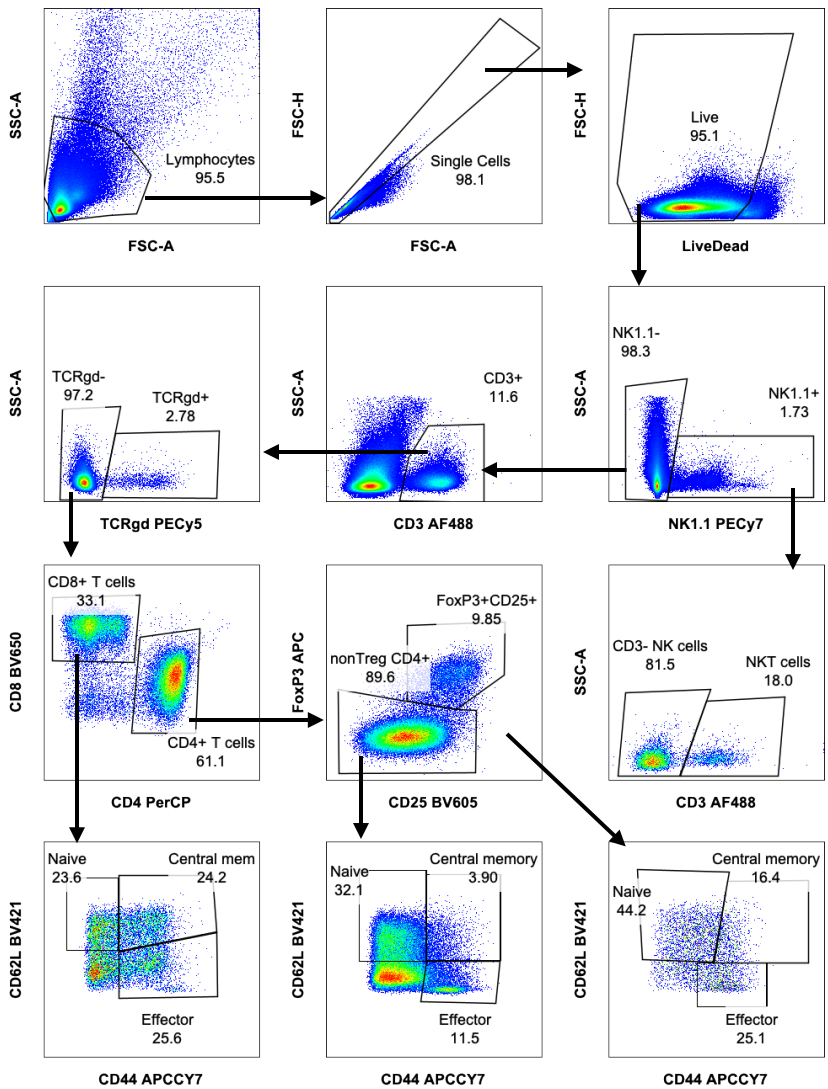
SSC-A
Lymphocytes
95.5
FSC-A
FSC-H
Single Cells
98.1
FSC-A
FSC-H
Live
95.1
LiveDead
SSC-A
TCRgd-
97.2
TCRgd+
2.78
TCRgd PECy5
SSC-A
CD3+
11.6
CD3 AF488
SSC-A
NK1.1-
98.3
NK1.1+
1.73
NK1.1 PECy7
CD8 BV650
CD8+ T cells
33.1
CD4+ T cells
61.1
CD4 PerCP
FoxP3 APC
FoxP3+CD25+
9.85
nonTreg CD4+
89.6
CD25 BV605
SSC-A
CD3- NK cells
81.5
NKT cells
18.0
CD3 AF488
CD62L BV421
Naive
23.6
Central mem
24.2
Effector
25.6
CD44 APCCY7
CD62L BV421
Naive
32.1
Central memory
3.90
Effector
11.5
CD44 APCCY7
CD62L BV421
Naive
44.2
Central memory
16.4
Effector
25.1
CD44 APCCY7

Figure S5.5 Gating strategy to analyse splenic NK, NKT and T cell subsets

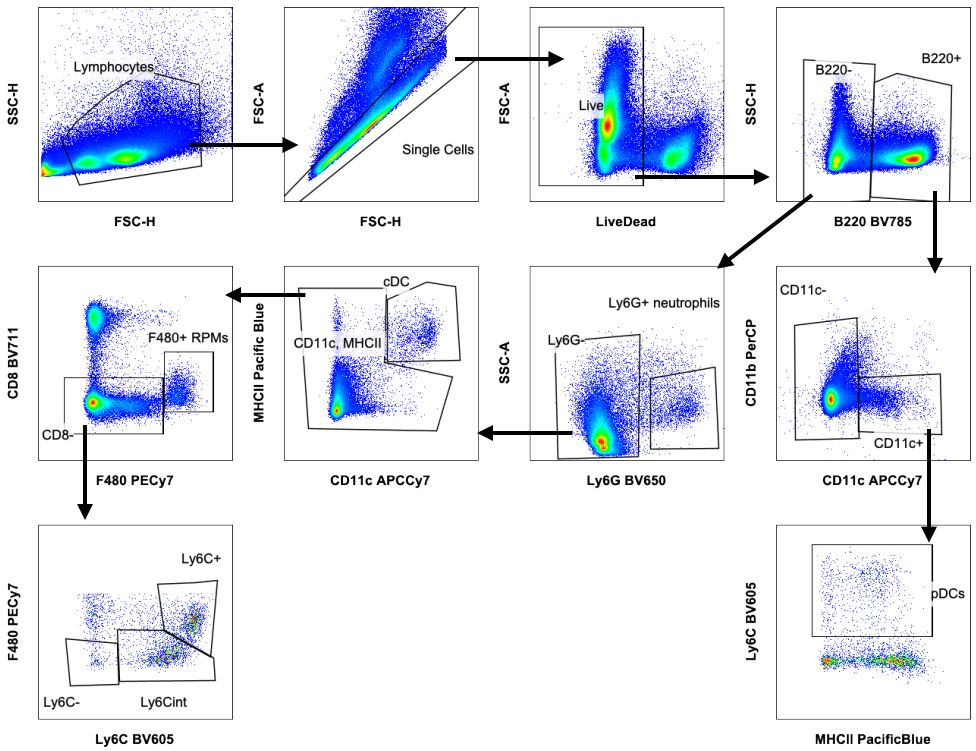
SSC-H
Lymphocytes
FSC-H
FSC-A
Single Cells
FSC-H
FSC-A
Live
LiveDead
SSC-H
B220-
B220+
B220 BV785
CD11b PerCP
CD11c-
CD11c+
CD11c APCCy7
SSC-A
Ly6G+ neutrophils
Ly6G-
Ly6G BV650
MHCII Pacific Blue
cDC
CD11c, MHCII
CD11c APCCy7
CD8 BV711
F480+ RPMs
CD8-
F480 PECy7
F480 PECy7
Ly6C+
Ly6C-
Ly6Cint
Ly6C BV605
Ly6C BV605
pDCs
MHCII PacificBlue

Figure S5.6 Gating strategy to analyse splenic myeloid subsets and B cells

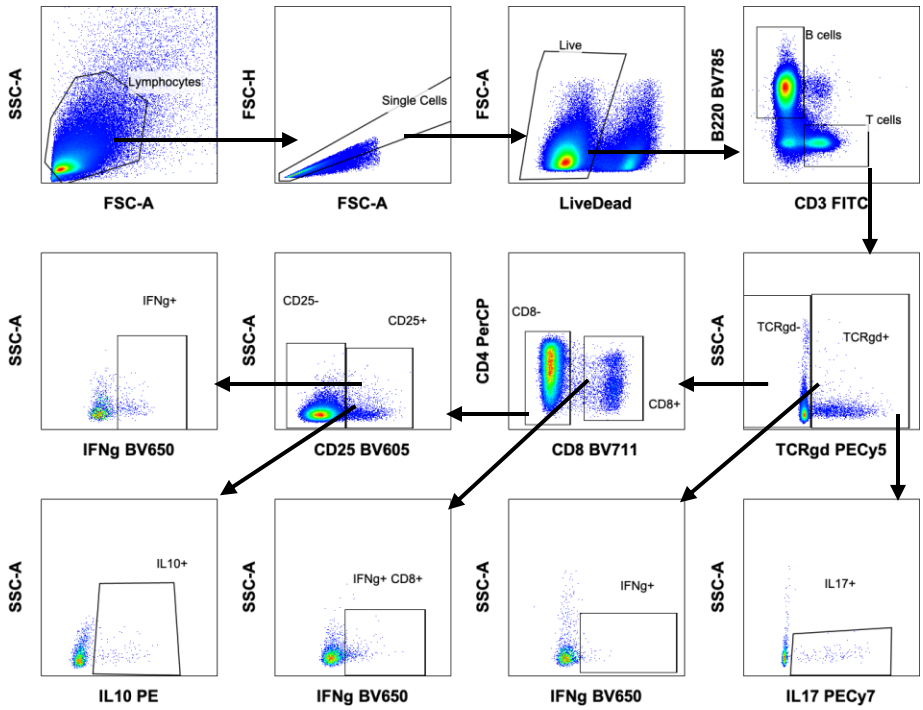
SSC-A
Lymphocytes
FSC-A
FSC-H
Single Cells
FSC-A
FSC-A
FSC-A
Live
LiveDead
B220 BV785
B cells
T cells
CD3 FITC
SSC-A
IFNg+
IFNg BV650
SSC-A
CD25-
CD25+
CD25 BV605
CD4 PerCP
CD8-
CD8+
CD8 BV711
SSC-A
TCRgd-
TCRgd+
TCRgd PECy5
SSC-A
IL10+
IL10 PE
SSC-A
IFNg+ CD8+
IFNg BV650
SSC-A
IFNg+
IFNg BV650
SSC-A
IL17+
IL17 PECy7

Figure S5.7 Gating strategy to analyse cytokine expression in splenic T cells stimulated *ex vivo*

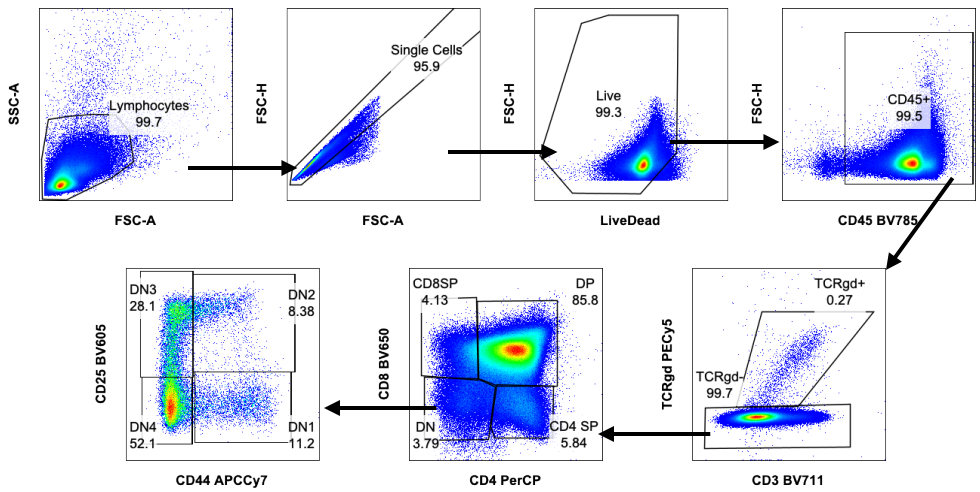
SSC-A
Lymphocytes
99.7
FSC-A
FSC-H
Single Cells
95.9
FSC-A
FSC-H
Live
99.3
LiveDead
FSC-H
CD45+
99.5
CD45 BV785
TCRgd PECy5
TCRgd+
0.27
TCRgd-
99.7
CD3 BV711
CD8 BV650
CD8SP
4.13
DP
85.8
DN
3.79
CD4 SP
5.84
CD4 PerCP
CD25 BV605
DN3
28.1
DN2
8.38
DN4
52.1
DN1
11.2
CD44 APCCy7

Figure S5.8 Gating strategy to analyse thymopoesis

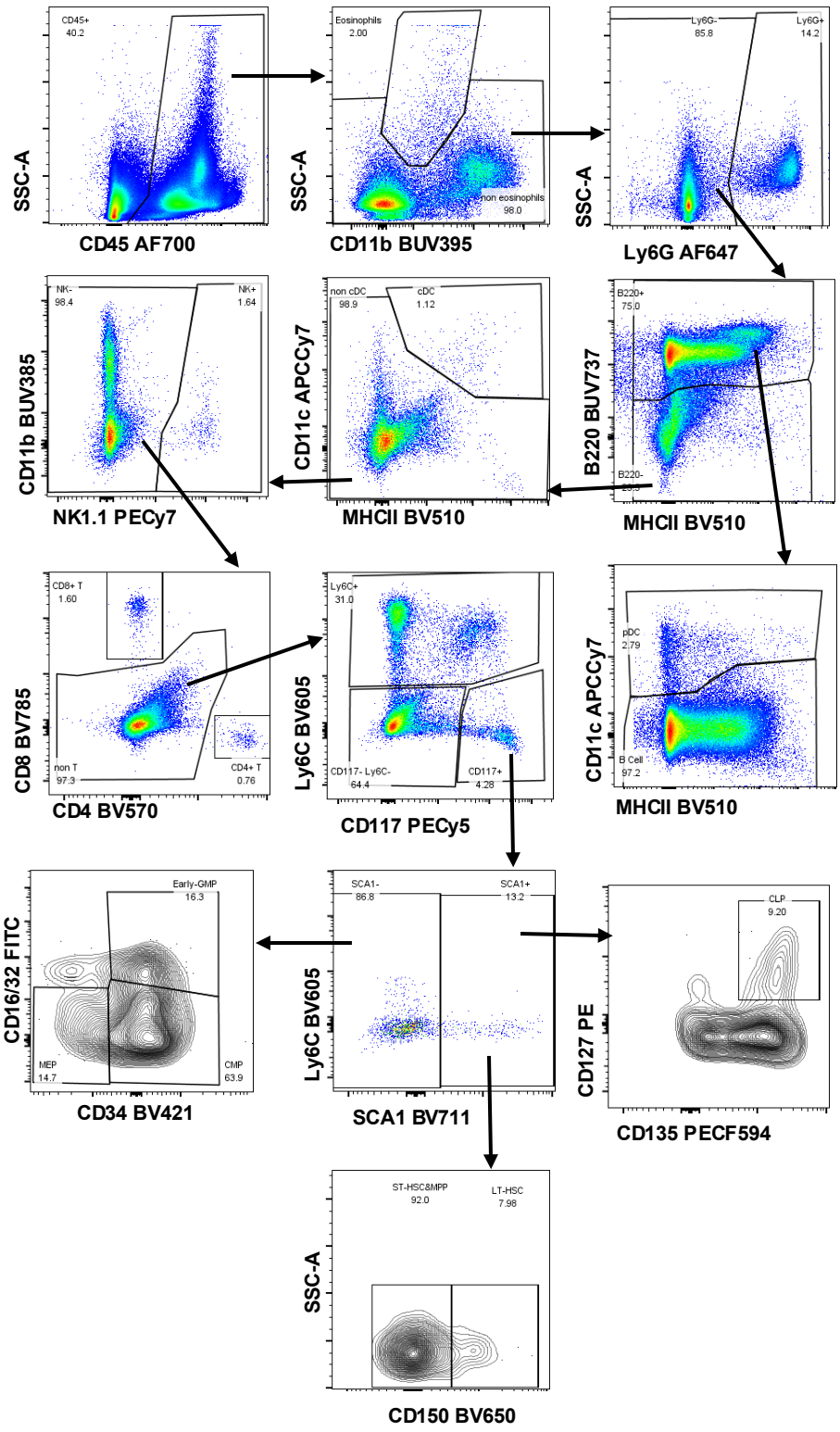
CD45+
40.2
SSC-A
CD45 AF700
Eosinophils
2.00
non eosinophils
98.0
SSC-A
CD11b BUV395
Ly6G-
85.8
Ly6G+
14.2
SSC-A
Ly6G AF647
NK-
98.4
NK+
1.64
CD11b BUV385
NK1.1 PECy7
non cDC
98.9
cDC
1.12
CD11c APCCy7
MHCII BV510
B220+
75.0
B220-
B220 BUV737
MHCII BV510
CD8+ T
1.60
non T
97.3
CD4+ T
0.76
CD8 BV785
CD4 BV570
Ly6C+
31.0
CD117- Ly6C-
64.4
CD117+
4.28
Ly6C BV605
CD117 PECy5
pDC
2.79
B Cell
97.2
CD11c APCCy7
MHCII BV510
Early-GMP
16.3
MEP
14.7
CMP
63.9
CD16/32 FITC
CD34 BV421
SCA1-
86.8
SCA1+
13.2
Ly6C BV605
SCA1 BV711
CLP
9.20
CD127 PE
CD135 PECF594
ST-HSC&MPP
92.0
LT-HSC
7.98
SSC-A
CD150 BV650

Figure S5.9 Gating strategy to analyse bone marrow leukocytes

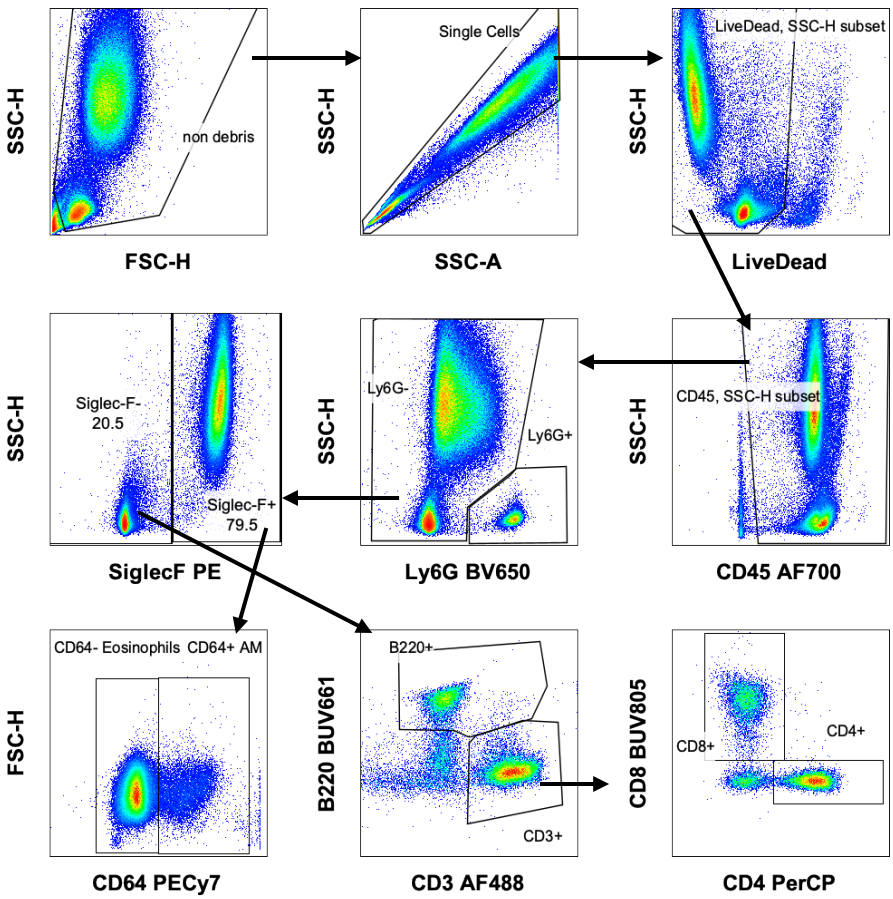
SSC-H
non debris
FSC-H
Single Cells
SSC-H
SSC-A
LiveDead, SSC-H subset
SSC-H
LiveDead
CD45, SSC-H subset
SSC-H
CD45 AF700
Ly6G-
Ly6G+
SSC-H
Ly6G BV650
Siglec-F-
20.5
Siglec-F+
79.5
SSC-H
SiglecF PE
CD64- Eosinophils
CD64+ AM
FSC-H
CD64 PECy7
B220+
CD3+
B220 BUV661
CD3 AF488
CD8+
CD4+
CD8 BUV805
CD4 PerCP

Figure S5.10 Gating strategy to analyse bronchioalveolar lavage fluid

References

Bitto, N.J., Kaparakis-Liaskos, M., 2017. The Therapeutic Benefit of Bacterial Membrane Vesicles. Int J Mol Sci 18, 1287. https://doi.org/10.3390/ijms18061287

Briaud, P., Carroll, R.K., 2020. Extracellular Vesicle Biogenesis and Functions in Gram-Positive Bacteria. Infection and Immunity 88, 10.1128/iai.00433-20. https://doi.org/10.1128/iai.00433-20

Cani, P.D., Amar, J., Iglesias, M.A., Poggi, M., Knauf, C., Bastelica, D., Neyrinck, A.M., Fava, F., Tuohy, K.M., Chabo, C., Waget, A., Delmée, E., Cousin, B., Sulpice, T., Chamontin, B., Ferrières, J., Tanti, J.-F., Gibson, G.R., Casteilla, L., Delzenne, N.M., Alessi, M.C., Burcelin, R., 2007. Metabolic endotoxemia initiates obesity and insulin resistance. Diabetes 56, 1761–1772. https://doi.org/10.2337/db06-1491

Chang, C.-J., Bai, Y.-C., Jiang, H., Ma, Q.-W., Hsieh, C.-H., Liu, C.-C., Huang, H.-C., Chen, T.-J., 2024. Microbiome analysis of serum extracellular vesicles in gestational diabetes patients. Acta Diabetol. https://doi.org/10.1007/s00592-024-02358-2

Chechushkov, A., Desyukevich, P., Yakovlev, T., Al Allaf, L., Shrainer, E., Morozov, V., Tikunova, N., 2024. Sterile Fecal Microbiota Transplantation Boosts Anti-Inflammatory T-Cell Response in Ulcerative Colitis Patients. Int J Mol Sci 25, 1886. https://doi.org/10.3390/ijms25031886

Chelakkot, C., Choi, Y., Kim, D.-K., Park, H.T., Ghim, J., Kwon, Y., Jeon, J., Kim, M.-S., Jee, Y.-K., Gho, Y.S., Park, H.-S., Kim, Y.-K., Ryu, S.H., 2018. Akkermansia muciniphila-derived extracellular vesicles influence gut permeability through the regulation of tight junctions. Exp Mol Med 50, e450. https://doi.org/10.1038/emm.2017.282

Choi, Y., Kwon, Y., Kim, D.-K., Jeon, J., Jang, S.C., Wang, T., Ban, M., Kim, M.-H., Jeon, S.G., Kim, M.-S., Choi, C.S., Jee, Y.-K., Gho, Y.S., Ryu, S.H., Kim, Y.-K., 2015. Gut microbe-derived extracellular vesicles induce insulin resistance, thereby impairing glucose metabolism in skeletal muscle. Sci Rep 5, 15878. https://doi.org/10.1038/srep15878

Chu, H., Mazmanian, S.K., 2013. Innate immune recognition of the microbiota promotes host-microbial symbiosis. Nat Immunol 14, 668–675. https://doi.org/10.1038/ni.2635

Cui, Y., Zhang, L., Wang, X., Yi, Y., Shan, Y., Liu, B., Zhou, Y., Lü, X., 2022. Roles of intestinal Parabacteroides in human health and diseases. FEMS Microbiol Lett 369, fnac072. https://doi.org/10.1093/femsle/fnac072

Elhenawy, W., Debelyy, M.O., Feldman, M.F., 2014. Preferential packing of acidic glycosidases and proteases into Bacteroides outer membrane vesicles. mBio 5, e00909-00914. https://doi.org/10.1128/mBio.00909-14

Ezeji, J.C., Sarikonda, D.K., Hopperton, A., Erkkila, H.L., Cohen, D.E., Martinez, S.P., Cominelli, F., Kuwahara, T., Dichosa, A.E.K., Good, C.E., Jacobs, M.R., Khoretonenko, M., Veloo, A., Rodriguez-Palacios, A., 2021. Parabacteroides distasonis: intriguing aerotolerant gut anaerobe with emerging antimicrobial resistance and pathogenic and probiotic roles in human health. Gut Microbes 13, 1922241. https://doi.org/10.1080/19490976.2021.1922241

Gedgaudas, R., Bajaj, J.S., Skieceviciene, J., Valantiene, I., Kiudeliene, E., Bang, C., Franke, A., Schreiber, S., Kupcinskas, J., 2023. Sterile Fecal Filtrate From A Healthy Donor Improves Microbial Diversity In Patients With Hepatic Encephalopathy. J Gastrointestin Liver Dis 32, 332–338. https://doi.org/10.15403/jgld-4906

Gomez de Agüero, M., Ganal-Vonarburg, S.C., Fuhrer, T., Rupp, S., Uchimura, Y., Li, H., Steinert, A., Heikenwalder, M., Hapfelmeier, S., Sauer, U., McCoy, K.D., Macpherson, A.J., 2016. The maternal microbiota drives early postnatal innate immune development. Science 351, 1296–1302. https://doi.org/10.1126/science.aad2571

Grieneisen, L., Dasari, M., Gould, T.J., Björk, J.R., Grenier, J.-C., Yotova, V., Jansen, D., Gottel, N., Gordon, J.B., Learn, N.H., Gesquiere, L.R., Wango, T.L., Mututua, R.S., Warutere, J.K., Siodi, L., Gilbert, J.A.,

Barreiro, L.B., Alberts, S.C., Tung, J., Archie, E.A., Blekhman, R., 2021. Gut microbiome heritability is near-universal but environmentally contingent. Science 373, 181–186. https://doi.org/10.1126/science.aba5483

Guo, J., Ren, C., Han, X., Huang, W., You, Y., Zhan, J., 2021. Role of IgA in the early-life establishment of the gut microbiota and immunity: Implications for constructing a healthy start. Gut Microbes 13, 1908101. https://doi.org/10.1080/19490976.2021.1908101

Heo, M., Park, Y.S., Yoon, H., Kim, N.-E., Kim, K., Shin, C.M., Kim, N., Lee, D.H., 2023. Potential of Gut Microbe-Derived Extracellular Vesicles to Differentiate Inflammatory Bowel Disease Patients from Healthy Controls. Gut Liver 17, 108–118. https://doi.org/10.5009/gnl220081

Hu, M., Eviston, D., Hsu, P., Mariño, E., Chidgey, A., Santner-Nanan, B., Wong, K., Richards, J.L., Yap, Y.A., Collier, F., Quinton, A., Joung, S., Peek, M., Benzie, R., Macia, L., Wilson, D., Ponsonby, A.-L., Tang, M.L.K., O'Hely, M., Daly, N.L., Mackay, C.R., Dahlstrom, J.E., Vuillermin, P., Nanan, R., 2019. Decreased maternal serum acetate and impaired fetal thymic and regulatory T cell development in preeclampsia. Nat Commun 10, 3031. https://doi.org/10.1038/s41467-019-10703-1

Huang, R., Wu, F., Zhou, Q., Wei, W., Yue, J., Xiao, B., Luo, Z., 2022. *Lactobacillus* and intestinal diseases: Mechanisms of action and clinical applications. Microbiological Research 260, 127019. https://doi.org/10.1016/j.micres.2022.127019

Iimura, M., Gallo, R.L., Hase, K., Miyamoto, Y., Eckmann, L., Kagnoff, M.F., 2005. Cathelicidin mediates innate intestinal defense against colonization with epithelial adherent bacterial pathogens. J Immunol 174, 4901–4907. https://doi.org/10.4049/jimmunol.174.8.4901

Ivanov, I.I., Atarashi, K., Manel, N., Brodie, E.L., Shima, T., Karaoz, U., Wei, D., Goldfarb, K.C., Santee, C.A., Lynch, S.V., Tanoue, T., Imaoka, A., Itoh, K., Takeda, K., Umesaki, Y., Honda, K., Littman, D.R., 2009. Induction of intestinal Th17 cells by segmented filamentous bacteria. Cell 139, 485–498. https://doi.org/10.1016/j.cell.2009.09.033

Joat, N., Bajagai, Y.S., Van, T.T.H., Stanley, D., Chousalkar, K., Moore, R.J., 2023. The temporal fluctuations and development of faecal microbiota in commercial layer flocks. Anim Nutr 15, 197–209. https://doi.org/10.1016/j.aninu.2023.07.006

Jones, E., Stentz, R., Telatin, A., Savva, G.M., Booth, C., Baker, D., Rudder, S., Knight, S.C., Noble, A., Carding, S.R., 2021. The Origin of Plasma-Derived Bacterial Extracellular Vesicles in Healthy Individuals and Patients with Inflammatory Bowel Disease: A Pilot Study. Genes (Basel) 12, 1636. https://doi.org/10.3390/genes12101636

Kaisanlahti, A., Turunen, J., Byts, N., Samoylenko, A., Bart, G., Virtanen, N., Tejesvi, M.V., Zhyvolozhnyi, A., Sarfraz, S., Kumpula, S., Hekkala, J., Salmi, S., Will, O., Korvala, J., Paalanne, N., Erawijantari, P.P., Suokas, M., Medina, T.P., Vainio, S., Medina, O.P., Lahti, L., Tapiainen, T., Reunanen, J., 2023. Maternal microbiota communicates with the fetus through microbiota-derived extracellular vesicles. Microbiome 11, 249. https://doi.org/10.1186/s40168-023-01694-9

Kaisanlahti, A., Turunen, J., Hekkala, J., Mishra, S., Karikka, S., Amatya, S.B., Paalanne, N., Kruger, J., Portaankorva, A.M., Koivunen, J., Jukkola, A., Vihinen, P., Auvinen, P., Leppä, S., Karihtala, P., Koivukangas, V., Hukkanen, J., Vainio, S., Samoylenko, A., Bart, G., Lahti, L., Reunanen, J., Tejesvi, M.V., Ruuska-Loewald, T., 2025. Gut microbiota-derived extracellular vesicles form a distinct entity from gut microbiota. mSystems 10, e0031125. https://doi.org/10.1128/msystems.00311-25

Kaliannan, K., Robertson, R.C., Murphy, K., Stanton, C., Kang, C., Wang, B., Hao, L., Bhan, A.K., Kang, J.X., 2018. Estrogen-mediated gut microbiome alterations influence sexual dimorphism in metabolic syndrome in mice. Microbiome 6, 205. https://doi.org/10.1186/s40168-018-0587-0

Khalesi, S., Bellissimo, N., Vandelanotte, C., Williams, S., Stanley, D., Irwin, C., 2019. A review of probiotic supplementation in healthy adults: helpful or hype? Eur J Clin Nutr 73, 24–37. https://doi.org/10.1038/s41430-018-0135-9

Knoop, K.A., Holtz, L.R., Newberry, R.D., 2018. Inherited Nongenetic Influences on the Gut Microbiome and Immune System. Birth Defects Res 110, 1494–1503. https://doi.org/10.1002/bdr2.1436

Kordjazy, N., Haj-Mirzaian, Arvin, Haj-Mirzaian, Arya, Rohani, M.M., Gelfand, E.W., Rezaei, N., Abdolghaffari, A.H., 2018. Role of toll-like receptors in inflammatory bowel disease. Pharmacological Research 129, 204–215. https://doi.org/10.1016/j.phrs.2017.11.017

Koren, O., Konnikova, L., Brodin, P., Mysorekar, I.U., Collado, M.C., 2024. The maternal gut microbiome in pregnancy: implications for the developing immune system. Nat Rev Gastroenterol Hepatol 21, 35–45. https://doi.org/10.1038/s41575-023-00864-2

Kubinak, J.L., Round, J.L., 2012. Toll-Like Receptors Promote Mutually Beneficial Commensal-Host Interactions. PLoS Pathog 8, e1002785. https://doi.org/10.1371/journal.ppat.1002785

Lauro, M.L., Burch, J.M., Grimes, C.L., 2016. The Effect of NOD2 on the Microbiota in Crohn's Disease. Curr Opin Biotechnol 40, 97–102. https://doi.org/10.1016/j.copbio.2016.02.028

Li, C.-C., Hsu, W.-F., Chiang, P.-C., Kuo, M.-C., Wo, A.M., Tseng, Y.J., 2023. Characterization of markers, functional properties, and microbiome composition in human gut-derived bacterial extracellular vesicles. Gut Microbes 15, 2288200. https://doi.org/10.1080/19490976.2023.2288200

Li, M., Sloboda, D.M., Vickers, M.H., 2011. Maternal Obesity and Developmental Programming of Metabolic Disorders in Offspring: Evidence from Animal Models. Journal of Diabetes Research 2011, 592408. https://doi.org/10.1155/2011/592408

Liu, J., Tan, Y., Cheng, H., Zhang, D., Feng, W., Peng, C., 2022. Functions of Gut Microbiota Metabolites, Current Status and Future Perspectives. Aging Dis 13, 1106–1126. https://doi.org/10.14336/AD.2022.0104

Ma, W., Wang, Y., Nguyen, L.H., Mehta, R.S., Ha, J., Bhosle, A., Mclver, L.J., Song, M., Clish, C.B., Strate, L.L., Huttenhower, C., Chan, A.T., 2024. Gut microbiome composition and metabolic activity in women with diverticulitis. Nat Commun 15, 3612. https://doi.org/10.1038/s41467-024-47859-4

Macia, L., Nanan, R., Hosseini-Beheshti, E., Grau, G.E., 2019. Host- and Microbiota-Derived Extracellular Vesicles, Immune Function, and Disease Development. Int J Mol Sci 21, 107. https://doi.org/10.3390/ijms21010107

Magne, F., Gotteland, M., Gauthier, L., Zazueta, A., Pesoa, S., Navarrete, P., Balamurugan, R., 2020. The Firmicutes/Bacteroidetes Ratio: A Relevant Marker of Gut Dysbiosis in Obese Patients? Nutrients 12, 1474. https://doi.org/10.3390/nu12051474

Marchesi, J.R., Adams, D.H., Fava, F., Hermes, G.D.A., Hirschfield, G.M., Hold, G., Quraishi, M.N., Kinross, J., Smidt, H., Tuohy, K.M., Thomas, L.V., Zoetendal, E.G., Hart, A., 2016. The gut microbiota and host health: a new clinical frontier. Gut 65, 330–339. https://doi.org/10.1136/gutjnl-2015-309990

Martel, J., Chang, S.-H., Ko, Y.-F., Hwang, T.-L., Young, J.D., Ojcius, D.M., 2022. Gut barrier disruption and chronic disease. Trends in Endocrinology & Metabolism 33, 247–265. https://doi.org/10.1016/j.tem.2022.01.002

Mazmanian, S.K., Liu, C.H., Tzianabos, A.O., Kasper, D.L., 2005. An immunomodulatory molecule of symbiotic bacteria directs maturation of the host immune system. Cell 122, 107–118. https://doi.org/10.1016/j.cell.2005.05.007

McKnight, C.G., Jude, J.A., Zhu, Z., Panettieri, R.A., Finkelman, F.D., 2017. House Dust Mite–Induced Allergic Airway Disease Is Independent of IgE and FcεRIα. Am J Respir Cell Mol Biol 57, 674–682. https://doi.org/10.1165/rcmb.2016-0356OC

McMillan, H.M., Kuehn, M.J., 2021. The extracellular vesicle generation paradox: a bacterial point of view. EMBO J 40, e108174. https://doi.org/10.15252/embj.2021108174

Menon, R., Khanipov, K., Radnaa, E., Ganguly, E., Bento, G.F.C., Urrabaz-Garza, R., Kammala, A.K., Yaklic, J., Pyles, R., Golovko, G., Tantengco, O.A.G., 2023. Amplification of microbial DNA from bacterial extracellular vesicles from human placenta. Front Microbiol 14, 1213234. https://doi.org/10.3389/fmicb.2023.1213234

Mishra, A., Lai, G.C., Yao, L.J., Aung, T.T., Shental, N., Rotter-Maskowitz, A., Shepherdson, E., Singh, G.S.N., Pai, R., Shanti, A., Wong, R.M.M., Lee, A., Khyriem, C., Dutertre, C.A., Chakarov, S., Srinivasan, K.G.,

Shadan, N.B., Zhang, X.-M., Khalilnezhad, S., Cottier, F., Tan, A.S.M., Low, G., Chen, P., Fan, Y., Hor, P.X., Lee, A.K.M., Choolani, M., Vermijlen, D., Sharma, A., Fuks, G., Straussman, R., Pavelka, N., Malleret, B., McGovern, N., Albani, S., Chan, J.K.Y., Ginhoux, F., 2021. Microbial exposure during early human development primes fetal immune cells. Cell 184, 3394-3409.e20. https://doi.org/10.1016/j.cell.2021.04.039

Molina-Tijeras, J.A., Gálvez, J., Rodríguez-Cabezas, M.E., 2019. The Immunomodulatory Properties of Extracellular Vesicles Derived from Probiotics: A Novel Approach for the Management of Gastrointestinal Diseases. Nutrients 11, 1038. https://doi.org/10.3390/nu11051038

Nabhani, Z.A., Dulauroy, S., Marques, R., Cousu, C., Bounny, S.A., Déjardin, F., Sparwasser, T., Bérard, M., Cerf-Bensussan, N., Eberl, G., 2019. A Weaning Reaction to Microbiota Is Required for Resistance to Immunopathologies in the Adult. Immunity 50, 1276-1288.e5. https://doi.org/10.1016/j.immuni.2019.02.014

Ott, S.J., Waetzig, G.H., Rehman, A., Moltzau-Anderson, J., Bharti, R., Grasis, J.A., Cassidy, L., Tholey, A., Fickenscher, H., Seegert, D., Rosenstiel, P., Schreiber, S., 2017. Efficacy of Sterile Fecal Filtrate Transfer for Treating Patients With Clostridium difficile Infection. Gastroenterology 152, 799-811.e7. https://doi.org/10.1053/j.gastro.2016.11.010

Park, J.-Y., Kang, C.-S., Seo, H.-C., Shin, J.-C., Kym, S.-M., Park, Y.-S., Shin, T.-S., Kim, J.-G., Kim, Y.-K., 2021. Bacteria-Derived Extracellular Vesicles in Urine as a Novel Biomarker for Gastric Cancer: Integration of Liquid Biopsy and Metagenome Analysis. Cancers 13, 4687. https://doi.org/10.3390/cancers13184687

Pellegrino, A., Coppola, G., Santopaolo, F., Gasbarrini, A., Ponziani, F.R., 2023. Role of Akkermansia in Human Diseases: From Causation to Therapeutic Properties. Nutrients 15, 1815. https://doi.org/10.3390/nu15081815

Rooks, M.G., Garrett, W.S., 2016. Gut microbiota, metabolites and host immunity. Nat Rev Immunol 16, 341–352. https://doi.org/10.1038/nri.2016.42

Sheflin, A.M., Melby, C.L., Carbonero, F., Weir, T.L., 2016. Linking dietary patterns with gut microbial composition and function. Gut Microbes 8, 113–129. https://doi.org/10.1080/19490976.2016.1270809

Taitz, J.J., Tan, J.K., Potier-Villette, C., Ni, D., King, N.J., Nanan, R., Macia, L., 2023. Diet, commensal microbiota-derived extracellular vesicles, and host immunity. Eur J Immunol 53, e2250163. https://doi.org/10.1002/eji.202250163

Tan, J., McKenzie, C., Potamitis, M., Thorburn, A.N., Mackay, C.R., Macia, L., 2014. The role of short-chain fatty acids in health and disease. Adv Immunol 121, 91–119. https://doi.org/10.1016/B978-0-12-800100-4.00003-9

Tan, J., Ni, D., Taitz, J., Pinget, G.V., Read, M., Senior, A., Wali, J.A., Nanan, R., King, N.J.C., Grau, G.E., Simpson, S.J., Macia, L., 2020. Dietary protein increases T cell independent sIgA production through changes in gut microbiota-derived extracellular vesicles. https://doi.org/10.1101/2020.11.30.405217

Tan, J., Taitz, J., Nanan, R., Grau, G., Macia, L., 2023. Dysbiotic Gut Microbiota-Derived Metabolites and Their Role in Non-Communicable Diseases. International Journal of Molecular Sciences 24, 15256. https://doi.org/10.3390/ijms242015256

Thorburn, A.N., McKenzie, C.I., Shen, S., Stanley, D., Macia, L., Mason, L.J., Roberts, L.K., Wong, C.H.Y., Shim, R., Robert, R., Chevalier, N., Tan, J.K., Mariño, E., Moore, R.J., Wong, L., McConville, M.J., Tull, D.L., Wood, L.G., Murphy, V.E., Mattes, J., Gibson, P.G., Mackay, C.R., 2015. Evidence that asthma is a developmental origin disease influenced by maternal diet and bacterial metabolites. Nat Commun 6, 7320. https://doi.org/10.1038/ncomms8320

Togo, A.H., Diop, A., Dubourg, G., Khelaifia, S., Richez, M., Armstrong, N., Maraninchi, M., Fournier, P.-E., Raoult, D., Million, M., 2019. *Anaerotruncus massiliensis* sp. nov., a succinate-producing bacterium isolated from human stool from an obese patient after bariatric surgery. New Microbes and New Infections 29, 100508. https://doi.org/10.1016/j.nmni.2019.01.004

Toyofuku, M., Nomura, N., Eberl, L., 2019. Types and origins of bacterial membrane vesicles. Nat Rev Microbiol 17, 13–24. https://doi.org/10.1038/s41579-018-0112-2

Toyofuku, M., Schild, S., Kaparakis-Liaskos, M., Eberl, L., 2023. Composition and functions of bacterial membrane vesicles. Nat Rev Microbiol 21, 415–430. https://doi.org/10.1038/s41579-023-00875-5

Turunen, J., Tejesvi, M.V., Suokas, M., Virtanen, N., Paalanne, N., Kaisanlahti, A., Reunanen, J., Tapiainen, T., 2023. Bacterial extracellular vesicles in the microbiome of first-pass meconium in newborn infants. Pediatr Res 93, 887–896. https://doi.org/10.1038/s41390-022-02242-1

Wan, J., Zhang, Y., He, W., Tian, Z., Lin, J., Liu, Z., Li, Y., Chen, M., Han, S., Liang, J., Shi, Y., Wang, X., Zhou, L., Cao, Y., Liu, J., Wu, K., 2022. Gut Microbiota and Metabolite Changes in Patients With Ulcerative Colitis and Clostridioides difficile Infection. Front Microbiol 13, 802823. https://doi.org/10.3389/fmicb.2022.802823

Wu, G.D., Chen, J., Hoffmann, C., Bittinger, K., Chen, Y.-Y., Keilbaugh, S.A., Bewtra, M., Knights, D., Walters, W.A., Knight, R., Sinha, R., Gilroy, E., Gupta, K., Baldassano, R., Nessel, L., Li, H., Bushman, F.D., Lewis, J.D., 2011. Linking long-term dietary patterns with gut microbial enterotypes. Science 334, 105–108. https://doi.org/10.1126/science.1208344

Xie, J., Li, Q., Haesebrouck, F., Hoecke, L.V., Vandenbroucke, R.E., 2022. The tremendous biomedical potential of bacterial extracellular vesicles. Trends in Biotechnology 40, 1173–1194. https://doi.org/10.1016/j.tibtech.2022.03.005

Xu, Y., Xie, C., Liu, Y., Qin, X., Liu, J., 2023. An update on our understanding of Gram-positive bacterial membrane vesicles: discovery, functions, and applications. Front Cell Infect Microbiol 13, 1273813. https://doi.org/10.3389/fcimb.2023.1273813

Yang, J., McDowell, A., Seo, H., Kim, S., Min, T.K., Jee, Y.K., Choi, Y., Park, H.S., Pyun, B.Y., Kim, Y.K., 2020. Diagnostic Models for Atopic Dermatitis Based on Serum Microbial Extracellular Vesicle Metagenomic Analysis: A Pilot Study. Allergy Asthma Immunol Res 12, 792–805. https://doi.org/10.4168/aair.2020.12.5.792

Chapter 6 Integrated discussion and future directions

6.1 Summary of results

The gut microbiota has been shown to influence almost all aspects of host physiology through diverse signalling mechanisms. Gut bacteria produce hundreds, to potentially thousands, of unique molecules, each with the potential to modulate key biological processes. Disruptions in microbial product signalling, such as altered SCFA production, are strongly linked to disease development and highlight the importance of understanding these microbial interactions. The aim of this thesis was to investigate the complex relationship between the gut microbiota and host, with a particular focus on MEVs, a class of bacterial products that are poorly defined in the context of gut microbiota-host communication. By exploring their influence on host physiology, this work identifies multiple pathways through which MEVs regulate host immunity and metabolism. Our findings establish MEVs as critical mediators of microbiota-host interactions, central to maintaining homeostasis and potentially contributing to disease pathogenesis.

We first demonstrated that antibiotic-mediated dysbiosis, while causing minimal changes to baseline immunity, primed immune cells towards enhanced TNF responses upon *ex vivo* stimulation. This chapter provides mechanistic insight into how antibiotic exposure might predispose individuals to inflammatory conditions. Secondly, we discovered a novel pathway linking diet and mucosal immunity, with increased dietary protein

modulating intestinal sIgA production, via increased MEVs release from a succinate-induced bacterial stress response. Thirdly, we identified a new role for gut MEVs as peripheral environmental cues (zeitgebers) that regulate hepatic gluconeogenesis in response to host glucose demand, highlighting an inter-kingdom synchronisation between host metabolism and microbiota-derived signals. Finally, we demonstrated that MEVs are not only a distinct fraction of the bacterial secretome, but they also actively regulate microbiota composition. Moreover, they serve as a novel pathway for maternal gut microbiota-mediated programming of offspring immunity.

Together, the findings of this thesis offer the first comprehensive characterisation of MEVs as fundamental mediators of microbiota-host communication. We have uncovered novel roles for MEVs across diverse biological processes, from immune and metabolic regulation to fetal programming, as well as modulating gut bacterial composition itself. This research not only highlights the dual role of MEVs in maintaining homeostasis and potentially driving disease pathogenesis, but also opens new avenues for therapeutic interventions, utilising MEVs to modulate immune disorders, improve metabolic health, and influence maternal-fetal programming.

6.2 The dysbiosis-TNF-autoinflammatory circuit

Our antibiotic study demonstrated that antibiotic-induced dysbiosis altered immune cell programming without triggering overt inflammation. Specifically, basal spleen and MLN cellular composition were largely unchanged except for expansion of pDC and cDC numbers, however, splenic T cells from antibiotic-treated mice exhibited a significantly enhanced TNF production phenotype. This priming effect provides mechanistic insights

into the epidemiological links between antibiotic exposure and development of TNF-associated autoinflammatory diseases, where alterations in gut microbiota are thought to contribute (Donald and Finlay, 2024; Guarner et al., 2024).

6.2.1 Does dysregulation originate within the gut?

Antibiotics disrupt gut homeostasis but whether this is an event that progresses to systemic immune changes (such as peripheral TNF priming), and to what extent, likely depends on multiple factors. Genetic mouse models demonstrate a clear relationship between TNF expression, microbiota composition, and disease development. TNF-deficient mice are resistant to colitis while mice overexpressing TNF develop spontaneous intestinal inflammation that advances to severe colitis in a microbiota-dependent manner (Noti et al., 2010; Schaubeck et al., 2016). Notably, progression is driven by dysbiotic shifts in bacterial composition (Roulis et al., 2016), suggesting that microbiota composition is a key determinant of TNF-mediated disease progression.

A major limitation of our study is that we did not assess gut barrier function or changes to gut-local cells, which would be crucial to understanding the dysbiosis-peripheral TNF link and clarify whether peripheral immune dysregulation originates from gut dysregulation, occurs concurrently, or develops independently. Future studies should characterise gut lamina propria immune populations, and in particular, assess whether tolerogenic cells (DCs, macrophages, and Tregs) are impaired in function or number, and whether gut immune cells generally display heightened priming or pro-inflammatory cytokine expression. Since our study only assessed immune changes at the experimental endpoint after four weeks of continuous antibiotic exposure, a longitudinal analysis that tracks microbiota composition, gut immunity and systemic priming at weekly intervals

could clarify how such changes may progress over time. This approach would help determine whether gut-local immune dysregulation precedes peripheral TNF priming and provide insight into how prolonged or cumulative antibiotic exposure (which may better mimic human antibiotic consumption) could contribute to immune dysfunction and disease risk.

6.2.2 Do antibiotics have a direct effect?

While enhanced peripheral TNF is unlikely to be a direct effect of systemically circulating antibiotics (given their poor oral bioavailability), we cannot exclude the possibility of antibiotics having direct immunomodulatory effects on gut cells, contributing to gut dysregulation and subsequent peripheral immune priming.

Short-term oral vancomycin (5mg/mouse/day) induced endoplasmic reticulum (ER) stress in goblet cells which impaired the mucus barrier, but exogenous supplementation with the bile acid tauroursodeoxycholic acid (TUDCA), an ER stress inhibitor, alleviated this effect (Sawaed et al., 2024). While our study used a lower vancomycin dose (2.5mg/mouse/day), both antibiotics in our regimen may have had a direct effect on gut-local cells, indirectly contributing to peripheral TNF priming. Thus, future studies should evaluate direct impacts of vancomycin and polymyxin B on both gut immune and epithelial cells. Although GF mice offer a means to examine microbiota-independent effects, their intrinsic gut immune deficiencies may limit capacity to identify direct effects. Therefore, *in vitro* approaches would be more suitable. Primary gut lamina propria immune cells could be treated with vancomycin and polymyxin B and assessed for functional responses and cytokine production. Intestinal organoids could also be used as more physiological models of the epithelial barrier and could determine whether

antibiotics impair other epithelial lineages (such as Paneth cells) and barrier integrity via TJ formation. Determining whether antibiotics have direct effects on gut cells could facilitate the identification of additional protective compounds, like TUDCA, which could be co-administered with antibiotics to mitigate such adverse direct effects. This may be particularly beneficial for patients requiring frequent or long-term antibiotic therapy, as well as those with genetic predispositions to autoinflammatory disease, who may be more susceptible to antibiotics-induced immune dysregulation.

6.2.3 Are gut microbiota metabolites responsible?

Our antibiotic-induced dysbiosis may have contributed to enhanced peripheral TNF priming by disrupting key microbiota-derived signals that normally regulate immune homeostasis and constrain excessive inflammation. This could occur through multiple overlapping pathways, including depletion of beneficial metabolites, accumulation of dysbiotic metabolites, and alterations in PRR ligands which provide tonic signalling essential for immune homeostasis (Ghosh et al., 2021; Tan et al., 2023).

We observed SCFAs, particularly butyrate and acetate, were significantly reduced by both vancomycin and polymyxin B. Acetate, the only SCFA that reaches systemic circulation, has been shown to reduce LPS-stimulated TNF expression *in vitro* when used as a pre-treatment, by influencing epigenetic histone acetylation and autophagy of the NLRP3 inflammasome (Fragas et al., 2022; Xu et al., 2019). Therefore, systemic reduction in acetate may have diminished an inhibitory effect on splenic TNF production. To investigate this, future studies could sort splenic T cells and perform a Western blot to assess histone acetylation or cleaved caspase-1 p20 levels, which would clarify whether

acetate depletion is key in driving TNF priming via altered epigenetics or inflammasome turnover.

Although butyrate is largely confined to the gut, its depletion may have indirectly driven systemic changes by disrupting gut homeostasis. Butyrate depletion shifts colonocyte metabolism towards oxygen production, favouring growth of pathogenic taxa over SCFA producers (Park et al., 2024). Additionally, butyrate stabilises HIF-1α, an essential transcription factor for gut barrier integrity (Colgan and Taylor, 2010; Kelly et al., 2015). Thus, to clarify if butyrate loss is central to initiating gut immune dysregulation, future studies could assess changes to colonocyte function, HIF-1α protein levels, and gut transcriptomic changes using a combination of Western blot, RNA-seq and RT-qPCR approaches.

Notably, anti-TNF therapies not only alleviate inflammatory disease symptoms but also improve gut microbiota composition in patients with Crohn's disease, IBD and rheumatoid arthritis (RA), often increasing SCFA-producers while reducing proinflammatory taxa such as *E. coli* (Busquets et al., 2015; Ditto et al., 2021; Picchianti-Diamanti et al., 2018; Ribaldone et al., 2019). This microbiota remodelling primarily occurs in TNF-responders, suggesting that resolving dysbiosis is integral to the success of anti-TNF inhibitors, and helps breaks the cycle of inflammation (Alshehri et al., 2021). Given this, testing our antibiotic model with concurrent SCFA supplementation could reveal the extent to which SCFAs counteract the TNF immune priming we observe in otherwise healthy mice.

6.2.4 Do alterations in gut MAMPs play a role?

A shift in the quantity and/or composition of circulating MAMPs could also explain enhanced peripheral TNF. One intriguing possibility is that certain microbes can actively disrupt immune tolerance, and antibiotic exposure may facilitate their abundance or systemic translocation. For example, the periodontal pathogen *Porphyromonas gingivalis* is implicated in RA pathogenesis by enzymatically citrullinating host proteins, triggering autoantibody production and breaking immune tolerance (Gómez-Bañuelos et al., 2019; Mikuls et al., 2012). Similarly, the enterovirus Coxsackievirus B is strongly associated with type 1 diabetes and is thought to initiate islet autoimmunity, although the precise mechanisms are under investigation (Nekoua et al., 2022). Emerging evidence also suggests the gut microbiota harbours cross-reactive antigens capable of promoting autoimmune diseases via molecular mimicry (English et al., 2023; Miyauchi et al., 2023). Thus, this could represent an understudied link between antibiotic exposure, dysbiosis and autoimmunity, and individuals who harbour higher levels of cross-reactive microbes in their gut may be at heightened risk of autoimmune disease following antibiotics use.

Before examining this, however, it would be crucial to clarify whether our antibiotic model directly increased translocation of microbial components into the periphery. Alongside assessing gut barrier function, future studies could quantify serum levels of bacterial DNA (via RT-qPCR for the 16s rRNA gene) or LPS by ELISA. However, these markers may reflect not only translocation of whole microbes or membrane components, but also levels of MEVs in circulation. As demonstrated in Chapter 3, gut MEVs can enter the periphery even in the absence of gut barrier dysfunction, suggesting they may be an overlooked, yet significant driver of antibiotic-mediated immune dysregulation.

6.2.5 Are MEVs the missing link?

While we did not directly investigate MEVs in Chapter 2, the rest of this thesis highlights their role as key mediators of gut-host interactions. Given this, we speculate that MEVs may play a significant role in the antibiotic-dysbiosis-disease axis. Antibiotics are known to stimulate MEV release *in vitro* (Toyofuku et al., 2019), but their impact on MEV dynamics *in vivo* has never been investigated, to our knowledge.

In Chapter 3, we demonstrated that MEVs directly modulate host gene expression, upregulating a range of immune mediators in the SI epithelium (CCL28, APRIL, BAFF, TGF-β, and TSLP) via TLR4/NF-κB signalling. While assessing TNF was outside the scope of that study, it is likely antibiotics could influence both the quantity as well as composition of gut MEVs, potentially driving changes in host immunity, such as enhanced TNF expression. Indeed, vancomycin significantly enriched *E. coli* in the gut, likely shifting the MEV profile towards vesicles solely from this genus. Notably, we observed a significant increase in sIgA levels in vancomycin-treated mice, raising the possibility that a profile of LPS-enriched MEVs may have stimulated sIgA production via the TLR4/NF-κB pathway we observed in Chapter 3. Thus, understanding how antibiotics influence both metabolite and vesicle profiles *in vivo* could provide critical mechanistic insights into dysbiosis-induced immune dysregulation. Future research should characterise how different antibiotics may induce changes to *in vivo* MEV quantities, bacterial origins, and molecular cargo, and assess whether such alterations to the MEV profile correlate with TNF priming or other immune alterations.

Additionally, the timing and dosing of antibiotics may play a crucial role in shaping MEV dynamics and their downstream effects on the host. As demonstrated in Chapter 4, gut

MEV production is closely aligned with host glucose demand and regulates hepatic gluconeogenesis. Factors such as multiple daily doses, or recommendations to take antibiotics with or without food, could significantly disrupt natural MEV oscillations, interfering with this metabolic synchronisation between microbiota and host. These disruptions may also contribute to an association between antibiotics and metabolic disorders (Vallianou et al., 2021; Yuan et al., 2020), revealing a mechanism beyond dysbiotic changes through which antibiotics may influence host metabolism.

A comprehensive investigation could include mapping gut MEV levels over 24-hour periods, in relation to antibiotic administration and host feeding patterns, which could reveal if and how antibiotics disrupt natural MEV oscillations. This could be complemented with monitoring changes in host glucose homeostasis and metabolism, to determine if antibiotic-MEV disruptions contribute to metabolic dysregulation. Immune profiling of intestinal and systemic compartments could examine how altered MEV dynamics directly affect gut local immunity (such as Tregs and gut barrier integrity), as well as distal immune responses (such as T cell priming). Conducting these experiments in the context of an autoimmune mouse model could also reveal whether MEVs serve as a direct link between antibiotic-induced dysbiosis and disease susceptibility. Additionally, comparing acute versus repeated antibiotic courses (which may better reflect human antibiotic usage patterns) could reveal how cumulative exposure progressively alters gut microbiota composition, MEV dynamics and host immune-metabolic homeostasis. This would provide mechanistic insight into how disrupted MEV homeostasis could drive both autoimmune and metabolic pathologies.

6.3 MEVs offer a novel therapeutic intervention for early life

As we found in Chapters 3-5, MEVs influence host immunity and metabolism, and this regulatory capacity presents novel therapeutic opportunities, particularly in early life, where MEVs could shape immune development and metabolic programming.

6.3.1 Could MEVs enhance breastmilk sIgA?

A potential therapeutic application of MEVs lies in enhancing maternal breastmilk sIgA levels. Breastmilk sIgA provides crucial protection against neonatal infection, promotes colonisation of beneficial gut bacteria, and fosters a tolerogenic environment in the infant gut, with breastfeeding significantly reducing infant mortality (Guo et al., 2021; Li et al., 2022). sIgA levels peak in colostrum, the milk produced within the 72 hours after birth, and decline thereafter. NCDs such as gestational diabetes mellitus are also associated with reduced sIgA milk levels (Akhter et al., 2021; Smilowitz et al., 2013). Since mammary IgA^+ plasma cells are believed to originate from intestinal IgA^+ cells that migrate to the mammary gland during late pregnancy via CCL28 (Guo et al., 2021; Wilson and Butcher, 2004), gestational MEV supplementation could enhance maternal sIgA levels, strengthening protective effects of breastfeeding. This strategy may be particularly valuable in reducing the risk of necrotising enterocolitis (NEC), a severe gastrointestinal infection that predominantly affects preterm infants and is the leading cause of their mortality. Since breastfeeding is one of the strongest protective factors against NEC due to the passive transfer of sIgA, MEV supplementation in high-risk pregnancies could serve as a novel approach to mitigate NEC incidence and severity (Cacho et al., 2017; Gopalakrishna et al., 2019).

In Chapter 5, we administered MEVs to female mice during gestation, however, we did not assess how MEVs induced changes to maternal physiology. A key future direction would be to examine the mammary gland for IgA^+ plasma cell abundance, which could determine whether MEV supplementation is in fact a viable strategy to enhance breastmilk sIgA. This also could reveal a potential confounding factor in our postnatal analysis of the MEV-exposed offspring. While we fostered litters to PBS-treated dams within 48 hours of birth, these pups would have still received colostrum which may have had an increased level of sIgA. This may have influenced subsequent microbiota colonisation patterns as well as colonic gene expression at our endpoint analysis. However, this could also highlight a synergistic role of MEVs in enhancing offspring health, by directly influencing the fetus *in utero* as well as enhancing neonatal immunity via milk sIgA.

6.3.2 Could MEVs directly promote fetal and neonatal health?

Regardless of whether gestational MEV supplementation impacts the fetus directly or indirectly through maternal physiology, we found MEV exposure resulted in lasting postnatal changes, including altered microbiota composition, modified colonic gene expression, increased peripheral immune organ cellularity, and enhanced peripheral IFNg production. In the context of rising NCDs, MEVs could be harnessed as a pregnancy supplement to optimise offspring health outcomes. The increasing prevalence of childhood allergic disease in Australia highlights the need for early interventions that promote appropriate immune development (Peters et al., 2017).

To advance our understanding of MEVs in fetal programming and their therapeutic potential, a key next step would be to assess whether administering MEVs to GF pregnant mice can normalise postnatal immune defects in the offspring. This would provide fundamental insight into the role of maternal gut MEVs in shaping immune development. Additionally, investigating whether MEVs derived from a high-fibre diet microbiota can replicate the allergy-protective effects of direct maternal fibre intake could open new therapeutic avenues (Thorburn et al., 2015). If fibre-enriched MEVs can promote tolerogenic immune programming *in utero*, this would offer a novel strategy to reduce childhood incidence of atopy, without requiring significant modifications to maternal diet.

MEVs could also serve as early-life supplements, providing a safer alternative to live probiotics due to their non-replicative nature. Formula-fed infants do not receive exposure to microbiota-derived components normally transmitted through breastmilk, which are believed to contribute to its long-term health benefits, including reduced risks of obesity, type 1 and 2 diabetes, asthma, and IBD (Dogaru et al., 2014; Lund-Blix et al., 2017; Owen et al., 2006; Xu et al., 2017; Yan et al., 2014). Incorporating even freeze-dried MEVs into infant formula, for example, could deliver key antigenic immunomodulatory signals that shape neonatal immunity to potentially reduce the risk of NCDs later in life. This would also avoid the limitations and risks associated with live probiotics, as discussed below.

6.4 The pros and cons of MEV therapeutics

6.4.1 The advantages of MEV therapeutics

MEV-based therapeutics offer several advantages over existing approaches aimed at modulating host-microbiota interactions. While diet modifications shape microbiota composition, such interventions often suffer from poor adherence and there is a lack of long-term data supporting sustained and consistent compositional changes (Downer et al., 2016; Voreades et al., 2014) Similarly, probiotic effectiveness varies due to poor colonisation, variations in individual responses, and infection risks in vulnerable populations (Ojima et al., 2022; Sanders et al., 2010). Moreover, most commercial probiotics are typically limited to *Lactobacillus* and *Bifidobacteria* strains which fail to replicate the complex signalling of a healthy microbiota (de Simone, 2019). While faecal microbiota transplantation (FMT) appears to be an effective approach for long-term microbiota modulation, its practical use is limited by the risk of adverse events, particularly the transmission of pathogenic or antibiotic-resistant strains (Michailidis et al., 2021).

MEVs overcome many of these limitations by providing a non-replicative yet bioactive means of delivering complex microbial signals. Unlike live probiotics or FMT, they pose minimal infectious risks, making them particularly suitable for vulnerable populations including infants, elderly people and individuals who are immunocompromised. As MEVs naturally encase their content in a lipid membrane bilayer, internal cargo is protected from degradation by proteases and nucleases, and studies indicate bacterial EVs are heat-stable, further supporting their potential as an oral therapeutic (Verbunt et al., 2024).

Our biodistribution studies in Chapters 3 and 4 revealed that under normal physiological conditions, orally administered MEVs translocate beyond the gut. Notably, they accumulate in the liver (likely due to hepatic portal vein drainage), which may reflect an evolutionary role in synchronising bacterial and host metabolism. Previous studies have shown isolated BEVs from specific gut bacteria exhibit tissue tropism after oral administration, implicating them in disease pathogenesis (Chelakkot et al., 2018; Choi et al., 2015). This raises the broader question of whether MEVs from dysbiotic microbiotas associated with specific diseases follow distinct distribution patterns. For example, do MEVs from obesity-associated microbiotas preferentially accumulate in adipose tissue, while those from neurodegenerative or psychiatric-associated microbiotas target to afferent vagal nerve fibres, or even the central nervous system? Identifying if there are disease-specific distribution patterns could provide crucial insight into pathogenesis mechanisms, as well as whether MEV tropism could be exploited to deliver targeted therapeutics.

6.4.2 The concerns about MEV therapeutics

The findings of this thesis also highlight important considerations that must be addressed before MEVs can be fully developed and harnessed as therapeutic agents. As we found in Chapter 4, MEVs actively regulate host gluconeogenesis, which highlights a potential contribution in conditions with disrupted metabolic homeostasis. Chronic exogenous MEV administration induced glucose intolerance and mild insulin resistance in adult male mice, suggesting that gestational MEV supplementation in Chapter 5 may have influenced maternal glucose metabolism, and, consequently, offspring metabolic programming. This represents another key limitation of our study in Chapter 5, as we did not assess if MEV exposure impacted maternal metabolic homeostasis, or programmed changes to

offspring metabolism. Given that maternal metabolic impairments can have detrimental long-term consequences on offspring metabolism (Godfrey et al., 2017; Li et al., 2011), it would be critical to determine whether gestational MEV supplementation alters offspring glucose homeostasis and increases susceptibility to metabolic disease. This is particularly relevant when considering MEV-based strategies to enhance maternal sIgA or reduce incidence of childhood atopy. Future studies should comprehensively assess offspring metabolic health by conducting glucose and insulin tolerance tests, measuring adiposity and food intake, and characterising the liver as well as susceptibility to obesogenic diets.

Optimising MEVs as therapeutics would also require careful consideration of timing and dosage to maximise potential benefits while minimising adverse effects. Aligning administration with endogenous rhythms of MEV production, for example, could mitigate potential metabolic disruptions. Another critical safety concern is the extent to which MEV therapeutics could transmit antibiotic resistance genes to recipient gut microbiota. While this would aid in preserving beneficial commensals during future antibiotic therapy, the risk of pathobionts acquiring resistance genes could be a significant safety concern. Thus, screening MEV preparations for the presence of antibiotic-resistance genes or plasmids would be a key factor in ensuring their safety profile.

Overall, as outlined in the following section, a comprehensive characterisation of how MEV preparations may vary in molecular composition, functional activity, and stability is essential for their therapeutic translation. A deeper understanding of these properties is crucial for determining the suitability of MEVs as therapeutic agents for pregnancy, early life, and metabolic dysregulation.

6.5 Unpacking MEVs further

6.5.1 An integrated approach

The molecular composition of MEVs represents a key area for future research, as this thesis primarily focused on their quantitative effects rather than qualitative differences in MEV composition or bacterial origin. For example, in Chapter 4 we observed identical doses of MEVs from different diets activated TLR4 to similar levels. However, MEV composition likely varied, which could influence their immunomodulatory properties in a different biological context. Similarly, in Chapter 5, while we demonstrated that supplementing MEVs during gestation above physiologically circulating levels altered offspring outcomes, we did not investigate whether MEVs isolated from different dietary conditions could have distinct effects on offspring development and immunity.

Comprehensive characterisation of MEV cargo, including proteins, lipids, metabolites, and nucleic acids, would be essential for understanding their therapeutic potential and deciphering the precise mechanisms behind their effects, which may vary across biological contexts. MEVs have been shown to exacerbate liver steatosis by delivering bacterial DNA that activates the cGAS/STING pathway, but systemic activation of this pathway via MEV-DNA enhances systemic antiviral immunity (Erttmann et al., 2022; Luo et al., 2022). These findings illustrate the need to dissect how specific MEV components and their associated signalling pathways may contribute to distinct physiological and pathological processes.

Understanding how environmental and dietary factors shape MEV composition is equally critical to understand the link between diet, microbiota, and host physiology and disease.

A multi-omics approach, integrating proteomics, lipidomics, metabolomics, and 16S rRNA profiling, would provide the most comprehensive strategy to systematically map relationships between diet, microbiota composition, MEV profile and composition, and host responses. This could enable the development of tailored MEV formulations, designed to elicit specific immune or metabolic effects, advancing the field of precision-based medicine and microbiota therapeutics.

6.5.2 Overlooked cargo and co-isolating components

Beyond the intrinsic molecular cargo of MEVs, co-isolating microbiota components may also contribute to the effects of MEV preparations. Recent studies showing sterile faecal filtrates can be as effective as FMT in treating dysbiosis suggest that microbiota-derived products, rather than live bacteria, are the key therapeutic mediators. The MEV isolation strategy used in this thesis was selected for total yield, ensuring consistent batch and dosing for our *in vivo* administration studies. While more stringent isolation methods such as size-exclusion chromatography or density-gradient ultracentrifugation can isolate purer vesicle populations, they result in significantly reduced yield. Therefore our isolation method, while still comprising predominantly bacterial-derived vesicles, likely contained co-isolating molecules such as bacterial flagellar and pili fragments, and protein aggregates (Tulkens et al., 2020).

Bacteriophages may represent a significant co-isolating component in MEV preparations as they can be directly encapsulated within bacterial vesicles (Champagne-Jorgensen et al., 2021; Toyofuku et al., 2019). These viruses outnumber even bacteria within the gut and are increasingly appreciated for their role in regulating bacterial composition, and, consequently, host health (Łusiak-Szelachowska et al., 2017). The first study of sterile

faecal filtrates identified bacteriophages as the main therapeutic factor in improving dysbiosis (Ott et al., 2017). Thus, in Chapter 5, when we observed MEV administration altered gut bacterial composition in adult male mice, it is possible that bacteriophages contributed to this effect. As bacteriophages are likely to be inherently co-isolated with bacterial vesicles, measuring their prevalence within MEV preparations would be crucial for understanding mechanistically how MEVs influence gut microbiota composition and thus regulate host-microbiota interactions.

6.6 Conclusion

The complex interplay between modern lifestyle factors and health is increasingly linked to alterations in gut microbiota. This thesis establishes that MEVs are fundamental mediators of host-microbiota communication, with implications for both disease pathogenesis and therapeutic development. We identified that MEVs influence diverse areas of host biology, from immunity to metabolism, suggesting they may be key in explaining the rising incidence of NCDs in industrialised nations. Environmental factors, such as changes in diet and antibiotic use, likely alter MEV signalling to potentially influence disease susceptibility. Understanding these mechanisms also presents new therapeutic opportunities, particularly given the limitations of current microbiota-targeted interventions. Further research is needed to define how environmental factors shape gut MEVs, the downstream effects on host physiology, and how this may be utilised therapeutically. Collectively, this thesis advances our understanding of host-microbiota communication, positioning MEVs as crucial mediators of this cross-talk.

References

Akhter, H., Aziz, F., Ullah, F.R., Ahsan, M., Islam, S.N., 2021. Immunoglobulins Content in Colostrum, Transitional and Mature Milk of Bangladeshi Mothers: Influence of Parity and Sociodemographic Characteristics. J Mother Child 24, 8–15. https://doi.org/10.34763/jmotherandchild.20202403.2032.d-20-00001

Alshehri, D., Saadah, O., Mosli, M., Edris, S., Alhindi, R., Bahieldin, A., 2021. Dysbiosis of gut microbiota in inflammatory bowel disease: Current therapies and potential for microbiota-modulating therapeutic approaches. Bosn J Basic Med Sci 21, 270–283. https://doi.org/10.17305/bjbms.2020.5016

Busquets, D., Mas-de-Xaxars, T., López-Siles, M., Martínez-Medina, M., Bahí, A., Sàbat, M., Louvriex, R., Miquel-Cusachs, J.O., Garcia-Gil, J.L., Aldeguer, X., 2015. Anti-tumour Necrosis Factor Treatment with Adalimumab Induces Changes in the Microbiota of Crohn's Disease. Journal of Crohn's and Colitis 9, 899–906. https://doi.org/10.1093/ecco-jcc/jjv119

Cacho, N.T., Parker, L.A., Neu, J., 2017. Necrotizing Enterocolitis and Human Milk Feeding: A Systematic Review. Clin Perinatol 44, 49–67. https://doi.org/10.1016/j.clp.2016.11.009

Champagne-Jorgensen, K., Jose, T.A., Stanisz, A.M., Mian, M.F., Hynes, A.P., Bienenstock, J., 2021. Bacterial membrane vesicles and phages in blood after consumption of lacticaseibacillus rhamnosus JB-1. Gut Microbes 13, 1993583. https://doi.org/10.1080/19490976.2021.1993583

Chelakkot, C., Choi, Y., Kim, D.-K., Park, H.T., Ghim, J., Kwon, Y., Jeon, J., Kim, M.-S., Jee, Y.-K., Gho, Y.S., Park, H.-S., Kim, Y.-K., Ryu, S.H., 2018. Akkermansia muciniphila-derived extracellular vesicles influence gut permeability through the regulation of tight junctions. Exp Mol Med 50, e450. https://doi.org/10.1038/emm.2017.282

Choi, Y., Kwon, Y., Kim, D.-K., Jeon, J., Jang, S.C., Wang, T., Ban, M., Kim, M.-H., Jeon, S.G., Kim, M.-S., Choi, C.S., Jee, Y.-K., Gho, Y.S., Ryu, S.H., Kim, Y.-K., 2015. Gut microbe-derived extracellular vesicles induce insulin resistance, thereby impairing glucose metabolism in skeletal muscle. Sci Rep 5, 15878. https://doi.org/10.1038/srep15878

Colgan, S.P., Taylor, C.T., 2010. Hypoxia: an alarm signal during intestinal inflammation. Nat Rev Gastroenterol Hepatol 7, 281–287. https://doi.org/10.1038/nrgastro.2010.39

de Simone, C., 2019. The Unregulated Probiotic Market. Clinical Gastroenterology and Hepatology 17, 809–817. https://doi.org/10.1016/j.cgh.2018.01.018

Ditto, M.C., Parisi, S., Landolfi, G., Borrelli, R., Realmuto, C., Finucci, A., Caviglia, G.P., Ribaldone, D.G., Astegiano, M., Zanetti, A., Carrara, G., Scirè, C.A., Antivalle, M., Sarzi-Puttini, P., Fusaro, E., 2021. Intestinal microbiota changes induced by TNF-inhibitors in IBD-related spondyloarthritis. RMD Open 7, e001755. https://doi.org/10.1136/rmdopen-2021-001755

Dogaru, C.M., Nyffenegger, D., Pescatore, A.M., Spycher, B.D., Kuehni, C.E., 2014. Breastfeeding and Childhood Asthma: Systematic Review and Meta-Analysis. American Journal of Epidemiology 179, 1153–1167. https://doi.org/10.1093/aje/kwu072

Donald, K., Finlay, B.B., 2024. Experimental models of antibiotic exposure and atopic disease. Front Allergy 5, 1455438. https://doi.org/10.3389/falgy.2024.1455438

Downer, M.K., Gea, A., Stampfer, M., Sánchez-Tainta, A., Corella, D., Salas-Salvadó, J., Ros, E., Estruch, R., Fitó, M., Gómez-Gracia, E., Arós, F., Fiol, M., De-la-Corte, F.J.G., Serra-Majem, L., Pinto, X., Basora, J., Sorlí, J.V., Vinyoles, E., Zazpe, I., Martínez-González, M.-Á., 2016. Predictors of short- and long-term adherence with a Mediterranean-type diet intervention: the PREDIMED randomized trial. International Journal of Behavioral Nutrition and Physical Activity 13, 67. https://doi.org/10.1186/s12966-016-0394-6

English, J., Patrick, S., Stewart, L.D., 2023. The potential role of molecular mimicry by the anaerobic microbiota in the aetiology of autoimmune disease. Anaerobe 80, 102721. https://doi.org/10.1016/j.anaerobe.2023.102721

Erttmann, S.F., Swacha, P., Aung, K.M., Brindefalk, B., Jiang, H., Härtlova, A., Uhlin, B.E., Wai, S.N., Gekara, N.O., 2022. The gut microbiota prime systemic antiviral immunity via the cGAS-STING-IFN-I axis. Immunity 55, 847-861.e10. https://doi.org/10.1016/j.immuni.2022.04.006

Fragas, M.G., Oliveira, D.M. de, Hiyane, M.I., Braga, T.T., Camara, N.O.S., 2022. The dual effect of acetate on microglial TNF-α production. Clinics (Sao Paulo) 77, 100062. https://doi.org/10.1016/j.clinsp.2022.100062

Ghosh, S., Whitley, C.S., Haribabu, B., Jala, V.R., 2021. Regulation of Intestinal Barrier Function by Microbial Metabolites. Cellular and Molecular Gastroenterology and Hepatology 11, 1463–1482. https://doi.org/10.1016/j.jcmgh.2021.02.007

Godfrey, K.M., Reynolds, R.M., Prescott, S.L., Nyirenda, M., Jaddoe, V.W.V., Eriksson, J.G., Broekman, B.F.P., 2017. Influence of maternal obesity on the long-term health of offspring. The Lancet Diabetes & Endocrinology 5, 53–64. https://doi.org/10.1016/S2213-8587(16)30107-3

Gómez-Bañuelos, E., Mukherjee, A., Darrah, E., Andrade, F., 2019. Rheumatoid Arthritis-Associated Mechanisms of Porphyromonas gingivalis and Aggregatibacter actinomycetemcomitans. Journal of Clinical Medicine 8, 1309. https://doi.org/10.3390/jcm8091309

Gopalakrishna, K.P., Macadangdang, B.R., Rogers, M.B., Tometich, J.T., Firek, B.A., Baker, R., Ji, J., Burr, A.H.P., Ma, C., Good, M., Morowitz, M.J., Hand, T.W., 2019. Maternal IgA protects against the development of necrotizing enterocolitis in preterm infants. Nat Med 25, 1110–1115. https://doi.org/10.1038/s41591-019-0480-9

Guarner, F., Bustos Fernandez, L., Cruchet, S., Damião, A., Maruy Saito, A., Riveros Lopez, J.P., Rodrigues Silva, L., Valdovinos Diaz, M.A., 2024. Gut dysbiosis mediates the association between antibiotic exposure and chronic disease. Front Med (Lausanne) 11, 1477882. https://doi.org/10.3389/fmed.2024.1477882

Guo, J., Ren, C., Han, X., Huang, W., You, Y., Zhan, J., 2021. Role of IgA in the early-life establishment of the gut microbiota and immunity: Implications for constructing a healthy start. Gut Microbes 13, 1908101. https://doi.org/10.1080/19490976.2021.1908101

Kelly, C.J., Zheng, L., Campbell, E.L., Saeedi, B., Scholz, C.C., Bayless, A.J., Wilson, K.E., Glove, L.E., Kominsky, D.J., Magnuson, A., Weir, T.L., Ehrentraut, S.F., Pickel, C., Kuhn, K.A., Lanis, J.M., Nguyen, V., Taylor, C.T., Colgan, S.P., 2015. Crosstalk between Microbiota-Derived Short-Chain Fatty Acids and Intestinal Epithelial HIF Augments Tissue Barrier Function. Cell Host Microbe 17, 662–671. https://doi.org/10.1016/j.chom.2015.03.005

Li, M., Sloboda, D.M., Vickers, M.H., 2011. Maternal Obesity and Developmental Programming of Metabolic Disorders in Offspring: Evidence from Animal Models. Journal of Diabetes Research 2011, 592408. https://doi.org/10.1155/2011/592408

Li, R., Ware, J., Chen, A., Nelson, J.M., Kmet, J.M., Parks, S.E., Morrow, A.L., Chen, J., Perrine, C.G., 2022. Breastfeeding and post-perinatal infant deaths in the United States, A national prospective cohort analysis. The Lancet Regional Health – Americas 5. https://doi.org/10.1016/j.lana.2021.100094

Lund-Blix, N.A., Dydensborg Sander, S., Størdal, K., Nybo Andersen, A.-M., Rønningen, K.S., Joner, G., Skrivarhaug, T., Njølstad, P.R., Husby, S., Stene, L.C., 2017. Infant Feeding and Risk of Type 1 Diabetes in Two Large Scandinavian Birth Cohorts. Diabetes Care 40, 920–927. https://doi.org/10.2337/dc17-0016

Luo, Z., Ji, Y., Zhang, D., Gao, H., Jin, Z., Yang, M., Ying, W., 2022. Microbial DNA enrichment promotes liver steatosis and fibrosis in the course of non-alcoholic steatohepatitis. Acta Physiol (Oxf) 235, e13827. https://doi.org/10.1111/apha.13827

Łusiak-Szelachowska, M., Weber-Dąbrowska, B., Jończyk-Matysiak, E., Wojciechowska, R., Górski, A., 2017. Bacteriophages in the gastrointestinal tract and their implications. Gut Pathog 9, 44. https://doi.org/10.1186/s13099-017-0196-7

Michailidis, L., Currier, A.C., Le, M., Flomenhoft, D.R., 2021. Adverse events of fecal microbiota transplantation: a meta-analysis of high-quality studies. Ann Gastroenterol 34, 802–814. https://doi.org/10.20524/aog.2021.0655

Mikuls, T.R., Thiele, G.M., Deane, K.D., Payne, J.B., O'Dell, J.R., Yu, F., Sayles, H., Weisman, M.H., Gregersen, P.K., Buckner, J.H., Keating, R.M., Derber, L.A., Robinson, W.H., Holers, V.M., Norris, J.M., 2012. Porphyromonas gingivalis and disease-related autoantibodies in individuals at increased risk of rheumatoid arthritis. Arthritis Rheum 64, 3522–3530. https://doi.org/10.1002/art.34595

Miyauchi, E., Shimokawa, C., Steimle, A., Desai, M.S., Ohno, H., 2023. The impact of the gut microbiome on extra-intestinal autoimmune diseases. Nat Rev Immunol 23, 9–23. https://doi.org/10.1038/s41577-022-00727-y

Nekoua, M.P., Alidjinou, E.K., Hober, D., 2022. Persistent coxsackievirus B infection and pathogenesis of type 1 diabetes mellitus. Nat Rev Endocrinol 18, 503–516. https://doi.org/10.1038/s41574-022-00688-1

Noti, M., Corazza, N., Mueller, C., Berger, B., Brunner, T., 2010. TNF suppresses acute intestinal inflammation by inducing local glucocorticoid synthesis. J Exp Med 207, 1057–1066. https://doi.org/10.1084/jem.20090849

Ojima, M.N., Yoshida, K., Sakanaka, M., Jiang, L., Odamaki, T., Katayama, T., 2022. Ecological and molecular perspectives on responders and non-responders to probiotics and prebiotics. Current Opinion in Biotechnology 73, 108–120. https://doi.org/10.1016/j.copbio.2021.06.023

Ott, S.J., Waetzig, G.H., Rehman, A., Moltzau-Anderson, J., Bharti, R., Grasis, J.A., Cassidy, L., Tholey, A., Fickenscher, H., Seegert, D., Rosenstiel, P., Schreiber, S., 2017. Efficacy of Sterile Fecal Filtrate Transfer for Treating Patients With Clostridium difficile Infection. Gastroenterology 152, 799-811.e7. https://doi.org/10.1053/j.gastro.2016.11.010

Owen, C.G., Martin, R.M., Whincup, P.H., Smith, G.D., Cook, D.G., 2006. Does breastfeeding influence risk of type 2 diabetes in later life? A quantitative analysis of published evidence2. The American Journal of Clinical Nutrition 84, 1043–1054. https://doi.org/10.1093/ajcn/84.5.1043

Park, B., Kim, J.Y., Riffey, O.F., Walsh, T.J., Johnson, J., Donohoe, D.R., 2024. Crosstalk between butyrate oxidation in colonocyte and butyrate-producing bacteria. iScience 27, 110853. https://doi.org/10.1016/j.isci.2024.110853

Peters, R.L., Koplin, J.J., Gurrin, L.C., Dharmage, S.C., Wake, M., Ponsonby, A.-L., Tang, M.L.K., Lowe, A.J., Matheson, M., Dwyer, T., Allen, K.J., 2017. The prevalence of food allergy and other allergic diseases in early childhood in a population-based study: HealthNuts age 4-year follow-up. Journal of Allergy and Clinical Immunology 140, 145-153.e8. https://doi.org/10.1016/j.jaci.2017.02.019

Picchianti-Diamanti, A., Panebianco, C., Salemi, S., Sorgi, M.L., Di Rosa, R., Tropea, A., Sgrulletti, M., Salerno, G., Terracciano, F., D'Amelio, R., Laganà, B., Pazienza, V., 2018. Analysis of Gut Microbiota in Rheumatoid Arthritis Patients: Disease-Related Dysbiosis and Modifications Induced by Etanercept. International Journal of Molecular Sciences 19, 2938. https://doi.org/10.3390/ijms19102938

Ribaldone, D.G., Caviglia, G.P., Abdulle, A., Pellicano, R., Ditto, M.C., Morino, M., Fusaro, E., Saracco, G.M., Bugianesi, E., Astegiano, M., 2019. Adalimumab Therapy Improves Intestinal Dysbiosis in Crohn's Disease. Journal of Clinical Medicine 8, 1646. https://doi.org/10.3390/jcm8101646

Roulis, M., Bongers, G., Armaka, M., Salviano, T., He, Z., Singh, A., Seidler, U., Becker, C., Demengeot, J., Furtado, G., Lira, S., Kollias, G., 2016. Host and microbiota interactions are critical for development of murine Crohn's-like ileitis. Mucosal Immunol 9, 787–797. https://doi.org/10.1038/mi.2015.102

Sanders, M.E., Akkermans, L.M., Haller, D., Hammerman, C., Heimbach, J., Hörmannsperger, G., Huys, G., Levy, D.D., Lutgendorff, F., Mack, D., Phothirath, P., Solano-Aguilar, G., Vaughan, E., 2010. Safety assessment of probiotics for human use. Gut Microbes 1, 164–185. https://doi.org/10.4161/gmic.1.3.12127

Schaubeck, M., Clavel, T., Calasan, J., Lagkouvardos, I., Haange, S.B., Jehmlich, N., Basic, M., Dupont, A., Hornef, M., von Bergen, M., Bleich, A., Haller, D., 2016. Dysbiotic gut microbiota causes transmissible Crohn's disease-like ileitis independent of failure in antimicrobial defence. Gut 65, 225–237. https://doi.org/10.1136/gutjnl-2015-309333

Smilowitz, J.T., Totten, S.M., Huang, J., Grapov, D., Durham, H.A., Lammi-Keefe, C.J., Lebrilla, C., German, J.B., 2013. Human Milk Secretory Immunoglobulin A and Lactoferrin N-Glycans Are Altered in Women with Gestational Diabetes Mellitus123. J Nutr 143, 1906–1912. https://doi.org/10.3945/jn.113.180695

Tan, J., Taitz, J., Nanan, R., Grau, G., Macia, L., 2023. Dysbiotic Gut Microbiota-Derived Metabolites and Their Role in Non-Communicable Diseases. Int J Mol Sci 24, 15256. https://doi.org/10.3390/ijms242015256

Thorburn, A.N., McKenzie, C.I., Shen, S., Stanley, D., Macia, L., Mason, L.J., Roberts, L.K., Wong, C.H.Y., Shim, R., Robert, R., Chevalier, N., Tan, J.K., Mariño, E., Moore, R.J., Wong, L., McConville, M.J., Tull, D.L., Wood, L.G., Murphy, V.E., Mattes, J., Gibson, P.G., Mackay, C.R., 2015. Evidence that asthma is a developmental origin disease influenced by maternal diet and bacterial metabolites. Nat Commun 6, 7320. https://doi.org/10.1038/ncomms8320

Toyofuku, M., Nomura, N., Eberl, L., 2019. Types and origins of bacterial membrane vesicles. Nat Rev Microbiol 17, 13–24. https://doi.org/10.1038/s41579-018-0112-2

Tulkens, J., De Wever, O., Hendrix, A., 2020. Analyzing bacterial extracellular vesicles in human body fluids by orthogonal biophysical separation and biochemical characterization. Nat Protoc 15, 40–67. https://doi.org/10.1038/s41596-019-0236-5

Vallianou, N., Dalamaga, M., Stratigou, T., Karampela, I., Tsigalou, C., 2021. Do Antibiotics Cause Obesity Through Long-term Alterations in the Gut Microbiome? A Review of Current Evidence. Curr Obes Rep 10, 244–262. https://doi.org/10.1007/s13679-021-00438-w

Verbunt, J., Jocken, J., Blaak, E., Savelkoul, P., Stassen, F., 2024. Gut-bacteria derived membrane vesicles and host metabolic health: a narrative review. Gut Microbes 16, 2359515. https://doi.org/10.1080/19490976.2024.2359515

Voreades, N., Kozil, A., Weir, T.L., 2014. Diet and the development of the human intestinal microbiome. Front Microbiol 5, 494. https://doi.org/10.3389/fmicb.2014.00494

Wilson, E., Butcher, E.C., 2004. CCL28 Controls Immunoglobulin (Ig)A Plasma Cell Accumulation in the Lactating Mammary Gland and IgA Antibody Transfer to the Neonate. J Exp Med 200, 805–809. https://doi.org/10.1084/jem.20041069

Xu, L., Lochhead, P., Ko, Y., Claggett, B., Leong, R.W., Ananthakrishnan, A.N., 2017. Systematic review with meta-analysis: breastfeeding and the risk of Crohn's disease and ulcerative colitis. Alimentary Pharmacology & Therapeutics 46, 780–789. https://doi.org/10.1111/apt.14291

Xu, M., Jiang, Z., Wang, C., Li, N., Bo, L., Zha, Y., Bian, J., Zhang, Y., Deng, X., 2019. Acetate attenuates inflammasome activation through GPR43-mediated Ca2+-dependent NLRP3 ubiquitination. Exp Mol Med 51, 1–13. https://doi.org/10.1038/s12276-019-0276-5

Yan, J., Liu, L., Zhu, Y., Huang, G., Wang, P.P., 2014. The association between breastfeeding and childhood obesity: a meta-analysis. BMC Public Health 14, 1267. https://doi.org/10.1186/1471-2458-14-1267

Yuan, J., Hu, Y.J., Zheng, J., Kim, J.H., Sumerlin, T., Chen, Y., He, Y., Zhang, C., Tang, J., Pan, Y., Moore, M., 2020. Long-term use of antibiotics and risk of type 2 diabetes in women: a prospective cohort study. International Journal of Epidemiology 49, 1572–1581. https://doi.org/10.1093/ije/dyaa122